SILVANUS

D*6.2* - Model of Ecological Resilience

This project has received funding from the European Union's Horizon 2020 research and innovation programme under Grant Agreement No 101037247

Project Acronym	SILVANUS
Grant Agreement number	101037247 (H2020-LC-GD-2020-3)
Project Full Title	Integrated Technological and Information Platform for Wildfire Management
Funding Scheme	IA – Innovation action

DELIVERABLE INFORMATION

Deliverable Number:	D6.2
Deliverable Name:	Report on SILVANUS resilience programme for forest management, v1
Dissemination level:	PU
Type of Document:	R
Contractual date of delivery:	30/09/2023 (M24)
Date of submission:	30/09/2023
Deliverable Leader:	AMIKOM
Status:	Final
Version number:	V0.5
WP Leader/ Task Leader:	WP6 – AMIKOM
Keywords:	Ecological resilience, wildfire adaptation, restoration, soil analysis
Abstract:	Deliverable D6.2 provides conceptual model of ecological resilience analyse from 5 European Pilot and 1 non-European Pilot Areas. Soil analysis methods, considering the important soil variable on burned and unburned forest also deeply elaborated. Moreover, to facilitate monitoring program of the ecological resilience processes, this deliverable elaborates a design of Open Forest Map Tool. Open Forest Map enable big data analysis for all possible related aspects of ecological resilience for further analysis by the expert user.

Lead Author(s):	Kusrini (AMIKOM)
Reviewers:	VTG, CERTH, UTH

Disclaimer

All information in this document is provided “as is" and no guarantee or warranty is given that the information is fit for any particular purpose.

The user there of uses the information at its sole risk and liability. For the avoidance of all doubts, the European Commission has no liability in respect of this document, which is merely representing the authors view.

Document History			
Version	**Date**	**Contributor(s)**	**Description**
V0.1	30-3-2023	AMIKOM	Outline
V0.2	5-9-2023	WP6 contributors	First round of input contributions consolidated
V0.3	16-10-2023	AMIKOM, AUA, IST, PNRT, TUZVO, LETS, ASSET, Z&P	Second round of input contributions consolidated
V0.4	24-10-2023	VTG, CERTH, UTH	Internal review feedback collected
V0.5	28-10-2023	AMIKOM, AUA, PNRT	Final version released for submission after integrating feedback from internal review

List of Contributors

Partner	Author(s)
ZANASI ALESSANDRO SRL (Z&P)	Domenica Casciano, Alexandre Lazarou
GEOPONIKO PANEPISTIMION ATHINON (AUA)	Konstantinos Demestichas, Spyridon Kaloudis, Dimitrios Sykas, Stavroula Galanopoulou
ASSOCIACAO DO INSTITUTO SUPERIOR TECNICO PARA A INVESTIGACAO E DESENVOLVIMENTO (IST)	Inês Ribeiro, Vânia Proença, Leonor Themudo Barata, Ivo Gama (Terraprima)
LETS ITALIA srls (LETS)	Gianpiero Lacovara (LETS); Marcello Sacchetti (LETS); Eva Canarslan (LETS)
Parco Naturale Regionale di Tepilora (PNRT)	Marianna Mossa, Alessandro Salvatore Pala, Marino Satta
KENTRO MELETON ASFALEIAS (KEMEA)	Georgios Sakkas, Nikolaos Kalapodis
ELLINIKI OMADA DIASOSIS SOMATEIO (HRT)	Iosif Vourvachis, Alexandros Giordanis
PERIFEREIA STEREAS ELLADAS (PSTE)	Sofia Katsifou, Socratis Boutsis
Hrvatska vatrogasna zajednica (HVZ)	Zeljko Cebin
TECHNICKA UNIVERZITA VO ZVOLENE (TUZVO)	Andrea Majlingová, Maroš Sedliak, Ján Bahýľ
Obcianske zdruzenie Plamen Badin (PLAMEN)	
Yayasan AMIKOM Yogyakarta (AMIKOM)	Kusrini, Arief Setyanto, Gardyas Bidari Adninda, Renindya Azizza Kartikakirana, Kumara Ari Yuwana, Fitria Nucifera

List of acronyms and abbreviations

ACRONYM	Description
ACE	acenaphthene
ACY	scenaphthylene
ADD	Aeolian Dust Deposition
AGB	Above Ground Biomass
AIB	Anticendi Boschivi (Forest Fire Fighting, Italy)
ANT	anthracene
AVI	Advance Vegetation Index
AWC	Available Water Capacity
BaA	benzo(a)anthracene
BaP	benzo(a)pyrene
BbF	benzo(b)fluoranthene
BghiP	benzo (g,h,i) perylene
BGI	Biogeochemical Index
BI	Bare Soil Index
BkF	benzo(k)fluoranthene
BMG	Badan Meteorologi dan Geofisika (Meteorologu and Geophysics Agency, Indonesia)
C_f	Contamination factor
CHR	chrysene
CITES	Convention on International Trade of Endangered Species
CSI	Contamination security index
DBA	Dibenzo (a,h) anthracene
DBH	Diameter at Breast Height
DEM	Digital Elevation Model
DTM	Digital Terrain Model
EEC	European Economic Community
EF	Enrichment factor
EFFIS	European Forest Fire Information System
EPM	Erosion Potential Method
ER	Ecological Resilience
ERL	Effects Range Low
ERM	Effects Range Median

ACRONYM	Description
EU	European Union
FCD	Forest Canopy Density
FES	Forest Ecosystem Services
FHD	Foliage Height Difference Index
FLT	fluoranthene
FLU	fluorene
FoReSTAS	Agenzia Forestale Regionale per lo Sviluppo del Territorio e l'Ambiente della Sardegna (Regional Forestry Agency for the Development of the Territory and the Environment of Sardinia, Italy)
GC	Gas Chromatography
GDP	Gross Domestic Product
GIS	Geographic Information System
HNMS	Hellenic National Meteorological Service
HP	Hutan Produksi (Production Forest, Indonesia)
HPC	Hutan Produski Convertible (Convertible Production Forest, Indonesia)
HPLC	High Performance Liquid Chromatography
IBA	Important Bird Areas
Igeo	Geoaccumulation Index
IND	indene (1,2,3-cd)pyrene
IPCC	Intergovernmental Panel on Climate Change
IUCN	International Union for Conservation of Nature
JRC	Joint Research Centre
LAI	Leaf Area Index
LIBS	Laser-Induced Breakdown Spectroscopy
LiDAR	Light Detection and Ranging
LOI	Loss-On-Ignition
MEC	Multi-element contamination
MODIS	Moderate Resolution Imaging Spectroradiometer
MSAVI2	Modified Soil Adjustment Vegetation Index
MUSLE	Modified Universal Soil Loss Equation
NAP	Naphthalene
NASA	National Aeronautics and Space Administration

ACRONYM	Description
NDVI	Normalised Difference Vegetation Index
NIR	Near-InfraRed band
PAHs	Polycyclic Aromatic Hydrocarbons
pH	Soil Reaction
PHE	phenanthrene
PI	Single Pollution Index
PMPF	General and forestry police regulations of the Sardinia region
PLA	Protected Landscape Area
PLI	Pollution Load Index
PYR	pyrene
R	Red band
RMMF	Revised Morgan – Morgan – Finney
RUSLE	Revised Universal Soil Loss Equation
RUSLE	Revised Universal Soil Loss Equation
SAAD	Sensitive, Avoiders, Adaptive, Dependent
SAC	Special Area of Conservation
SAR	Synthetic Aperture Radar
SAVI	Soil Adjustment Vegetation Index
Sb	Shrub Biomass
SCS	Soil Conservation Services
SCS	Soil Conservation Services
SCS-CN	Soil Conservation Service Curve Number
SEM-EDS	Scanning Electron Microscopy – Energy Dispersive Spectroscopy
SI	Shadow Index
SSI	Scaled Shadow Index
SWAT	Soil and Water Assessment Tool
SWIR	Short-Wave InfraRed band
TI	Thermal Index
USDA	United States Department of Agriculture
USEPA	United States Environmental Protection Agency
USLE	Universal Soil Loss Equation
USPED	Unit Stream Power - based Erosion Deposition

ACRONYM	Description
VD	Vegetation Density
WaTEM/SEDEM	Water Erosion Prediction Program/SEdiment Delivery Model
WDPT	Water drops penetration time test
WEPP	Water Erosion Prediction Project
WWF	World Wide Fund Nature
XRD	X-ray Diffraction

List of beneficiaries

No	Partner Name	Short name	Country
1	UNIVERSITA TELEMATICA PEGASO	PEGASO	Italy
2	ZANASI ALESSANDRO SRL	Z&P	Italy
3	INTRASOFT INTERNATIONAL SA	INTRA	Luxembourg
4	THALES	TRT	France
5	FINCONS SPA	FINC	Italy
6	ATOS IT SOLUTIONS AND SERVICES IBERIA SL	ATOS IT	Spain
6.1	ATOS SPAIN SA	ATOS SA	Spain
7	EMC INFORMATION SYSTEMS INTERNATIONAL	DELL	Ireland
8	SOFTWARE IMAGINATION & VISION SRL	SIMAVI	Romania
9	CNET CENTRE FOR NEW ENERGY TECHNOLOGIES SA	EDP	Portugal
10	ADP VALOR SERVICOS AMBIENTAIS SA	ADP	Portugal
11	TERRAPRIMA - SERVICOS AMBIENTAIS SOCIEDADE UNIPESSOAL LDA	TP	Portugal
12	3MON, s. r. o.	3MON	Slovakia
13	CATALINK LIMITED	CTL	Cyprus
14	SYNTHESIS CENTER FOR RESEARCH AND EDUCATION LIMITED	SYNC	Cyprus
15	EXPERT SYSTEM SPA	EAI	Italy
16	ITTI SP ZOO	ITTI	Poland
17	Venaka Treleaf GbR	VTG	Germany
18	MASSIVE DYNAMIC SWEDEN AB	MDS	Sweden
19	FONDAZIONE CENTRO EURO-MEDITERRANEOSUI CAMBIAMENTI CLIMATICI	CMCC F	Italy
20	EXUS SOFTWARE MONOPROSOPI ETAIRIA PERIORISMENIS EVTHINIS	EXUS	Greece
21	RINIGARD DOO ZA USLUGE	RINI	Croatia
22	Micro Digital d.o.o.	MD	Croatia
23	POLITECHNIKA WARSZAWSKA	WUT	Poland
24	HOEGSKOLAN I BORAS	HB	Sweden
25	GEOPONIKO PANEPISTIMION ATHINON	AUA	Greece
26	ETHNIKO KENTRO EREVNAS KAI TECHNOLOGIKIS ANAPTYXIS	CERTH	Greece
27	PANEPISTIMIO THESSALIAS	UTH	Greece
28	ASSOCIACAO DO INSTITUTO SUPERIOR TECNICO PARA A INVESTIGACAO E DESENVOLVIMENTO	IST	Portugal
29	VELEUCILISTE VELIKA GORICA	UASVG	Croatia

No	Partner Name	Short name	Country
30	USTAV INFORMATIKY, SLOVENSKA AKADEMIA VIED	UISAV	Slovakia
31	POMPIERS DE L'URGENCE INTERNATIONALE	PUI	France
32	THE MAIN SCHOOL OF FIRE SERVICE	SGPS	Poland
33	ASSET - Agenzia regionale Strategica per lo Sviluppo Ecosostenibile del Territorio	ASSET	Italy
34	LETS ITALIA srls	LETS	Italy
35	Parco Naturale Regionale di Tepilora	PNRT	Italy
36	FUNDATIA PENTRU SMURD	SMURD	Romania
37	Romanian Forestry Association - ASFOR	ASFOR	Romania
38	KENTRO MELETON ASFALEIAS	KEMEA	Greece
39	ELLINIKI OMADA DIASOSIS SOMATEIO	HRT	Greece
40	ARISTOTELIO PANEPISTIMIO THESSALONIKIS	AHEPA	Greece
41	Ospedale Israelitico	OIR	Italy
42	PERIFEREIA STEREAS ELLADAS	PSTE	Greece
43	HASICSKY ZACHRANNY SBOR MORAVSKOSLEZSKEHO KRAJE	FRB MSR	Czechia
44	Hrvatska vatrogasna zajednica	HVZ	Croatia
45	TECHNICKA UNIVERZITA VO ZVOLENE	TUZVO	Slovakia
46	Obcianske zdruzenie Plamen Badin	PLAMEN	Slovakia
47	Yayasan AMIKOM Yogyakarta	AMIKOM	Indonesia
48	COMMONWEALTH SCIENTIFIC AND INDUSTRIAL RESEARCH ORGANISATION	CSIRO	Australia
50	FUNDACAO COORDENACAO DE PROJETOS PESQUISAS E ESTUDOS TECNOLOGICOS COPPETEC	COPPETEC	Brazil

List of Glossary

This section is provided for easy access to the deliverable. The glossary is a part of Deliverable 2.1, and there are additional vocabularies from Deliverable 6.2.

Term	Definition	Source
Climate	Weather conditions prevailing in an area in general or over a long period	IPCC Glossary
Climate Change	Change in the average conditions — such as temperature and rainfall — in a region over a long period of time	IPCC Glossary
Forest	Land with tree crown cover of more than 10 percent and area of more than 0.5 hectares. The trees should be able to reach a minimum height of 5 meters at maturity.	FAO/GFMC Wildland Fire Management Terminology
Planting	The act of placing seeds or seedlings into soil	European Glossary for Wildfires and Forest Fires
Recovery	Recovery or engineering resilience regards the ability of an ecosystem to return to its former condition after a disturbance	Oliver et al. (2015)
Rehabilitation	A collective term for any actions taken to repair damage to an area of land that has been caused by wildfire or wildfire suppression activities	European Glossary for Wildfires and Forest Fires
Restoration	A collective term for any actions taken to reduce and manage the impacts of a wildfire on a particular environment	European Glossary for Wildfires and Forest Fires
Maleability	The degree to which the stable state that is established after a disturbance differs from the original steady state	(E. Westman, 1986).
Elasticity	The rapidity at which a system can return to a stable state after a disturbance	(E. Westman, 1986).
Trend	The oscillations between post-recovery and pre-disturbance measurements of forest greenness and landscape metrics	(Czerwinski et al., 2014, Sankey, Temuulen, et al., 2021).
Remote Sensing	The acquisition and interpretation of images of the Earth's surface, where images are usually acquired by cameras and scanners carried on aircraft or orbiting satellites. Optical images simultaneously record visible and invisible reflected light in several different wavelengths; when combined, these images (or 'bands') can be used to map burn scars, different types of fuel and fuel moisture. Thermal images record emitted heat from active fires and the Earth's surface. Radar remote sensing	European Glossary for Wildfires and Forest Fires

Term	Definition	Source
	uses artificial microwave energy to produce images of burn scars through clouds and at night	
Resilience	The capacity of forest ecosystems to absorb the disturbance and maintain its normal patterns after being subjected to damage caused by an ecological disturbance	(Holling et al. (1995), Levin and Simon. (2023))

Index of figures

Index of tables

Executive Summary

This deliverable focuses on the process of returning biodiversity and ecosystems that were previously affected by forest fire. The concept of ecological resilience is one of the discussions on this deliverable to measure the forest's capacity to bounce back into pristine condition. The resiliency model has been drawn for each pilot area by measuring elasticity, malleability, and trend.

The deliverable also concerns significant fire impact on soil and hydrological conditions. The degradation of forest caused by fire occurrence is connected to physical and chemical water quality. Same as it might destroy soil structure and organic matter.

To evaluate the proposed approach of rehabilitation, we have used the pilot sites as a test bed. In each pilot area, rehabilitation and restoration become parts of forest management conducted by forest owners. Natural regeneration and planting program applied in the pilot areas, for each program supported with more detailed activities. The conceptual model proposed for forest resilience, which is consist of forest type, bioregions, ecoregions, climate type, fire regime, fire weather index, time span, magnitude, malleability, and elasticity.

To minimize the limitations of forest management, we designed a platform called Open Forest Map. Open Forest Map aimed to provide long-term monitoring of the ecological resilient process, mainly on forest ecosystems. This application applies historical earth monitoring images, recorded historical climate-related data, and other variables such as wildfire incidents, restoration, and rehabilitation programs carried out in the past.

1 Introduction

The aim of the deliverable is to outline the activities carried out in Task 6.2 and 6.3. Task 6.2 discussing on the development of forest rehabilitation and restoration policies, which is accommodate in this deliverable and continue to the next Deliverable 6.4. Meanwhile, Task 6.3 focusing on the impact of forest fire on the hydrology and soil properties.

The elaboration of this deliverable is a continuation of Deliverable 6.1. The previous deliverable examines the ecological resilience programs in the pilot areas, taken part of which are 5 EU pilot areas and 1 non-EU pilot area in phase C of the project (Rehabilitation and Restoration). In this deliverable, we explain the scope of ecological resilience model towards forest sustainability and design the tools for monitoring ecological resilience processes.

Observing and modelling ecological resilience requires a long terms historical context of the forest. The state of forest before, during, and after a disturbance need to be considered. To enable the long terms analysis, interconnected variables need to be defined and recorded in an integrated analysis. The historical data availability becomes crucial in this study since we cannot rely on field study in the past.

The variables derived from earth monitoring which is mentioned in this deliverable, such as the greenness level of the forest and its changes, the temperature of the landscape, and the level of severity after the ecological disturbance caused by fire, are some available historical data. Climate related data, such as temperature and, precipitation, are also available over time. The societal related variables such as population density and gross national product (GNP) are others related available variables in historical time series. Those data are available in various format, spatial and temporal resolution.

In the other hand, soil is an important component of the forest. Healthy soils are necessary for sustaining diverse ecosystem services in forest ecosystem. If ecological disturbances occurred, for example forest fire, it significantly influences to the soil properties. Fires usually prevent the dominance of a few species and release the nutrients locked in vegetation, stimulating nutrient cycling, and enhancing soil fertility over the short term. The significant effects on ecosystem functioning are those related to the following domains: (1) soil structure, which can influence water infiltration; (2) soil nutrients, which determine soil fertility; (3) soil carbon, as this is one of the major carbon sinks and thus a critical element in climate regulation; and (4) soil microorganisms, microbiota and mesofauna.

This deliverable presents our proposal for assessing ecological resilience based on historical data. It covers a study of rehabilitation programs aimed at enhancing the condition of forests within the historical context in six pilot regions across both Europe and non-European areas. The document includes an analysis of the ecological resilience of these pilot areas and the relevant variables, with a focus on strategies for improving forest conditions and reforestation.

Additionally, this deliverable discusses the methods used to assess soil properties, particularly in the context of fire impact. Samples are collected from both burned and unburned areas in nearby locations to evaluate the effects of forest fires on hydrology and soil physical properties, which are analysed through chemical processes. The analysis considers factors such as the severity and duration of the forest fires, as well as the causes and spread of these fires.

To ensure the sustainability of our solution, this deliverable also outlines the design of a tool for managing historical time series data and presents all variables in a standardized plot to facilitate further analysis. The tool also considers the temporal changes in global climate conditions and their impact on restoration programs. The tool records the policies and programs implemented in the pilot areas, allowing for the analysis and modelling of both current and future ecological resilience.

The deliverable reports on the activities carried out towards proposing a model of resilience processes adopted for forest restoration. The proposed model considers the impact and severity of wildfires and social

aspects for the affected populations. The deliverable reports on the exhaustive literature survey that has been carried out important literature related to the discussion and is followed by the result, which is explaining the model. This deliverable reports the initial model and shows the beta version of the model.

Ecological resilience has been computed under considering elasticity, malleability and magnitude variables of elasticity, malleability, and magnitude. Elasticity measures the period needed by the affected forest to rebound to its pre-disturbance condition. Malleability measures the absolute degradation of the forest after recovery periods. Magnitude assesses the immediate impact of the disturbance. The rehabilitation programs carried out in the area under study and related variable are collected. Descriptive model developed considering those collected variables in the pilot areas. The current version of the model areas limited by the data availability. To cover a wider area and longer periods of time this deliverable proposes a technology solution for ecological resilience monitoring. The design of the presented tools will become the solution of monitoring and ecological resilience modelling.

The structure of the deliverable consists of the following discussion:

1. Introduction

   Chapter 1 outlines the scope of the deliverable, explaining the aims and what to discuss in the overall chapters.

2. Forest Rehabilitation, Restoration, and Resilience

   Chapter 2 explains a brief resilience concept (detailed concept described in Deliverable 6.1) with the supporting element related to ecological resilience.

3. Soil Analysis

   Chapter 3 elaborates on soil analysis as one of the essential parameters that is affected by forest fires. The chapter discusses fire's impact on soil, soil resilience, and the analysis of soil samples.

4. Conceptual Model of Ecological Resilience

   Chapter 4 explains the proposed concept of the ecological resilience model, including the explanation of the ecological resilience program in European and non-European pilots.

5. Open Forest Map Tool

   Chapter 5 reports the idea of creating an Open Forest Map as a tool for ecological resilience monitoring. This chapter points out the process of designing the tool until the data analysis process.

6. Conclusion

   Chapter 6 concludes the overall chapters of Deliverable 6.2.

2 Forest Rehabilitation, Restoration, and Resilience

Forest Transition theory has been used to explain the change from shrinking to expanding forest cover (Mather, 2007). According to Mather (2007), forest transition refers to a change in forest cover over a given area from a period of net forest area loss to a period of net gain. Whether transitioning from deforestation to reforestation can lead to improved ecosystem services, depends on the quality and characteristics of the newly established forest (Zhai et al., 2020). Forest clearance or deforestation is the removal of a forest or stand of trees from land that is then converted to non-forest use. Deforestation is responsible for the shrinking of forest areas. Afforestation is an activity to convert non forest area into a forest, therefore afforestation is responsible for expanding on the forest. Reforestation or forest restoration aims to re-establishing forests that have either been cut down or lost due to wildfire, storm, flood, and many other forest disturbances.

Forest restoration is an essential process for recovering biodiversity and ecosystem services in areas that have been modified and degraded due to various disturbance factors. The goal of forest restoration, as well as ecological restoration in general, is to restore the ecosystem to its native condition, considering its compositional, structural, and functional dimensions. While achieving full recovery could become a long-term goal, the recovery rate depends on the extent of ecosystem modification of its original state and the ecosystem's resilience.

According to the conceptual model of the restoration staircase (Chazdon, 2008) as illustrated in **Figure 1** the type of restoration actions to be implemented in a degraded area should consider several factors. These factors include the level of ecosystem modification, the feasibility of achieving full recovery, as well as the management goals and associated costs.

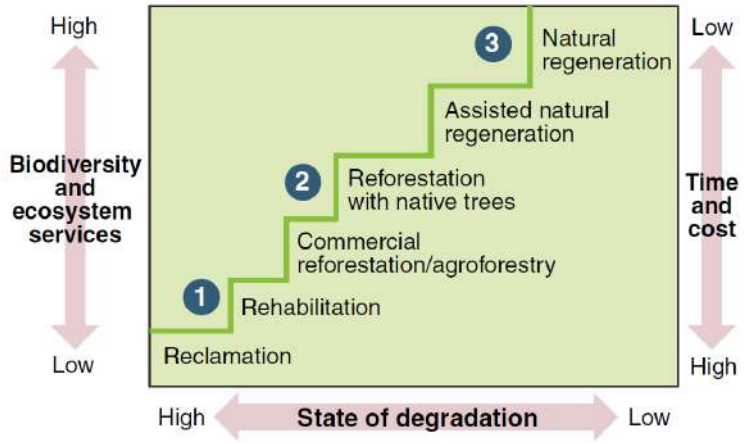

Figure 1. The Restoration Staircase.

The restoration staircase. Depending on the state of degradation of an initially forested ecosystem, a range of management approaches can at least partially restore levels of biodiversity and ecosystem services given adequate time (years) and financial investment (capital, infrastructure, and labour). Outcomes of restoration approaches are (1) restoration of soil fertility for agricultural or forestry use; (2) production of timber and nontimber forest products; or (3) recovery of biodiversity and ecosystem services. Source: (Chazdon, 2008)

In areas of severe degradation, where native ecosystems have lost their ability to withstand and recover from disturbances (i.e., their resilience), rehabilitation actions aimed at restoring specific components of the ecosystem (e.g., soil fertility, plant cover) instead of aiming at the entire ecosystem may be better suited (Hobbs & Harris, 2001). This targeted restoration can prioritize essential ecosystem services and enhance the potential for continued restoration and existing biodiversity (Suding et al., 2015). The objective here is not to fully restore the intervened ecosystem to its native state, but to improve enhance its capacity to provide selected and priority ecosystem services while sustaining biodiversity. Importantly, rehabilitation

actions may be necessary to improve conditions for achieving a higher level of ecosystem recovery towards its native condition in the long term.

On the other hand, if the level of degradation is moderate or low, actions involving assisted regeneration (such as shrub control to prevent encroachment or reintroduction of key species) represent the best options for restoring biodiversity and ecosystem services. The same case is if the ecosystem inherently possesses resilience (e.g., a forest with species capable of resprouting after a fire or employing other fire-related strategies), which could bring the ecosystem closer to its native condition with natural regeneration (with minimal intervention).

Promoting natural regeneration offers the advantage of being governed by natural ecological processes, making it potentially more effective in recovering ecosystem functions and services (Chazdon, 2008; Chazdon and Guariguata, 2016). However, there may be less control over the composition of the restored communities, as it is influenced by the existing species pool, including invasive species.

In addition to the state of the forest after disturbance, the selection of restoration actions should also consider the time required to achieve the desired restoration goals and the associated costs. In brief, the level of intervention chosen level of intervention directly impacts the costs involved (Chazdon, 2008). For example, natural regeneration comes with virtually no costs, but it is only a viable option when the level of modification is low and/or the ecosystem demonstrates good resilience capacity.

The time required for recovery will depend on the level of degradation and the ecosystem's resilience, as well as the urgency of fully or partially restoring the ecosystem, its biodiversity, and ecosystem services. Even if an ecosystem has the potential to reach a native condition through natural regeneration, the process may take an extended period (e.g., decades), which might not be socially acceptable, particularly if there is a need to recover critical ecosystem services promptly.

Furthermore, it's important to consider that the ecosystem may only be partially recovered in terms of its structure, composition, and functions (Suding, 2011). In such cases, the choice of restoration actions, including rehabilitation measures, should establish realistic goals for the area that align with stakeholder needs.

Overall, when intervening in a degraded forest ecosystem, it is crucial to focus on ecological resilience. This involves either restoring the ecosystem to a state equivalent to its native condition or transforming it into a new state (e.g., incorporating plant species better adapted to the level of degradation or anticipated climate changes) that aligns with the management goals for the area and ensures the ecosystem's ability to withstand disturbances.

2.1 Forest Rehabilitation and Restoration

Forest rehabilitation, as defined by (Chokkalingam et al., 2005) is "a coordination of efforts supported by policy agents to bring back tree cover on formerly forested grasslands, brushlands, scrublands or barren areas through planting, seeding and assisted natural regeneration for the purposes of producing industrial timber, sustaining livelihoods or restoring forest environmental functions."

Forest restoration is a deliberate human endeavour focused on undoing the effects of forest loss and degradation. Restoration projects aim to reclaim ecosystems that have been devastated or harmed, typically due to human activities. These activities often include deforestation, illegal fires, poorly managed practices lacking proper environmental oversight, and instances of abandonment. As a result, restoration efforts are primarily targeted at areas facing critical conditions caused by human actions (Redda+, 2022).

Forest ecosystem restoration encompasses more than just reducing hazardous fuels. It plays a vital role in reinstating the overall structure and functionality of forests and ensuring the protection and recovery of

essential habitat, riparian areas, watersheds, and various other characteristics. According to the Society for Ecological Restoration, ecological restoration is the process of aiding the recovery of ecosystems that have experienced degradation, damage, or destruction (SER, 2004).

The restoration techniques and treatments applied to a burned region can be categorized as either active or indirect (Vallejo et al., 2012). Active restoration program involves techniques like plantations and direct seeding, which can be expensive due to various requirements such as site preparation, labor, seedlings from nurseries, fertilizers, and tree shelters (Moreira & Vallejo, 2009). The survival of planted seedlings can be variable, particularly for broadleaved trees, and direct seeding often has a low success rate with only a small proportion of seeds able to germinate and thrive (Pausas et al., 2004). Indirect restoration involves natural regeneration, either passive or assisted. Passive restoration protects the area and allows ecological succession to occur (Lamb & Gilmour, 2003). In burned areas, regeneration may happen from seeds (e.g., Pausas et al., 2004), resprouting of burned trees and stumps (mostly basal resprouting) (e.g., Espelta et al., 2003), or resprouting of burned shrubs or herbs. Tree resprouts offer significant advantages over seedlings or planted trees, having an established root system, increasing their survival and growth probabilities (e.g., Moreira & Vallejo, 2009).

Assisted restoration includes activities like thinning, selecting shoots, controlling unwanted vegetation, or protecting from grazing animals (Lamb & Gilmour, 2003; Moreira & Vallejo, 2009). Despite its benefits, indirect restoration is often overlooked, with some governments subsidizing active restoration even in areas with natural regeneration (e.g., burned areas) (Pausas et al., 2004).

2.2 Forest Resilience

Resilience, as defined by (Holling, 1973) refers to an ecosystem's ability to bounce back and restore itself to its original condition after being disturbed. This includes the maintenance of its essential characteristics, such as taxonomic composition, structures, ecosystem functions, and process rates. In the context of forests, resilience can be understood as the forest's capacity to withstand external pressures and absorb disturbances (Oliver et al., 2015) (**Figure 2**). Over time, a resilient forest ecosystem can recover and return to its pre-disturbance state. When observed over an appropriate time frame, a resilient forest maintains its unique "identity" in terms of taxonomic composition, structural elements, ecological functions, and rates of various processes (Thompson et al., 2009). The forest resilience has been measured in Deliverable D6.1.

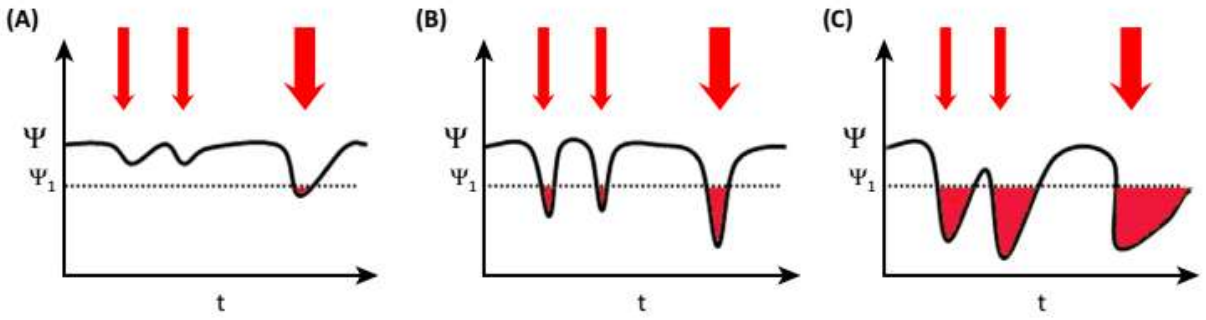

Figure 2. Schematic Showing Varying Levels of an Ecosystem Function to Environmental Pertubations/ Disturbance

Panel (A) shows a system with high resistance but slow recovery; panel (B) shows a system with low resistance but rapid recovery; panel (C) shows a system with both low resistance and slow recovery. Lack

of resilience (vulnerability) could be quantified as the length of time that ecosystem functions are provided below some minimum thresholds set by resource managers (this threshold shown with the symbol C1) or the total deficit of ecosystem function (i.e., the total shaded-red area). Note that, in the short term, mean function is similar in all systems but in the longer term mean function is lower and the extent of functional deficit is higher in the least resilient system (C) (Oliver et al., 2015).

A forest system naturally has a capacity to combat any kind of disturbance and to try to restore the natural state of pre-disaster. In this way, the forest has its resilience which maintains the stability of the forest structure, composition, and function. Tropical forests have higher levels of biodiversity than temperate and boreal forests. Various hypotheses have been proposed to explain this diversity, including the metabolic theory of ecology (J. H. Brown et al., 2004), neutral theory, (Hubbell, 2005), and landscape heterogeneity (Tuomisto et al., 2003), all of which probably contribute in some way to the overall understanding. Stand-level (alpha diversity) richness of tree species is between 100-300 in tropical forests, with regional (gamma) species richness of 4,000+ (Tuomisto et al., 2003).

A forest ecosystem can respond in different ways to disturbances and perturbations. Depending on the capacity of forests' capacity to cope with the degree of change, the characteristic taxonomic composition, vegetation structure, and rates of ecosystem processes may or may not be altered. Various drivers, both natural and anthropogenic, can influence forest resilience (Ibáñez et al., 2019) including forest quality, drivers of forest change, socioeconomic parameters, and forest policy programs is essential for promoting and enhancing forest resilience in the face of global change ((Reyer et al., 2015; Triviño et al., 2023). The overall metrics for assessing the forest resilience has been reported in Deliverable D6.1.

2.2.1 Forest Quality

Forest quality is an instrument in regional forest planning and management (Wang & Bao, 2011). Besides being necessary for forest management, forest quality is also a tool for ecological function evaluations (Zhao et al., 2019). Forest quality was first developed by WWF International and The World Conservation Union/ The International Union for Conservation of Nature (IUCN) as their lobbying and communication tool to pursue the importance of the forest (Dudley et al., 2006). The term "forest quality" highlights how well forests can accommodate humans' expanding ecological, economic, and social needs, and it is related to forest resource quality and forest ecological quality (Guo et al., 2023).

There are many forest quality definitions based on the level or scale of the forest area. So, forest quality is often assessed at the landscape and stand level (Wang & Bao, 2011). The explanation of forest quality at the landscape level is the importance and value of all forest landscape aspects, including its ecological, social, and economic components (Dudley et al., 2006). At this level, the assessment will explain the effect of a forest on both the natural environment and human society (Wang & Bao, 2011). At the stand level, forest quality refers to the forest structure and function in a small region or on a local scale (Wang & Bao, 2011). One of the forest quality assessments uses the analytic hierarchy process (AHP).

(Guo et al., 2023) have reviewed 16 papers of forest quality assessment according to many forest scales (forest stand and landscape) and have clustered them into five dimensions involved (Forest structure, Ecological function, Green Vitality, and Stability). Each of the dimensions has indicator factors that can be seen in **Table 1** below.

Table 1. Forest Ecosystem Quality Assessment Indicators

Dimensions Involved	Indicator Factors
Forest structure	Stand origin, community structure, stand age, canopy structure, stand density, tree species composition, depression
Ecological function	Water conservation, soil conservation, carbon sequestration and nutrient sequestration, forest recreation, etc.
Green Vitality	Normalized difference vegetation index (NDVI), stand volume. Leaf area index, biomass, forest growth per unit area, litter thickness
Stability	Net primary productivity (NPP) stability, NDVI stability
Site Conditions	Elevation, slope direction, slope, slope position, soil thickness, soil fertility, soil erosion degree, etc.

Source: (Guo et al., 2023)

Guo et al., (2023) have also clustered their review of papers into four forest ecosystem quality assessment methods: comprehensive evaluation method, remote sensing assessment method, process modelling method, and machine learning method. They have made a comparison of all the methods (see **Table 2**).

Table 2. Comparison of Forest Ecosystem Quality Assessment Methods

Methods	Main Features	Input Data	Advantages	Disadvantages
Comprehensive evaluation method	Combination of qualitative and quantitative	Ground monitoring data	Simple method; intuitive evaluation results with high accuracy; high information utilization	The evaluation results may be biased by obscuring some factors that have a greater impact
Remote sensing assessment method	High assessment efficiency; suitable for large-scale forest quality assessment	Ground monitoring data; multi-source remote sensing data	Saves human and material resources; fast evaluation; high evaluation efficiency	Remote sensing images are often affected by satellite type, weather, cloudiness, etc. Remote sensing inversion of forest quality-related indicators needs to be verified by ground monitoring data
Process modeling method	Lateral reflection of forest quality	Ground monitoring data; multi-source	Expression formulas are clear, can capture the	Limitations in input data, model structure, and

Methods	Main Features	Input Data	Advantages	Disadvantages
	through assessment of forest ecological functions	remote sensing data	intrinsic linkages of ecosystem services, and are highly interpretable	model parameters make simulation results subject to large uncertainties
Machine learning method	Adept at handling high-dimensional data and non-linear ecological relationships	Ground monitoring data; model simulation data; multi-source remote sensing data	It is self-learning and self-adaptive, greatly reducing the influence of subjective weights on evaluation results; it can couple ecological big data, process models, and use artificial intelligence to invert key parameters or optimize model parameters, thus improving evaluation accuracy	Its data demand is large, over-fitting or under-fitting problems may occur, and the interpretability of simulation results needs to be improved.

Source: (Guo et al., 2023)

2.2.2 Drivers of Forest Change

Global climate change influences various aspects of human life. IPCC stated that increasing global temperature by more than 2.5 ^{o}C is predicted to impact changing temperature, precipitation, and frequency of extreme events (Linden, 2015). Those changes in climate parameters triggered an exaggerated impact on many ecosystems, including the forest ecosystem. Forest ecosystem and climate change have a mutual relationship. Forests work on climate through exchanges of energy, water, and carbon dioxide (Bonan, 2008). Climate change also affects the forest ecosystem through climate-related disasters such as drought, flood, and wildfire (Allen et al., 2010). The disturbance related to climate change influences various aspects of the forest ecosystem, such as the replacement of native species due to the changing biophysical environment (Bal-Price et al., 2010)). The replacement of native species triggers biodiversity losses in forest ecosystems (Landsberg & Waring, 1997). Temperature and precipitation are the climate change parameters that have the most influence on the forest ecosystem.

a. Temperature

Increasing temperatures due to the global warming effect raises potential evapotranspiration and vapor pressure deficits, which alter water usage by plants and worsen the drought effect (Enríquez-de-Salamanca, 2022). This temperature change has different effects on different types of forests. In tropical forests, warmer temperatures would decrease forest growth by up to 40% (Aubry-Kientz et al., 2019). Raising temperatures in the northern boreal forest seems advantageous for forest growth, especially in the wetter locations (Ruiz-Pérez & Vico, 2020).

b. Precipitation

In addition to raising temperatures, heavy precipitation is another impact of climate change that has a significant effect on forest ecosystems. Extreme precipitation events, such as heavy rainfalls, floods, and landslides, can have significant effects on forest ecosystems (Bathurst et al., 2011). These events can cause both direct and indirect impacts on forest structure, function, and biodiversity. Aboveground biomass dropped as the result of extreme precipitation (Mann et al., 2017; Padilla et al., 2019).

Climate change is intensifying the occurrence and effects of forest disturbances worldwide. Seidl et al., (2017) highlighted the significant role that disturbances, such as wildfires, insect outbreaks, pathogens, windstorms, and drought, play in shaping forest ecosystems (**Figure 3)**. The article discussed how climate change is altering the frequency, severity, and spatial extent of these disturbances, with profound implications for forest resilience and biodiversity. Insect, fire, and drought disturbances tend to occur in warmer and drier conditions, but wind and pathogen disturbances could be worsened by warmer, wetter situations.

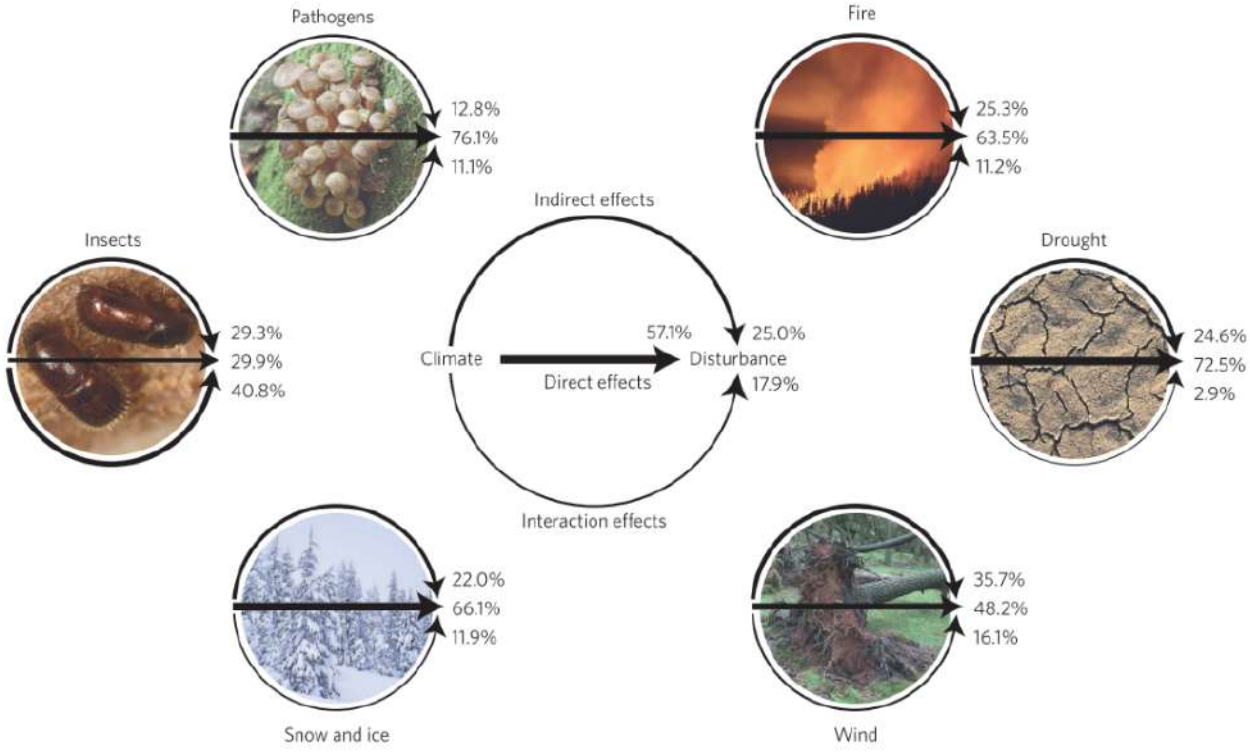

Figure 3. The direct, indirect, and interaction effects of climate change on forest disturbance agents
Source: Seidl et al., (2017)

c. Fire

As temperatures rise and precipitation patterns shift, forests become more susceptible to ignition, which can lead to devastating wildfires (Abatzoglou & Williams, 2016). In addition, climate change can also weaken forest resilience by disrupting ecological processes and altering the composition of forest ecosystems (Seidl et al., 2017). Climate change has increased the likelihood of extreme fire weather conditions, such as high temperatures, low humidity, and strong winds, in many parts of the world (Jolly et al., 2015). Forest fires could be more likely to occur due to those conditions.

d. Drought

Drought conditions, intensified by climate change, reduce tree vitality, and increase susceptibility to other disturbances. One of the primary effects of drought on forest ecosystems is water stress (Cook et al., 2014)

As water availability decreases during a drought, trees face challenges in maintaining their water balance. Drought-induced water stress leads to reduced leaf water potential, stomatal closure, and decreased photosynthesis (Allen et al., 2010). Prolonged and severe droughts resulted in tree mortality, particularly for species that are less tolerant of water scarcity.

e. Windstorm

Changing wind patterns and more frequent extreme weather events due to climate change contribute to increased wind damage in forests. Strong winds during windstorms can uproot or break trees, leading to tree damage and mortality (Romagnoli et al., 2023). Windstorms also influence forest dynamics by affecting tree growth and regeneration. Trees that survive wind events may experience physical damage to their stems, branches, or root systems, which can impact their growth and overall health (Seidl et al., 2017).

f. Insect outbreak

Warmer temperatures and altered phenological patterns are disrupting the natural checks and balances that regulate insect populations. This leads to outbreaks that can result in extensive tree mortality, impacting forest composition and ecosystem dynamics.

g. Pathogens

Climate change disrupts the balance between hosts and pathogens by influencing host physiology and immune defences (Coakley et al., 1999). Higher temperatures and increased humidity enhanced pathogen growth and reproduction, making hosts more susceptible to infection. Additionally, changes in plant phenology and distribution due to climate change created new opportunities for pathogen establishment and expansion.

The impacts of climate change on forest resilience are also becoming increasingly apparent. Climate change can disrupt ecological processes, alter species composition, and increase the risk of disturbances such as forest fires, which can reduce forest resilience (Thompson et al., 2009). The resilience of tropical, dry, and temperate forests is significantly decreasing, most likely because of water scarcity and climate variability (Forzieri et al., 2022). But boreal forests show different patterns, with an increasing trend in resilience because of warming temperatures and CO_2 fertilization.

2.2.3 Societal Parameters

Many factors, such as climate, fuel, physiography, and human activities, cause wildfires (Rodrigues et al., 2018). Over 95% of Europe's fires are due to human causes (San-Miguel-Ayanz et al., 2013). Human activities are mostly linked to wildfires (Martínez et al.,2009; Pozo et al., 2022), either purposefully or accidentally (Pozo et al., 2022).

Wildfire activity was also associated with socio-economic variables such as human population density, indigenous population proportion, and unemployment (Pozo et al., 2022). For any given year, population density significantly influences the burned area and the probability of fire occurrence (McWethy et al., 2018). Considering most fires are caused by people, fire occurrence should increase with population density (Pozo et al., 2022). There is a positive correlation between population density and fire occurrence (Collins et al., 2015; Miranda et al., 2011; Sjöström & Granström, 2023). Increased population increases the probability of anthropogenic fire ignition (Arora & Melton, 2018; Kloster et al., 2012).

Fire occurrences are also related to conflicts with local indigenous communities. Therefore, if there are more indigenous people, it could increase the occurrence of fire (Pozo et al., 2022). Fire occurrence could also increase with the proportion of unemployed because fire management also creates jobs in many regions. So, the social aspect must be included in the forest fire management and restoration analysis.

Socio-demographic variables influence the socio-economic contribution of plantation forestry activities to households (Kainyande et al., 2023). The socio-demographic variables are education, migration, and employment.

2.2.4 Forest Policy and Programs

According to the EU forest strategy for 2030, 43.5% of land in Europe consists of forest and wooded land, which is valuable for the community and other living things. Thus, the regulation for providing the best strategy becomes one of the main agenda topics in Europe. They are focused on forest management to be closer to nature and employ their forest strategy (Larsen et al., 2022).

The ownership of forests has an impact on their management. In several forests, the ownership could be a national or local authority, a factory, or a combination of both. That is why the policies applied to each forest are different from one another. Forest policies at the national level needed to set a certain standard for forest management, specifically on the restoration program.

The performance of policies in forest management is effectively proven. It improves the stability of the forest leadership (Schultz et al., 2016) and might affect the performance of the restoration programs. The availability of a regulation has a better impact on forest management.

3 Soil Analysis

3.1 Soil Resilience

How an ecosystem reacts to a disturbance depends on its resistance and resilience. The term resistance according to (McCann Kevin Shear, 2000), and (Diaz-Delgado et al., 2002) expresses "*the degree to which an ecosystem variable (e.g., canopy cover, vegetation composition or species richness) remains unchanged in the face of disturbance, and resilience the rate of recovery to the pre-disturbance value"*. According to (Dakos & Kéfi, 2022), (Cañizares et al., 2021) "*resilience is the ability of a system to cope with disturbances, bounce back, and maintain its state and functionality".*

One of the most important factors that can disrupt an ecosystem is forest fires. The fire can lead to the vegetation mortality, alteration of biodiversity, changes in the microclimate, soil erosion etc. The resistance of a forest to fire is related to the concept of stability and depends on the sensitivity of dominant trees and forest structure to fire (R. T. Brown et al., 2004); (Fernandes, 2009). Forest resilience is directly related to the characteristics of the various species in the plant community i.e., the degree to which they can recolonize the environment after fire (Pausas & Vallejo, 1999).

Significant are the effects of forest fires on the soil, which supports and affect the life of both plant and living in the soil organisms. Soil resilience "*is the ability of a soil system to regain new dynamic equilibrium after any sort of interruption or its ability to resist unfavorable alterations owing to different ecological and land-use conditions and to restore its original dynamic equilibrium after disturbance"* (Rawat et al., 2020). Soil resilience plays an important role in soil sustainability. Some of the major factors that affect soil resilience are climate, soil type, biota, land use vegetation, the disturbances that the soil undergoes during their duration etc. In recent decades, due to climate change and global population growth, the frequency and intensity of forest fires have increased, with damaging effects on the environment, the forest ecosystem and human. Some of them are destruction of forest vegetation and reduction of regeneration, biodiversity loss, degradation of soil properties, pollution, soil erosion, etc. (Rawat et al., 2020).

Forest fires cause significant changes in the physico-chemical properties of soil. The high temperatures that develop near the ground and the deposition of ash on its surface alter the soil pH, the availability of nutrients and lead to a loss of organic matter. The pH in most cases increases favoring the solubility of the various cations.

After a forest fire, the soil becomes a recipient of persistent pollutants such as heavy metals and hydrocarbons. Heavy metals are released into the soil directly and become mobile and toxic. Hydrocarbons are released into the atmosphere when forest vegetation is burned and then deposited in the soil.

The impact of forest fires on soil biodiversity is also significant. The heat released by fire can kill soil microorganisms either directly or indirectly by changing the chemical properties of the soil. Furthermore, it can lead to changes in the resilience of tolerant or resistant organisms relative to those more sensitive to pollutants. In heavy metal-contaminated soils, the ratio of resistant to sensitive bacteria increases in the contaminated soil, and metal-resistant bacteria are much less efficient at decomposing certain organic pollutants than trace-sensitive bacteria (Breure, 2004). When the stressors, such as for example a toxic chemical substance, act for a long period of time on soil then the effect on soil biota may initially not be substantial, remaining at the level of biochemical and cellular processes, but over time the DNA may be affected and have effects on the evolution of organisms (Breure, 2004).

These changes in biota, pH, disruption of the soil carbon and nutrients cycle etc. lead to a degradation of soil quality and a reduction in its resilience and strength, ultimately affecting the forest productivity (Pastor & Post, 1986). There is a direct relationship between soil quality and soil resilience. The properties of the soil that affect its quality are the ones that also control its resilience (Rawat et al., 2020).

The social impacts of soil quality degradation are also significant. Soil pollution for example has a direct impact on food production, thus endangering the health of people especially in the poorest areas. Moreover, as the loss of biodiversity intensifies, the risk of infectious epidemics is visible, with serious consequences for the health of the population and their quality of life (Adebayo, 2019).

Soil periodical physicochemical analysis after a fire event provides evidence of the status of physical soil characteristics as well as its pollution level. This information is useful a) for taking preventive actions for the protection of human and animal populations in cases where they could be affected. Such cases are the grazing of livestock in polluted areas that could end up a threat to human health through the food chain, direct health damage to the workers in the forest and in agricultural production by the respiration of polluted particles that drifted by the wind, and the pollution of freshwater reservoirs. Depending on the soil pollution degree more systematic analysis of freshwater reservoirs and air quality may be needed. b) For taking managerial measures for forest and animal recovery adapted to local environmental conditions, such measures are related to soil protection from erosion, the suspension of grazing both for facilitation of vegetation recovery and avoid risks for human health through the food chain, the adaptation of the expected time of forest recovery to the previous status of the fire.

Based on the results of soil analysis, adapted forest resilient standards related to vegetation composition, main and secondary forest uses, intensity of silvicultural treatments, and fire risk reduction through the adaptation of the forest structure (see **subchapter 4. Conceptual Model of Ecological Resilience**) could be established for the increase of future forest resilience.

3.2 Soil Analysis Methods

In this Sub Section, the effects of forest fires on hydrology, soil erosion and on the physical and chemical properties of soils are highlighted. The main factors affecting the soil are described, and several models/indices are presented for the calculation of hydrological and geomorphological characteristics of the soil as well as soil quality and pollution after the forest fire. These models will be useful for the assessment of fire effects on soil and hydrology in the Silvanus project.

3.2.1 Fire impact on hydrology

Fire occurrences, whether naturally triggered or caused by humans, are on the rise globally, hampering ecosystems' capacity to deliver vital services. While fires play a natural role in certain forest ecosystems, the escalating instances of devastating mega fires typically result in increased runoff, faster flow rates, and heightened erosion potential. Consequently, the growing prevalence of wildfires underscores the importance of comprehending the hydrological threats that follow fires, as well as the runoff, erosion, and sedimentation reactions of affected watersheds. It also emphasizes the need to implement strategies that bolster the resilience of forest ecosystems.

The degree to which fires alter soil hydrology largely hinges on the fire's intensity (meaning the speed at which energy is released) and its severity (indicating the scale of disruption in the burned environment), as highlighted by Zavala LM and others (Zavala et al., 2014).

To devise effective policies that mitigate the aftermath of fires and reduce the risk or consequences of fires, it's crucial to understand the impact of fires on the structure and function of watersheds.

Fires can change the landscape immediately, extensively and with long-term effects such as:

1. Vegetation burning combined with changes in soil physicochemical properties modify soil hydrology by increasing surface runoff, as well as rates of soil erosion and degradation.

2. Fire reduces (in case of a low-severity fire) or completely removes (for a high-severity fire) the tree canopy and ground cover of vegetation and litter. Additionally, bare soil due to vegetation burning, becomes more susceptible to raindrop impact and particle detachment. Therefore, interception and evapotranspiration are reduced, leading to more water available for runoff (Vieira, Malvar, et al., 2018); (Zituni et al., 2019).
3. The hydrological response can be indirectly affected by the disturbances of soil properties of the area. Their potential to disrupt a wide range of ecological processes and functions such as interception, infiltration, evapotranspiration, and storage can lead to higher runoff rates resulting in floods and mass movements and landslides, increased risks to human life and property.
4. The effects of fires on soil properties can be distinguished into a) direct and b) indirect.
    a. Direct impacts, related to burning duration and fire temperatures, are usually small and limited to the upper soil layer (a few centimetres from the surface).

    b. The indirect effects of fire depend on several factors, such as ash release, vegetation, morphology, as well as weather patterns and post-fire management (Pereira et al., 2018) (Pereira et al., 2018); (Keesstra et al., 2017); (Robichaud et al., 2020); (Salis et al., 2019). More specifically, ash is a key driver of the hydraulic response of burned soils (depending on its depth and type). Ash can either increase soil water retention and reduce soil water repellence, or it can seal the soil surface, reducing water infiltration and increasing surface runoff and flooding (Wittenberg et al., 2020); (Inbar et al., 2014); (Plaza-Álvarez et al., 2019). The ash impact on hydrological characteristics of burned soil depends on its colour; in more details, black ash, generated by lower fire temperatures, acts as a mulch with a wettable cover for the soil, retaining rainwater and improving infiltration, while gray to white ashes of higher severity fires, clog the soil pores and generate surface sealing, increasing overland flow, and erosion processes (Thomaz, 2018). As a result of wildfire impacts, in the burnt areas, sealing, surface crust formation, pore clogging, and bulk density increase; moreover, soil organic matter and macro-nutrients are lost, and its structure can be modified by the fire. The depletion of soil organic matter has a substantial effect on soil properties such as structure, as well as chemical and biological properties (Keesstra et al., 2017). In turn, these effects on soil physicochemical characteristics can influence the hydraulic properties, such as water repellence, water retention, hydraulic conductivity, and sorptivity. Wildfire particularly impacts the aggregate stability and water repellence of soils, and these effects on soils also depend on temperature and duration. Soil aggregate stability is not altered or slightly increases at temperatures up to 220 °C, while it is strongly reduced between 380 and 460 °C (Varela et al., 2010). Soil structure is irreversibly disrupted over 460 °C (Shakesby & Doerr, 2006), while, in contrast, clayey soils can show increased aggregate stability at high temperatures (Shakesby, 2011). Soil water repellence does not noticeably change at temperatures under 200 °C, increases between 250 and 300 °C, and completely disappears over 300–400 °C (Pereira et al., 2018); (Varela et al., 2010) (**Figure 4**).

Destruction of topsoil organic matter, leading to destabilization of soil structure and increased soil cover by ash, can exacerbate the effects of water repellence. These impacts may also lead to degradation of physical and chemical water quality, with potentially significant and long-term impacts on freshwater, such as the supply of drinking water supplies or recreational water uses. Fire also modifies the physicochemical properties of the land surface in a variety of ways that affect the hydrologic response to precipitation events based on the heat released (Certini, 2005); (Inbar et al., 2014) (**Figure 4**).

Post-fire background hydrological conditions tend to recover over periods ranging from a few months to several years, i.e., after vegetation has re-established and the extent of soil erosion has decreased (Vieira et al., 2018); (Zituni et al., 2019).

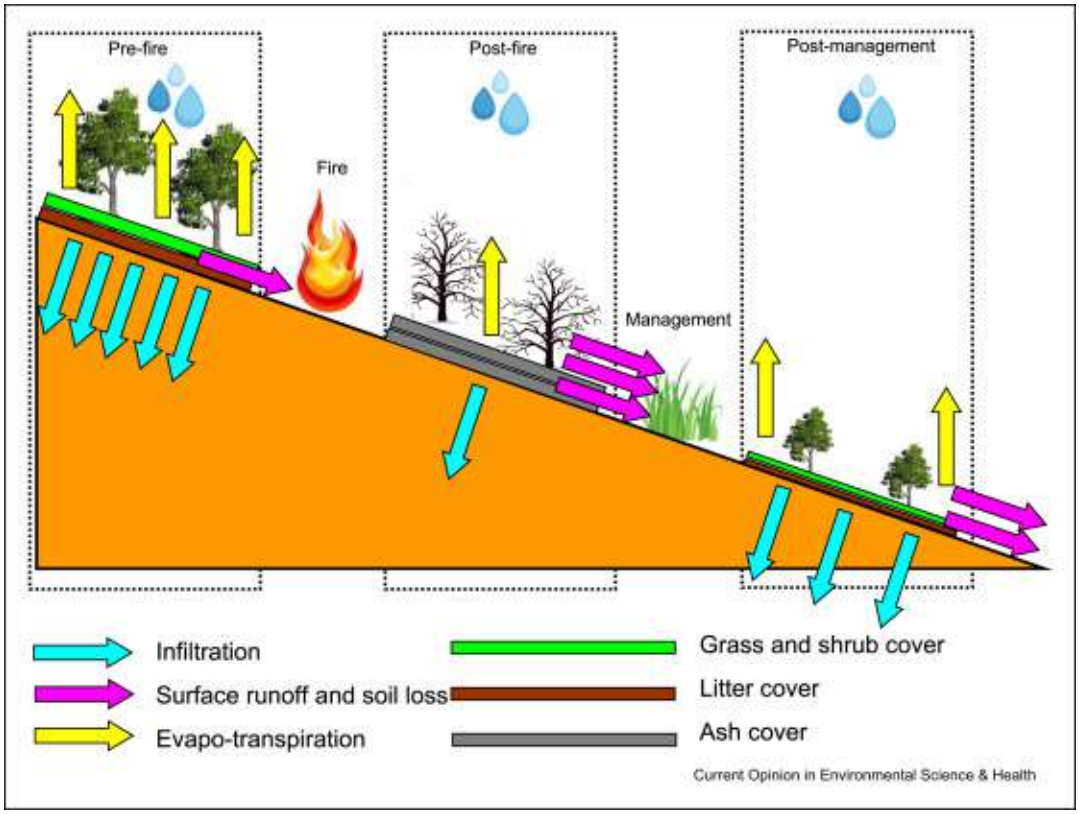

Figure 4. Scheme of the hydrological processes acting before and after wildfire with the effects of postfire management (Zema, 2021) **/adapted from Ref.** (Vieira et al., 2018**)**

3.2.1.1 Fire effect on soil erosion. Methods of soil erosion estimation

The wide recognition of wildfires as a driver for runoff and erosion in burnt forest areas has created a strong demand for model-based tools for predicting post-fire hydrological and erosion response models capable of reproducing the hydrological and erosive processes occurring in burned forest areas (**Table 3**).

In regions hit by intense fires, precise hydrological forecasts using digital models assist land custodians in choosing the best strategies for mitigating post-fire land degradation and planning restoration, as noted by Zema et al. (Zema et al., 2020).

Both straightforward empirical and semi-empirical models (like the Universal Soil Loss Equation or USLE, the Morgane et al. (Morgan et al., 1984)/MMF model, and their updated versions) and more intricate physical models (like the Water Erosion Prediction Project or WEPP and the Soil and Water Assessment Tool or SWAT) have undergone extensive testing. Generally, their outcomes have demonstrated commendable reliability, as cited by various researchers including Zema D.A. (Zema, 2021), Lucas-Borja M.E et al. (Lucas-Borja et al., 2019), and Schmeer S.R et al. (Schmeer et al., 2018). These modelling endeavours adapted pre-existing hydrological models to account for the impacts of fires.

Most models often overlook how fires influence vegetation and soil attributes. The RUSLE model seems particularly suited for assessing risk in fire-affected zones, largely due to its straightforwardness and minimal data needs. In contrast, intricate models are better suited for evaluating diverse land management

possibilities. Zema and colleagues in 2020 introduced an innovative approach to post-fire hydrology modeling, suggesting an artificial neural network prediction that yielded promising results for surface runoff and soil erosion in areas with Mediterranean climates.

The research available on post-fire hydrological modelling is not evenly spread worldwide, as pointed out by Lopes and others (Lopes et al., 2020). While the USA has advanced erosion modelling and frequently employs post-fire prediction models, other regions might have unique hydrological processes. For instance, Mediterranean burned areas possess distinct characteristics, such as shallow soils and specific hydrological patterns. In these settings, standard hydrological models, crafted for different climatic conditions, might not be as effective and could need specific adjustments, as mentioned by Vieira D.C.S. and others (Vieira, Malvar, et al., 2018; Vieira, Serpa, et al., 2018). Given the intricate nature of burned area hydrology, influenced by numerous factors, and the diverse post-fire management techniques, modelling the hydrological reactions of burned and managed soils remains a challenging task that warrants more investigation, as highlighted by Schmeer S.R. and others (Schmeer et al., 2018).

Table 3. Soil erosion- models

1. MODEL
Indices Hydraulics (sediment discharge rating curves, runoff (Q) -sediment discharge (Qs) curves)
Conceptual (Empirical)-bosed models /Revised Universal Soil Loss Equation (RUSLE)
Conceptual (Empirical)-bosed models /Modified Universal Soil Loss Equation (MUSLE)
G2 (Panagos et al., 2012)
Conceptual (Empirical)-bosed models /Universal Soil Loss Equation (USLE)
Revised Morgan-Morgan-Finney (RMMF)
Conceptual (Empirical)-bosed models /Gavrilovic (Erosion Potential Method, (EPM)
Conceptual (Empirical)-bosed models/Unit Stream Power - based Erosion Deposition (USPED)
Conceptual (Empirical)-bosed models/Water Erosion Prediction Program (WaTEM/SEDEM)
Geomorphological equation
Koutsoyiannis and Tarla
BQART model
ART model
Moulder and Syvitski
Lu et al.
Dendy and Bolton
Avendano Salas et al.
Webb and Griffiths

A. Soil Erosion Models/ indices for Soil Erosion:

a. Universal Soil Loss Equation (USLE)

The Universal Soil Loss Equation (USLE) estimates the average yearly erosion rate on a field slope, considering factors like rainfall, soil type, landscape, crops, and management methods. It specifically gauges soil loss from sheet or rill erosion on one slope, but doesn't include losses from gully, wind, or tillage erosion. While designed for certain farming and management systems, the USLE is also relevant for non-farming scenarios like construction sites. It allows for comparisons of soil loss from specific fields, crops, and management methods to acceptable erosion rates. It can also assess the effectiveness of conservation strategies in different farming setups.

To determine soil loss at a site, the USLE uses five primary factors. Each represents a specific condition impacting erosion severity. Due to fluctuating weather, the erosion figures these factors produce can differ significantly. As such, USLE values best represent long-term averages.

The principal equation for the USLE model family (Wischmeier & Smith, 1978) is below:

$$A = R \times K \times LS \times C \times P \quad [1]$$

Where:

A = long-term average annual soil loss (measured in tonnes per hectare per year) (ton x ha^{-1} x $year^{-1}$)

R = rainfall and runoff factor by geographical location (MJ * mm * ha^{-1} * $hour^{-1}$ * $year^{-1}$)

K = soil erodibility factor (ton * ha *hr* ha^{-1} * MJ^{-1} * mm–)

L = slope length factor (unitless)

S = slope steepness factor (unitless)

C = crop and management factor (unitless)

P = support practice factor (unitless)

The R and K factors of an area **cannot be altered**, but it is possible to reduce soil loss by constructing terraces, changing crops, or modifying agricultural practices.

b. Revised Universal Soil Loss Equation (RUSLE)

The Revised Universal Soil Loss Equation (RUSLE) is an enhanced version of the USLE and isn't tied to a specific land use. It's applicable to farmlands, disrupted forests, rangelands, construction areas, mined territories, restored lands, military training sites, landfills, waste disposal locations, and other areas vulnerable to soil erosion from rainfall and overland flow. Introduced by the USDA Soil and Water Conservation Service in 1993, RUSLE retains the same formula as USLE to calculate sheet and rill erosion (K. G. , Renard et al., 1994; K. G. Renard et al., 1991, 1997).

$$A=R*K*L*S*C*P \quad [2]$$

Where:

A is computed soil loss,

R is the rainfall-runoff erosivity factor,

K is a soil erodibility factor,

L is the slope length factor,

S is the slope steepness factor,

C is a cover management factor, and

P is a supporting practices factor.

Compared to USLE, RUSLE introduces significant updates. It offers improved values for erosion influenced by vegetation cover and more precise calculations for slope factors, coupled with enhanced computerization. RUSLE recognizes the erosion-reducing capabilities of surface residues and those mixed near the soil's top layer. Unlike USLE, which assumed consistent runoff across an area, RUSLE understands that some runoff forms channels, rills, and gullies. It also better identifies that prolonged rain can saturate soil, resulting in decreased absorption and increased erosive runoff. RUSLE can manage varying terrains and identify regions with sediment accumulation.

Another RUSLE update is its consideration of rock fragments in and on the soil. Surface rock fragments are treated similarly to mulch, while adjustments are made for rocks within the soil to account for their impact on water permeability and subsequent runoff.

c. Modified Universal Soil Loss Equation (MUSLE)

The MUSLE is utilized in hydrological models to gauge sediment outputs from various catchment sizes (Williams, 1975). However, the challenges of spatial scale dependency in determining MUSLE parameters haven't been sufficiently tackled. Without comprehensive data on hydrological behaviour and sediment output, certain analytical methods and theoretical examples are provided to highlight the main concerns. The findings indicate that the techniques for determining both erosivity and topographic elements are influenced by scale, especially when using a generalized or semi-distributed model. The takeaway is that if spatial-scale dependencies aren't properly grasped and addressed, they'll increase the uncertainties in MUSLE's application. A recommended method is to apply the erosivity formula to a consistent, small representative area and then expand it to the entire catchment. This method acknowledges the fluctuation of averaged parameters over diverse spatial scales.

The USLE, crafted to predict long-term yearly erosion, is typically deemed unsuitable for assessing erosion or sediment outputs from specific storm events across vast regions, as noted by Kinnell (Kinnell, 2005). This is because the USLE doesn't directly factor in runoff. Williams and Berndt (Williams & Berndt, 1977) introduced the modified USLE (MUSLE) to estimate sediment outputs from individual storms. It uses runoff attributes, instead of rainfall, to determine the erosivity factor (R). The general structure of MUSLE is:

$$Sy=R*K*LS*C*P \quad [3]$$

$$R=\alpha*(Q*qp) \quad [4]$$

Where:

Sy is the sediment yield (in t) for an individual storm for the entire catchment;

R is the erosivity index for the storm;

Q is the volume or runoff (in m^3);

qp is the peak flow rate (in $m^2\ s^{-1}$);

K, LS, C and P are the soil erodibility, topographic factor (accounting for slope length and steepness effects), crop management and soil erosion control practice factors, respectively; and a and b are location-specific coefficients. Subsequently, the MUSLE has been widely applied (Banasik & Walling, 1996); (Kinnell & Risse, 1998); (S. H. R. Sadeghi et al., 2007, 2014), and is the core sediment yield estimation method in the frequently used Soil and Water Assessment Tool (SWAT) hydrological model (Arnold et al., 1998). Many reported applications of the MUSLE have assumed fixed values for the a and b coefficients, of 11.8 and 0.56, respectively (S. H. R. Sadeghi et al., 2014), and part of the reason is that, for many practical applications at the basin scale, there will be little or no data available to calibrate the coefficients. An alternative form of Equation **[3]** estimates Sy in t ha^{-1} (Williams & Berndt, 1977)and uses values of total runoff depth (QD) in mm and peak runoff (qdp) in mm h^{-1} in Equation **[5]**. This equation can be derived by simply substituting QD·Area·10 for Q and qdp·Area·10/3600 for qp in Equation **[4]** and then dividing by Area (to obtain t ha^{-1} as the result, instead of t):

$$R=1.586\ (QD*qdp\ )0.56\ *\ (Area)0.12 \qquad [5]$$

where Area is the total catchment area (in ha).

While several studies ((Jha et al., 2004); (M. Sadeghi et al., 2013)) have discussed how to apply the MUSLE, there remains a lack of clarity about the spatial scale dependencies when using MUSLE across diverse catchment scenarios. This work evaluates these dependencies as part of a project aimed at creating a straightforward erosion and sediment transport model for South African catchments, as detailed by Bryson (Bryson, 2015). This model is intended to join a set of interconnected models that predict water amount and quality, both in natural and altered states. The water quality and sediment models, as described by Slaughter et al. (Slaughter et al., 2017), are meant to connect with existing monthly rainfall-runoff and water resource yield models through a monthly-to-daily breakdown sub-model, as noted by Hughes and Slaughter (Hughes & Slaughter, 2015).

Upon examining the initial sediment model version by Bryson (Bryson, 2015), it was clear that MUSLE outputs can greatly vary based on the spatial scale of application. The associated rainfall-runoff and water resource yield models operate on a semi-distributed spatial system, where the scale can differ significantly across applications. This variability also applies to grid-based models, where grid dimensions can change depending on the total modelled basin area. Thus, understanding MUSLE's spatial scale dependencies is crucial when using current models or developing new ones.

To pinpoint the scale-dependent aspects of MUSLE, earlier research that employed MUSLE was analysed to detect any spatial scale constraints and see how past researchers addressed scale dependency issues. This paper further delves into the potential scale effects using analytical techniques and theoretical examples.

d. G2

G2 is an empirical model for soil erosion rates at month-time intervals and has evolved with time into a quantitative tool with two distinct modules: one for soil loss and one for sediment yield (Panagos et al., 2012). The soil loss module, labeled as G2los, draws its foundational principles and many of its equations from the Universal Soil Loss Equation (USLE) by Wischmeier and Smith (Wischmeier & Smith, 1978) and its successor, the Revised-USLE (RUSLE) by Renard et al. (K. G. Renard et al., 1997). Ferro and Porto (Ferro & Porto, 2000) believe that the USLE is a sturdy empirical model that logically organizes the variables

simulating the erosion process. The data needed for G2's functions can be sourced from geodatabases that European or other global institutions provide freely and consistently.

Conversely, the sediment yield module, termed G2sed, incorporates the sediment delivery ratio (SDR) equation from the Erosion Potential Method (EPM) as cited by Gavrilovic (Gavrilovic, 1970) and da Silva et al. (Da Silva et al., 2014). Its primary data source is a detailed digital elevation model (DEM), which helps derive the necessary topographic and hydrographic attributes. The G2sed module takes the results from the G2los module and the computed EPM values to generate maps showing sediment yield, as noted by Karydas & Panagos (Karydas & Panagos, 2018).

$$E=(R/V)\times S\times(T/I) \quad [6]$$

Where:

E=Actual soil loss (t ha^{-1})

R=Rainfall-runoff erosivity factor (MJ mm ha^{-1} h^{-1} y^{-1})

V=Vegetation retention factor (dimensionless)

S=Soil erodibility factor (t ha h MJ^{-1} ha^{-1} mm^{-1}),

T=Topographic influence (dimensionless)

I=Interception of slope length (dimensionless)

e. USPED (Unit Stream Power - based Erosion Deposition)

USPED (Unit Stream Power - based Erosion Deposition) is a simple model which predicts the spatial distribution of erosion and deposition rates for a steady state overland flow with uniform rainfall excess conditions for transport capacity limited case of erosion process. The model is based on the theory originally outlined by Moore and Burch (Moore & Burch, 1986) with numerous improvements. For the transport capacity limited case, we assume that the sediment flow rate $\mathbf{q}_S(\mathbf{r})$ is at the sediment transport capacity T(**r**), **r**=(x,y) which is approximated by Julien and Simons (Julien & Simons, 1985).

$$|\mathbf{q}_S(\mathbf{r})| = T(\mathbf{r}) = K_t(\mathbf{r})\,|\mathbf{q}(\mathbf{r})|^m \sin b(\mathbf{r})^n \quad [7]$$

where b(**r**) (deg)is slope, **q**(**r**) is water flow rate, Kt(**r**) is transportability coefficient dependent on soil and cover, m, n are constants depending on the type of flow and soil properties. For overland flow the constants are usually set to m=1.6, n=1.3 (Foster et al., 1997). Steadu state water flow can be expressed as a function of upslope contributing area per unit contour width A(**r**)(m).

$$|\mathbf{q}(\mathbf{r})| = A(\mathbf{r})\, i \quad [8]$$

where i(m) is uniform rainfall intensity (note: approximation by upslope area neglects the change in flow velocity due to cover). For the uniform soil and cover properties represented by Kt=const., the net erosion/deposition rate is estimated as a divergence of the sediment flow (see Appendix in (Mitas & Mitasova, 1998)):

$$ED(\mathbf{r}) = \text{div } \mathbf{qs}(\mathbf{r}) = K_t \{ (\text{grad } h(\mathbf{r})) \cdot \mathbf{s(r)} \sin b(\mathbf{r}) - h(\mathbf{r}) (kp(\mathbf{r}) + kt(\mathbf{r})) \} \quad \textbf{[9]}$$

In the given formula, s(r) represents the unit vector pointing in the direction of the steepest slope, while h(r) (in meters) calculates the water depth based on the upslope area A(r). The terms kp(r) and kt(r) denote the profile curvature (the terrain's curvature in the steepest slope direction) and the tangential curvature (curvature tangential to a contour line projected onto a normal plane), respectively. These topographic parameters, s(r), kp(r), and kt(r), are derived from the primary and secondary derivatives of the terrain surface, as exemplified by methods like RST (Mitášová & Mitas, 1993); (Mitášová & Hofierka, 1993); (Krcho, 1992). As per the 2D framework, the spatial patterns of erosion and deposition are influenced by variations in overland flow depth (the first component) and the terrain's local geometry (the second component), which encompasses both profile and tangential curvatures. This two-variable approach highlights that local flow acceleration in both gradient and tangential directions (associated with the mentioned curvatures) are equally pivotal in determining where erosion or deposition happens. The interaction between water flow changes and the two types of terrain curvature, as presented in this bivariate approach, dictates whether erosion or deposition takes place.

For the USPED model, no experimental efforts were made to derive the necessary parameters. As a result, we resort to using parameters from USLE or RUSLE to factor in the effects of soil and cover, aiming to achieve a relative approximation of net erosion and deposition. It's assumed that sediment flow at its transport capacity can be estimated as follows:

$$T = R\ K\ C\ P\ A^m (\sin b)^n \quad \textbf{[10]}$$

where $R \sim i^m$, $KCP \sim Kt$ and $LS = A^m \sin b^n$, and m=1.6, n=1.3 for prevailing rill erosion while m=n=1 for prevailing sheet erosion. Then the net erosion/deposition is estimated as

$$ED = \text{div } (T.\ \mathbf{s}) = d(T*\cos a)/dx + d(T*\sin a)/dy \quad \textbf{[11]}$$

where the parameter a (deg) is aspect of the terrain surface. This equation is equivalent to the relationship with curvatures presented above, however the computational procedure is simpler.

Caution should be used when interpreting the results because the USLE parameters were developed for simple plane fields and detachment limited erosion therefore to obtain accurate quantitative predictions for complex terrain conditions they need to be re-calibrated.

f. WaTEM/SEDEM model

WaTEM/SEDEM was applied to simulate soil loss and deposition rates at European scale (Van Oost et al., 2000)**;** (Van Rompaey et al., 2001). The long-term annual rates of soil loss, sediment transfer and deposition were modelled with WaTEM/SEDEM. The model has been extensively employed to estimate net fluxes of sediments across landscape, catchment- and regional-scale level. To the best of our knowledge, this study represents the first application at the continental scale. WaTEM/SEDEM is a spatially explicit sediment delivery model involving two components. In the first stage, the soil loss potential is computed according to the multi-parameter scheme of the Revised Universal Soil Loss Equation (RUSLE) (Eq. **[12]**).

$$SL=R\cdot K\cdot LS_{2D}\cdot C\cdot P \quad [12]$$

where SL is the mean soil loss (Mg ha^{-1} yr^{-1}) which is the product of the rainfall intensity factor R (MJ mm ha^{-1} h^{-1} yr^{-1}), the soil erodibility factor K (Mg h MJ^{-1} mm^{-1}), the two-dimensional slope and slope-length factor LS_{2D} (Desmet & Govers, 1996), the cover-management factor C (dimensionless) and the conservation support practice factor P (dimensionless).

In the second step, the displaced soil amount (gross erosion) is routed downslope across each pixel from hillslopes to the riverine systems according to the **transport capacity** (TC in Mg yr^{-1}) (equation**[13]**) computed on the base of topography and land cover.

$$TC = k_{tc}\cdot E_{PR} = k_{tc}\cdot R\cdot K\cdot (LS_{2D}-4.1\cdot S_{IR}) \quad [13]$$

where TC is the transport capacity (Mg ha^{-1} yr^{-1}), k_{tc} (m) is the transport capacity coefficient, R, K, LS_{2D} are the aforementioned RUSLE input factors and S_{IR} (m m^{-1}) **(Equation [14])** is the inter-rill slope gradient computed based on Govers and Poesen (1988) **(Equation [13]):**

$$S_{IR} = 6.8\cdot S_g^{0.8} \quad [14]$$

where S_g represent the slope gradient (m m^{-1})

g. Gavrilovic (Erosion Potential Method, (EPM))

The Gavrilović method, also known as the Erosion Potential Method (EPM), is a semi-quantitative empirical model introduced by Gavrilović (Gavrilovic, 1970). It was developed based on erosion studies in the Morava River basin in Serbia and includes tasks like erosion mapping, sediment quantity prediction, and torrent categorization. Since its inception in 1968, this method has been widely used for addressing erosion and torrent issues in the Balkans. Nowadays, its application spans globally, from European countries like Switzerland, Croatia, Serbia, and Italy to nations like Iran and Chile, as cited by Bemporad et al. (Bemporad et al., 1997).

One of the strengths of the Gavrilović method is that it doesn't delve into the intricate physics of erosion processes. This makes it particularly useful in regions with limited data or where prior erosion studies are scarce.

The method not only offers predictions about sediment production and transport but also gauges the intensity of erosion and pinpoints areas at risk of erosion. In a study of the Dubračina basin in Croatia, the method's uncertainties in predicting annual sediment production were examined, especially when using varied land cover/use inputs. Three distinct land cover/use datasets were employed: a CORINE land cover map, a Spatial Plan, and a Landsat 8 image. This study showcased how different land cover/use data can influence the results produced by the Gavrilović method.

For a detailed breakdown of the Gavrilović method, including its equations and parameter descriptions, refer to De Vente & Poesen (de Vente & Poesen, 2005):

$$W_a = T \times P_a \times \pi \times \sqrt{Z^3} \times F \quad [15]$$

$$T=\sqrt{\frac{T0}{10}+0.1} \quad [16]$$

$$Z=Y\times X_a\times(\phi+\sqrt{J_a}) \quad [17]$$

$$\xi=\sqrt{\frac{O\ X\ Z}{lp+10}}\times D_d \quad [18]$$

$$D_d=\frac{lp+l\alpha}{F}=\frac{L}{F} \quad [19]$$

$$Gy=\xi\times Wa \quad [20]$$

Wa – total annual volume of detached soil (m^3/year)
T – temperature coefficient (–)
Pa – average annual precipitation (mm)
Z – erosion coefficient (–)
F – study area (km^2)
T0 – average annual temperature (°C)
Y – soil erodibility coefficient (–)
Xa – soil protection coefficient (–)
ϕ – coefficient of type and extent of erosion (–)
Ja – average slope of the study area (%)
ξ – sediment delivery ratio (–)
O – perimeter of the study area (km)
z – mean difference in elevation of the study area (km)
Dd – drainage density (km/km^2)
lp – length of the principal waterway (km)
la – cumulated length of the secondary waterways (km)
L – cumulated length of the principal and the secondary waterways (km)
Gy – actual sediment yield (m^3/year)

h. Koutsoyiannis and Tarla 1987

This study is an attempt to draw conclusions from the available sediment measurement data in Greece. It includes: (a) a brief report on the regime of sediment measurements in Greece, as well as their processing and utilization; (b) investigation of the effects of hydrological, climatic, topographical and geological factors on the sediment yield, based on the gauged data of Northwestern Greece with an attempt to interpret the effect of these factors; (c) derivation by statistical methods of an empirical formula for the sediment yield estimation from hydrological and geological data of the watershed (Koutsoyiannis & Tarla, 1987).

$$G=15\gamma e^{3P} \quad [21]$$

G =Mean annual suspended sediment discharge (t km^{-2})
P =mean annual precipitation depth (mm)
γ=geological coefficient

i. ART model

Syvitski and Morehead (J. P. Syvitski & Morehead, 1999) applied dimensional analysis to predict a river basin long-term sediment load, emphasizing the parameters Qs [M/T], A [L2], R [L], fluid density ρ [M/L3], and gravity g [L/T2]. Their analysis recovered two dimensionless supervariables designed to reflect (1) agravity-driven sediment yield (left side of eq. [23]) and (2) a potential-energy term (right side of equation **[23]**), such that

$$Q_s = \alpha A^{0.41} R^{1.3} \quad \textbf{[22]}$$

$$Q_s / \rho g^{1/2} A^{5/4} = \alpha (R/A^{1/2})^n \quad \textbf{[23]}$$

They assumed, n=1.5, based on equation **[22]**, and thus

$$Q_s = arg^{1/2} A^{1/2} R^{3/2} \quad \textbf{[24]}$$

where *α* is a constant of proportionality and Syvitski and Morehead (J. P. M. Syvitski et al., 2003; J. P. Syvitski & Morehead, 1999) suggested that a varies according to the temperature of the basin. Syvitski et al. (J. P. M. Syvitski et al., 2003), in an experiment to test equation **[24]** for regionality in temperature, divided the river basins by climate: polar, cold temperate, warm temperate, and tropical regions, both north and south of the equator.
They realized the role that average basin temperature played and officially rewrote the equation **[25]** as

$$Q_s = \alpha_3 A^{\alpha 4} R^{\alpha 5} e^{KT} \quad \textbf{[25]}$$

where k and the various as are empirical coefficients that define the major climate zones. Basin temperature was used here as a proxy for climate, and the global distribution of precipitation, vegetation, and weather dynamics. Syvitski et al. (J. P. M. Syvitski et al., 2003) saw that the exponent n of equation **[23]** varied according to climatic regions, from 0.4 to 1.5. Also, because the k factor varies between climate zones it was considered indicative of the changing effect of weathering (physical to chemical), depending on geographic location. Bias in the ART model predictions suggested that other parameters, not included in the model, must affect a river's sediment flux. When the discontinuities between the regions were removed using a globally averaged value of n=1 (equation **[23]** and *k*=0.13 [equation **[25]**) and applied to global observations on 488 rivers, the climate zone–free ART model accounted for just 57% of the global variance.

j. BQART model SUMMARY

Syvitski and Morehead (J. P. Syvitski & Morehead, 1999) employed dimensional analysis to the problem of predicting a river basins long-term sediment load, concentrating on the parameters Qs (M/T), A (L2), R (L), fluid density ρ (M/L3), and gravity g (L/T2). Two dimensionless variables were shown to reflect gravity-driven sediment yield (left side of Equation **[26]**), and a basins' potential energy (right side of Equation **[26]**):

$$Q_s / \rho g^{1/2} * A^{5/4} = \alpha (R/A^{½})^n \quad \textbf{[26]}$$

Using the globally-averaged value of n=1 (see Syvitski et al., 2003), and the global

relationship between discharge, Q, in m^3/s, and drainage area, A, in km^2 ($Q = 0.075\ A^{0.8}$), then Syvitski and Milliman showed that:

$$Q_s = w\ B.Q^{0.31}\ A^{0.5}\ R * T \qquad \text{for } T \geq 2°C \qquad \textbf{[27]}$$

$$Q_s = 2\ w\ B.Q^{0.31}\ A^{0.5}\ R \qquad \text{for } T < 2°C \qquad \textbf{[28]}$$

Where w =0.02 for units of kg/s, or w =0.0006 for units of MT/y, Q is in km^3/y, A is in km^2, R is in km, and T is in °C. The B term expands as:

$$B = I.L.(1-T_E)\ .E_h \qquad \textbf{[29]}$$

I is the glacier erosion factor defined as $I=(1+0.09A_g)$, where Ag is the area of the drainage basin as a percent of the total drainage area. TE is the trapping efficiency of lakes and man-made reservoirs, such that $(1-T_E) \leq 1$.

The basin-averaged lithology factor (L) is defined as: L= 0.5 for basins comprised principally of hard, acid plutonic and/or high-grade metamorphic rocks, L=0.75 for basins of mixed, mostly hard lithology, sometimes including shield material, L=1.0 for basins of volcanic, mostly basaltic rocks, or carbonate outcrops, or mixture of hard and soft lithology, L=1.5 for basins with a predominance of softer lithologies, but a significant area of harder lithologies. L=2.0 for fluvial systems draining a significant proportion of sedimentary rocks, unconsolidated sedimentary cover, or alluvial deposits, and L=3 for basins with an abundance of exceptionally weak material (crushed rock, loess deposits).

E_h is the human-influenced soil erosion factor, which may provide either a positive or negative influence on a river's sediment flux, and is based on population density and GNP per capita:

E_h=0.3 for basins with a high-density population PD >200 km^2, and a GNP/capita >$15K/y. E_h =1 for basins with a low human footprint (PD < 50 km^2) or those containing a mixture of the competing influences of soil erosion and conservation. E_h=2.0 for basins where the population is high (PD > 200 km^2), but GNP/capita is low (≤$2.5K/y), and where basins have not received the resources to engineer solutions to problems of soil erosion.

Finally, BQART may be rewritten in terms of catchment yield Y_s for suspended load:

$$Y_s = w\ B.Q^{0.31}\ A^{-0.5}\ R\ .T \qquad \textbf{[30]}$$

B. <u>Erosion models /indices Geomorphological - Topographic</u>

a. Dendy and Bolton

Dendy & Bolton formula (Dendy & Bolton, 1976) is used to determine sediment yield of all types of erosion such as sheet and rill Erosion, gully Erosion, channel Bed and bank erosion and mass movement. Area of watershed by Arc GIS and Runoff of the basin is used to determine sediment yield in the Dendy Bolton method.

The Dendy and Bolton (Dendy & Bolton, 1976) **[31]**) was developed based on sediment yield values, estimated for the antecedent catchments of 800 reservoirs throughout the USA, taking into consideration their sedimentation rate.

$$S_y=674A^{-0,16} \quad \textbf{[31]}$$

where
Sy=mean annual sediment yield (t km^{-2} y^{-1})
A=the catchment area (km^2)

Their individual factors do not display annual variation. Additionally, they oversimplify the complex erosion processes correlate sediment yield or discharge only with the basin area.

b. Avendano Salas et al.

Avendaño Salas et al. (Avendaño Salas et al., 1997) published a database with mean annual sedimentation rates for the 60 Spanish reservoirs. The reservoirs are distributed all over Spain, in various climatic, geologic and geomorphologic regions of the country, with a concentration along the relatively dry Mediterranean coast but without representation of the relative humid North western area. The age of the reservoirs varies between ca. twenty and just over hundred years and the measured mean area-specific. As a result of these and other findings, the original plan was extended to include studies of reservoirs that were suggested by the different River Authorities, given that these bodies are in the best position to understand the problems of their own basins.

$$SY=4139A^{(-0.43)} \quad \textbf{[32]}$$

where
Sy mean annual sediment yield (t km^{-2} y^{-1})
A the catchment area (km^2)

c. Lu et al.

The Lu et al. (2003) equation (**[33]**) was developed based on sediment discharge data from 248 gauging sites in the Upper Yangtze basin in China.

$$SY=849.15A^{(-0.0785)} \quad \textbf{[33]}$$

where
Sy mean annual sediment yield (t km^{-2} y^{-1})
A the catchment area (km^2)

d. Webb and Griffiths (Webb & Griffiths, 2001)

Webb and Griffiths (Webb & Griffiths, 2001) developed an equation (Equation **[34]**) for the estimation of mean annual sediment discharge based on data from 37 catchments in northern Arizona

$$Qs=193A^{1.04} \quad \textbf{[34]}$$

where
Q_s is the long-term sediment load (kg s^{-1}),
A the catchment area (km^2),

e. Mulder and Syvitski

A marine hyperpycnal plume is a particular kind of turbidity current occurring at a river mouth when the concentration of suspended sediment is so large that the density of river water is greater than the density of sea water. The plume can then plunge and possibly erode the seafloor to become self-maintained for a particular period (hours to weeks). The frequency of hyperpycnal plumes emanating from river discharge can be predicted with knowledge of rating curve characteristics, particularly during flood conditions. Examples of these curves are shown for middle-sized North American rivers. Semi-empirical relationships among average discharge, average sediment concentration, and the discharge during a flood are proposed and applied to 150 world rivers. Results show the importance of small and medium sized rivers in their ability to trigger underflow at their mouths. There are at least nine ''dirty'' rivers that may trigger underflows during one or more periods of the year. Most other rivers are cleaner and have hyperpycnal plumes only during floods. Large rivers do not generate underflows at their mouths because sediment retention within their expansive coastal flood plains effectively reduces the upper limit of the suspended concentration. Underflow transport may be an important process in marine-delta construction and should be considered in sedimentary basin-fill modelling. Proposed equations and nomograms may assist engineers in infrastructure design seaward of a river mouth (Mulder & Syvitski, 1996).

$$\log(Q_s)=0.406_{\log}(A)+1.279\log(H_{max})-3.679 \quad \textbf{[35]}$$

where
Qs is the mean annual sediment discharge (t y^{-1})
A is the catchment area (km^2)
H_{max} is the maximum catchment elevation (m)

f. Geomorphological - Topographic models

Correlation of mean annual sediment yield with the Hypsometric Integral (HI), Bifurcation Ratio (R_B) and USLE Soil Erodibility Factor (K) (Lykoudi & Zarris, 2004; Zarris et al., 2007)

$$S_y = 40.23 * HI^{1.06} * {R_B}^{1.40} * K^{0.59}, \qquad R^2 = 0.74 \quad \textbf{[36]}$$

Hypsometric Integral (HI): Distribution of elevation with catchment

Bifurcation Ratio (RB): Internal processes index, branches development grade, stream network dynamic equilibrium

USLE Soil Erodibility Factor (K): Main source of erosion processes

g. Revised Morgan – Morgan – Finney (RMMF)

The RMMF model separates the soil erosion process into two phases: the water phase and the sediment phase. The water phase determines the energy of the rainfall available to detach soil particles from the soil mass and the volume of runoff. In the erosion phase, rates of soil particle detachment by rainfall and runoff

are determined along with the transport capacity of runoff (Morgan, 2001). The difference from the MMF model is the stimulation of soil particle detachment by raindrop that takes account of plant canopy height and leaf drainage, and a component has been added for soil particle detachment by flow (Morgan, 2001). The details of the RMMF model can be described as follows (Morgan, 1995):

1) Rainfall energy

The procedure followed for the rainfall energy calculation considers the way precipitation is partitioned when it reaches the vegetation canopy. The canopy acts as a protective layer, since the interception of rainfall mitigates its kinetic energy (leaf drainage/stem flow) and additionally abates its volume reaching the soil surface unhindered (direct throughfall). The effectiveness of the canopy depends on the plant height, cover, and ground cover density.

Initially, the effective rainfall (ER, mm) – defined as the amount of precipitation that is added and stored in the soil before becoming available to the plant – is estimated.

$$ER=R\times A \quad \textbf{[37]}$$

where R (mm) is the mean annual precipitation and A (%) the rainfall interception coefficient (describes the precipitation amount retained from vegetation or crop cover, taking values between 0 and 1).

The ER is partitioned into two portions – one that reaches the soil surface unhindered as direct throughfall (DT) and one that is intercepted by the plant canopy, reaching the surface as leaf drainage (LD). The partition is determined by the percentage canopy cover (CC), expressed as a proportion between 0 and 1.

$$LD=ER\times CC \quad \textbf{[38]}$$

$$DT=ER-LD \quad \textbf{[39]}$$

The kinetic energy (KE(DT), J m^{-2}) of direct throughfall is calculated as a function of rainfall intensity (I, mm h^{-1}). Regarding the relationship between the kinetic energy of precipitation (KE, J m^{-2} mm^{-1}) and its intensity, different empirical equations have been developed for various climatic conditions worldwide (Zanchi & Torri, 1980) etc.). The equation developed by (Zanchi & Torri, 1980) for Central Italy is considered more suitable for Mediterranean-type climates (Morgan, 2001). In the absence of field measurements, a typical value of I per climatic region is used (10 for temperate climates, 25 for tropical climates, 30 for climates with intense seasonal variations like Mediterranean type/monsoon).

$$KE=9.81+11.25\log_{10}I \quad \textbf{[40]}$$

$$KE(DT)=DT(9.81+11.25\log_{10}I) \quad \textbf{[41]}$$

The kinetic energy of leaf drainage (KE(LD), J m^{-2}) is calculated as a function of the plant canopy height (PH) using the Brandt (1990) formula.

$$KE(LD)=15.8\times PH0.5-5.87 \quad \textbf{[42]}$$

where PH (m) is the height from which raindrops fall from the crop/vegetation cover to the ground surface. When Equation **[42]** yields a negative value, the KE(LD) parameter is set equal to zero.

Overall, the total energy of the ER (KE, J m^{-2}) is calculated by:

$$KE=KE(DT)+KE(LD) \quad \textbf{[43]}$$

2) Runoff

Runoff is estimated based on the methodology introduced by Kirkby (Kirkby, 1976), if runoff occurs when daily precipitation exceeds the moisture storage capacity of the soil and that daily precipitation can be described by an exponential frequency distribution (Morgan, 2001).

$$Q=R\times\exp(-Rc/Ro) \quad \textbf{[44]}$$

$$Ro=R/Rn \quad \textbf{[45]}$$

$$Rc=1000\times MS\times BD\times EHD\times Et/Eo \quad \textbf{[46]}$$

where,

Q (mm) is the annual runoff

R (mm) the mean annual rainfall

R_c (mm) the moisture storage capacity of the soil, R_o (mm) the mean rain per erosive rain day

R_n (rain days) the number of rain days per year

MS (% w w^{-1}) the moisture content of the soil at field capacity or 1/3 bar tension

BD (Mg m^{-3}) the bulk density of the topsoil layer

EHD (m) the effective hydrological depth of the soil (the depth within which the moisture storage capacity controls the generation of runoff; depends on vegetation/crop cover, presence or absence of surface crust, presence of impermeable layer within 0.15 m of the surface)

E_t/E_o the actual (E_t) to potential (E_o) evapotranspiration ratio.

In general, R_c can be used as an indicator of a soil's runoff potential. The coefficient is inversely related to Q **[44]** For instance, a reduction of the EHD implies low vegetation cover; E_t/E_o values, thus high runoff generation potential and unhindered transition downstream. The latter will decrease R_c, and by extension will increase Q. Equally important is the role of precipitation, regarding its mean annual depth (R) and the mean rain per erosive rain day (R_o) coefficient. Additionally, an increase of BD can hinder the movement of air, water and nutrients within the topsoil layer (Doran, 2002), while high BD values can increase overland flow by decreasing the infiltration and water holding capacity of soil.

3) Soil particle detachment by raindrop impact

Soil particle detachment by raindrop impact (F, kg m^{-2}) is estimated by:

$$F=K\times KE\times 10-3 \quad \textbf{[47]}$$

where K(g j^{-1}) is the soil detachability index and KE is the total energy of the ER(Jm^{-2}).

The soil detachability index, denoted as K, represents the amount of soil removed from the soil mass for each unit of rainfall energy and serves as an indicator of the soil's susceptibility to erosion. As Morgan (Morgan, 2005) points out, this index fluctuates based on the soil's inherent mechanical attributes (like texture, aggregate stability, shear strength, and infiltration capacity) and chemical characteristics (such as organic matter content, pH, cation exchange capacity, and carbon to nitrogen ratio). These internal factors are influenced by external elements like rainfall, landform, geology, vegetation, and human-induced disruptions (examples being farming, deforestation, and excessive grazing). In terms of soil texture, larger, heavier particles are harder to move, whereas smaller, cohesive particles tend to be more resilient against detachment.

4) Soil particle detachment by runoff

According to Quansah (Quansah, 1982), soil particle detachment by runoff (H, kg m^{-2}) is estimated as a function of runoff (Q, mm), slope steepness (S, °), ground cover (GC, %; expressed as a proportion between 0 and 1) and the resistance of soil to erosion (Z) given its cohesion (COH, kPa; describes its shear strength, being a measure of particle detachability from raindrop impact and overland flow) (Rauws and Govers 1988). For loose, non-cohesive soils, Z is set equal to eq. **[49]** assumes that soil particle detachment by runoff occurs only where the soil is not protected by ground cover (Morgan, 2001):

$$Z=1/(0.5\times COH) \quad \textbf{[48]}$$

$$H=Z\times Q1.5\times \sin S\times (1-GC)\times 10-3 \quad \textbf{[49]}$$

The rooting system (expressed by GC) acts complementary to the canopy, enhancing soil structure and stability, additionally reducing the speed (thus energy) of overland flow by increasing its roughness. It is defined by the plant's morphology, density, and height. All in all, soil loss decreases exponentially as vegetation cover increases (Gyssels et al., 2005), with the greatest runoff reductions being observed for dense, spatially uniform vegetation covers.

5) Transport capacity of runoff

The transport capacity of runoff (TC, kg m^{-2}) is estimated:

$$TC=C\times Q2\times \sin S\times 10-3 \quad \textbf{[50]}$$

where C is the crop cover management factor which combines the C and P factors of USLE, and S (°) is the slope steepness.

According to Morgan et al. (Morgan et al., 1984), the sine of slope steepness is used (instead of the tangent) to prevent high predictions at high slope angles (at low slope angles this choice makes very little difference).

6) Erosion estimation

The total annual detachment rate of soil (D) is estimated as the sum of the soil particle detachment by raindrop impact (F) and runoff (H) components.

$$D=F+H \quad \textbf{[51]}$$

The detachment rate is compared to the annual transport capacity of runoff (TC) and the lesser of the two values is the annual erosion rate or gross erosion (GE, kg m^{-2}). GE values are transformed to be expressed in t ha^{-1} $year^{-1}$.

$$GE=\min(D\times 10, TC\times 10) \quad \textbf{[52]}$$

Fire effect on Runoff. Methods of Runoff calculation

7) SCS-CN Method to estimate Runoff

The Soil Conservation Service Curve Number (SCS-CN) method, developed by Soil Conservation Services (SCS) of USA in 1969, is a simple, predictable, and stable conceptual method for estimation of direct runoff depth based on storm rainfall depth. It relies on only one parameter, CN. The details of the method are described in this section.

The SCS-CN method is based on the water balance equation of the rainfall in a known interval of time Δt (**Figure 5**), and from the continuity principle it can be expressed as;

$$P = I\alpha + F\alpha + P\mathrm{e} \quad \textbf{[53]}$$

where,

P = total precipitation,

Iα= initial abstraction,

Fα = Cumulative infiltration excluding Ia and,

Pe = direct surface runoff (all in units of volume occurring in time Δt)

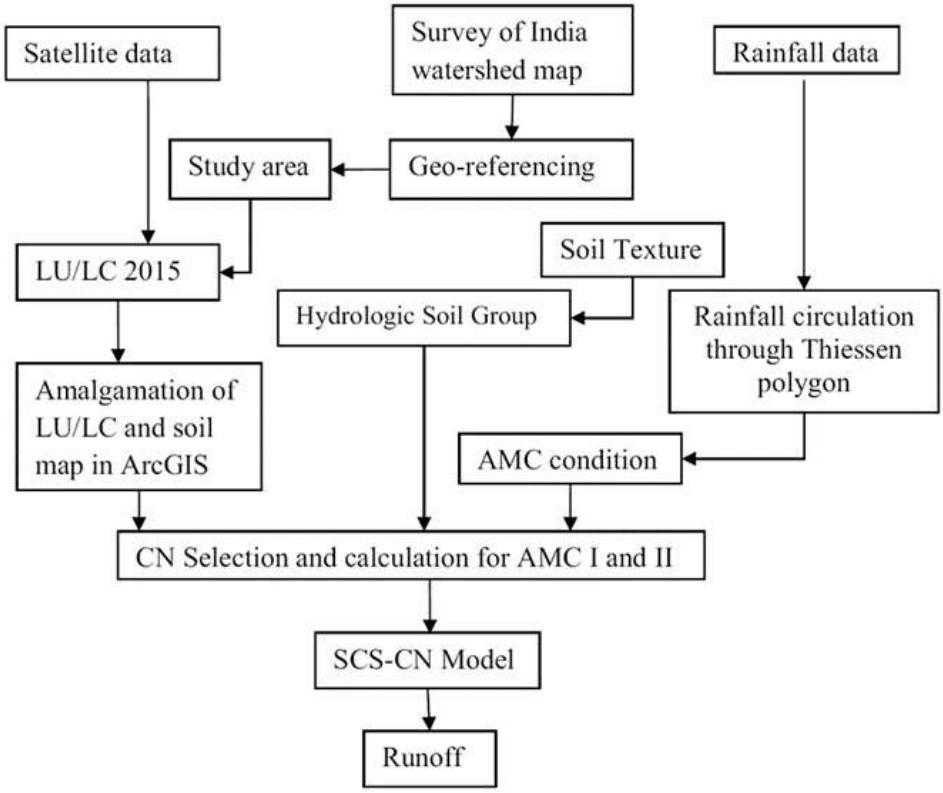

Figure 5. Flow chart of Methodology for Rainfall – Runoff (Satheeshkumar et al., 2017)

3.2.1.2 Fire effect on sediment discharge. Sediment discharge calculation methods

Physically-based models/indices Hydraulics (sediment discharge rating curves, runoff (Q) -sediment discharge (Qs) curves)

Sediment yield is the amount of sediment, adjusted for the size of the catchment area, that results from both erosion and deposition activities within a basin. Currently, predictions of sediment yield primarily rely on straightforward empirical models. These models connect the yearly sediment delivery to a river with various catchment attributes such as drainage area, landscape, climate, and vegetation features, as noted by Hosseini M, et al. (Hosseini et al., 2018) and Inbar A., et al. (Inbar et al., 2014). Out of these attributes, the catchment area stands out as the most crucial and often serves as the sole factor used in sediment yield predictions. Over recent decades, sediment discharge rating curves have become a popular tool to determine a catchment's sediment yield. This curve, which statistically relates suspended sediment discharge to stream discharge, typically follows a power-law equation:

$$Q_{is} = aQ_i b\, n_i \quad \textbf{[54]}$$

where Q_{is} is the sediment discharge (M/T, kg/s), Q is the river discharge (M^3/T, m^3/s), a and b are the sediment rating coefficient and exponent correspondingly, and η is the multiplicative error term which exhibits a lognormal distribution (Keesstra et al., 2017). Estimates of sediment yield based on rating curve calculations will in most cases involve greater error than those obtained from direct measurements, and this can be ascribed primarily to the scatter associated with the rating relationship. Several researchers

(Koutsoyiannis & Tarla, 1987) have analyzed such scatter in detail and have described controls associated with season, water temperature, hysteretic effects related to rising and falling stage of the hydrograph, exhaustion effects and varying patterns of tributary inflow. The mathematical technique which is used to construct the rating curve and the adequacy of the number of data points have also been shown to be significant controls on the accuracy of resultant calculations of sediment yield (Walling, 1983); (Keizer et al., 2018) shows that by using a single rating curve for the river Creedy in the UK may involve overestimation of the annual sediment discharge up to 60%.

Rating curves are suffering serious criticism from various researchers. For instance, Ferguson (Ferguson, 1986) and Keesstra (Keesstra et al., 2017) argues that when the rating parameters are resulted from a log-log regression between suspended sediment and river discharges, an underestimation of sediment yield is resulted. Another cause of the inaccuracies associated with the use of rating relationships is the fact that a large proportion of the total suspended sediment load is transported by a few major flood events, which represent only a very small proportion of the total time. In most cases, particularly in Mediterranean type catchments, most of the annual sediment load is transported in a few days around peak flow conditions. These observations indicate two important implications for the likely accuracy of rating curve estimates of suspended sediment load. Firstly, it means that a regular sampling programme is unlikely to provide samples representatives of those periods when the majority of the load is transported. Secondly it means that because the rating plot is fitted by least squares to the whole range of the available data, its trend maybe largely determined by the main mass of samples representative of low flows and sediment discharges and may therefore be unrepresentative of the conditions during which the majority of the load is transported.

A previously overlooked aspect in defining sediment rating curves is the identification of outliers. Contrary to stage-discharge rating curves, where hysteresis effects (identical stages at varying discharges during the hydrograph's rise or fall) don't stray much from the main curve, the suspended sediment discharge isn't as closely tied to the explanatory factor (river discharge), resulting in notable measurement variations. As a result, the suspended sediment transport rate is primarily influenced by the sediment's supply and presence within the catchment. This involves an intricate interplay between sediment creation and transportation mechanisms.

The broken line smoothing technique, proposed by Koutsoyiannis and Tarla (Koutsoyiannis & Tarla, 1987), serves as a straightforward substitute for numerical smoothing and interpolation methods. In this context, it's presented as an alternative to the standard single rating curve. This broken line consists of multiple straight-line segments. The number of these segments is determined by balancing two goals: reducing the fitting error and ensuring the line isn't too jagged. Given that the dominant river form is the gravel-bed type, a broken line with two segments is assumed. In such river forms, there's a clear-cut discharge level at which sediment begins to move. Below this level, the suspended sediment doesn't interact with the riverbed. However, once the discharge surpasses this threshold, the top layer of larger particles breaks apart, revealing a variety of smaller particles below, leading to a notable rise in the transport rate. Additionally, during high discharges, erosion of the riverbanks can increase the amount of sediment available in the riverbed.

3.2.2 Fire impact on soil

Soil is an important natural resource that is very difficult to renew. It consists of inorganic and organic components and supports plant growth and life in general. Forest vegetation acts protectively on the soil by preventing soil erosion and flooding. Some of the most important factors contributing to soil degradation in forest ecosystems are deforestation, fires, soil erosion, and pollution. Fires are considered one of the

most destructive factors in most forest ecosystems leading to soil degradation and nutrient losses through evaporation and erosion.

Fire severity is usually described in three classes: light, with surface temperatures around 250°C; moderate, with surface temperatures up to 400°C; and high, with surface temperatures more than 675°C. During forest fires, maximum ground temperatures typically range from 200 to 300 °C. In heavy fuels such as slash, where loadings can reach >400 Mg ha^{-}1, maximum soil surface temperatures typically range between 500-700 °C, but instantaneous temperatures greater than 1500 °C can be developed (Neary et al., 1999).

Forest fires cause soil changes that affect the chemical, physical, and biological characteristics of forest soils. These fires modify the physical and chemical properties of the topsoil layer by heating, combustion, and ash deposition. Intensity, duration, fuel load, soil characteristics, type and structure of vegetation, meteorological conditions, and topography play a significant role in the extent of these changes. Low-intensity fires do not cause enough soil heating to produce significant changes to soil physical properties. Low-severity fires can have beneficial effects on the soil as the temperatures reached are not high and the loss of nutrients through evaporation and smoke is reduced. However, high-severity fires combust a large amount of fuel and have extremely negative impacts on soil. The effects of these factors on the soil properties are complex. Soils are poor conductors of energy, so the heating caused by a forest fire is limited to the first few centimetres of soil.

Fire releases pollutants and suspends particles in the atmosphere. Hydrocarbons and high ash loads containing heavy metals are eventually deposited in soil, sediments, and water, resulting in their degradation. To be accurate, the assessment of the condition of the soil must be made comparatively before and after the fire. This is carried out:

- with physico-chemical soil analyses
- using soil quality indicators
- with the use of models.

Information on the changes to soil properties following fire helps to find sustainable and adaptable management practices of soils and forests.

3.2.2.1 Fire effect on soil physical properties. Determination methods of soil physical properties

The main physical properties of the soil affected by forest fires are:

a. Color. Soil color depends on mineral composition, element concentration, organic matter, and moisture content. It is the most noticeable alteration in burned soil. In soils where the fire temperature is higher, reddening of the soil matrix occurs and is due to the transformation of Fe oxides and the complete removal of organic matter (Ulery & Graham, 1993); (Certini, 2005). When the fire temperature is low to moderate the soil is covered by a layer of black or gray ash (Certini, 2005). Surface patches of the reddened soil indicate the place where soil was severely burned.

b. Texture. The soil textural components (sand, silt, and clay), as they have high temperature limits, are not easily affected by fire, except at high temperatures and at the surface of the mineral soil (horizon A). The most susceptible fraction to alteration is that of clay (Verma & Jayakumar, 2012). As the temperature increases the hydration of the clay and the clay lattice structure begin to break down. At high temperatures, complete destruction of the internal clay structure can be observed (Tadesse, 2016); (Neary et al., 2005). Where fires are severe (> 400 C) soil texture may be permanently altered and clay particles may aggregate into stable sand-sized particles, so that the soil texture becomes

coarser and more erodible. The intense erosion that can occur after a fire can led to the loss of fine materials and the retention of coarser particles or aggregates in the soil. According to Mataix-Solera et al. (Mataix-Solera et al., 2011), the main factors affecting soil aggregation are clay content and type, cations, attractive and cohesive forces between aggregate components, microbial activity, Fe and Al oxides and organic matter. After fire and loss of organic matter in the case of heavy rainfall before vegetation cover is restored, crusts may form on the surface of bare soils that reduce the infiltration rate and increase the velocity of runoff resulting in nutrient loss. Overall, high-severity fires cause significant changes in soil texture, but these depend to some extent on the type of soil affected.

Determination methods

Particle size analysis is a measurement of the size distribution of individual particles in a soil sample. There are numerous techniques for measurement. Particle size analysis data can be presented and used in several ways.

1) **Hydrometer method** (Gee & Bauder, 1986).
2) **Pipet method** (Gee & Bauder, 1986).

c. Bulk density. Forest fires result in an increase in soil bulk density (Boerner et al., 2009). This increase is due to the burning of soil organic matter which leads to the destruction of the soil structure (Choromanska & DeLuca, 2002). The bulk density, which is related to the porosity, increases due to the collapse of the aggregates and the plugging of the voids by the ash and dispersed clay minerals resulting in a decrease in the porosity and permeability of the soil (Certini, 2005). The increase in sand fraction that can be caused by the high temperatures due to fire may contribute to the reduction of the soil bulk density in the burned areas.

Determination methods

1) **Core method:** A cylindrical metal sampler is pressed or driven into the soil to the desired depth, and it is carefully removed to preserve a known volume of sample as it existed in situ. The sample is dried to 105 ^{o}C and weighed (Blake & Hartge, 1986).
2) **Excavation method:** A quantity of soil is excavated, dried, weighed and determined the volume of the excavation (Blake & Hartge, 1986).

d. Water repellency. The formation of a water-repellent layer on the surface soil or a few centimetres below is another effect of wildfires on the soil. It is due to the burning of organic matter, which can release volatile hydrophobic substances, a small part of which moves down and coats the soil particles, forming a hydrophobic layer when it condenses in a cooler part of the soil profile. The hydrophobic layer impedes the movement of water through the soil layers and leads to soil erosion and nutrient loss. Soil water repellency is not affected at soil temperatures below 175 °C but increases significantly at temperatures between 175 and 270 °C. Water repellency is produced in all types of soil texture, but the sandy fraction, due to its low specific surface area, is more sensitive to water repellency (Li et al., 2021); (Verma & Jayakumar, 2012). Fire brings also significant change in deterioration of soil structure, porosity, and permeability.

Determination methods

Water drops penetration time (WDPT) test. It involves placing droplets of distilled water onto the surface of a soil sample and recording the time for their complete infiltration (Dekker & Ritsema, 1994).

e. Moisture. Measures of soil water content are needed in every type of soil study. In the field, knowledge of the water content available for plant growth is important, and in the laboratory, many physical and chemical properties of the soil necessitate knowledge of water content (Gardner, 1986).

Determination methods

Gravimetric method. This method involves weighting the wet sample, removing the water, and reweighting the sample to determine the amount of water removed (Gardner, 1986).

3.2.2.2 Fire effect on soil chemical properties. Determination methods of soil chemical properties

The changes observed after the forest fire in the soil's chemical properties are more important than the changes in its biological and physical properties. The main chemical properties of the soil that are affected by forest fires are:

a. Soil Reaction (pH). When organic matter burns, basic cations are released, resulting in an increase in soil pH (Ulery & Graham, 1993). The extent and duration of soil pH changes are controlled by factors such as fire intensity, post-fire rainfall, initial fuel loading, etc. However, a significant increase in pH is only observed at higher temperatures (450-500 ^{o}C) (Certini, 2005) and the presence of ash can lead to an increase in soil pH due to the high pH of the ash. The increase in soil pH enhances the solubility of some cations, such as calcium, magnesium, sodium, and potassium, and reduces others, such as copper and zinc. In addition, pH is one of the major underlying variables determining the floristic variation within forest communities. All these factors can have direct or indirect effects on plants by limiting their growth due to the development and function of symbiotic associations with rhizobia, mycorrhizae, actinomycetes, and other rhizobacteria that promote plant growth (Soti et al., 2020).

Determination methods

1) **Colorimetric Determinations** of pH (Thomas, 1996)).
2) **Electrometric Measurements** (Thomas, 1996).

b. Total Organic Carbon. Total carbon (C) in soils is the sum of both organic and inorganic C. Organic C is present in the soil organic matter fraction, whereas inorganic C is largely found in carbonate minerals. Total organic carbon is one of the most important components of soil, due to its ability to affect plant growth both as an energy source but also for the availability of nutrients through mineralization.

Determination methods

1) Dry combustion.

2) Wet combustion.

The CO_2 liberated from organic and inorganic C is determined through spectrophotometric, volumetric, titrimetric, gravimetric, or conductimetric techniques (Nelson & Sommers, 1996).

c. Soil Organic Matter. Soil organic matter has been defined as the organic fraction of soil, including plant, animal, and microbial residues, fresh and at all stages of decomposition, and the relatively resistant soil humus.

The effect of fire on soil organic carbon and organic matter depends mainly on fire duration, available biomass, soil moisture content, and fire type and intensity (Reyes et al., 2015). The effects of fire on

soils are highly variable and indicate that low intensity fire usually results in little change in soil carbon, but intense fire or wildfire can result in a huge loss of soil carbon (Tadesse, 2016). The major changes in soil organic matter composition are presented at temperatures between 250 and 450 °C. Nearly all organic matter is consumed in regions of the soil heated to 450 °C.

The combustion of soil organic matter also leads to the destruction of soil aggregates. The loss of organic matter is extremely negative for soil quality.

Determination methods

1) Direct estimation of organic matter by **loss-on-ignition** (LOI) (Kalra & Maynard, 1991).
2) Organic carbon by **wet digestion** (Walkley-black method) (Walkley & Black, 1934), (Nelson & Sommers, 1996).

d. Nutrient dynamics. Fire can affect soil nutrient status in two ways: directly by adding available nutrients and indirectly by altering the soil environment. Nutrients present in live and dead plant material can either be lost by evaporation during a fire or released and deposited on the soil surface in a highly soluble form. These highly soluble forms of nutrients on the soil surface can be taken up by the root systems of plants or simply lost through erosion. Fires can reduce the number of soil nutrients through losses from volatilization, smoke, ash transport, leaching, and erosion. They can also contribute to the decrease/increase in the availability of some elements. For example, some nutrients released from organic matter and microbial biomass are finally removed from the ecosystem by runoff and leaching.

A direct effect of fire is the loss of soil N. This is due to its volatilization caused by the high temperatures developed during the fire. The nitrogen that is lost is usually in the form of ammonia and other related N gases. Nitrogen that after fire is not completely volatilized, is mineralized to NH_4^+-N and can be further nitrified to NO_3^- -N under favourable conditions (Agbeshie et al., 2020).

Fire can also lead to an increase in levels of non-volatile soil nutrients such as K, P, Ca, Mg etc., and total concentrations after low-intensity fires (Verma et al., 2019). The effect of the fire on available P is the increase in soil solution concentrations and the leaching of mineral forms of P. Increasing temperature causes a decrease in exchangeable Na in soils due to the aggregation of sand particles, leading to less extractability from water.

Ashes are produced by burnt soil and vegetation and show a very heterogeneous composition. Ashes generated by forest fires contain essential plant nutrients, such as calcium (Ca), magnesium (Mg), silicon (Si) potassium (K) and phosphorous (P), and in some cases may contain significant amounts of Al, Mn, Fe and Zn (Khanna et al., 1994). Ash may also include a considerable amount of trace elements like toxic elements (arsenic, lead, cadmium) and hazardous compounds, such as polycyclic aromatic hydrocarbons (PAHs). The release of such trace elements and PAHs into the environment poses an environmental risk as the leaching of these elements affects not only the soil, but also water systems, and can even alter the normal growth of plants (Escudey et al., 2015). Forest soil represents a major long-term reservoir for persistent pollutants including heavy metals and polycyclic aromatic hydrocarbons.

After the fire event, metals become more mobile due to the increase in soil surface exposure and the mobility associated with ash dispersal. Major and trace metals include Cd, Cr, Co, Cu, Hg, Mn, Ni, Pb, Zn and As are mobilized after fire with increased concentrations in soil and water resources (Abraham & Dowling, 2017). Heavy metals pose an increased risk to the environment due to their toxicity, environmental persistence and bioaccumulation and biomagnification tendency in food chain.

Polycyclic aromatic hydrocarbons (PAHs) are a group of hydrophobic compounds that consist of at least two connected aromatic rings. They are divided into subgroups depending on the number of rings they possess. The main source of these pollutants into the environment is incomplete combustion of fuels, such as coal, and organic materials. They can also be found in the environment as a result of natural processes (e.g., forest fires or products of garbage and oil burning). PAHs are also a group of major environmental concerns. Many of them are persistent, bioaccumulate in adipose tissues and have mutagenic, teratogenic, and carcinogenic activity in living organisms. According to the United States Environmental Protection Agency 16 PAHs are listed as major pollutants: naphthalene (NAP), acenaphthylene (ACY), acenaphthene (ACE), fluorene (FLU), phenanthrene (PHE), anthracene (ANT), fluoranthene (FLT), pyrene (PYR), benzo(a)anthracene (BaA), chrysene (CHR), benzo(a)pyrene (BaP), benzo(b)), fluoranthene (BbF), benzo(k)fluoranthene (BkF), indene (1,2,3-cd)pyrene (IND), dibenzo (a,h) anthracene (DBA) and benzo (g,h,i) perylene (BghiP). The PAH concentrations and toxicity levels in soils increase significantly after fires, and then declined to the levels of unaffected areas within one-two years. Soils and sediments can serve as an indicator of the contamination levels since they tend to accumulate PAHs as a result of their lipophilic character.

PAHs produced during combustion in fires are emitted into the atmosphere and they can be redistributed between vapors and particulate phases and then transported long distances and/or deposited in the terrestrial and aquatic environment via dry or wet deposition. They can be deposited on the soil surface, directly by burning vegetation or mineralization of organic matter or indirectly through interactions of the ash with the underlying soil, and from littering. In addition, they can be washed into the soil profile or transported by overland flow, impinging on surface and ground water bodies (Campos & Abrantes, 2021).

Determination methods

The concentration of the elements in soil is determined by atomic absorption spectrophotometry and atomic emission spectroscopy techniques, inductively coupled plasma emission spectrometry, and fluorescence spectroscopy. Some of the analytical methods for total elemental analyses are usually carried out after solubilization of the sample using techniques such as: (i) acid digestion or (ii) fusing agents (Hossner, 1996).

For the extraction of aromatic polycyclic hydrocarbons in soil Ultrasonic, Soxhlet and mechanical shaker are widely used. The chromatographic are the most method that is used for detecting. High Performance Liquid Chromatography (HPLC) and Gas Chromatography (GC) are recommended by USEPA to detect the PAHs compound in water, wastewater or in sediment (Erawaty Silalahi et al., 2021).

The most common soil parameters that usually used to assess the physicochemical soil properties are given in the **Table 4**.

Table 4. Common Parameters That Affect the Physicochemical Soil Properties.

Chemical elements	Chemical parameters	Physical parameters
Al	Soil pH	Particle size analysis (soil texture)
Mn	Total organic carbon in mineral soils and organic matter	Soil moisture
Fe	Polycyclic aromatic hydrocarbons	Bulk density
Ni		

Chemical elements	Chemical parameters	Physical parameters
Zn		
Cd		
Pb		
Cu		
Cr		
K		
S		
Mg		
Ca		
Total nitrogen in mineral soils		
Exchangeable Na		
0.03 M NF4 + 0.025 M HCl (Bray 1) P (mg/kg)		
pH 8.5, 0.5 M NaHCO3 (Olsen) P (mg/kg)		
Mineralogical composition		

3.2.2.3 Soil quality and pollution assessment methods

Many calculation methods based on different algorithms exist for the evaluation of environmental quality. Some of them may be inaccurate when used to estimate soil quality, so it is very important to choose the appropriate method of assessing soil quality for decision making and selection of sustainable management practices (Qingjie et al., 2008).

Soil quality is the capacity of a soil to function, within the ecosystem and land-use boundaries, to sustain productivity, maintain environmental quality, and promote plant and animal health (Doran & Parkin, 1994). Various physical, chemical, and biological soil characteristics are used to determine soil quality, either individually or in combination. Estimation of soil quality is a complex process and difficult task because soil constitutes solid, liquid, and gaseous phases, and soils can be used for a larger variety of purposes. Parent material, climate, topography, and hydrology are factors that may influence potential values of soil properties to such a degree that it is impossible to establish universal target values. Soil quality assessment thus needs to include baseline or reference values to enable identification of management effects (Bünemann et al., 2018).

Physical and chemical attributes are the main indicators used to assess soil quality. Soil organic carbon, total N and pH, among the chemical properties, and particle size distribution, bulk density, available water, soil structure, and aggregate stability among the physical characteristics, are the most widely used parameters to assess soil quality. Recently, new studies showed that soil organisms play a central role in soil functioning, therefore, adding biological and biochemical indicators can greatly improve soil quality assessments. Several techniques are currently available to determine soil microbial characteristics such as microbial biomass and respiration (e.g., chloroform fumigation extraction, substrate induced respiration, the 1-day CO2 test) (Muñoz-Rojas, 2018).

Pollution indices provide a complex assessment of soil environment contamination due to different geochemical backgrounds (Gu et al., 2016). The indices are used also to define if accumulation of heavy metals in soils is caused by natural processes or is the result of anthropogenic activities (Caeiro et al., 2005) and generally allow to determine ecological risk and help to protect the ecosystem.

The main models and indices used to assess soil quality and pollution are presented in **Table 5** and explained below.

Table 5. Description of Models/Indices

Model Name	Model/ Indices	Mathematical expression	Variable	Description	Range	Verbal
1	Soil Quality Index (SQI) (Amacher et al., 2007)	$Total\ SQI = \sum individual\ soil\ property\ index\ values$	SQI	Soil Quality Index		Higher index scores represent better soil quality
2	Geoaccumulation Index (Igeo) (Müller, 1969)	$\mathrm{I_{geo}} = \log_2[\frac{\mathrm{C_n}}{1.5\ \mathrm{GB}}]$	$\mathrm{I_{geo}}$	Geoaccumulation Index	Igeo ≤ 0 0 ≤ Igeo < 1 1 ≤ Igeo < 2 2 ≤ Igeo < 3 3 ≤ Igeo < 4 4 ≤ Igeo < 5 Igeo > 5	unpolluted unpolluted to moderately polluted Moderately polluted Moderately to strongly polluted Strongly polluted Strongly to extremely polluted Extremely high polluted
			$\mathrm{C_n}$	Concentration of individual heavy metal	>0	
			GB	Value of geochemical background	>0	
3	Single Pollution Index (PI) (Al-Anbari et al., 2015)	$\mathrm{PI} = \frac{\mathrm{C_n}}{\mathrm{GB}}$	PI	Single Pollution Index	PI < 1 1 < PI ≤ 3 3 ≤ PI	Unpolluted, low level of pollution Moderate polluted Strong polluted
			$\mathrm{C_n}$	the content of heavy metal in soil	>0	
			GB	values of the geochemical background	>0	
			EF		EF < 2 EF = 2–5	Deficiency to minimal

Model Name	Model/ Indices	Mathematical expression	Variable	Description	Range	Verbal
4	Enrichment factor (EF) (Abrahim & Parker, 2008)	$\mathrm{EF} = \frac{\left[\frac{\mathrm{C_n}}{\mathrm{LV}}\right]\mathrm{sample}}{\left[\frac{\mathrm{GB}}{\mathrm{LV}}\right]\mathrm{background}}$		Enrichment factor	EF = 5–20 EF = 20–40 EF > 40	enrichment Moderate enrichment Significant enrichment Very high enrichment Extremely high enrichment
			$\frac{\mathrm{C_n}}{\mathrm{LV}}$ sample	content of analyzed heavy metal (Cn) and one of the following metals Fe/Al/Ca/Ti /Sc/ Mn (LV) in the sample	>0	
			$\frac{\mathrm{GB}}{\mathrm{LV}}$ background	reference content of the analyzed heavy metal (Cn) and one of the following metals Fe/Al/Ca/Ti /Sc/Mn (LV)	>0	
5	Contamination factor (C_f) (Inengite et al., 2015)	$\mathrm{C_f} = \frac{\mathrm{C_m}}{\mathrm{C_{p-i}}}$	$\mathrm{C_f}$	Contamination factor	Cf < 1 1 < Cf ≤ 3 3 ≤ Cf ≤ 6 6 ≤ Cf	Low contamination factor Moderately contaminated factor Considerably contaminated factor Very high contaminated factor
			$\mathrm{C_m}$	mean content of heavy metal from	>0	

Model Name	Model/ Indices	Mathematical expression	Variable	Description	Range	Verbal
				at least five samples of individual metals		
			C_{p-i}	preindustrial reference value for the substances	>0	
6	Biogeochemical Index (BGI) (Mazurek et al., 2017)	$BGI = \frac{C_n O}{C_n A}$	BGI	Biogeochemical Index	>1	increased ability of heavy metal sorption by the O horizons of soil.
			$C_n O$	content of a heavy metal in the O horizon	>0	
			$C_n A$	content of a heavy metal in the A horizon	>0	
7	Pollution Load Index (PLI) (Varol, 2011)	$PLI = \sqrt[n]{PI_1 \times PI_2 \times PI_3 \times \ldots . PI_n}$	PLI	Pollution Load Index	PLI > 1 PLI = 1 PLI < 1	Polluted Baseline levels of pollution Not polluted
			PI	calculated values for the Single Pollution Index	>0	
			n	the number of analyzed heavy metals	>0	
8	Multi-element contamination (MEC) (Adamu & Nganje, 2010)	$MEC = \frac{(\frac{C_1}{T_1} + \frac{C_2}{T_2} + \frac{C_3}{T_3} + \ldots \frac{C_n}{T_n})}{n}$	MEC	Multi-element contamination	MEC>1	anthropogenic impact on heavy metal concentration
			C	content of heavy metal	>0	
			T	tolerable levels given by Kloke (1979)	>0	

Model Name	Model/ Indices	Mathematical expression	Variable	Description	Range	Verbal
			n	the number of heavy metals	>0	
9	Contamination security index (CSI) (Pejman et al., 2015)	$\mathrm{CSI}=\sum_{i=1}^{n} w\left(\left(\frac{C}{ERL}\right)^{\frac{1}{2}}+\left(\frac{C}{ERM}\right)^{2}\right)$	CSI	Contamination security index	<0.5 0.5-1 1-1.5 1.5-2 2-2.5 2.5-3 3-4 4-5 >5	uncontaminated very low severity low severity low to moderate severity moderate severity moderate to high severity high severity very high severity ultra-high severity
			w	computed weight of each heavy metal (Pejman et al. 2015)	>0	
			C	concentration of heavy metal	>0	
			ERL	values given by Long et al. (1995)	>0	
			ERM	values given by Long et al. (1995)	>0	
			n	number of investigated toxic elements	>0	

1) Soil Quality Index (SQI)

SQI is estimated following the method outlined by Amacher et al., 2007 (Amacher et al., 2007) according to the following equation:

$$Total\ SQI=\sum individual\ soil\ property\ index\ values \quad \textbf{[55]}$$

The soil quality index (SQI) integrates a number of measured physical and chemical properties of forest soils into a single number that serves as the soil's "vital sign" of overall soil quality. Mineral soil property threshold levels, interpretations, and associated soil index values are listed in **Table 6** according to Amacher et al., 2007 (Amacher et al., 2007). The SQI is a tool for establishing baselines and detecting forest health trends. It may also be an indicator of the potential for soil quality to change because of the influence of environmental stressors (**Table 5**).

Table 6. Soil quality index values and associated soil property threshold values and interpretations (Amacher et al., 2007).

Parameter	Level	Interpretation	Index
Bulk density (g/cm^3)	> 1.5	Possible adverse effects	0
	≤ 1.5	Adverse effects unlikely	1
Coarse fragments (percent)	> 50	Possible adverse effects	0
	≤50	Adverse effects unlikely	1
Soil pH	< 3.0	Severely acid - almost no plants can grow in this environment	-1
	3.01 to 4.0	Strongly acid - only the most acid tolerant plants can grow in this pH range and then only if organic matter levels are high enough to mitigate high levels of extractable Al and other metals	0
	4.01 to 5.5	Moderately acid - growth of acid intolerant plants is affected depending on levels of extractable Al, Mn, and other metals	1
	5.51 to 6.8	Slightly acid - optimum for many plant species, particularly more acid tolerant species	2
	6.81 to 7.2	Near neutral - optimum for many plant species except those that prefer acid soils	2
	7.21 to 7.5	Slightly alkaline - optimum for many plant species except those that prefer acid soils, possible deficiencies of available P and some metals (for example, Zn)	1
	7.51 to 8.5	Moderately alkaline - preferred by plants adapted to this pH range. possible P and metal deficiencies	1
	> 8.5	Strongly alkaline - preferred by plants adapted to this pH range, possible B and other oxyanion toxicities	0
Total organic carbon in mineral soils (percent)	>5	High - excellent buildup of organic C with all associated benefits	2
	1 to 5	Moderate - adequate levels	1
	< 1	Low - could indicate possible toss of organic C from erosion or other processes. particularly in temperate or colder areas	0
Total nitrogen in mineral soils (percent)	>0.5	High - excellent reserve of nitrogen	2
	0.1 to 0.5	Moderate - adequate levels	1

Parameter	Level	Interpretation	Index
	< 0.1	Low - could indicate loss of organic N	0
Exchangeable Na percentage (exchangeable Na/ECEC x 100)	>15	High - sodic soil with associated problems	0
	≤15	Adverse effects unlikely	1
K (mg/kg)	> 500	High - excellent reserve	2
	100 to 500	Moderate - adequate levels for most plants	1
	<100	Low - possible deficiencies	0 -
Mg (mg/kg)	>500	High - excellent reserve	
	50 to 500	Moderate - adequate levels for most plants	1
	<50	Low - possible deficiencies	0
Ca (mg/kg)	> 1000	High - excellent reserve, probably calcareous soil	2
	101 to 1000	Moderate - adequate levels for most plants	1
	10 to 100	Low - possible deficiencies	0
	< 10	Very low - severe Ca depletion, adverse effects more likely	-1
Al (mg/kg)	> 100	High - adverse effects more likely	0
	11 to 100	Moderate - only Al sensitive plants likely to be affected	1
	1 to 10	Low - adverse effects unlikely	2
	< 1	Very low - probably an alkaline soil	2
Mn (mg/kg)	> 100	High - Possible adverse effects to Mn sensitive plants	0
	11 to 100	Moderate - adverse effects or deficiencies less likely	1
	1 to 10	Low - adverse effects unlikely, possible deficiencies	1
	< 1	Very low - deficiencies more likely	0
Fe (mg/kg)	> 10	High - effects unknown	1
	0.1 to 10	Moderate - effects unknown	1
	< 0.1	Low - possible deficiencies, possibly calcareous soil	0
Ni (mg/kg)	>5	High - possible toxicity to Ni sensitive plants, may indicate serpentine soils, mining areas, or industrial sources of Ni	0
	0.1 to 5	Moderate - effects unknown	1
	< 0.1	Low - adverse effects highly unlikely	1

Parameter	Level	Interpretation	Index
Cu (mg/kg)	> 1	High - possible toxicity to Cu sensitive plants, may indicate mining areas or industrial sources of Cu	0
	0.1 to 1	Moderate - effects unknown but adverse effects unlikely	1
	< 0.1	Low - possible deficiencies in organic, calcareous, or sandy soils	0
Zn (mg/kg)	> 10	High - possible toxicity to Zn sensitive plants, may indicate mining areas or industrial sources of Zn	0
	1 to 10	Moderate - effects unknown, but adverse effects unlikely	1
	<1	Low - possible deficiencies in calcareous or sandy soils	0
Cd (mg/kg)	> 0.5	High - possible adverse effects	0
	0.1 to 0.5	Moderate - effects unknown. but adverse effects less likely	1
	< 0.1	Low - adverse effects unlikely	1
Pb (mg/kg)	> 1	High - adverse effects more likely, may indicate mining areas or industrial sources of Pb	0
	0.1 to 1	Moderate - effects unknown, but adverse effects less likely	1
	< 0.1	Low - adverse effects unlikely	1
S (mg/kg)	> 100	High - may indicate gypsum soils, atmospheric deposition, mining areas, or industrial sources	0
	1 to 100	Moderate - adverse effects unlikely	1
	<1	Low - possible deficiencies in some soils	0
0.03 M NF_4 + 0.025 M HCl (Bray 1) P (mg/kg)	> 30	High - excellent reserve of available P for plants in acid soils, possible adverse effects to water quality from erosion of high P soils	1
	15 to 30	Moderate - adequate levels for plant growth	1
	< 15	Low - P deficiencies likely	0
pH 8.5, 0.5 M $NaHCO_3$ (Olsen) P (mg/kg)	> 30	High - excellent reserve of available P in slightly acidic to alkaline soils, possible adverse effects to water quality from erosion of high P soils	1
	10 to 30	Moderate - adequate levels for plant growth	1
	< 10	Low - P deficiencies likely	0

2) Geoaccumulation Index (Igeo)

The Igeo values enable the assessment of heavy metal soil contamination by comparing the current levels of heavy metals in the topsoil to either the levels found in the bedrock or a specific geochemical background (Müller, 1969). The Igeo values are helpful to divide soil into quality classes (**Table 5**).

3) Single Pollution Index (PI)

The Single Pollution Index (PI) is used to determine which heavy metal represents the highest threat to a soil environment. This is also necessary for the calculations of some complex indices (Kowalska et al., 2018); (Al-Anbari et al., 2015) (**Table 5**).

4) Enrichment factor (EF)

EF is used to assess the possible impact of anthropogenic activity on the concentration of heavy metals in soil. To identify the expected impact of anthropogenesis on the heavy metal concentrations in the soil, the content of heavy metals characterized by low variability of occurrence (LV) is used as a reference, both in the analyzed samples and in GB. Reference elements are usually Fe, Al, Ca, Ti, Sc or Mn (Abrahim & Parker, 2008) (**Table 5**).

5) Contamination factor (C_f)

The contamination factor (C_f) is used to evaluate heavy metal contamination. This index enables the assessment by taking into account the content of heavy metals on the surface of the soil and values of pre-industrial reference levels given by Bemporad et al. (Bemporad et al., 1997); Kowalska et al. (Kowalska et al., 2018) and Inengite et al. (Inengite et al., 2015) (**Table 5**).

6) Biogeochemical Index (BGI)

This index is used to evaluate the degree of heavy metal concentration in the O horizon of soils under forest and grassland vegetation. For the calculations, knowledge of the heavy metal content in the O horizon and the directly underlying A horizon is necessary. It can be assumed that the higher the BGI values, the greater the capability of the O horizon to sorb heavy metals and neutralize xenobiotics, as well as reduce phytotoxicity (Mazurek et al., 2017) (**Table 5**).

7) Pollution Load Index (PLI)

The pollution load index is used for the total assessment of the degree of contamination in soil and it easily demonstrates the deterioration of the soil conditions as a result of the accumulation of heavy metals (Kowalska et al., 2018); (Varol, 2011) (**Table 5**).

8) Multi-element contamination (MEC)

The MEC index provides a measurement for assessing contamination by considering the heavy metal content in surface soil horizons, taking into account the limits given by Kloke (Kloke, 1979) and Adamu and Nganje (Adamu & Nganje, 2010) (**Table 5**).

9) Contamination security index (CSI)

CSI gives information about the intensity of the concentration of heavy metals in the soil. In order to calculate the CSI, effects range low (ERL) and effects range median (ERM) values given by Long et al. (Long et al., 1995) were used. This index is also used to determine the limit of toxicity above which the adverse impact on the soil environment is observed (Pejman et al., 2015).

The effects range low (ERL) and the effects range median (ERM) values were used also to identify the ecological risk of polycyclic aromatic hydrocarbons (PAHs) in soil (Long et al., 1995) (**Table 5**).

3.2.3 Fire effect on soil minerals. Determination methods of soil minerals

As already mentioned, the effect of fire on soil properties is highly dependent on the intensity and the duration of the fire (Agbeshie et al., 2022). The high temperatures that induced by the fire, decrease in depth due to the low thermal conductivity of the soil, thus the possibility of effecting on minerals could be observed in the upper few centimetres, while samples from deeper layers may remain unchanged mineralogically. Soil surface temperatures during fire, even during an intensive one, typically range between 200 and 700 °C (Shtober-Zisu & Wittenberg, 2021). For example, during controlled burns in Ocala National Forest and Archbold Biological Station in Florida, the temperature in the surface of the soil reached approximately 600 °C, while at the 2 cm depth was less than half but with a longer duration (Carrington, 2010). Therefore, alterations of minerals in the upper layers of soil, due to the rapidly increasing temperatures, may occur. Iron oxides, like goethite, could form hematite at about 300 – 400 °C, clay minerals, like kaolin, can be decomposed at about 420 – 550 °C yielding to amorphous aluminosilica material, as well as phyllosilicates like montmorillonite which can also be thermally decomposed (Ulery et al., 2017). A decrease in clay content with the increase of temperature is reported in several studies (Parlak, 2011); (Araya et al., 2016). Moreover, the generation of thermal cracks in feldspars and other soil aggregates could accelerate weathering due to increased surface area and may result to loss of K, Ca and Mg through leaching (Arocena & Opio, 2003).

Determination methods

The mineralogical analysis of soils after the fire involves the following techniques:

Macroscopic and microscopic observation, i.e., under the stereomicroscope. Microphotographs will be acquired to support the observations. These observations provide information for the following soil properties that usually change after fire: soil structure, texture (i.e., aggregation), porosity, wetability, infiltration rates, and water holding capacity.

Mineralogical analysis with the X-ray diffraction method for identification of soil minerals and their possible transformation during fire. XRD analyses could also lead to an estimation about the developed temperature in the soil. For example, the presence of kaolinite in burnt areas suggests that the temperature should not exceed 550 °C, in which kaolinite has decomposed (Ulery et al., 1996). Moreover, temperatures exceeding 600 °C noticeably reduce gibbsite concentration and convert goethite into ultra-fine maghemite, while quartz intensity is diminished, probably due to the encapsulation of quartz particles in a glassy matrix (Ketterings et al., 2000). At a lower temperature of approximately 300 °C goethite is transformed to a disordered hematite (Nørnberg et al., 2009), (Yusiharni & Gilkes, 2012). On the other hand, carbonates resist temperatures up to 1000 °C and thus, they are not affected by fire (Certini, 2005).

Sample preparation is necessary to identify the above possible differentiations. Pulverization of dried samples with particle sizes less than 50 μm, and randomization of crystalline orientation are needed. Minerals with very low quantities of a few percent of volume in the sample will not be detected because they will be covered by the noise in the diffraction pattern.

However, minor crystalline mineral phases can be detected with microRaman spectroscopy. No sample preparation is needed; the soil can be analysed as is. This method could cover the limitations of XRD for minerals in very low quantities.

To assist the mineralogical interpretation, chemical analysis will be performed with two techniques:

a. EPMA analyses (X-rays) with electron microscopy. The SEM will also be used for detailed inspection of the samples at the micron scale. The morphology and microstructure of soil minerals can be observed, such as cracks in the morphology of feldspars and iron oxides due to the fire. Moreover, a qualitative elemental analysis can be carried out without altering the sample. However, sample preparation is needed to acquire a semi-quantitative chemical analysis. Soil is a non-conductive material, and the use of a high vacuum for this kind of analysis will negatively charge its surface. Thus, a coating of a conductive film (e.g., gold, carbon etc.), a few nm thick, is needed.
b. Bulk chemical analyses with the LIBS technique (Laser Induced Breakdown Spectroscopy). This technique can detect all elements of the periodic table, starting with hydrogen, and then lithium, boron, and all other elements. Qualitative analysis is straightforward and easy with this technique; however, quantification is possible after calibration of the system. Analysis with this method can be made on all kinds of materials (inorganics and organics) and material phases (solid, liquid, gas).

With the above techniques it is possible that charcoal particles that usually remain after fire enhance the water retentive purposes. It is also possible to investigate the dehydration level of some phases, and after calibration to estimate this parameter. New minerals can also form, i.e., carbonates from the decomposition of oxalates. The formation of calcite crystals ($CaCO_3$) in burned soils could be occurred due to the transformation of calcium oxalate during the combustion of vegetal tissue, especially wood (Wattez & Courty, 1987); (Ulery & Graham, 1993); (Iglesias et al., 1997). Comparisons with the regolith or soils that have not been exposed to fire will provide evidence on such mineralogical neoformations or transformations (i.e., possibly calcite-lime-portlandite). Raman is a very interesting method to detect these changes.

3.2.4 Soil sampling methods

3.2.4.1 Preparation of sampling – Office work

a. Prior to sampling, the area is studied through topographic, geological, and vegetation maps to identify the sub-areas of the greatest interest (e.g., areas with different geological and topographic characteristics, burnt and unburned areas, and locations with different types of vegetation).
b. The access road network should also be known.
c. Sampling should not take place immediately after rainfall, but at least ten days after the rainfall.
d. The number of samples and the method of selecting the sample positions are then determined.

3.2.4.2 Selection of sampling positions

Soil samples are taken from different geological formations in both burned and unburned areas.

Number of samples

A representative number of surface samples (15-30) from the depth of 0-10 cm is required. The number of the samples depends on the size of area, the geology, the terrain, the vegetation cover, and the cost.

3.2.4.3 Soil sampling methods

a. The most used sampling design for many field studies is systematic sampling using either transects or grids. The choice of a transect or grid depends on several factors, such as the complexity of landforms at the sampling site, etc. (Petersen & Calvin, 1996). Where the above methodologies cannot be applied, random sampling or a combination of random and systematic sampling may be selected.

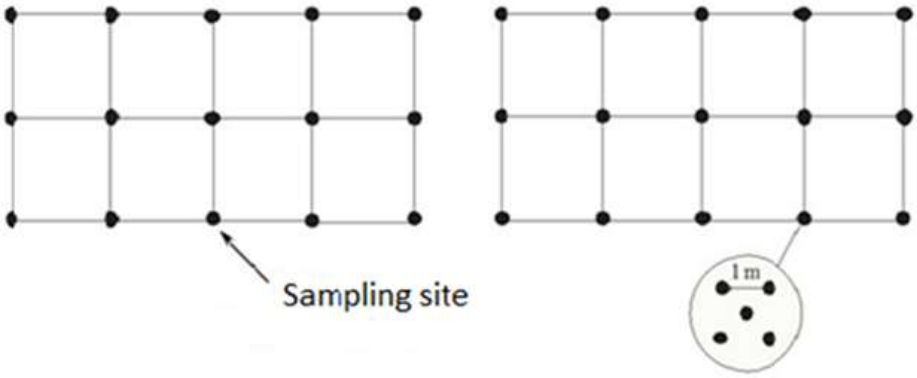

Figure 6. Soil Sampling Protocol (Systematic Sampling) (opencourses.uoa.gr)

Grid Sampling

In this sampling design, a grid system is imposed over each field or subsection of a field. One simple or one composite sample from each grid node is sent for laboratory analysis. In the case of a composite sample at each sampling site, one composite sample must be collected by mixing five sub-samples from the corners and the centre of a 10 m square in sealable plastic bags (**Figure 6).**

b. When the topography of the pilot area does not allow the above types of sampling, soil sampling can be carried out at various points based on the geological background.

The tools required for the soil sampling are:

1. common hand tools, such as shovels, trowels, spatulas, etc. for surficial soil sample collection
2. a core sampler
3. GPS
4. plastic soil bags
5. permanent markers

The sampler should avoid sampling a typical area such as eroded knolls, depressions, saline areas, fence lines, old roadways and yards, water channels, manure piles, and field edges. There must be a record of each plot such as geographic coordinates, altitude, slope, vegetation, etc. (soil sampling protocol) (**Table 7)**.

Table 7. Soil Sampling Protocol

<table>
<tr><th colspan="6">SOIL SAMPLING PROTOCOL</th></tr>
<tr><td colspan="3">Number of soil profile:</td><td colspan="3">Date:</td></tr>
<tr><td colspan="3">Number of sample:</td><td colspan="3">Horizon:</td></tr>
<tr><td colspan="3">Sampling site</td><td colspan="3" rowspan="2">Projection system:</td></tr>
<tr><td>Country:</td><td colspan="2">Location:</td></tr>
<tr><td colspan="3" rowspan="2"></td><td colspan="3">Sampling position coordinates</td></tr>
<tr><td colspan="2">X:</td><td>Y:</td></tr>
<tr><td colspan="3">Altitude:</td><td colspan="3">Soil slope:</td></tr>
<tr><td colspan="3">Depth of sampling:</td><td>0-10º</td><td>10-35º</td><td>>35º</td></tr>
<tr><td colspan="3">Type of sampling</td><td colspan="3">Type of sampler:</td></tr>
<tr><td colspan="2">Undisturbed:</td><td>Disturbed:</td><td colspan="3">Responsible of the sampling:</td></tr>
<tr><td colspan="6">DESCRIPTION OF CLIMATOLOGICAL CONDITIONS OF THE DAY SAMPLING</td></tr>
<tr><td colspan="6">VEGETATION DESCRIPTION - LAND USE</td></tr>
<tr><td colspan="6">LOCATION DESCRIPTION-TOPOGRAPHY</td></tr>
</table>

3.2.4.4 Sampling procedure

Before soil collection: The surface must be cleared of living plants, plant litter and surface rocks.

Collection of samples: A quantity of topsoil from depth 0 to 10 cm is collected, about 1-2 kg in weight and then transferred into a numbered plastic bag (use of a permanent marker). Additionally, paper with the sample number written in pencil (not pen) is placed inside the bag, which is closed very tightly (not to lose sample moisture).

Soil cores

a. For more detailed soil analysis and if it is possible, soil cores can be collected in order to study soil properties changes according to depth.
b. Soil cores are usually taken up to the depth of 30 cm. Alternatively, samples can be collected from a soil profile.
c. The core sampler should be inserted vertically into the soil.
d. After the extraction of a sample, it is carefully stored undisturbed, for example in a plastic bag or in a tube.

After sampling procedure

a. Collected samples should be transported to the laboratory as soon as possible.
b. In the case of the measurement of organic compounds (e.g., hydrocarbons) part of the samples should be kept frozen (<-10 ^{o}C) to prevent nutrient transformations caused by microorganisms.
c. The rest of the samples should be air-dried or dried in an oven at the temperature of 40 °C and stored, until the analysis, in the refrigerator (4 ^{o}C) or in a cool place.
d. The moisture content of the samples is determined immediately after their arrival at the laboratory to avoid soil moisture loss.

3.2.4.5 Treatment of subsampling

a. For the preparation process, living macroscopic roots and all particles, mineral and organic, with a diameter larger than 2 mm, should be removed from the samples by dry sieving (2-mm sieve).
b. The particles not passing the 2-mm sieve are weighed separately for the determination of the coarse fragment content (required only for bulk density).
c. For those analyses for which finely ground material is required (e.g., Carbonate content, Total Organic Carbon, Total Nitrogen and Total Elements) pulverization is done.

3.2.5 Indicative plan for soil resilience

Usual measures could be applied to protect the soil are the following:

3.2.5.1 Before the fire:

Measures taken to reduce the fire risk should not harm the soil and should not intensify erosion. An example is the compaction of the soil due to overgrazing, the excessive thinning of the crown or the understory of the vegetation, etc.

3.2.5.2 After the fire:

Usual measures (experience from Greece):

a. Anti-erosion works.
b. Flood protection works.
c. Reforestation
d. Post-fire vegetation monitoring
e. Protection of natural regeneration

Anti-erosion and flood protection works:

In Greece, the following projects are preferred:

a. Soil retention works made of logs (deadened by fire)
b. Soil retention works made of tree branches (deadened by fire)
c. Wooden fences

Their lifespan is between three (3) and five (5) years.

The construction of logs and twigs should be carried out with special care, along the contours.

Branching grids and logs should be placed on the ground very well to avoid soil loss .

3.2.6 Work done and planning

Up to now, the research methodology has been designed, and the first soil sampling has been carried out in some pilot areas. The collected soil samples have been processed and are ready for analysis. Some initial measurements have been made in the pilot area of Portugal. Furthermore, fieldwork for measuring soil erosion in pilot burned areas has started. Existing models and indicators of soil characteristics (erodibility, geomorphological features, soil quality, pollution, etc.) on which to base the experimental data processing are gathered.

The work that remains to be carried out in the next period includes field and laboratory work such as:

1. Supplementary soil sampling in different parts of the pilot area and in different time periods.
2. Physicochemical and mineralogical analysis of soil samples.
3. Additional field work to monitor soil erosion.
4. Determination of measures for the restoration of the burnt areas in the pilot area.

3.3 Soil Analysis

3.3.1 Initial results from the Greek pilot area

3.3.1.1 Initial results from soil physicochemical analysis

Up to now in the pilot area of Greece in North Evia, surface soil sampling has been carried out in April 2023 based on the geological background **(**Figure 18**)**. Eleven (11) simple surface soil samples (0-10cm) and eleven (11) cores (up to 30cm) have been collected from burned and unburned areas with the same geological background. Subsequently, physicochemical analyses were performed on these samples **(Table 8).**

Table 8. Results of pH and particle size analysis of surface soils of the North Evia region.

Sample	pH	Sand%	Silt%	Clay%	Soil texture
E1	7,09	51,01	23,81	25,18	Sandy Clay Loam
E2	7,19	55,77	22,86	21,37	Sandy Clay Loam
E3	7,46	60,53	27,62	11,85	Sandy Loam
E4	7,49	51,96	29,52	18,51	Sandy Loam
E5	6,82	54,82	24,76	20,42	Sandy Clay Loam
E6	6,58	53,18	25,71	21,10	Sandy Clay Loam
E7	5,92	49,10	30,10	20,80	Loam
E8	6,46	68,15	20,95	10,90	Sandy Loam
E9	7,51	68,15	19,05	12,80	Sandy Loam
E10	7,78	52,91	32,38	14,70	Sandy Loam
E11	7,62	85,30	8,95	5,75	Loamy Silt

a. Particle size analysis was carried out by the hydrometer method (Gee & Bauder, 1986). The percentages % of sand, silt, and clay were placed on the soil textural triangle, and the texture of each sample was determined (**Figure 7**). The soil texture triangle is used to convert particle size distribution into a recognized texture class based on the relative amounts of sand, silt, and clay as a percentage.

Based on the results, the soils of the study area are classified into four categories. Four samples belong to the 'Sandy Clay Loam' category, one sample to the 'Loam' category, five samples to the 'Sandy Loam' category, and finally one sample belongs to the 'Loamy Silt' category. It is observed that in most of the samples the sand fraction predominates, followed by the silt and clay fractions.

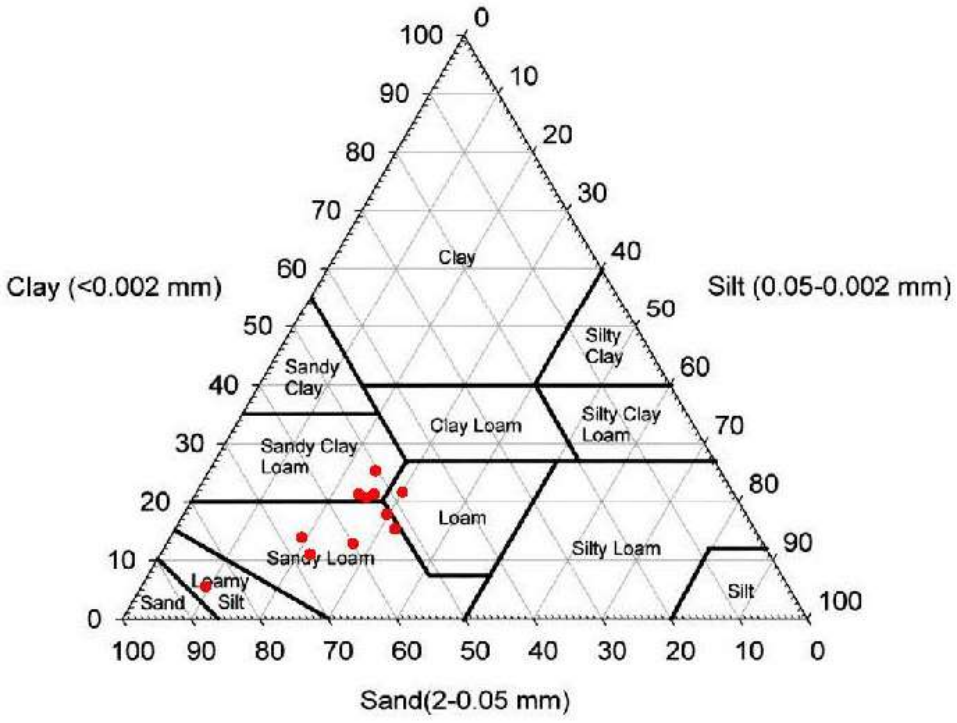

Figure 7. Soil textural Triangle (Ternary diagram of the USDA soil texture classification (Gee & Bauder, 1986)

b. The pH was determined in the soil samples of the pilot area by the electrometric measurement method (Thomas, G., 1996). This ranged between 5.92 and 7.78 (**Table 8).** According to the United States Department of Agriculture Natural Resources Conservation Service, soils with pH values between 5.6 and 6 are classified as moderately acidic, 6.1 and 6.5 slightly acidic, 6.6 and 7.3 neutral, 7.4 and 7.8 slightly alkaline, and those with values between 7.9 and 8.4 moderately alkaline. Thus, according to the above classification, five (5) samples are classified as slightly alkaline, four (4) samples as neutral, one (1) sample as slightly acidic and one (1) sample as moderately acidic.

According to the above results regarding soil texture and pH, no clear differences are observed between the soils of the burned and unburned areas. Analyzes of a larger number of samples are expected to provide more detailed data.

3.3.1.2 Initial results from mineralogical soil analysis

The research is based on analyses of soil from a mapped area in North Evia, Greece, affected by wildfires in the summer of 2021. For the acquisition of the samples, drilling was preceded in 11 spots of a specific area with hollow plastic tubes with a length of approximately 35 cm. The core samples were removed from the tubes with a self-made piston and separated at every 2 cm (**Figure 8**)**.** They classified from 'a to k', where 'a' represents the deeper part of the core sample into the ground.

Figure 8. a) Hollow plastic tube, filled with the core sample, b) removing the core sample with a piston and dividing it in every 2 cm, c) storage of each sample, d) dehydration at 50°C, e) dehydrated samples, and e) final storage of the dehydrated samples in the desiccator.

The samples were analysed with X-ray Diffraction (XRD) for mineralogical identification. Scanning Electron Microscopy – Energy Dispersive Spectroscopy (SEM-EDS) and Laser-Induced Breakdown Spectroscopy (LIBS) were performed for a qualitative elemental information of the samples. The progress of the analyses in each sample is presented below **(Table 9)**.

Table 9. Progress of the soils' analyses.

Deeper parts → upper parts of the soil										
	2cm	2cm	2cm	2cm	2cm	2cm	2cm	2cm	2cm	2cm
1	**a**	**b**	**c**	**d**	**e**					
	Dehydration 50°C		Dehydration 50°C		Dehydration 50°C					
	XRD		XRD		XRD					
	SEM-EDS				SEM-EDS					
					LIBS					
2K	**a**	**b**	**c**	**d**	**e**	**f**				
	Dehydration 50°C		Dehydration 50°C		Dehydration 50°C	Dehydration 50°C				
	XRD				XRD	XRD				
	SEM-EDS				SEM-EDS	SEM-EDS				
						LIBS				
3A	**a**	**b**	**c**	**d**	**e**	**f**	**g**	**h**	**i**	**j**
	Dehydration 50°C		Dehydration 50°C		Dehydration 50°C		Dehydration 50°C		Dehydration 50°C	Dehydration 50°C
	XRD		XRD		XRD		XRD		XRD	XRD
	SEM-EDS								SEM-EDS	SEM-EDS
										LIBS
4A	**a**	**b**	**c**	**d**						
	Dehydration 50°C			Dehydration 50°C						
	XRD			XRD						
	SEM-EDS			SEM-EDS						
				LIBS						
5K	**a**	**b**	**c**	**d**	**e**					
	Dehydration 50°C			Dehydration 50°C	Dehydration 50°C					
	XRD			XRD	XRD					
	SEM-EDS				SEM-EDS					

					LIBS					
6K	**a**	**b**								
	Dehydration 50°C	Dehydration 50°C								
	XRD	XRD								
	SEM-EDS	SEM-EDS								
		LIBS								
7K	**a**	**b**	**c**	**d**	**e**	**f**	**g**			
	Dehydration 50°C					Dehydration 50°C	Dehydration 50°C			
	XRD					XRD	XRD			
	SEM-EDS						SEM-EDS			
							LIBS			
8A	**a**	**b**	**c**	**d**						
	Dehydration 50°C			Dehydration 50°C						
	XRD			XRD						
	SEM-EDS			SEM-EDS						
				LIBS						
9K	**a**	**b**	**c**	**d**						
	Dehydration 50°C		Dehydration 50°C	Dehydration 50°C						
	XRD		XRD	XRD						
	SEM-EDS			SEM-EDS						
				LIBS						
10K	**a**	**b**	**c**	**d**	**e**	**f**				
	Dehydration 50°C				Dehydration 50°C	Dehydration 50°C				
	XRD				XRD	XRD				
	SEM-EDS					SEM-EDS				
						LIBS				
11A	**a**	**b**								
	Dehydration 50°C	Dehydration 50°C								
	XRD	XRD								
	SEM-EDS	SEM-EDS								
		LIBS								

3.3.1.2.1 XRD analyses

A Bruker D8 Focus instrument was used for the analyses (**Figure 9, a**), with an X-ray lamp operating at 40 kV and 40 mA, an angle scan range of 3–75 degrees, an angle resolution of 0.02 of a degree, and an integration time: 1 sec per step (angle) (**Figure 9, b**). For the evaluation were used the EVA Bruker software, for the acquisition and the preliminary processing and the Profex version 5.2.1 software for refined processing (https://www.profex-xrd.org). Profex version 4.3.6 was also used due to hardware requirements. The EVA Bruker software includes a full database for phase identification; thus, it is the appropriate software for the preliminary identification of an unknown mixture, from the defined 2-theta angles with the corresponding intensities for each mineral. The Profex software includes a limited database (for example for clay minerals there are only few representative minerals from specific groups, like the nontronite from the smectite group and not the montmorillonite, but the peak fitting that provides, illustrates better the presence of each phase. Furthermore, Profex with the tool for the convergence progress, evaluates and leads to the optimum fitting of phases in the diagram when the red line that derives from the selected to be identified phases is below the acceptance limit. The combination of these two software was considered necessary to obtain the best possible result. Moreover, preparation of the samples is mandatory for the analysis with the XRD, thus, they dehydrated at 50 °C to be pulverized and resulting to a powder.

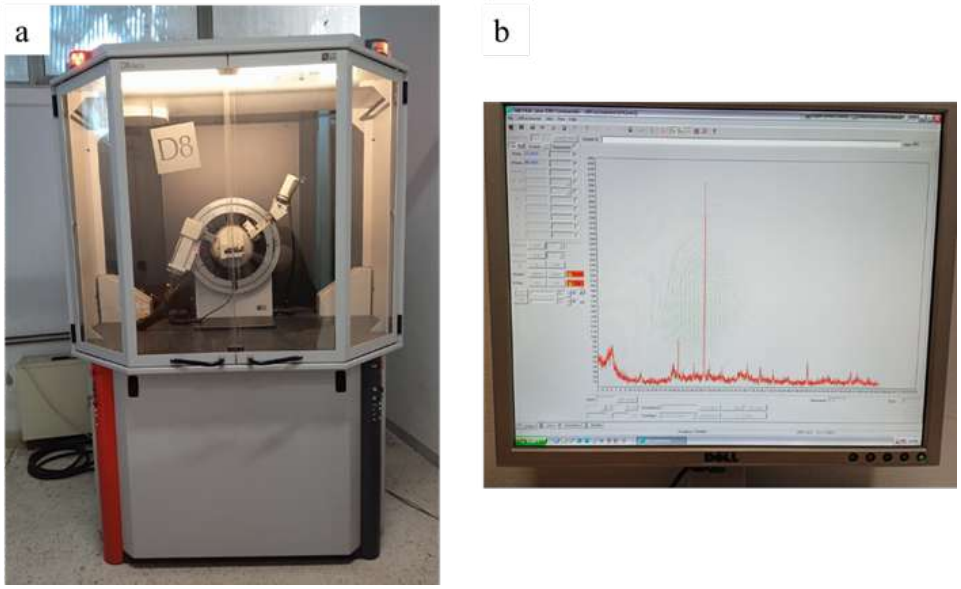

Figure 9. a) XRD D8 Bruker with b) XRD Commander software.

Preparation of samples for the XRD analyses

- Use of agate mortar and pestle in multiple sizes (from 12.5 cm to 5 cm in diameter) in order to pulverize a small part of the dehydrated soil of each sample (**Figure 10, a**).
- Special sample holders with an embossed area in the middle have been used to insert the sample for analysis.
- In the embossed area, a volume of dust is inserted and slightly agitated to randomize the crystalline orientation.
- A flat surface is created by quickly pressing the sample with a glass plate in an effort to avoid parallelization of the crystallites (**Figure 10, b**).

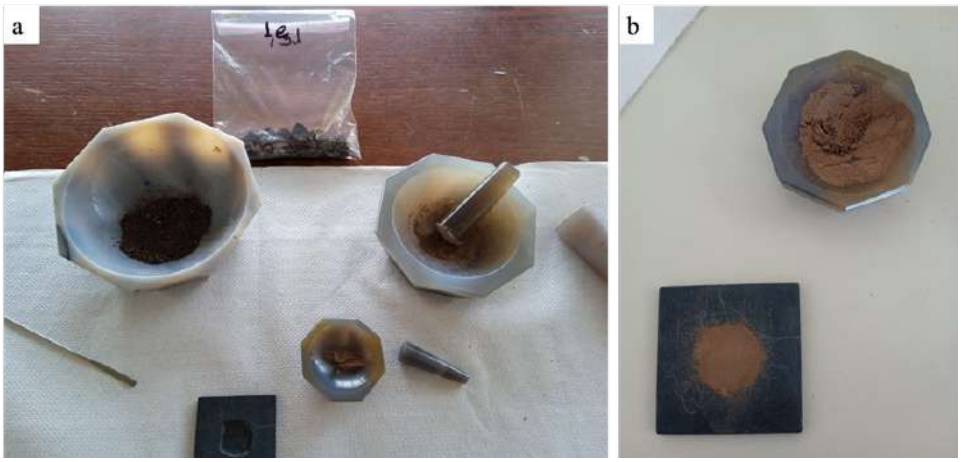

Figure 10. Preparation of the soils for the XRD analyses. a) Use of agate mortars in multiple sizes in order to pulverize the soil and b) the produced powder is placed in the sample holder.

XRD diagrams

XRD diagrams from spots 1, 2K, 3A, 4A, 5K, 6K, 7K, 8A, 9K, 10K and 11A have been acquired and identified. From the analyses, for example, along the 3A core sample from an unburnt area, there is no identified mineralogical differentiation in the 6 analysed samples across its length (**Figure 11, a**). Minerals like quartz, calcite, dolomite, and feldspar were identified in each one of them, which is in agreement with the geology of the sampling area which is characterized by conglomerates; these minerals consist of the binding material.

Similarly, with the samples from the 4A spot, which are also deriving from an unburnt area with conglomerate (**Figure 11, b**). Montmorillonite is analysed in these samples with similar peaks across the length of the core sample, as expected because the area has not been affected by the fire.

Samples from 8A and 11A spots from unburnt areas vary in their mineralogical components, even though they also derive from clastic rocks but from distant areas. Quartz, mica, and feldspar are mainly detected in 8A, with similar XRD diagrams across the length of the core sample (**Figure 12, a**), while in 11A spot chlorite, serpentine, quartz, feldspar and carbonates are detected with little identified differences, mainly in feldspar, which is more intense in the deeper sample (11A, a) (**Figure 12, b**).

In the samples from the burnt areas, a differentiation is observed in the 2K and 5K spots in the concentration of montmorillonite. In the samples that were deeper in the ground (2K, a and 5K, a) the existence of the clay mineral is more apparent (pointed out with black arrows) (**Figure 13**, **a and b**), while it diminishes in the upper two samples from 2K (2K, e and 2K, f) and 5K (5K, d and 5K, e), especially in the 5K, e (surface sample). The decomposition of the clay mineral due to the fire could be a possibility, which requires further research.

The differences in mineralogy of the core samples 2K and 5K are also obvious. The 2K core sample derives from marl soil with carbonate, clay minerals and quartz analyzed in the XRD diagram (**Figure 13**, **a**), while the 5K from ophiolitic soil, thus serpentine prevails in the diagram (**Figure 13**, **b**).

In the 6K spot (**Figure 13**, **c**). it's worth noting that it also originates from a burnt area. Similar XRD diagrams were obtained from the sample, possibly due to its small size of only 4 cm, which may have been entirely exposed to the effects of the fire. This core sample derives from melange soils, complex mixtures of marl, conglomerates, clay, etc. Thus, quartz, chlorite (clay) and albite (plagioclase feldspar) prevail in this diagram. Similarly, the samples from 10K spot present no identified difference in the clay minerals across the length

of the core sample, with slight variations in quartz and feldspar in the deeper sample in the ground (10K, a) (**Figure 13, d**).

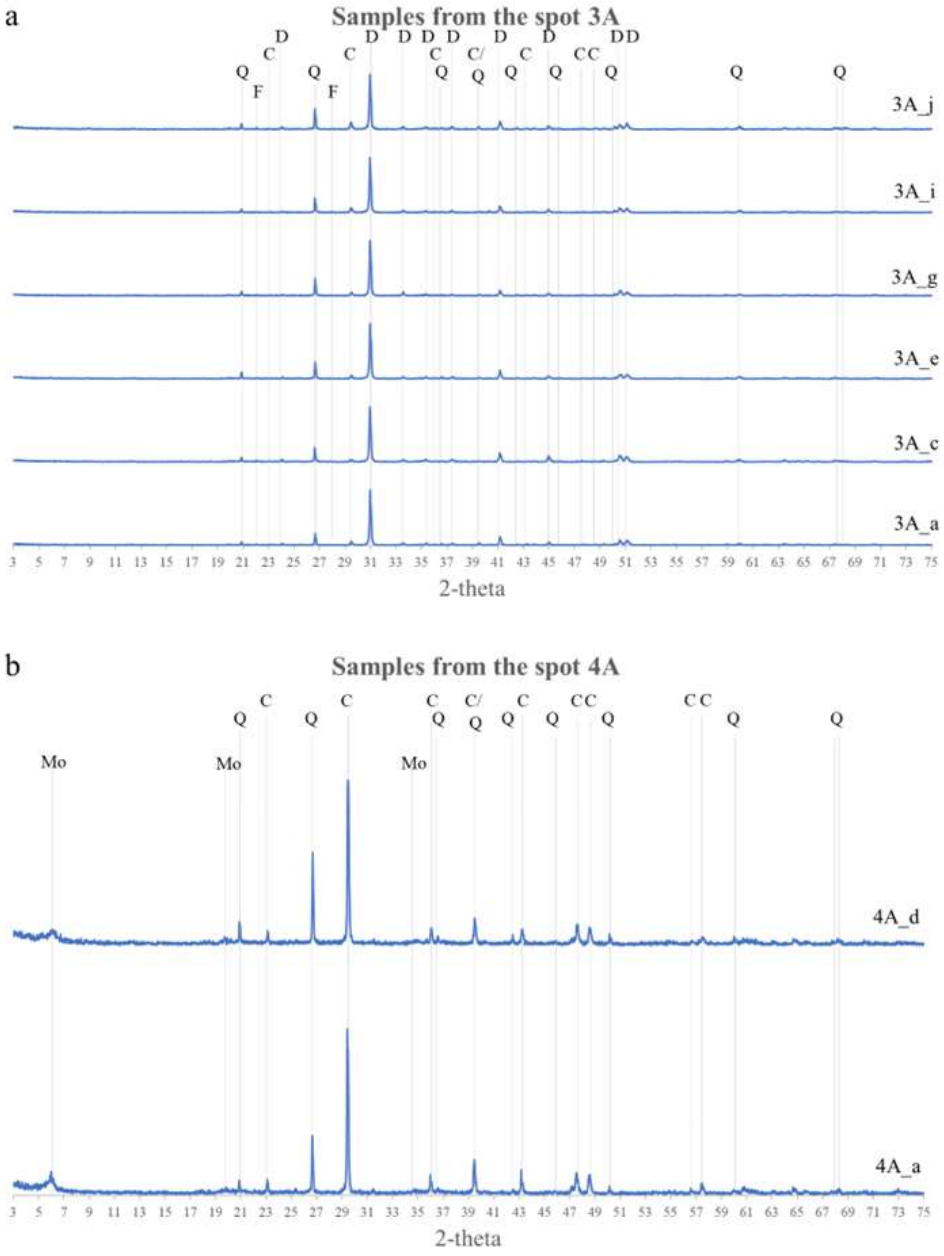

Figure 11. XRD diagrams from the spots 3A and 4A. The identification was carried out with Profex software, where D: dolomite, C: calcite, Q: quartz, F: feldspar and Mo: montmorillonite are identified.

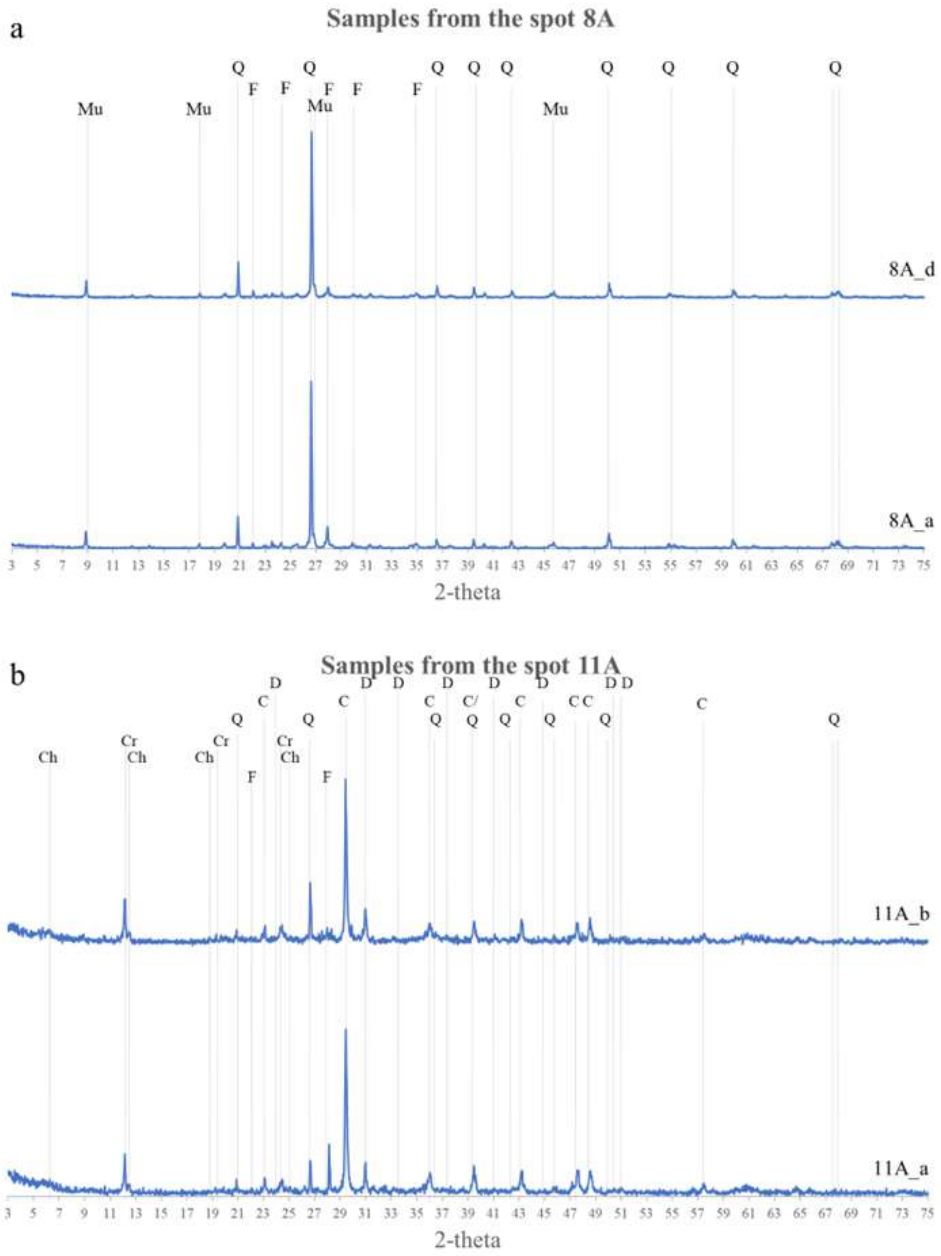

Figure 12. XRD diagrams from the spots 8A and 11A. The identification was carried out with Profex software, where D: dolomite, C: calcite, Q: quartz, F: feldspar, Mu: muscovite, Cr: chrysotile and Ch: chlorite are identified.

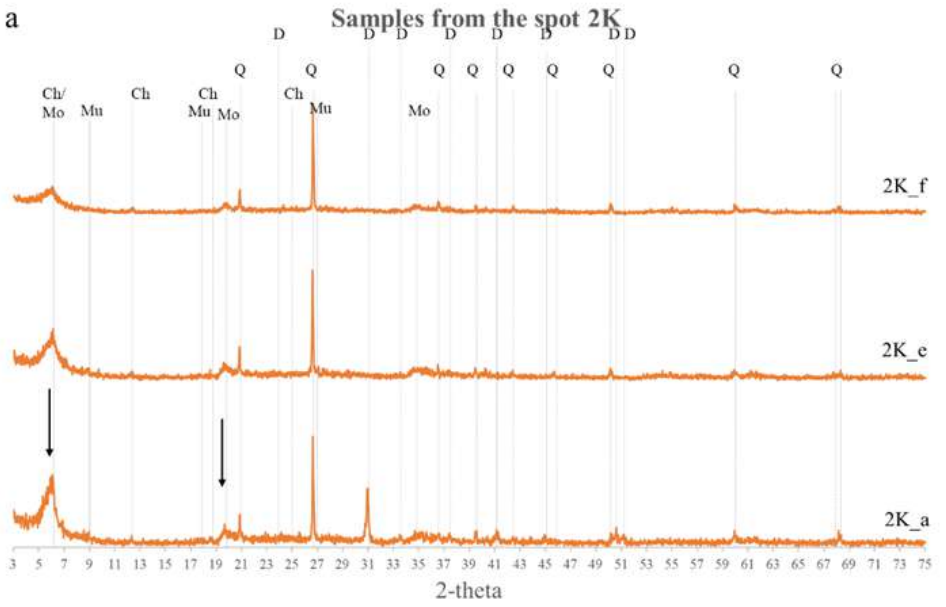
a
Samples from the spot 2K
Ch/ Mo
Mu
Ch
Ch Mu
Mo
Ch
Mu
Mo
D
Q
2K_f
2K_e
2K_a
2-theta

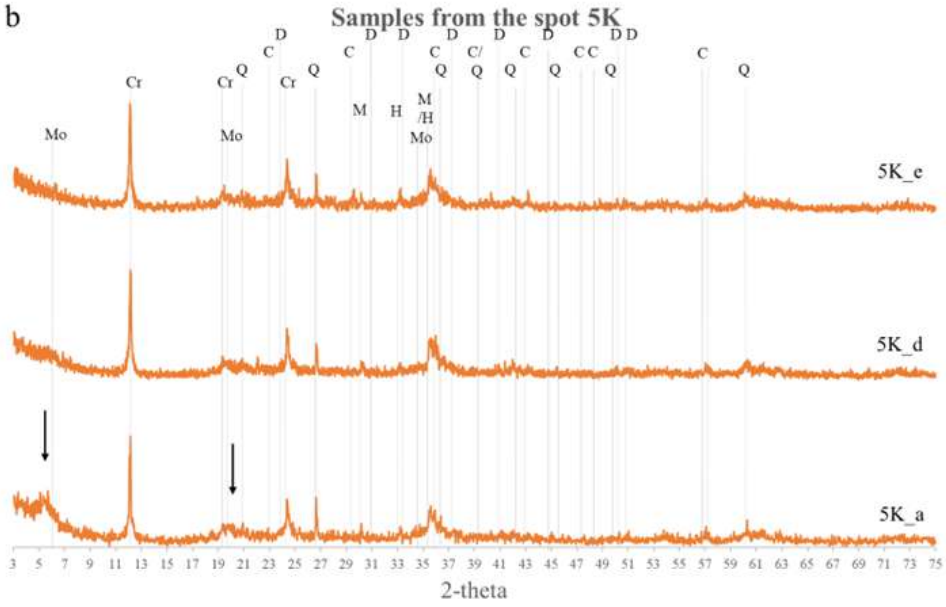
b
Samples from the spot 5K
Mo
Cr
Cr Q
Mo
Cr
Q
C
D
M
H
M /H
Mo
C/ Q
C
Q
5K_e
5K_d
5K_a
2-theta

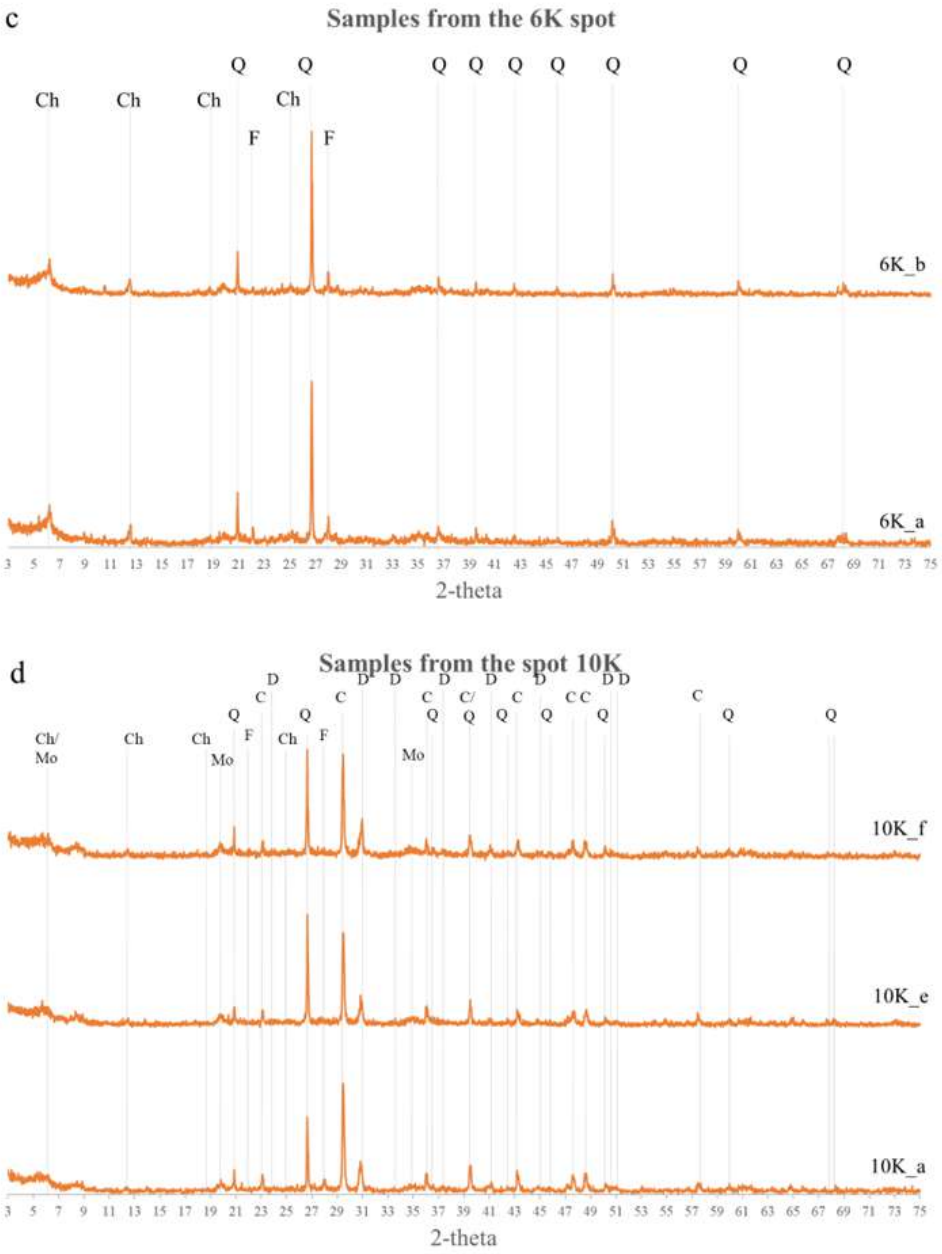

Figure 13. XRD diagrams from a) 2K spot, b) 5K spot, c) 6K spot and d) 10K spot.

The black arrows point out the more apparent indication of the clay mineral in 2K and 5K. The identification was carried out with Profex software, where D: dolomite, C: calcite, Q: quartz, Ch: chlorite, Cr: chrysotile, Mo: montmorillonite, F: feldspar, Mu: muscovite, M: maghemite and H: hematite are indicated.

The decomposition of the detected clay minerals is also observed in a lower degree in the diagrams from burnt areas 1, 7K and 9K. 1 and 7K are from areas with mainly clay minerals, while in 9K carbonates are also detected (**Figure 14**)**.** Moreover, XRD diagrams from the upper 2 cm, from all the analyzed spots, with the identified minerals are also presented (**Figure 15**).Minerals like calcite, dolomite, quartz, serpentine (chrysotile), clay minerals (chlorite, montmorillonite), feldspar (albite), mica (muscovite), titanium oxide (rutile) and iron oxides (hematite, maghemite) are identified in the analyzed spots.

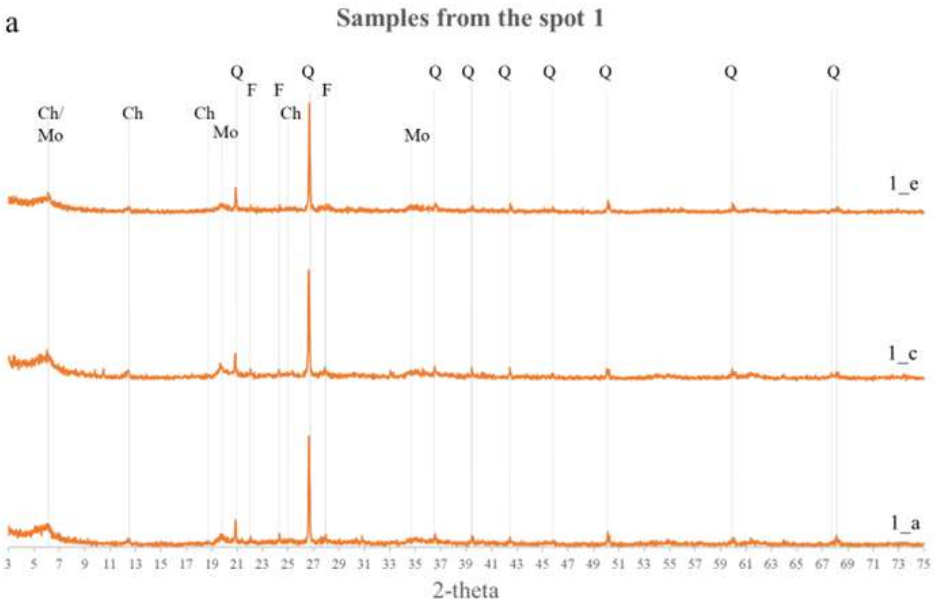
a
Samples from the spot 1
Ch/
Mo
Ch
Ch
Mo
F
F
Ch
Q
F
Q
F
Mo
Q
Q
Q
Q
Q
Q
Q
1_e
1_c
1_a
3 5 7 9 11 13 15 17 19 21 23 25 27 29 31 33 35 37 39 41 43 45 47 49 51 53 55 57 59 61 63 65 67 69 71 73 75
2-theta

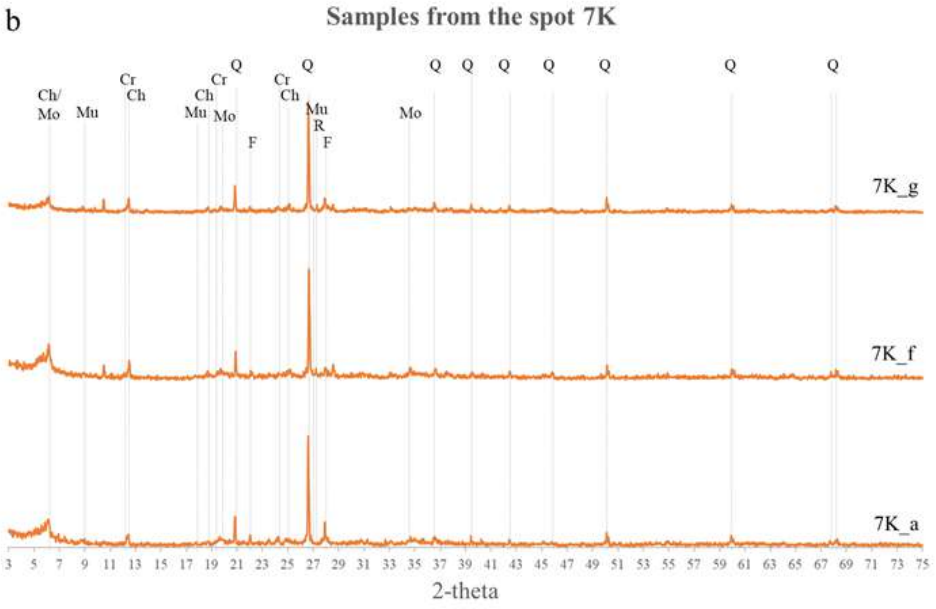
b
Samples from the spot 7K
Ch/
Mo
Mu
Cr
Ch
Ch
Mu
Cr
Mo
F
Q
Cr
Ch
Q
Mu
R
F
Mo
Q
Q
Q
Q
Q
Q
Q
7K_g
7K_f
7K_a
3 5 7 9 11 13 15 17 19 21 23 25 27 29 31 33 35 37 39 41 43 45 47 49 51 53 55 57 59 61 63 65 67 69 71 73 75
2-theta

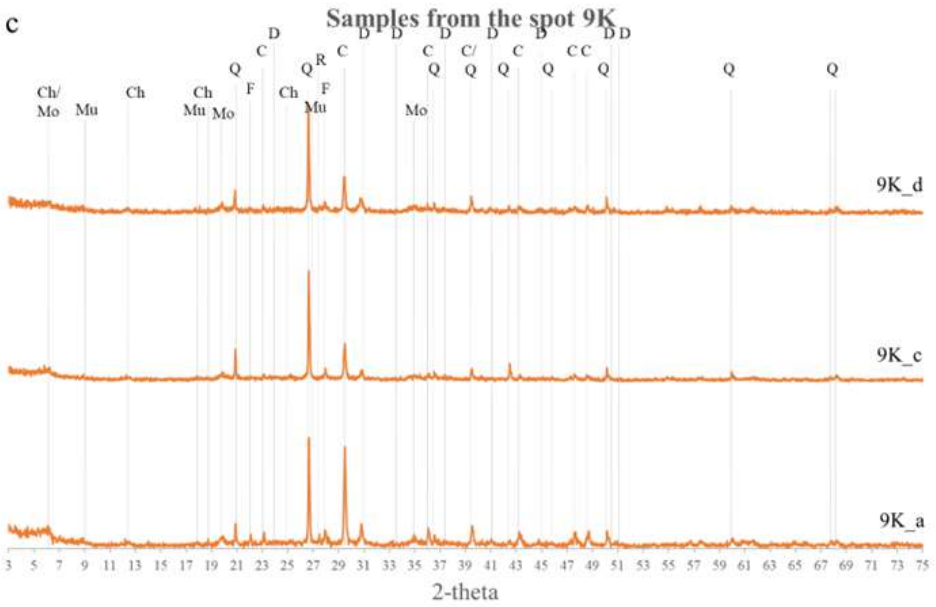

Figure 14. XRD diagrams from a) 1 spot, b) 7K spot and c) 9K spot.

The identification was carried out with Profex software, where D: dolomite, C: calcite, Q: quartz, Ch: chlorite, Cr: chrysotile, Mo: montmorillonite, F: feldspar, Mu: muscovite, and R: rutile are indicated.

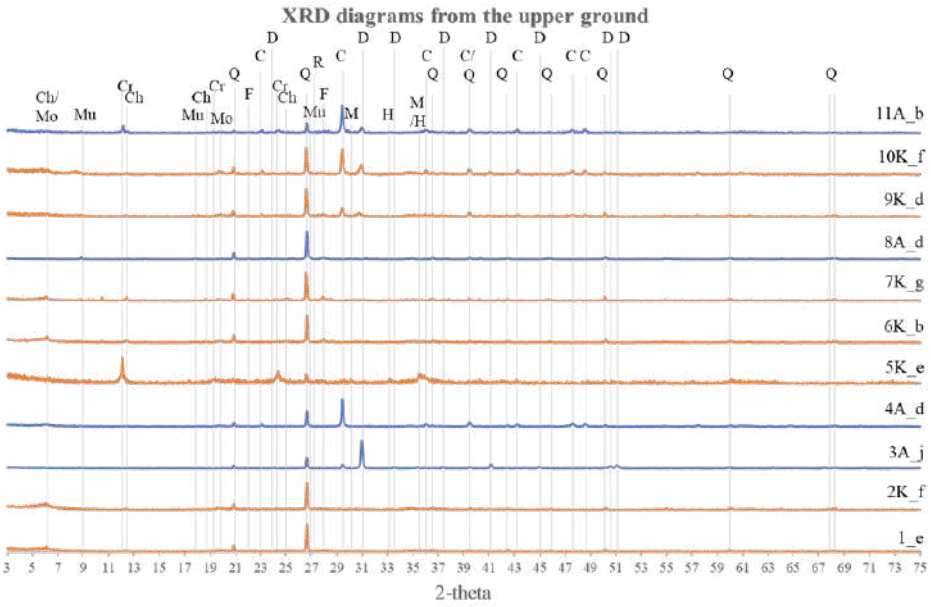

Figure 15. XRD diagrams from the upper 2 cm (surface) of burnt (1_e, 2K_f, 5K_e, 6K_b, 7K_g, 9K_d, 10K_f)

Orange color and unburnt areas (3A_j, 4A_d, 8A_d, 11A_b) – blue color. The identification was carried out with Profex software, where D: dolomite, C: calcite, Q: quartz, Ch: chlorite, Cr: chrysotile, Mo: montmorillonite, F: feldspar, Mu: muscovite, R: rutile, M: maghemite and H: hematite are indicated.

3.3.1.2.2 SEM-EDS analyses

The SEM-EDS analysis is performed with a Jeol 6380LV system and an EDS system using the INCA software from Oxford Instruments (**Figure 16**). The SEM instrument is operating at 20kV (primary electron beam) and a filament current of 58–60 mA. The samples were analyzed as powders on carbon tape and they are deriving from the upper one or two sections of each sample, and the deeper one into the ground (**Figure 17**), using the low vacuum mode of the electron microscope, which was set at 30 Pa to avoid charging. This eased the operation without any modifications of the sample during coating (i.e., elevated temperatures, carbon deposition on the surface).

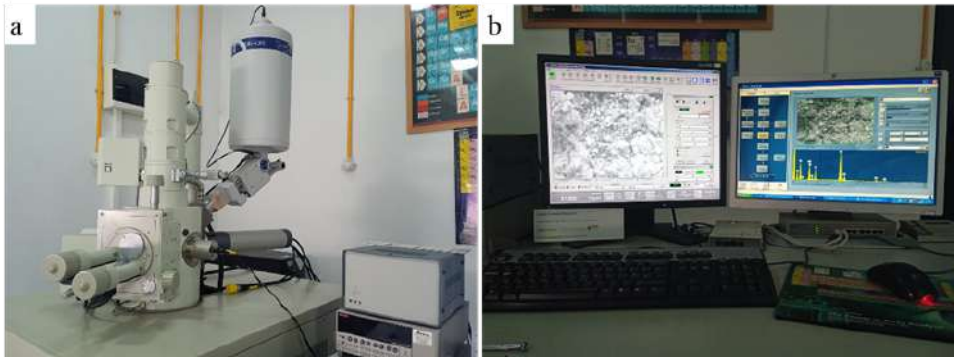

Figure 16. a) Jeol 6380LV with EDS system and b) the two computers for the handling of the SEM analysis (left side computer) and the elemental analysis (right side computer).

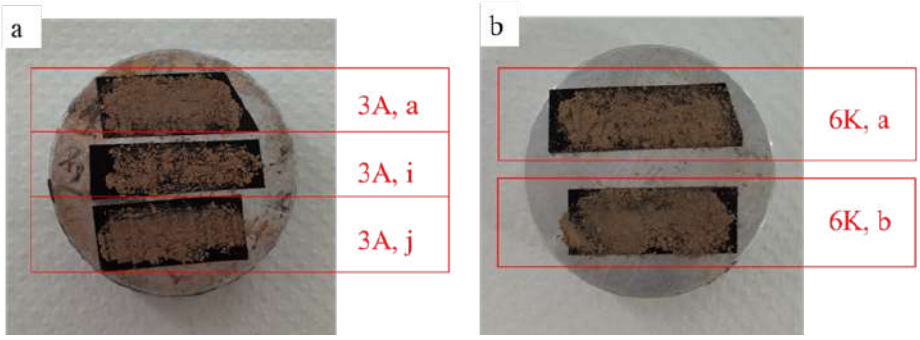

Figure 17. a) Powder from the sample 3A on carbon tapes, with 'a' representing the deeper part of the sample into the ground, while 'i' and 'j' representing the upper two sections from the surface, b) similar with the sample 6K, with 'a' representing the deeper part and 'b' the upper part of the ground's surface.

Elemental composition of the samples with SEM-EDS

In general, the mineralogy shares similarities in burnt and unburnt areas because it regards the same territory. Elements like Na, Mg, Al, Si, K, Ca, and Fe are mainly analyzed in all the samples with SEM-EDS, while small average atomic percentages up to 1% of Ti, Cr, Mn, Co and Ni were also detected.

The chemical elements Mg, Si, Ca, and Fe are the main elements that present fluctuations due to the samples' mineralogy. Sampling from nearby areas with similar geology leads to similar EDS analyses, like 1 and 2K, 3A and 4A, also in 6K and 7K, and in 9K and 10K (**Figure 18, and Table 10**). The XRD diagrams are also similar in these locations.

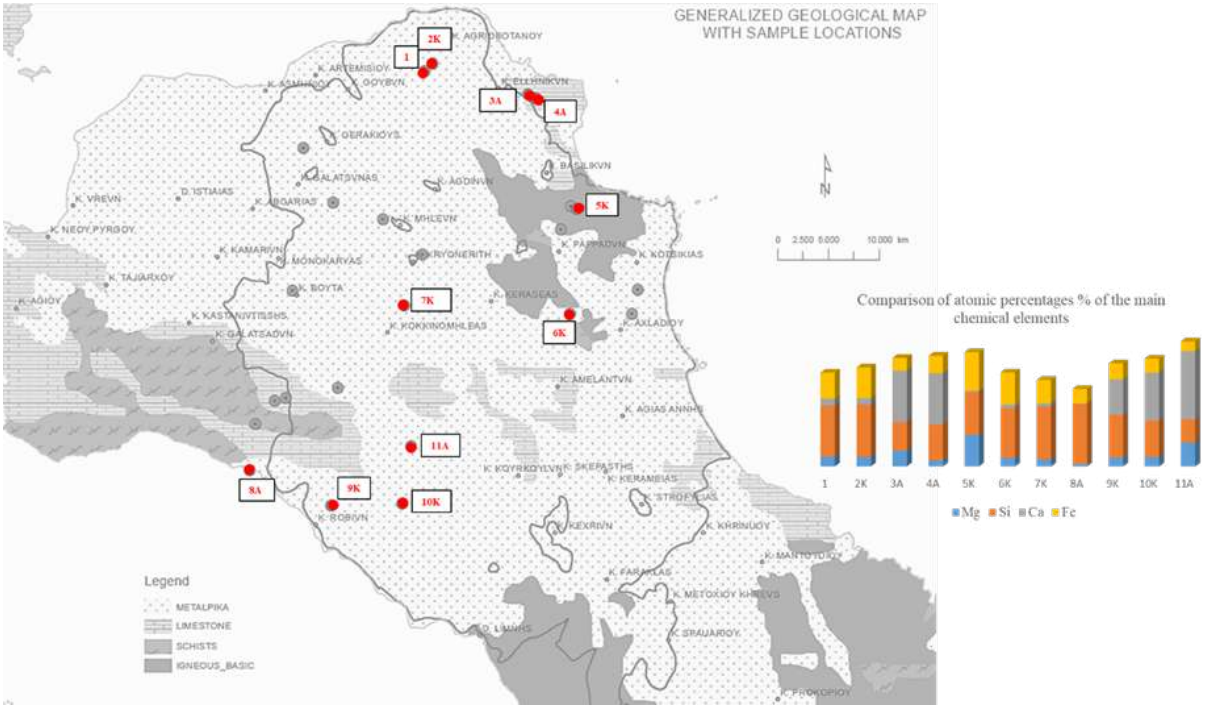

Figure 18. Generalized geological map with the sampling locations and the chart with the comparison of the atomic percentages % of Mg (blue color), Si (orange color), Ca (grey color), and Fe (yellow color) in each location (Sampling locations pointed with red dots and arabic numbers, K=burnt, A=unburnt).

Table 10. Average atomic percentages of each sampling location, with highlighting in blue the main chemical element/ elements in each location.

	Na	Mg	Al	Si	K	Ca	Ti	Cr	Mn	Fe	Co	Ni	O
1	0,30	4,78	6,79	24,99	1,42	3,20	0,42	0,00	0,23	12,76	0,00	0,00	45,14
2K	0,00	4,63	4,95	25,52	1,16	3,10	0,55	0,00	0,00	15,00	0,00	0,22	44,87
3A	0,00	7,71	6,19	13,82	1,40	25,16	0,12	0,00	0,00	6,20	0,00	0,00	39,40
4A	0,00	2,91	4,82	17,42	0,94	25,16	0,22	0,00	0,00	8,49	0,00	0,00	40,07
5K	0,00	15,34	2,19	20,91	0,36	0,70	0,00	0,10	0,00	18,77	0,00	0,00	41,64
6K	0,66	4,14	6,49	24,17	1,11	1,82	0,66	0,18	0,47	15,71	0,00	0,00	44,62
7K	2,35	3,41	8,45	25,68	1,45	1,75	0,98	0,00	0,00	11,28	0,00	0,00	44,69
8A	1,44	1,04	9,12	29,45	4,98	0,26	0,44	0,00	0,00	7,03	0,00	0,00	46,27
9K	0,18	4,28	6,02	20,74	1,69	17,39	0,35	0,00	0,00	7,76	0,00	0,00	41,60
10K	0,00	4,54	5,68	17,62	1,41	23,54	0,36	0,00	0,00	6,86	0,00	0,00	40,00
11A	0,00	11,70	1,96	11,17	0,25	33,29	0,00	0,00	0,00	4,77	0,00	0,00	36,87

Comparing the samples of 1 and 2K spots from burned nearby areas, it can be observed that the samples are chemically similar (**Figure 19**, **a**). The samples from the 3A and 4A spots and from nearby unburnt areas are also chemically similar, with a slight difference in the percentage of Mg, due to the intense presence of dolomite in 3A (**Figure 19**, **b**).

The samples from 6K and 7K spots from nearby burnt areas also share similar chemistry with small variations in the concentration of Fe which increases in the deeper samples (6K, a and 7K, a), possibly due to a mineralogical difference that is still investigated (**Figure 19**, **c**). On the other hand, the spot 5K is

chemically different from the above samples, mainly in the Mg content. 5K is in a geologically different area and the elevated percentage of Mg is probably due to the presence of serpentine.

Comparing the samples from the south-west areas, it can be observed that only the samples from the spots 9K and 10K present elemental similarities, while the samples from the unburnt areas 8A and 11A differ chemically, with Si along with K are dominating in 8A spot and Mg along with Ca in 11A (**Figure 19**, **d**).

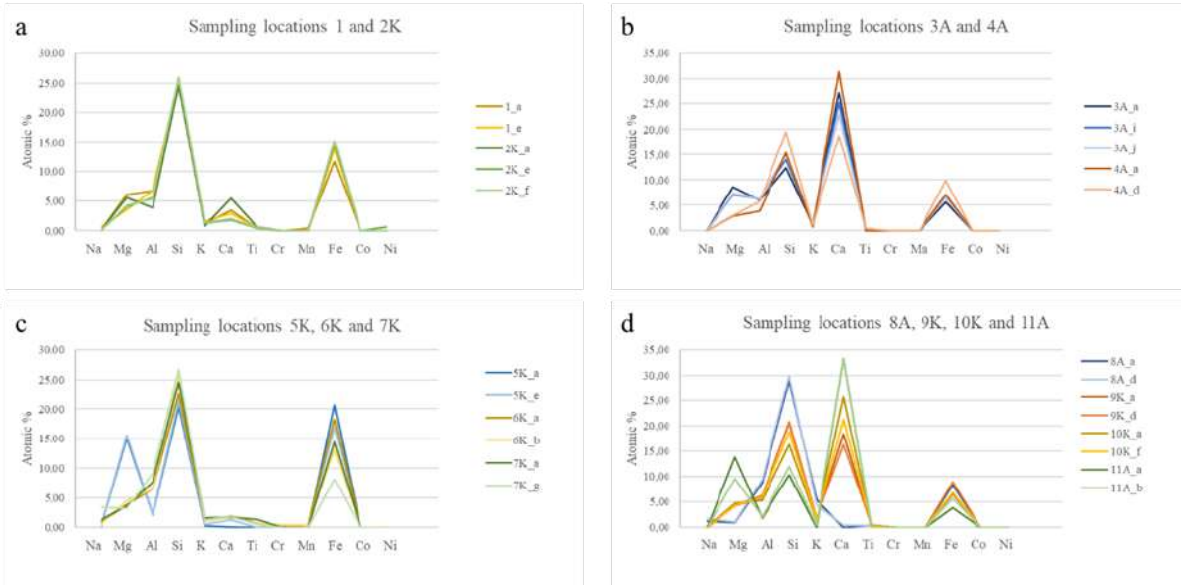

Figure 19. SEM-EDS analyses in atomic % a) from the samples 1 – yellow hues and 2K – green hues, b) from the samples 3A – blue hues and 4A – orange hues, c) from the samples 5K – blue hues, 6K – yellow hues and 7K – green hues, and d) from the samples 8A – blue hues, 9K – orange hues, 10K – yellow hues and 11A – green hues.

SEM-EDS analyses were also performed in single grains, where Cr, Ti, Mn, Co and Ni were identified, while in the analyses in large areas, their presence could not be detected in all the cases, probably due to their small concentration. For example, in the sample 2K, a, Ti was undoubtedly detected (**Figure 20, a and b**). In the sample 6K, a, Co and Ni were identified along with Mn in a well-defined grain (**Figure 20, c and e**), while the chemistry of the surroundings differs with Fe prevailing (**Figure 20, c and d**). Moreover, Cr was detected in the 11A, a sample along with Mg, Al, Si, Ca, and Fe (**Figure 20, f and g**).

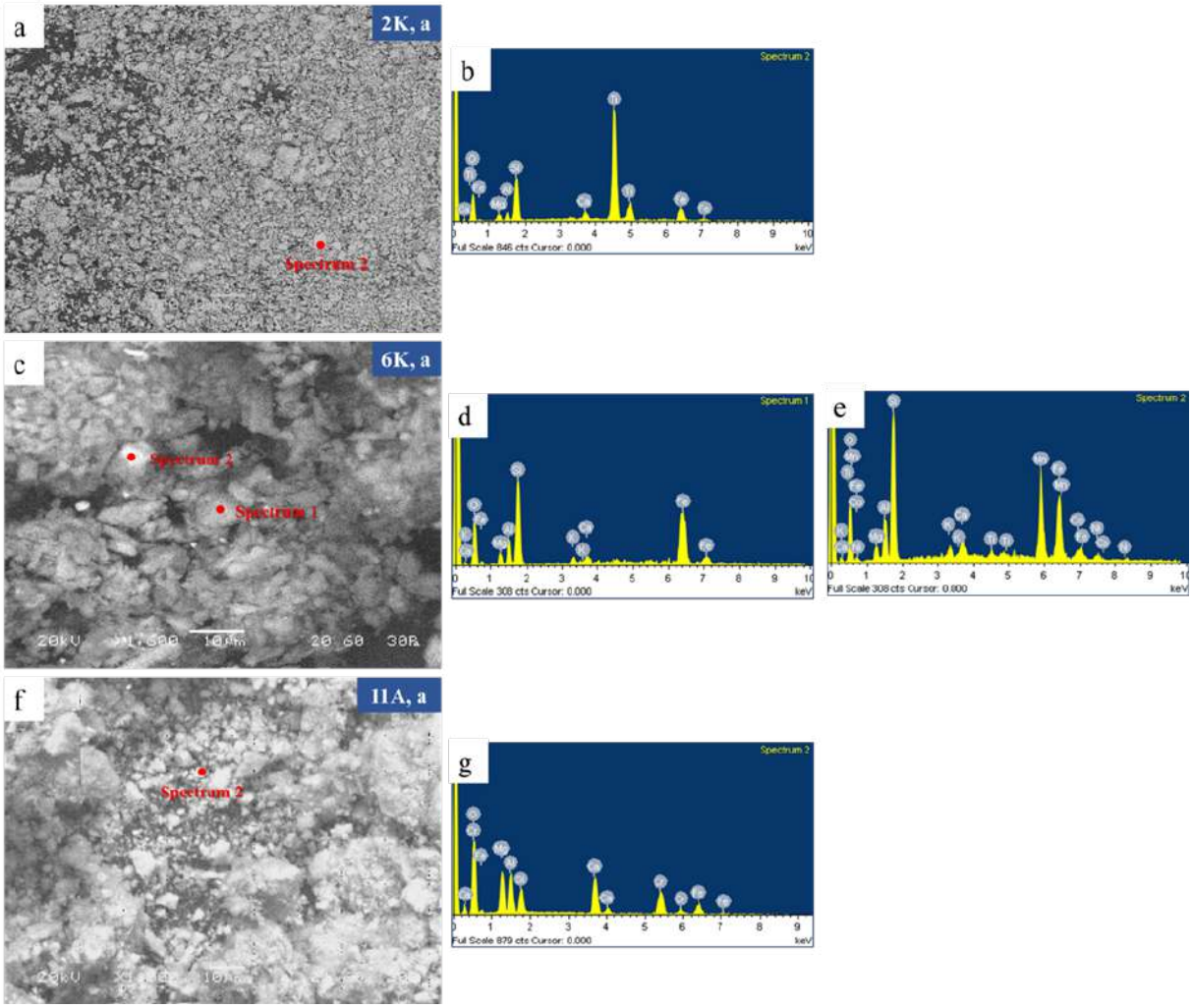

Figure 20. SEM-EDS analyses in single grains from the deeper samples of 2K, 6K, and 11A spots. a) Analysis of a single grain in the 2K, a sample and b) spectrum with the detection of Ti. c) The chemical differences of two grains in 6K, a sample, which diameter is less than 5 µm, with d) Spectrum 1 from the grey granule and e) Spectrum 2 from the white granule. The colours in the BSE image are due to the chemical differences of the two granules, the heavier elements are illustrated with brighter colours. f) SEM image from the 11A, a sample and g) Spectrum with the identification of Cr.

3.3.1.2.3 LIBS analyses

LIBS analyses were performed with a Q-Switched Nd:YAG laser at 1064 nm with a pulse duration of 8 ns. The spectra were acquired from two spectrometers, one in the UV range and the other in the Visible/IR range. The spectral coverage of the two spectrometers is from 200 nm to 1045 nm. The processing is performed with in-house software for laboratory use with a built-in database with the majority of the chemical elements of the periodic table (89 chemical elements).

For the analyses, the dehydrated samples from the upper 2 cm of each core sample were used, with no further preparation. A small volume of the soil was pressed into an aluminium case, and a flat surface was created. The flat surface is a requirement in order to acquire representative spectra across the sample with no changes in the geometry of the focal length and the position of the optical fibres for the acquisition of the spectra (**Figure 21**).

Figure 21. The LIBS system for the chemical analyses from a fast cooling plasma produced by the intense pulse of a laser beam (8ns at 1064 nm). Left is the Nd:YAG laser, while on the right is the laser focusing lens and the two optical fibres which collect the light emission form the plasma and guide it to the two spectrometers.

Elemental composition of the samples with LIBS

Similarly, to SEM-EDS, LIBS analyzed Na, Mg, Al, Si, K, Ca, Ti, Cr, Mn, Fe along with H and O in the surficial samples of each spot (**Figure 22**). Na, Ti and Mn were detected in all the upper samples with LIBS, while K was not detected in all of them. Co and Ni were not analyzed in these samples. More focused analyses with SEM-EDS could probably provide more results about their presence.

The most intense peaks of Na are observed in 6K, 7K and 8A spots (**Figure 22**) and the Ca has high intensities in 3A, 4A, 9K, 10K and 11A spots. The higher intensity of Si and Al is in 8A spot, while Fe diminishes in 9K, 10K and 11A spots. K is observed with more intense peaks in 3A and 8A spots, while it is also detected in 9K and 10K in extremely low intensities. Ti and Mn are detected in all the spots with similar intensities, while Cr is detected in 5K, 6K and 11A spots, however, in extremely low intensities, and indications of its presence were observed in the rest of the spots.

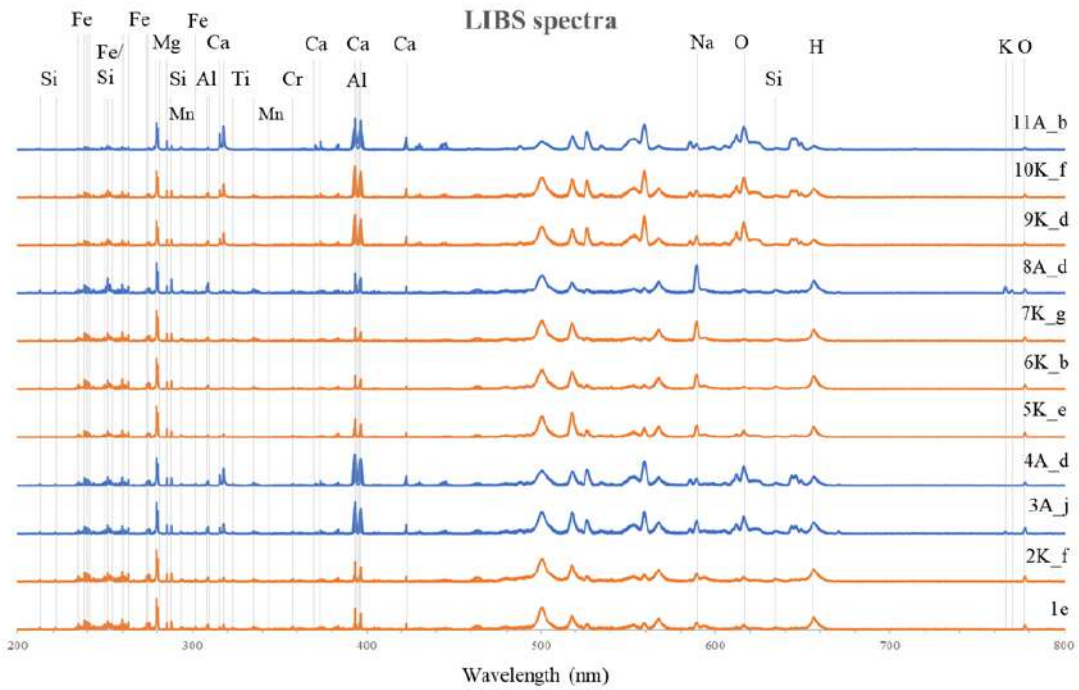

Figure 22. LIBS analyses of the upper parts of the 11 spots from burnt – orange color and unburnt areas – blue color, where Na: sodium, Mg: magnesium, Al: aluminum, Si: silicon, K: potassium, Ca: calcium, Ti: titanium, Cr: chromium, Mn: manganese, Fe: iron, H: hydrogen and O: oxygen are identified.

3.3.1.2.4 Discussion

SEM-EDS and LIBS along with XRD analyses could be proven to be very powerful tools for the investigation of soil affected by fire, providing useful information when they are implemented together. The main chemical elements were confirmed by both SEM-EDS and LIBS and their concentrations in the samples were corresponding. The analysed minerals with XRD were mostly in agreement with the identified chemical elements (**Table 11**). However, chemical elements like Cr, Mn, Co and Ni are not a part of the analysed minerals by XRD, probably due to their low concentration or because they substituted another element like Fe in the crystals' structure.

Na, Ti, and Mn were detected more easily with LIBS, while K with EDS. Heavy elements like Co and Ni were also analysed by SEM-EDS in single grains, as mentioned before, in only two analyses (both Co and Ni in the sample 6K, a, and solely Ni in 2K, e). Both analyses were from samples of 2 cm to 4 cm below the surface of the ground.

LIBS provides fast analyses of a large volume of the sample compared to EDS, which outweighs in focused analyses. The analysis of a larger volume of samples with EDS will be a time-consuming process. Thus, their implementation together could provide concise and direct results.

Clay minerals seem to diminish in the XRD diagrams of the upper samples from the burnt areas, especially in spots 2K and 5K. This is also observed in the spots 1, 7K and 9K but in a lower degree, while spots 6K and 10K present similar characteristics across their length, as in the spots 4A and 11A from unburnt areas. The decomposition of montmorillonite could probably be an explanation for these differences, and this could imply that the temperature of the fire exceeded 500 °C on the surface of the ground.

Regarding carbonates analysed with XRD, the only fluctuation was observed in the 9K spot, where the most intense peak of calcite was from the deeper sample in the ground (9K, a). If calcite was affected by the fire, the temperature in the area may have exceeded 1000 °C in the surface of the ground. Macroscopically, the

samples from the 9K spot had the most apparent colour differentiation, from dark brown in the upper sample and lighter hues in the deeper ones. The colour of the soil is an indication that the fire was very intensive in the area.

In general, sampling from nearby, geologically similar burnt and unburnt areas have not led to further results until now, mainly due to the mineralogical differences. However, two nearby spots from similar areas geologically, the 10K spot from a burnt area and 11A from an unburnt area, slightly differ mineralogically, and could be compared. In both spots, minerals like dolomite, calcite, quartz, feldspar, and chlorite were detected, the only difference is that in the 10K spot montmorillonite was also detected, while in the 11A chrysotile (serpentine) was identified. From the observation of their XRD diagrams across the length of the core samples, the main similarities are that the most intense peaks of feldspar were identified in the deeper samples (10K, a and 11A, a), in contrast to the peaks of quartz which were diminished in the same samples. These observations in both burnt and unburnt areas probably regard the similar geology of the area and they are not an effect of the fire.

Future research with samples from unburnt areas with clay minerals could lead to further indications about the possible decomposition of minerals like montmorillonite due to the fire.

Table 11. Detection of chemical elements with EDS and/ or LIBS and the identified minerals with XRD.

	Na	Mg	Al	Si	K	Ca	Ti	Cr	Mn	Fe	Co	Ni	Minerals
	EDS/ LIBS	EDS/ LIBS	EDS/ LIBS	EDS/ LIBS	EDS/ LIBS	EDS/ LIBS	EDS/ LIBS	EDS/ LIBS	EDS/ LIBS	EDS/ LIBS	EDS/ LIBS	EDS/ LIBS	XRD
1	+/ +	+/ +	+/ +	+/ +	+/ -	+/ +	+/ +		+/ +	+/ +			Q, F, Ch, Mo
2K	-/ +	+/ +	+/ +	+/ +	+/ -	+/ +	+/ +		-/ +	+/ +		+/ -	D, Q, Ch, Mo, Mu
3A	-/ +	+/ +	+/ +	+/ +	+/ +	+/ +	+/ +		-/ +	+/ +			D, C, Q, F
4A	-/ +	+/ +	+/ +	+/ +	+/ -	+/ +	+/ +		-/ +	+/ +			C, Q, Mo
5K	-/ +	+/ +	+/ +	+/ +	+/ -	+/ +	-/ +	+/ +	-/ +	+/ +			D, C, Q, Mo, Cr, M, H
6K	+/ +	+/ +	+/ +	+/ +	+/ -	+/ +	+/ +	+/ +	+/ +	+/ +	+/ -	+/ -	Q, F, Ch
7K	+/ +	+/ +	+/ +	+/ +	+/ -	+/ +	+/ +		-/ +	+/ +			Q, F, Ch, Mo, Mu, Cr, R
8A	+/ +	+/ +	+/ +	+/ +	+/ +	+/ +	+/ +		-/ +	+/ +			Q, F, Mu
9K	+/ +	+/ +	+/ +	+/ +	+/ +	+/ +	+/ +		-/ +	+/ +			D, C, Q, F, Ch, Mo, Mu, R
10K	-/ +	+/ +	+/ +	+/ +	+/ +	+/ +	+/ +		-/ +	+/ +			D, C, Q, F, Ch, Mo
11A	-/ +	+/ +	+/ +	+/ +	+/ -	+/ +	-/ +	+/ +	-/ +	+/ +			D, C, Q, F, Ch, Cr

Abbreviation	Mineral	Chemical Formula
D	Dolomite	$CaMg(CO_3)_2$
C	Calcite	$CaCO_3$
Q	Quartz	SiO_2
F	Feldspar/ Albite	$NaAlSi_3O_8$
Ch	Chlorite	$(Mg,Fe)_3(Si,Al)_4O_{10}(OH)_2\cdot(Mg,Fe)_3(OH)_6$
Mo	Montmorillonite	$(Na,Ca)_{0.33}(Al,Mg)_2(Si_4O_{10})(OH)_2\cdot nH_2O$
Mu	Muscovite	$KAl_2(AlSi_3O_{10})(F,OH)_2$
Cr	Serpentine/ Chrysotile	$Mg_3(Si_2O_5)(OH)_4$
M	Maghemite	γ-Fe2O3
H	Hematite	α-Fe2O3
R	Rutile	TiO2

3.3.2 Initial results from the Portuguese pilot area

Soil samples were collected at sixteen locations, within the pilot oak forest site (**Figure 23**).

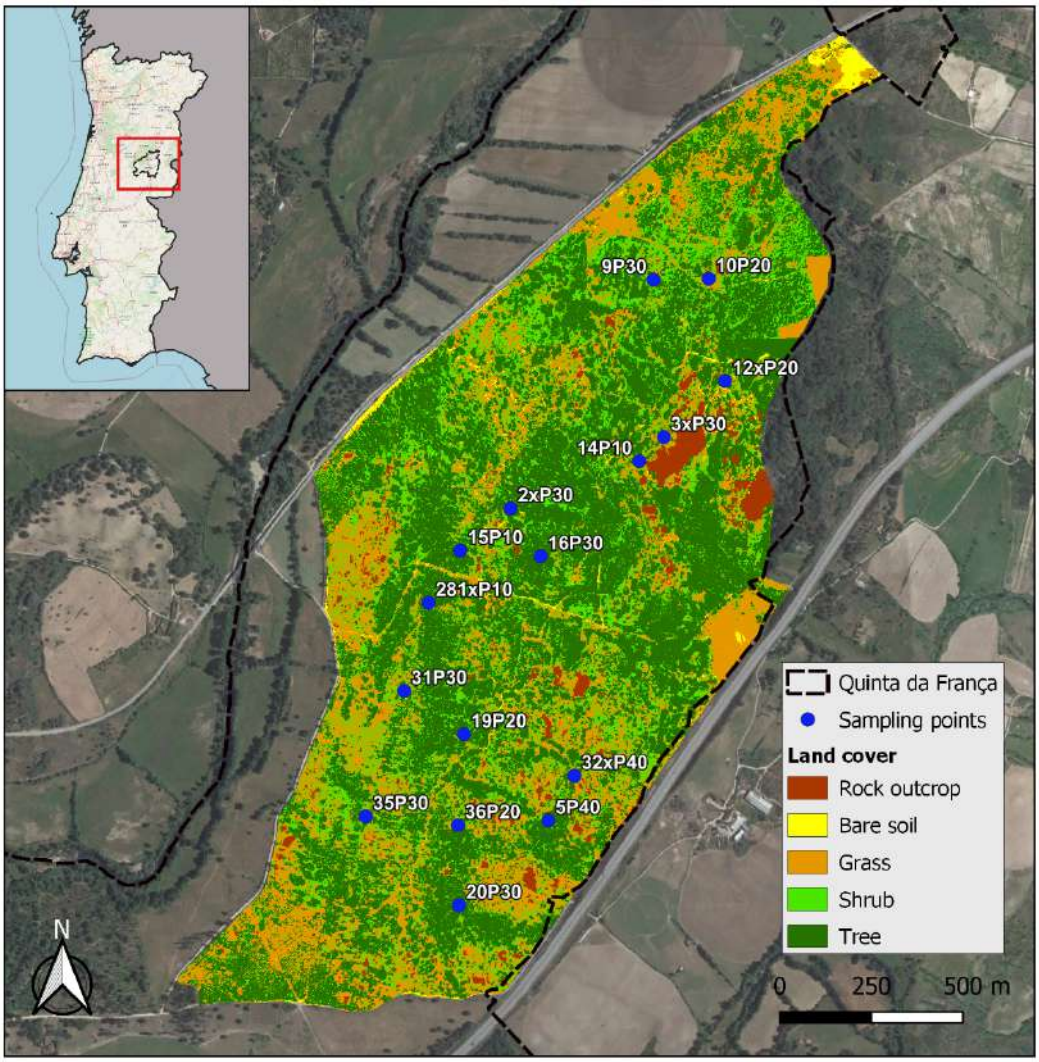

Figure 23. Map with location of soil sampling points, within the oak forest pilot site at Quinta da França. The inset figure shows the location of the Cova da Beira region in Portugal, where Quinta da França is located.

Sampling locations were distributed across the pilot site and covered different types of vegetation cover (i.e., the microhabitat scale within the oak forest). Each soil sample consisted of five probes (soil cores) collected at a depth of 20 cm. The probes were collected from the centre and sides of a 10 m x 10 m quadrat. Each composite soil sample was dried in a 36ºC oven for two to four days (depending on the moisture content). Subsequently, the samples were sent to the Soil and Plant Laboratory at the University of Trás-os-Montes and Alto Douro (UTAD) for laboratory analysis. Each soil fraction was analysed for: organic matter content (% SOM), phosphorus content (mg P2O5/kg) using two different analyses (Égner-Riehm and Olsen methods), soil pH (water and KCl), total nitrogen content (g N/kg), and potassium content (mg K2O/kg). These measurements refer to previous research and were carried out on forest areas that are showing regeneration as they were burned at least 25 years ago. These measurements can be used as a basis for comparison reasons in case future fire event as well as for the assessment of current soil status.

The first results of the analyses of the physical and chemical soil properties of the 16 soil samples from the Portuguese pilot, are presented in **Table 12**. The completion and interpretation of these results will follow soon.

Table 12. Initial results from soil analysis in the Portuguese pilot area. All sampling points are located within the oak forest pilot site.

Sampling point	Coordinates	Tree cover (%)	Soil texture	pH (water)	pH (KCl)	SOM (%)	P (mg P_2O_5 kg^{-1}) - ER	P (mg P_2O_5 kg^{-1}) - Olsen	K (mg K_2O kg^{-1}) - ER	N total (g N kg^{-1})
10P20	40.29165075, -7.40753671	90%	Coarse	5,11	4,13	3,78	74,33	57,16	70,37	2,03
12xP20	40.28912294, -7.40712537	54%	Coarse	5,21	4,18	2,49	54,36	46,30	69,09	1,43
14P10	40.287232, -7.40997	34%	Coarse	5,22	3,99	1,59	8,89	14,47	54,92	0,99
15P10	40.284978, -7.41324	95%	Coarse	5,08	4,06	3,19	20,34	38,47	74,36	1,80
16P30	40.280679, -7.415902	96%	Coarse	5,54	4,49	4,97	23,31	26,34	96,63	2,49
19P20	40.276481, -7.416254	84%	Coarse	4,90	3,95	3,45	12,18	38,61	44,49	1,91
20P30	40.285186, -7.415816	86%	Coarse	5,38	4,18	2,86	10,40	55,42	122,97	1,61
281xP10	40.283936, -7.416885	98%	Coarse	5,11	4,04	2,37	9,25	41,49	121,58	1,39
2xP30	40.286183, -7.414153	94%	Coarse	5,45	4,28	4,21	9,21	28,81	159,08	2,18
31P30	40.28179159, -7.41776692	36%	Coarse	4,71	3,69	2,30	12,14	37,14	63,57	1,36
32P40	40.278744, -7.419141	12%	Coarse	5,24	4,30	3,08	14,98	51,75	51,00	1,75
35P30	40.27955729, -7.4124084	38%	Coarse	4,70	3,91	5,29	77,68	35,68	38,62	2,65
36P20	40.278446, -7.416199	94%	Coarse	5,07	4,06	3,17	28,08	30,14	57,30	1,82
3xP30	40.28779835, -7.40915554	38%	Medium	5,00	4,05	4,33	49,56	42,50	50,88	2,21
5P40	40.278484, -7.413297	98%	Coarse	5,09	4,15	3,13	5,95	17,50	77,94	1,76
9P30	40.29167557, -7.40930399	<1%	Coarse	5,14	4,03	1,56	39,75	41,72	93,79	0,91

In this subsection are given: a) the main models/indices of assessing soil status, namely, indices for assessing soil erosion, sediment transport, soil quality and soil pollution. These models/indices are useful for monitoring soil status before and after a fire event. Based on the soil properties changes due to a fire event it is possible to select and apply measures for improving soil resilience b) the first results of the soil physicochemical analyses from two pilot areas, Greece, and Portugal. Specifically, in the Greek pilot area, soil texture, pH and mineralogical composition of the soil samples have been determined so far. These

preliminary results show that dominant soil fraction is sand, followed by silt and clay. Most of the samples are classified as 'Sandy loam' and 'Sandy Clay Loam'. In terms of pH, most soil samples are characterized as slightly alkaline and neutral. According to the results concerning soil texture and pH there were not found differences between burnt and unburned areas. From the mineralogical analysis, an estimation of fire intensity (temperature) was attempted since the mineral's decomposition occurs at specific temperatures. Based on the results of the analysis the decomposition of montmorillonite (clay mineral) in some soil samples, is an indication that the temperature in the soil surface exceeded 500 ^{o}C in these sample areas. We didn't find carbonate minerals alterations that occurs at temperatures exceeding 1000 ^{o}C, that means that fire temperature in the ground was under 1000 ^{o}C. Further measurements will show in more details of fire intensity in the Greek study area. In the Portuguese pilot area, the measurements refer to a forest that have been burned at least 25 years ago and will be useful for comparison reasons in case future fire event and for the assessment of current soil status.

4 CONCEPTUAL MODEL OF ECOLOGICAL RESILIENCE

4.1 Methods

4.1.1 Data Collection

Silvanus Project covers comprehensive forest management integrated technology in all phases: Phases A, B, and C. The conceptual model of ecological resilience is in the area for Phase C in both European and non-European pilots. Calculation of ecological resilience requires the following data:

a. History of wildfire event
   It is essential to access historical wildfire data to determine the timing and locations of wildfires. Each pilot project will select a subset of significant wildfire events, considering those with the most substantial impact on the region.
a. Timeseries Landsat Satellite Imagery
   Landsat satellite imagery is utilized to monitor wildfires at specific time and location as mentioned before. This monitoring was carried out before the fire event, immediately after the fire, and during the post-fire recovery phase. The assessment of forest conditions was based on the NDVI (Normalized Difference Vegetation Index) value.

4.1.2 Data Analysis

In this report, we assessed ecological resilience by using parameters including malleability, elasticity, and trend analysis. The outcomes of these resilience assessments are presented in a qualitative and comparative analysis across the pilot project sites. The determination of resilience combines the evaluation of vegetation health, with the Normalized Difference Vegetation Index (NDVI) serving as a proxy (Cui et al., 2013). NDVI is a widely utilized vegetation index for quantifying forest resilience, as it offers valuable insights into vegetation structure and its relationship with plant characteristics and productivity (Pan et al., 2018). The process of calculating resilience (Liu et al., 2021) involves several steps:

1. Disturbance magnitude calculations

The identification of the fire event location and timing relies on fire historical data from each pilot project. Disturbance magnitude is determined by measuring the difference in NDVI values before the fire event and immediately after it.

$$\text{Disturbance magnitude } (D) = NDVI_{pre} - NDVI_{post} \quad \textbf{[56]}$$

2. Recovery time

Forests require a specific duration to return to their initial state prior to the occurrence of a fire event. The recovery time (T) is computed by tracking the period from the onset of the fire until the forest ecosystem regains at least 70% of its initial condition (Rezaei & Ghaffarian, 2021). This temporal assessment is carried out manually by monitoring the changes in NDVI monthly.

3. Recovery magnitude calculations

Recovery magnitude is the difference in NDVI values between the recovery period and the initial state. This measurement describes alterations in forest conditions both before the fire and upon its recovery. A higher recovery magnitude indicates a less stable forest ecosystem.

$$\text{Recovery magnitude (R)} = |NDVIrec - NDVIpre| \quad [57]$$

4. Elasticity

Elasticity is an indicator of the recovery rate after experiencing disturbance. This elasticity metric is derived from the recovery magnitude and the recovery time. A higher elasticity value indicates faster recovery of the forest ecosystem.

$$Elasticity = \frac{R}{T} \quad [58]$$

5. Malleability

Malleability reflects the extent of deviation from the initial state after a fire event. A greater malleability value indicates a less stable ecosystem, whereas a lower malleability value suggests a stable and more resilient ecosystem. The maximum malleability value is 100% or 1.

$$Malleability = \frac{|R - D|}{D} \; x \; 100\ \% \quad [59]$$

6. Trends

Time series analysis is calculated based on the average NDVI value per month after a fire event. Trend analysis was carried out using the Mann Kendal method. The significance of identifying decreasing, increasing, or stable trends in forest resilience lies in their potential to indicate the degradation, improvement (evolution), or stability of the forest ecosystem's characteristics (**Figure 24**). These trends offer valuable insights into the ecosystem's overall health and capacity to withstand disturbances.

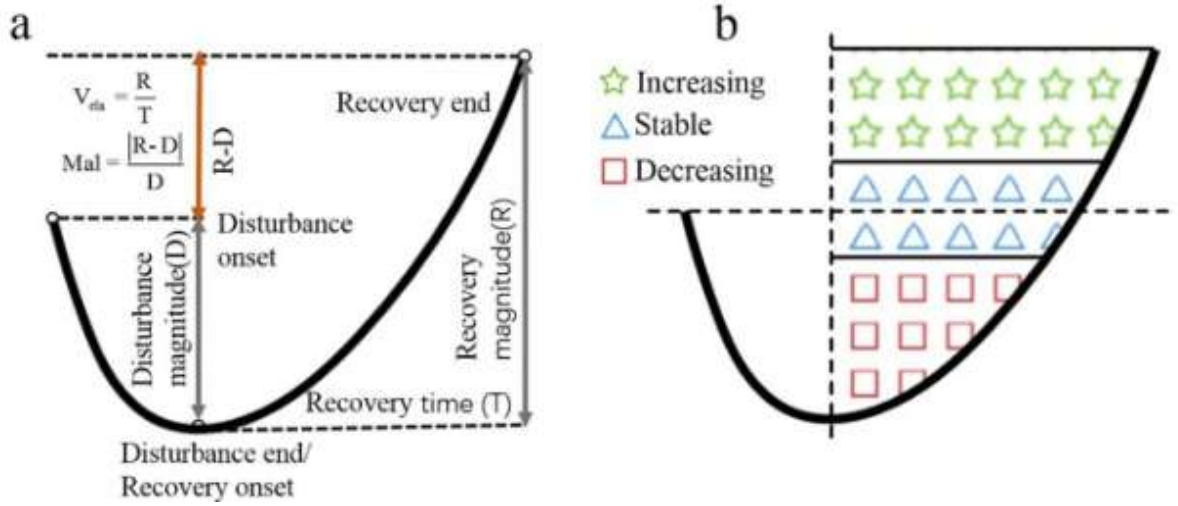

Figure 24. Indicators for ecology resilience: a) Elasticity and malleability; b) Trend

4.2 ECOLOGICAL RESILIENCE PROGRAMS

4.2.1 European Pilot

4.2.1.1 Gargano Park - Italy

4.2.1.1.1 Location/ Administrative

The historical and physical subregion of Gargano is in the province of Foggia in the Apulia region of southeast Italy. It is made up of a large, solitary mountain range with multiple peaks and highland that serves as the spine of the Gargano Promontory, which extends into the Adriatic Sea. According to Article 19 of Law 394/91, the governing law for protected areas, Gargano National Park was founded in 1991. It is one of the Italian project pilots, along with the Park of Tepilora in Sardinia. Gargano Park's region, as seen in **Figure 25.** Over 118,000 hectares of the region, which is in Apulia's northeast, are made up of 18 municipalities in the province of Foggia.

Figure 25. Map of the Gargano Park

The park's proximity to the Mediterranean Sea results in a year-round climate of high temperatures, humidity, and precipitation. The yearly temperature variation is gradual and mild, with January having the lowest average high temperature of 52.9 degrees Fahrenheit and July having the highest average high temperature of 88.9 degree.

4.2.1.1.2 History of Fires

The Territorial Coordination for the Environment of the State Forestry Corps provided the events referring to the ten-year period 2003–2012, which were taken into consideration for the analysis of the historical series of fires. These events also demonstrate that fires in the Gargano occur almost exclusively in the summer. **Table 13** presents the historical fire series data. The data summarized in the table was obtained through the processing of the raw data, and it shows that a total of 379 fires took place over the inquiry period, though the number of fires per year varies greatly, from a low of 13 in 2009 to a maximum of 72 in 2007. Even the annual extent varies; in 2009, 90.98 ha is taken total were burned, with an average area per fire of 7 ha. Following unusually large and destructive fires in 2007, a total of 5,762.4 hectares were burned,

with an average of 80 ha per fire. The average annual number was 37.9 and the average fire area was 23.3 hectares.

In the same decade, the total area burned by fire was 8,836 ha, which 63% (ha 5,603.4) involved wooded areas, while the remaining 37% (ha 3,233.4) involved non-wooded areas (pastures, uncultivated land). It shown in **Figure 26.**

Table 13. Historical Series of Fire in Gargano Park

	2012	2011	2010	2009	2008	2007	2006	2005	2004	2003	Tot.
Number of wildfires [ha]	55	40	21	13	24	72	23	27	33	71	379
Wooded area [ha]	258.32	297.66	55.04	27.82	380.16	4,189.48	42.31	55.54	44.94	252.20	5,603.38
Unforested area wooded. [ha]	128.98	390.03	84.72	63.16	531.11	1,572.95	63.40	109.44	133.73	155.86	3,233.38
Total area [ha]	387.30	687.68	139.76	90.98	911.28	5,762.43	105.71	164.89	178.67	408.06	8,836.76
Avg. fire area [ha]	7.04	17.19	6.66	7.00	788.08	80.03	4.60	6.11	5.41	6.75	927.87

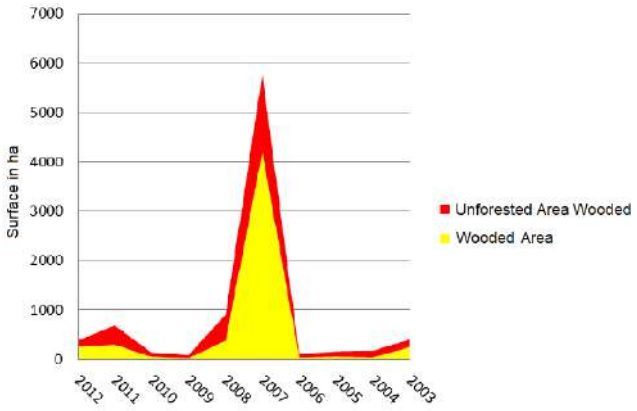

Figure 26. Wooded and Non-wooded Areas of Gargano Park Burned by Fire in 2003-2012

The Coordinamento Territoriale per l'Ambiente del Corpo Forestale dello Stato (State Forestry Corps' Territorial Coordination for the Environment) released the historical analysis on wildfire incidents for the 2010–2019 decade. According to the data, wildfires in the Gargano virtually always occur in the summer, particularly in the months of July and August. As shown in **Table 14** there were 483 wildfires in total over the study period, with a considerable variation in frequency from 20 in 2014 to 106 in 2017. Additionally, the annual extension varies greatly. For example, in 2018, 17,42 ha burned, with an average of 0,6 ha per wildfire, whereas in 2017, after numerous breakouts and a particularly dry summer, 2149,04 ha burned, with an average of 20,27 ha per wildfire. Between 2010 and 2019, there were 48,3 wildfires on average every year, with an average burned area of 23,3 ha.

Table 14. Yearly Distribution of Wildfires in The Gargano Park in the 2010-2019 Decade

	2010	2011	2012	2013	2014	2015	2016	2017	2018	2019	Tot.
N° of wildfires [ha]	21	40	55	34	20	72	41	106	29	65	483
Wooded area [ha]	55.04	297.66	258.32	94.79	10.08	299.94	74.46	1378.07	10.08	155.45	2642.27
Non wooded area [ha]	84.72	390.03	128.98	14.07	39.66	324.21	51.98	770.97	7.33	418.47	2230.43
Total area [ha]	139.76	687.68	387.30	108.87	58.12	624.15	126.44	2149.03	17.42	573.92	4872.70
Avg. area per wildfire [ha]	6.66	17.19	7.04	3.20	2.91	8.67	3.08	20.27	0.6	8.83	10.1

Throughout the same decade, wildfires affected 4872,70 hectares in total, with wooded regions being affected on 54,23% (2642,27 ha) and non-wooded regions (pastures, uncultivated lands), on 45,77% (2230,42 ha). It is shown in **Figure 27.**

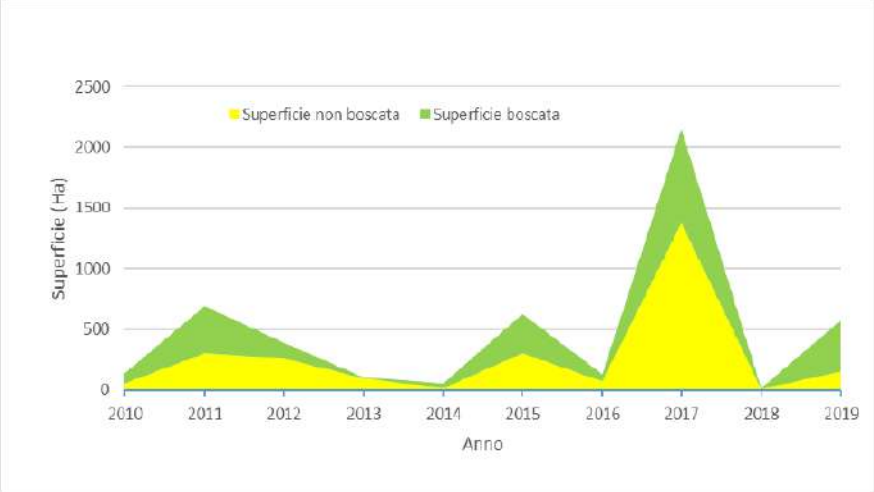

Figure 27. Wooded and Non-wooded Areas of Gargano Park Burned by Fire in 2010-2019

4.2.1.1.3 Forest management, prevention, and restoration activities/programmes/strategies

Based on the AIB Plan of Gargano National Park, interventions to restore forest cover following a fire must be based on retracing, in full, the developmental stages of the secondary succession of the implicated vegetation type. This evolution may occur naturally or with the assistance of forestry practices that are consistent in floristic and zoological terms with the range of local vegetation. The passing of another fire occurrence and this cannot coexist. If wildfires become more intense and frequent, the forest vegetation's accumulated adaptations to the passage of fire will be insufficient to maintain a forest ecosystem. Fire has the potential to transform from an ecological disturbance to a catastrophic one if the incidents occur frequently (a phenomena known as recurrence), take a long time to recover from, or do significant harm to the ecosystem. As a result of the destruction of seed-bearing plants in that area, the ecology is unable to respond by establishing natural regeneration, and forest areas may regress to a bushy, spotty, or prairie structure. Furthermore, the resulting lack of vegetation cover may encourage erosion, causing further harm

to the impacted habitats. In these situations, a more direct and active restoration intervention (active reconstitution) of the forest ecosystem is beneficial and/or required. This enables the quick reconstruction of the forest stand, which should preserve the form and functionality of the one that was destroyed.

It is important to assess on a case-by-case basis whether intervention is necessary to restore the forest cover burned by the wildfire or to allow nature to take its course (natural restoration) in an area of high naturalistic and landscape value, such as Gargano Park. In the first scenario, the characteristics of the pre-existing forest and the evolutionary dynamics of the vegetation in the intervention region must be established in relation to the silvicultural operation. Natural restoration should be preferred wherever possible.

An important educational component of integrated forest fire prevention planning is understanding the impact of fire on vegetation as well as the various possibilities and diverse dynamics of natural reconstitution of forest stands, which may allow for the detection of cases that require active intervention. This anticipates the balancing and harmonizing of forecasting, preventive, active defence, and environmental restoration. Additionally, the location and size of the wildfire need to be taken into account. In fact, the harm is proportionate to the afflicted region, all other things being equal. Therefore, it is crucial to complete the reconstitution following significant fires, even with only minimal intervention in some of the affected areas. The intervention that must be made is extremely sensitive. Coniferous woods have occasionally been rebuilt using deciduous trees to ensure recovery in the event of future fires. As deciduous trees are not suited to the environmental circumstances following a significant fire, this usually results in failure. It is often debatable and only justified for the aesthetics of the landscape to trim and remove dead plants. Burned trees may not always promote spontaneous regrowth, which benefits from the protection provided by standing dead trees. Where no intervention was made, regeneration has frequently been more abundant.

Additional issues result from the law's prohibition on reforestation and environmental engineering in the burned region for five years following a fire (L 353/2000, art. 10). The reconstitution cannot be effectively allocated over time due to this extremely rigid regulation. In fact, not much time needs to pass before it is necessary to analyse both the actual plant death and the restart of the renewal. The intervention, carried out at the proper time, encourages secondary succession, while a delayed intervention will disturb it.

4.2.1.2 Tepilora Park – Italy

4.2.1.2.1 Location/ Administrative

The Regional Natural Park of Tepilora is a Regional Park established in 2014 (pursuant to Regional Law No. 21 of 24 October 2014). It is managed by the Regional Natural Park Authority of Tepilora. The park is entirely part of the region of Sardinia, province of Nuoro and covers an area of about 7,877 hectares. It includes in part, 4 municipalities: Bitti, Lodè, Posada and Torpè. **Figure 28** shows the map of the Tepilora Regional Natural Park.

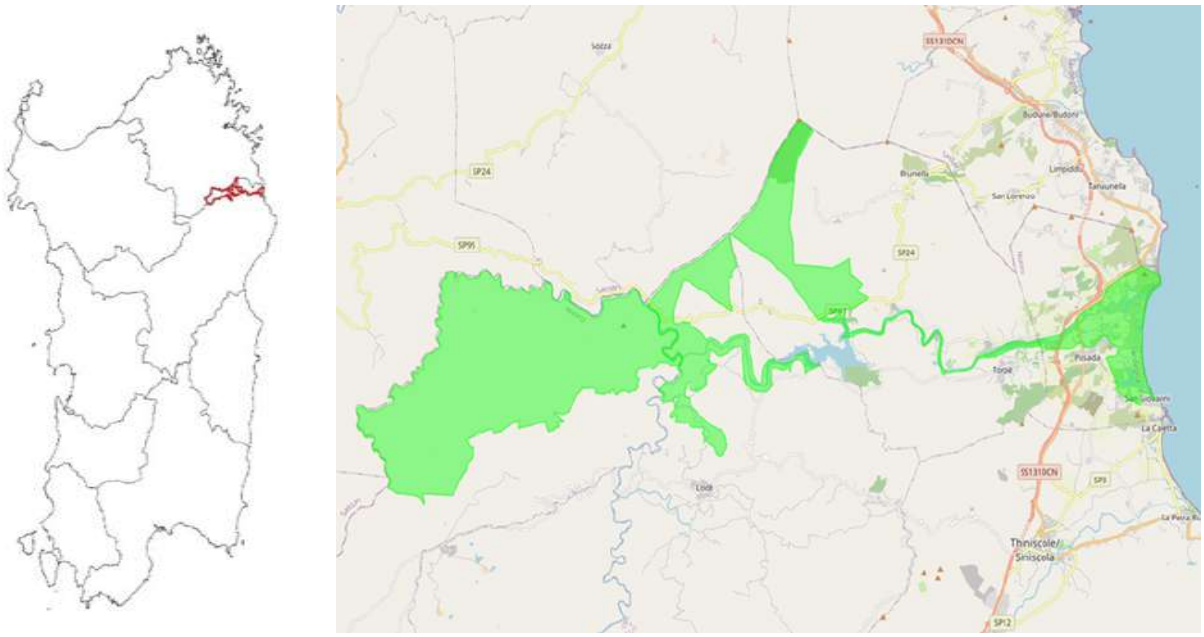

Figure 28. Map of the Tepilora Regional Natural Park.

Located in the north-west of Sardinia, the Tepilora Regional Natural Park includes a vast territory that insists on four municipalities: Torpè, Posada, Lodè and Bitti. The park extends from the Tepilora forest to the mouth of the Rio Posada; its fulcrum is Mount Tepilora (m.528 s.l.m.), a rocky tip with a triangular profile that stands out in the densely wooded area of Littos and Crastazza and looks towards Lake Posada. Once intended for grazing and cutting wood, in the 1980s the area was afforested for 16% of the total and was equipped for hiking and fire protection, becoming a nature reserve.

Wildfires in the Tepilora Park occur almost exclusively in summer (in June, July, August, September). The main cause of fire in Sardinia was found to be 60% of arson, 35% of involuntary origin and 5% of accidental origin (Source - Civil Protection). As for fires of involuntary and accidental origin, they are mainly due to cigarette butts, or the removal of plant remains (burning stubble).

All the monitoring processes are currently human based. In the Park there are three fire lookout posts; they are masonry buildings, in good condition and regularly used. Furthermore, in the neighbouring municipalities there are watch towers. This implies more difficulties in the timely management of concurrent and/or distant fire events.

4.2.1.2.2 History of fires

The analysis of the historical series of fires was carried out considering the events referring to the period 20 12-2019 elaborated by the Forestry and Environmental Surveillance Corps of the Autonomous Region of Sardinia. The analysis brought up that the fires in the Territory of the four Municipalities that make up the Tepilora Park occurs almost exclusively in the summer period (June, July, August, September). The processing of the raw data allowed to obtain the data summarized in Table 15, which shows that a total of 78 fires occurred in the period under review, but their annual number is extremely variable, going from a minimum of 4 in 2018 to a maximum of 18 in 2019. The annual extension is also not constant. In 2019, because of exceptional and extensive fires, the total area burned was 595.80 hectares with an average area per fire of 33.1 hectares. In the same period, the total area burned by the fire was 898.95 Ha, of which 58% (Ha 539.12) concerned wooded areas, while the remaining 37% (Ha 359.83) involved non-wooded areas (pastures, uncultivated land).

Table 15. History of Fires in Tepilora Park

	2012	2013	2014	2015	2016	2017	2018	2019	Tot.
Number of fires	6	8	10	10	10	12	4	18	78
Wooded area (Ha)	23,64	7,31	12,59	18,6	10,41	139,28	1,12	326,15	539,12
Total area (Ha)	**49,70**	**27,08**	**19,99**	**38,86**	**25,01**	**139,58**	**2,93**	**595,80**	**898,95**
Average fire area (Ha)	8,28	3,38	1,99	3,88	2,50	11,63	0,73	33,10	65,49

In 2016 wiildfire caused the destruction of about 3 hectares of forest. The extinguishing operations were conducted by the Forestry and Environmental Surveillance Corps of the Sardinian Region, supported by Forestas Agency workers and volunteers.

PNRT does not have a planting or regeneration plan/program for forest recovery in case of fire. It is necessary to comply with current legislation, as described below, where several restrictions must be respected.

4.2.1.2.3 Forest management, prevention, and restoration activities/programmes/strategies

a. <u>Restriction on areas covered by fire</u>

Rehabilitation strategies in wooded areas covered by fires are essentially due to constraints.
The Law 21/11/2000 n. 353, "Framework law on forest fires", which contains prohibitions and requirements deriving from the occurrence of forest fires, provides for the obligation for municipalities to census the areas covered by fires, also making use of the surveys carried out by the Forestry Corps, in order to apply the constraints that limit the use of the land only for those areas that are identified as wooded or intended for pasture, with different time frames, namely:

1. **fifteen-year constraints:** the intended use of wooded areas and pastures whose stands have been crossed by fire cannot be changed compared to the pre-existing fire for at least fifteen years. In these areas it is allowed only the realization of public works that are necessary for the protection of public safety and the environment. It follows the obligation to insert on the aforementioned areas an explicit constraint to be transferred in all the deeds of sale stipulated within fifteen years of the event;
2. **ten-year constraints:** in wooded areas and pastures whose stands have been crossed by fire, the construction of buildings as well as structures and infrastructures aimed at civil settlements and production activities is prohibited for ten years, except in cases where municipal authorization acts have already been issued for this realization on a date prior to the fire on the basis of the urban planning instruments in force on that date. Grazing and hunting are prohibited in such areas;
3. **five-year constraints:** on the aforementioned stands it is forbidden to carry out reforestation and environmental engineering activities supported with public financial resources, except in the case of specific authorization granted either by the Minister of the Environment, for state protected natural areas, or by the competent region, for documented situations of hydrogeological instability or for particular situations in which an intervention to protect environmental and landscape values is urgent.

Active forest management - post-fire forest reconstitution in Montiferru-Planargia

In the summer of 2021 around 13,000 hectares of forest, shrubland, meadow-grassland and uncultivated land were affected by the fire, involving no less than 11 municipalities - Bonarcado, Santu Lussurgiu, Cuglieri, Sennariolo, Scano di Montiferro, Tresnuraghes, Flussio, Tinnura, Magomadas, Suni and Sagama - affected to varying degrees and intensities (**Figure 29 and Figure 30**). The fire was triggered by the breakdown of a car that caught fire along the S.P.15 Bonarcado – Santu Lussurgiu on 23 July. Initially it had affected approximately 20 hectares and it had been contained by fire engines and then cleared. The next day (July 24, 2021) however, at the height of a period of persistent drought and scorching heat (confirmed by fire risk warning bulletin from the Civil Protection) with maximum temperatures above 30 °C and locally measured above 40 °C, with sirocco winds with an average speed of around 14 km/h and maximum speeds of up to 35 km/h, the fire was reactivated. The geomorphological structure of places with narrow gullies carved and shaped by the water and vegetated on both sides produced flame heights of 30-40 meters indicated by the testimonies of firefighting personnel.

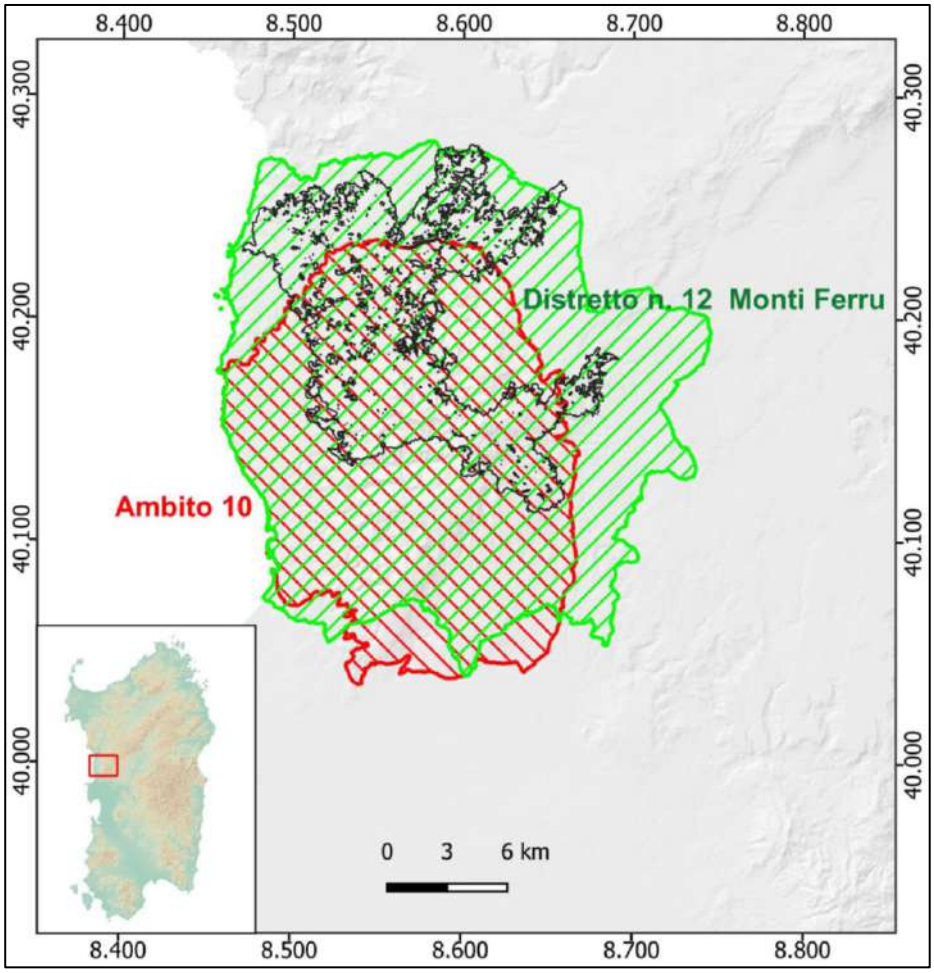

Figure 29. Montiferru territory included in Area 10 of the Regional Landscape Plan (red) and in District 12 of the Regional Forestry and Environmental Plan (green). The area covered by the fire is in black

Within one day the flames involved thousands of hectares of forest, various types of crops and pasture, arriving at the gates of the Municipality of Santu Lussurgiu and surrounding and besieging, in a subsequent phase, Cuglieri, Sennariolo, Tresnuraghes and Scano di Montiferro. Many productive activities were affected by the great event which presented itself as a critical fire rural urban interface and to safeguard

the physical safety of people and property, the mayors, more resumed, they had to arrange for the evacuation of several families. The fire spread towards the internal areas, towards the south and towards the north, reaching the coast in Porto Alabe, proving physically difficult to contain and therefore classified as a Mega fire (Extreme Wildfire Events) with characteristics that exceed the machine's ability to control organizational (exceeding 10,000 kWm-1, propagation speed of 3 km/h).
On July 25th, 2021, the emergency was proclaimed, and the Department of National Civil Protection has requested the activation of the so-called Civil Protection Mechanism of the European Union (EUCPM), following which France sent two Canadairs from the European Civil Protection Group and two others were sent later from Greece by the Center Emergency Response Coordination (ERCC). These four vehicles joined the five already operatives who supported the helicopters in operation to support the ground teams of the Fire Brigade Fire, FoReSTAS, Forestry Corps, Civil Protection, volunteers, and law enforcement.

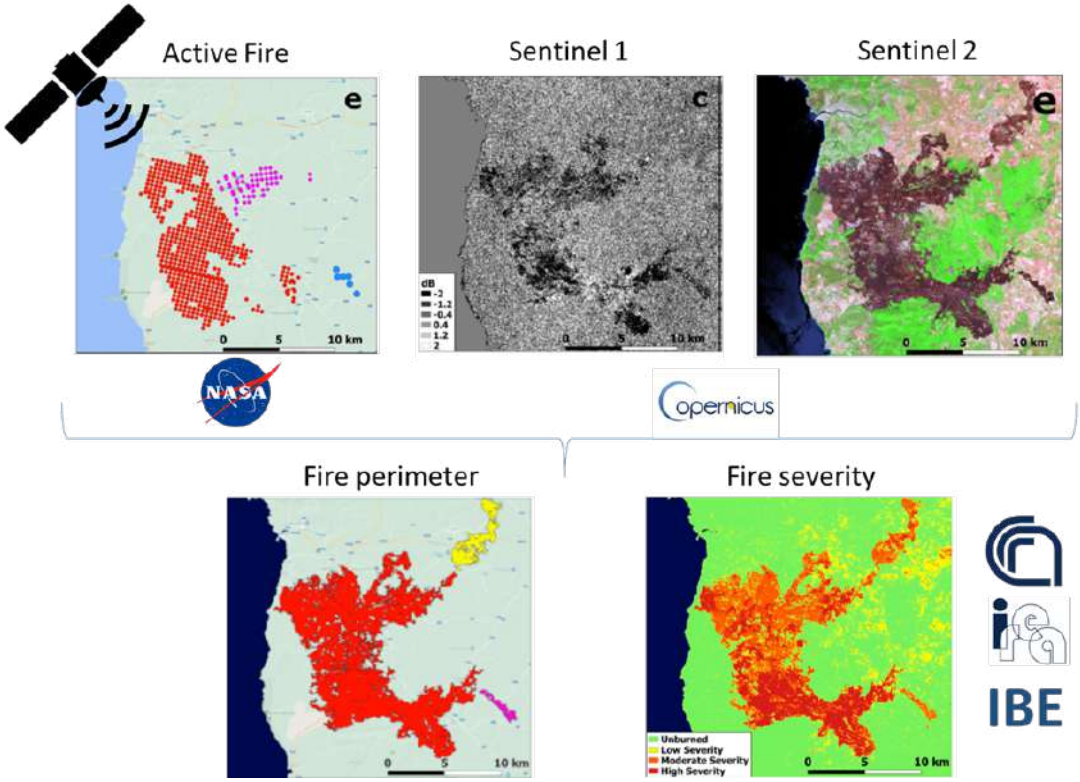

Figure 30. Top: satellite data used for the analysis of the event (Active Fire, Sentinel-2 and Sentinel-1 optical images). Below: maps of the results obtained (extension of burned areas and severity of the fires)

The forest formations affected were mainly *P. pinea, P. halepensis, P. pinaster, P. canariensis and Quercus ilex and suber* made artificially and followed by reforestation in the 90s. The undergrowth was mainly made up of scrub evolved meditteranea such as *Ardutus unedo, Erica scoparia, Phillerea angustifolia, Callicotome spinosa, Cistus sp, Mirtus communis, Juniperus sp.* and sp. various. Furthermore, in the "Riu Suelzu" area, a portion of artificial cork forest was affected by the fire, and in some area's portions of medium and poorly developed Mediterranean scrub (**Figure 31**).

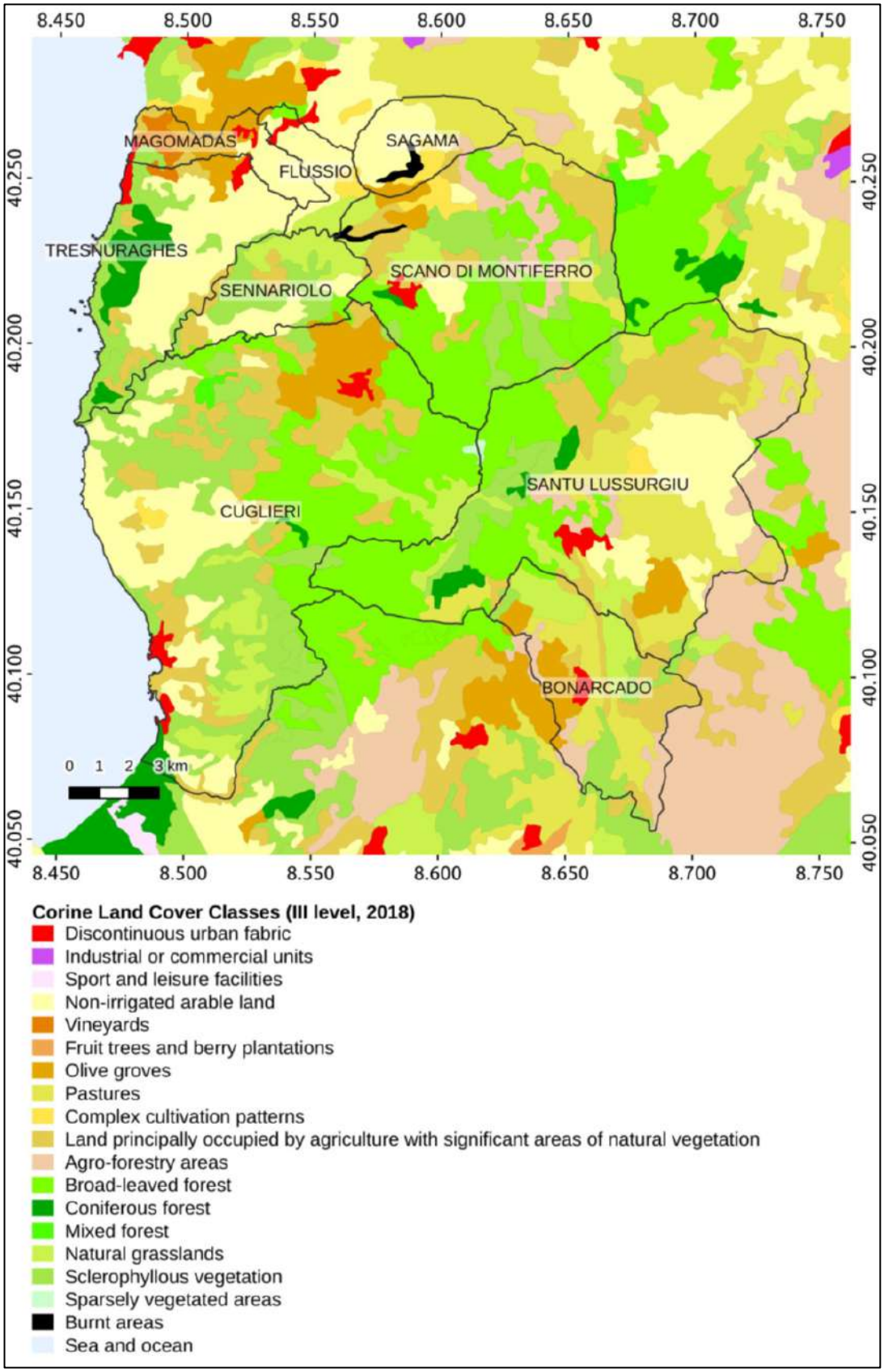

Figure 31. Land cover map. Processing using third level classification of the Corine Land Cover 2018

In the areas affected by the fire of July 2021 in the areas of public property of the municipality of Santu Lussurgiu-Cuglieri under a 30-year concession and those of the municipality of Tresnuraghes, forest reconstitution interventions will be carried out by cutting dead or severely compromised trees as a result

of the fire. The intervention essentially consists in the elimination of the burnt and dead aerial parts, following cutting with the aid of chainsaws at the collar of the trees. The resulting materials may be arranged according to contour lines in areas with a greater slope, ensuring adequate soil coverage and limiting runoff phenomena as much as possible. In areas where the road system allows it, woody material of an adequate size will be given in concession to local populations through special assignment notices. Forest reconstitution can be carried out by following three routes as a priority:

1. Mechanical forest reconstruction, in areas affected by fire, with the aid of specific mechanical means. consisting of the cutting and clearing of dead or compromised individuals as a result of the July 2021 fire. This includes the following operations: cutting, felling, and hauling. If necessary, limbing, depeeling, removal of the resulting material, any succession or tramming of single individuals or stumps or groups of individuals on broad-leaved trees of the Mediterranean maquis. Felling of all conifers burnt or compromised as a result of the fire. Operations will be carried out on land with high operational difficulties. Felling may be carried out with the aid of mechanical means such as an excavator or harvester or wheeled tractor equipped with hydraulic forestry pincers or shear or cutting system with hydraulic saw or similar.
2. Manual forestry reconstruction, in areas affected by fire, with the aid of professional chainsaws consisting of the felling and trimming of plants that cannot be reached due to unfavourable conditions by mechanical means. The intervention will be carried out with a specialised operator. In addition, manual trimming will be carried out on broadleaf tree stumps following the passage of mechanical means that, for various reasons, cannot be carried out at the collar. If necessary, the resulting stumps will be placed in an orderly manner on the fall bed.
3. Mixed forest reconstruction, in areas affected by fire, with the aid of mechanical means and chainsaws.

The various steps described above must be followed in part, depending on local conditions.

Debarking from the fall bed of woody material in whole trees or parts of trees-trunks (firewood or other low-value assortments) with a useful diameter greater than or equal to 8 cm, from the felling site to the imposed, (depending on local conditions) placed at the edge of the slope in plots and stacked in homogeneous and orderly piles. Felling must be carried out using mechanical equipment (skidder or forwarder) or a 4x4 wheeled tractor equipped with a 4x4 tractor and/or a 4x4 towed forestry winch with hydraulic loading clamp or other suitable equipment with the same or better characteristics.

Formation of rows and arrangement parallel to the contour lines, in areas with a steep slope and where runoff is possible, the felled branches and trunks will be arranged in rows parallel to the contour lines to limit runoff and soil leaching. Chopping of the resulting material, special chippers will be used to grind the material and release it on the ground.

These interventions aim to achieve, in the medium term, the reconstitution of the mixed broadleaf stand affected by the fire, operating according to the methods seen for coppice (succession, tramming and coppicing, pruning of dead or severely compromised branches) and undergrowth control interventions aimed at reducing potentially combustible biomass and thus preventing fires. Interventions aimed at encouraging both gamic and agamic regeneration of the stands affected by the July 2021 fires. Within the Forest Presidia, the area affected by the fire that is to be subjected to forest reconstitution intervention, is mainly characterised by the presence of a variegated stand depending on the genesis and climatic and edaphic conditions, which can be summarised as follows.

- Interventions of forest reconstitution on stands of natural origin such as holm oak or holm oak forests with a strong component of evolved Mediterranean scrub;
- Interventions of forest reconstitution on stands with the main component being Mediterranean scrub in the various evolutionary phases;

- Interventions of forest reconstitution on stands with garrigue;
- Interventions of forest reconstitution on stands of artificial origin with coniferous stands;
- Interventions of forest reconstitution on stands of artificial origin with coniferous and broadleaf stands with components of the Mediterranean maquis;
- Interventions of forest reconstitution on stands partly of artificial origin with predominant cork and more or less evolved Mediterranean scrub component with the presence of pinus sp and eucalyptus sp (Presidio Forestale Tresnuraghes);
- Other marginal plant components;

The described stands, especially those mixed with planted broadleaf and coniferous trees, consist of different types such as: portions of weakly maturing coppice, limited coniferous areas and, finally, vast areas with artificial plantations of Mediterranean and non-Mediterranean conifers (which have never been subjected over the years to gradual deconiferament interventions aimed at renaturalising the forest stand) that dominate the underlying planes made up, in the most fertile areas, of holm-oak coppice and, in the poorest and most degraded areas, of more or less evolved Mediterranean scrub. There are residual areas with the presence of a mixed broadleaf stand made up of vegetation types such as: weakly maturing coppice portions and areas with coniferous holm-oak coppice.

In carrying out the above-mentioned forest reconstitution operations, particular care and attention must be adopted to manage the numerous and extensive pine regeneration nuclei that will be created in the coming years. In fact, a well-known phenomenon, following the passage of fire on coniferous stands, it is evident that the pyrophilous species renew themselves with great vigour. Therefore, in the following years, the evolution of these stands will have to be monitored to create the best conditions for a prompt and rapid colonisation of the area covered by fire. Transects and witness areas will be identified in these areas, where useful and valuable surveys on regeneration (density, distribution, height, and vegetative state of seedlings) will be carried out for a few years and, therefore, on the capacity for vegetative recovery following the passage of fire.

Through these operations, the intention is to reconstitute the vegetation cover and improve the ecological conditions of the stands damaged by the July 2021 fire. The interventions will also bring, in the long run, undoubted productive and economic benefits.

Post-forest replanting of fire-affected areas

On the portions subject to forest reconstitution interventions, areas affected by fire or in the clearings and places where there is no concrete existing forest matrix, it is necessary to proceed with the planting of forestry post-humans from Forestas nurseries. Holes will be drilled by hand in the vicinity of clusters and clearings that existed before the fire or that were formed following the passage of the fire, with the aim of renaturalising the areas, recovering degraded forest systems and thus restoring the vegetal cover with undoubted benefits from the point of view of: hydrogeological defence, aesthetic-landscape function, nature, fauna (with species that are also suitable for wild animals such as cherry trees, walnut trees, hazelnuts), etc. etc.

The replanting of young plants will allow a prompt environmental recovery of the areas devastated by the fire and will also ensure the feeding of wild animals over time.

Regularisation of agamic and gamic regeneration after forest restoration in fire-affected areas

On the portions subjected to forest reconstitution interventions in the previous year or previous years of the areas affected by fire, it is necessary to regularise and optimise the natural regeneration that will be

established in the years following the main intervention, i.e., forest reconstitution. The main objectives include the following interventions on active and passive pyrophilous species:

- Control the regeneration of seed-born conifers on the regeneration cores that will be created both in space and time;
- Control and regularise the suckers of forest species on individual stumps;
- Adopting appropriate silvicultural measures depending on the species and local conditions;
- Defending natural regeneration from possible interference by wildlife (mouflon, deer, etc.);

The interventions will ensure the success of recolonisation and will allow a prompt environmental recovery of the areas devastated by the fire, the recovery of degraded forest systems and therefore the restoration of the vegetal cover with undoubted benefits from the point of view of hydrogeological defence, aesthetic-landscape function, naturalistic function, fauna, etc.

Cultivation care after forest restoration in fire-affected areas

In some areas it is necessary to proceed with the cultivation of the young plants planted with the replanting carried out in previous years, with the main objective of speeding up the recovery of degraded forest systems and thus restoring the vegetation cover with undoubted benefits in terms of hydrogeological defence, aesthetic landscape function, naturalistic function, fauna, etc.

Cultivation care for the young plants planted with replanting will allow a prompt environmental recovery of the areas devastated by the fire.

b. <u>Interventions related to coniferous forest management and mixed management.</u>
Thinning and thinning operations of conifer-dominated artificial stands

On the artificial stands, predominantly coniferous, operations will be carried out with the objective of renaturalising the areas, with the recovery of degraded forest systems. This intervention will take place in the Montresta PF, where there are several reforestation systems created, in the 'Tucuralvure' and 'Cugurrera' areas, by the municipality in the 1980s. These are pine forests at maturity stage, with a strong presence of broadleaf trees, particularly holm and downy oak and cork and other scrub essences, which have undergone modest silvicultural interventions in the past, limited to partial stripping and an initial thinning phase. Therefore, it is necessary to intervene by means of stripping and thinning operations in the other parts to be renaturalised, with the ultimate objective of obtaining a quality stand, with a multi-species and multi-layered composition that ensures, at the same time, the improvement of the conditions of stability. The intervention will produce evolutionary processes that create the ecological prerequisites for the establishment and further affirmation of the natural regeneration of species other than those present on the dominant plane, with the regular development of the deciduous subjects already present, to allow for the increased resistance and resilience of the biocoenosis to parasite attacks (insects and fungi) and with the increase in available biomass. In the continuation of the interventions, it will be essential to monitor the evolutionary dynamics to verify the functionality and degree of the regeneration and affirmation processes. In particular, work will be carried out on the most promising conifers in terms of retractable assortments by means of limbing aimed at reducing the knottiness of the stems and, therefore, favouring greater mechanical homogeneity of the wood, with the ultimate objective of producing construction timber of better technological and, therefore, commercial quality.

On the one hand, the removal of the released trees will ensure the start of the renaturalisation process with the gradual establishment of the native vegetation, development, and establishment of the seedlings of the understorey, and on the other hand, the improvement of the resinous stand left standing. Wood

piles will be produced and given to the local population. The resulting materials may be given to the local population and the others arranged in cordons or chipped or chopped according to local conditions.

Moderate thinning of simple or matriculated coppice

The thinning of holm oak and downy oak coppice or mixed coppice with the release of matricinees, in numbers even higher than those provided for by the current PMPF (General and forestry police regulations of the Sardinia region), is an intervention that favours the coexistence of coppice and high forest, determining greater stability of the stand in the short term. The resulting material may be given to the local population and the others arranged in cordons or chipped or chopped according to local conditions. The cut will concern underdeveloped, malformed, perishing, and supernumerary suckers, releasing one to three per stump and the most vigorously developing matricinas. Intervention will have to be particularly cautious in that, at least at present, although this is feared in the future, interventions will not be carried out in any way like those of start-up, but rather to reshape the traditional methods of coppice treatment in the form of less intensive use. Interventions will therefore be extremely gradual and targeted, to allow, on the one hand, the achievement of the long-term objective of partial conversion into a forest, and on the other, the temporary maintenance of the current form of governance.

The intervention to be carried out on the simple or matriculated coppice, is aimed at favouring greater homeostasis of the forest stand, by increasing stability and ecological resilience. The long-term result is a mixed, biplane (with the shrub component consisting of Mediterranean garrigue) and uneven-aged stand, to be treated according to the modern dictates of naturalistic silviculture. The intervention also aims to regularise the strong presence of downy oak, which is particularly exrophilous and competitive with cork and holm oak. Wood piles will be produced and given to the local population. Through these operations, the intention is to reconstitute the vegetal mantle and improve the ecological conditions of the stands damaged by biotic and abiotic adversities; in the long term, the interventions will also bring undoubted productive and economic benefits.

Reconstruction of forest on cork oak forest affected by fire

Cork tree reconstitution will be carried out on areas degraded by fire and on cork tree areas in a precarious vegetative condition in the "Riu Suelzu" locality within the Tresnuraghes PF. The viability of the species and its survival are certainly correlated to the extent of the damage to the aerial apparatus, the thickness of the cork, the degree of ground cover and the presence of other species present in the vicinity of the cork trees.

In this case, in the "Riu Suelzu" locality, there is a cork oak forest, partly of artificial origin, dating back some 20/30 years, and a spontaneous component deriving from the old matrix that existed in the past. The planned recovery intervention consists of simple pruning on individuals that have passed the critical phase, with the elimination of the portions of dead branches. On some individuals that show damage to the leaf apparatus, pruning will be carried out to allow for a balanced reconstitution of the foliage and thus favour growth and productivity recovery processes. Another fundamental operation to be performed during the reconstitution phase is coppicing, which consists in cutting the poorly formed, over-numbered, overgrown suckers, mostly originating from the development of adventitious buds. The cut, carried out using a chainsaw, must be performed in a workmanlike manner, creating a convex surface to avoid water stagnation and possible attack by parasites.

The interventions described represent the most effective action to favour the regeneration of a stand that has been severely compromised by fire or damaged by other factors, and allow, in the long term, the establishment of a climatic vegetation in dynamic equilibrium with the parameters of the climate and edaphic parameters. Obviously, the intensity of the operations, particularly coppicing, is in relation to the

intensity of the damage and the initial conditions of the stand. These interventions will ensure that the treated plants will quickly return to production or reach, after about 15 years, the circumference diameters that will allow eventual demasking with consequent putting into production of the individuals that have reached the decortication diameter.

Interventions related to utilisation and cultivation cuts or forest reconstitution

Within the framework of the various forestry utilisations, a series of complementary interventions are foreseen that are closely connected to forest cutting and utilisation. Sometimes these are necessary to allow the products to be used promptly and the stand to be maintained. They concern, first, the removal of timber from the fall bed at the first useful transportation point, to be carried out by hand or with the aid of polyethylene paddles in the appropriate slope conditions. Another onerous but necessary operation is the removal of the branches, which can be used to make bundles or, where possible, to arrange them in windrows, which can also be useful, if properly carried out, to form erosion barriers. Obviously, removing brushwood from the stand means performing an effective preventive action against forest fires. The same is valid for preventive forest clearing to be carried out conditions to facilitate subsequent silvicultural operations. The resulting material will be burned (in conditions of difficult natural mineralisation) or deposited/returned in the areas affected by cutting in order to feed the organic component of the forest soil or, to a small extent, taking into account the obstacles to transit represented by the morphology of the sites, chipped with the aid of special chipping machines carried by tractors.

It seems obvious that the interventions described are essential for proper silvicultural action and sustainable forest management. Furthermore, consideration will be given to the possibility that subjects outside the Agency may be interested in the utilisation of combusted or partially combusted biomass for use as an energy resource to feed biomass power plants. Expressions of interest will therefore be made, and plots will be assigned to cooperatives or companies operating in the forestry sector and having specialisations and equipment suitable for this intervention. Therefore, the forest reconstitution interventions, as described above, will be carried out in part by workers belonging to the Montiferru Planargia Forestry Corps and in part delegated to entrepreneurial subjects, in single or associated form, registered in the business register at the competent Chamber of Commerce and operating in Sardinia, in other Italian regions or in EU Member States.

4.2.1.3 Sterea Ellada – Central Greece

4.2.1.3.1 Location/ Administrative

The pilot area for Greece is the island of Evia, and more specifically its northern part as well as apart from the center of the island due to its characteristic mountainous area of Dirfys.

The island extends along the northeastern shores of Attica, which is separated by Northern and Southern Evia Bays. The eastern coasts of the island are in the Aegean Sea, while the western coasts are in Evoikos gulf. In terms of geographical coordinates Evia spans from the latitude of 39.00 N (northernmost part - Cape Artemision) to 37.95 N (southern part – Cape Mandili) and a longitude of 22.81E (western part) to 24.59E (most eastern part). The total pilot area is approximately 1.868 km^2 (**Figure 32).**

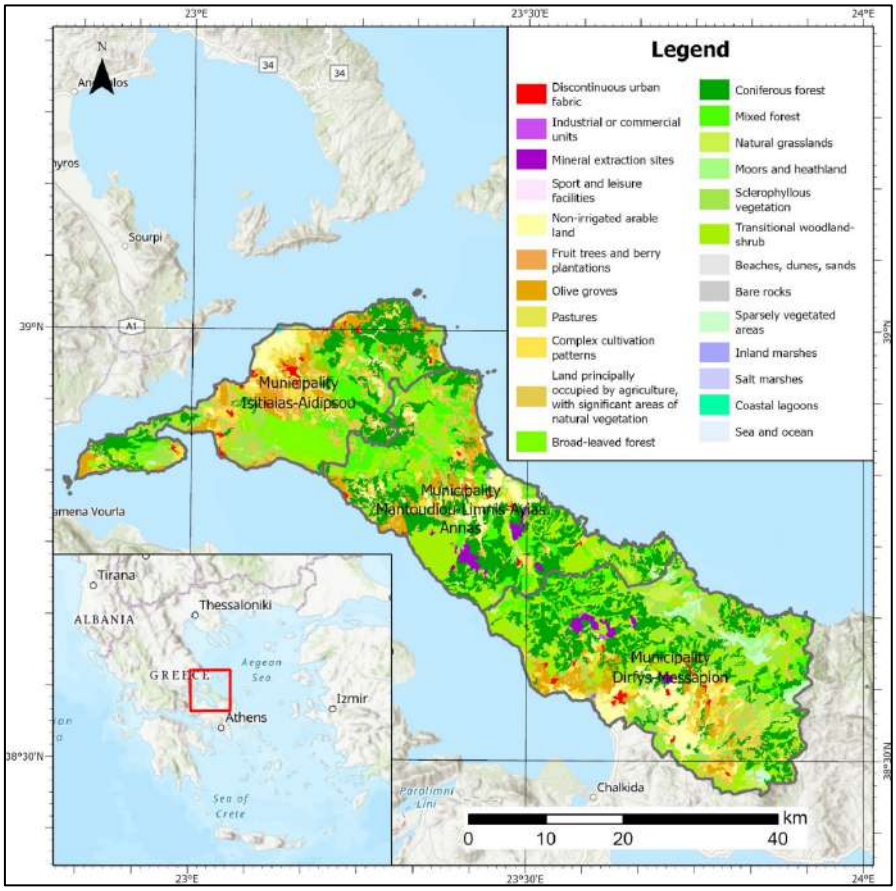

Figure 32. Land cover of North Evia pilot area from CORINE 2018-2021 (D6.1).

In terms of administrative borders, three municipalities are in the pilot area, specifically the municipality of Istiaia-Aidipsos, the municipality of Limni-Mantoudi-Ayia Anna, and the municipality of Dirfys-Messapion.

The forested part of the study area is under the administration of the corresponding local forest services that belong to the Ministry of Environment and Energy.

The maximum altitude of the area is equal to 989 m, while the average altitude is 331 m. 27% of the area that burned during the August 2021 fire has an altitude of less than 200 m, 35% of it is between 200 and 400 m, while only 9% is above 600 m. The slopes in the area vary. The average slope is 32.8%, while the area with a slope of more than 50% is 19%. For the SILVANUS study area (the whole North Evia of three municipalities) the mean slope is (25%) 14°, slightly different as plains and valleys are also included. Nevertheless, as many forests in the area occur in the mountains an average slope of 33% is more representative.

Vegetation: The forest species that dominate in the forests of Evia are Aleppo pine (Pinus halepensis), fir (Abies cephalonicae), Black pine (Pinus nigra), and from the broadleaf, oak (Quercus *sp.*), chestnut (Castanea sativa) and, in small areas other species, such as *Platanus orientalis* and *Acer sp*. More specifically:

- *Pinus halepensis,* occupies a significant area, especially in the northern part of the Evia and forms pure clusters up to 500 m by altitude.
- *Abies cephalonica,* occupies areas above 500m in altitude and is found either pure or mixed by person, groups, and lochs with Black Pine (*Pinus nigra*).
- *Pinus nigra,* occupies a small area, shows good growth, and where there is a mix of fir forms dense clusters.
- *Platanus sp*., develops on the banks of rivers and in the large streams that exist in the study area.

- Quercus *sp.* Usually found in mixed forests with pine or develop small forests on its own**.**

4.2.1.3.2 History of Fires

The number of fire events in Evia ranged from 76 to 114 per year. The fire season in Evia typically occurs from May 1 to October 31, with the highest forest fire numbers observed in June, July, and August. There is also a notable occurrence of fires in March, possibly due to negligence or arson for the creation of pastures. The climatic conditions based on data of neighbouring stations (Skyros and Lamia) for the fire period are as follows: a) winds in Evia are from the north to the northeast (N-NE) with an average speed of about 4 m/s; b) average temperatures, the average minimum is equal to 18.5 °C and the average high 28.6 °C, daily maximum temperatures can exceed 40° C, d) average air humidity for the fire season is 61% e) average precipitation, only for July and August, is about 5 mm in (Technical Chamber of Greece, 2010).

Most of the fires in Evia burn relatively small areas. Approximately 98.8% of fires burnt less than 30 ha, 98% burnt less than 10 hectares, and 93% burnt less than 1 hectare. Nevertheless, 1,2% of fires are more than 30 ha, and the mega-fire of 2021 burned more than 500,000 hectares (Hellenic Fire Service[1]).

Fire durations varied, with observed fires lasting from a few minutes to more than 3 days. The 2021 mega-fire in Evia lasted at least 10 days. Many fires (62%) had a duration of 1 to 12 hours, while approximately 4% lasted more than 72 hours. Fires lasting less than 1 hour accounted for around 18% of the total, while fires lasting 1 to 3 days accounted for approximately 6.4%.

Figure 33. Representative pre-fire pine forest status in the Greek pilot area.

The fires in Evia are a mix of surface and crown fires, with crown fires being the predominant type due to the prevailing pine tree species and the accumulation of big quantities of forest fuel due to poor forest management (**Figure 33**).

[1] https://www.fireservice.gr/el_GR/synola-dedomenon

4.2.1.3.3 Forest management, prevention, and restoration activities/programmes/strategies

In general, the restoration process of a burned forested area is given in the Deliverable D6.1 and specifically in the subchapter "6.1.3 Sterea Ellada - Central Greece".

Post-fire management: According to Greek law every burned area, public or private, that had been characterized by the Forest Service as a forest including shrubs, is officially declared as "under reforestation". This area cannot change character or use and remains intact for a period of 25 years maximum, to be reforested naturally or by artificial planting. In such areas, grazing is prohibited for the facilitation of the reforestation process.

Natural regeneration is the preferable method of reforestation due to the usual successful vegetation recovery by native species, as well as the access problems due to steep terrain and the high cost of artificial planting in such terrains. Only in some specific cases, artificial regeneration is the first-choice method, namely, in areas prone to soil erosion with poor expectations for natural regeneration, or in peri-urban aesthetic forests.

A catastrophic fire event happened during the August of the year 2021. The fire burned in the North Evia from 3 August 2021 to 11 August 2021. The report of the local Forest Service stated that in several local communities, the percentage of the burned area has exceeded 80% of the total area, and in some cases reaches up to 100% (Apostolidis et al., 2022). Mega fire of August 2021 is presented (**Figure 34**).

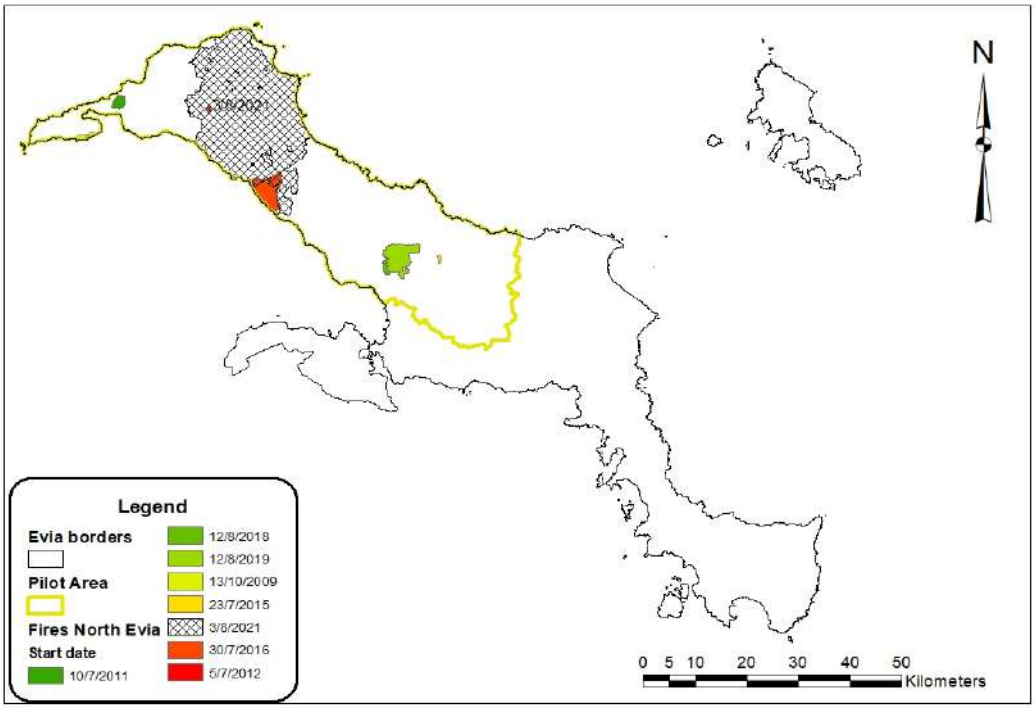

Figure 34. Bigger forest fires in the Greek pilot area.

The fire burned a large area, more than 50,000 ha, which included many types of ecosystems. Most of the 38,000 ha of burned forest consisted of pine. It is estimated that the populations of 800 to 900 plant species, were affected by the fire. It is expected that many of these species will recover by natural regeneration since they have developed adaptation mechanisms to fire.

Almost all known populations of 4 rare local endemic species suffered the effects of the fire. Among them is the Evia-Oak (*Quercus trojana subsp. euboica*). The fire has also affected the largest part of the population of 6 more local endemic species. A total of 10 local endemic species have been significantly affected by the fire.

Fauna impact assessment: In field missions, after the fire and until recently significantly fewer animals were recorded than before the fire. From the mammal fauna recorded the species: wild boar (Sus scrofa), fox (Vulpes vulpes), hare (Lepus europaeus), beech marten (martes foina). In terms of poultry, most species were recorded in riparian ecosystems, in orchards and crops near the settlements, and on the borders of burned and unburned lands. Within the burned areas and at a considerable distance from unburnt areas hawk and snipe species were recorded.

Main management goals and intervention plan

In the pilot area, up to now, the forest vegetation has successfully recovered in most of the burned areas by the natural regeneration of pine and shrub species (**Figure 35, a**). Also, in areas with relatively high soil moisture such, as in the bed and banks of currents, where broadleaved tree species prevailed, these tree species survived the fire and were sprouting leaves again (**Figure 35, b**). The ability of the local broadleaved trees to restrain the fire characteristics and transition as well as their survivability to the fire make them ideal natural candidates for future forest resilience increase.

After the destruction of the vegetation by the fire the soil erosion risk is high until the vegetation cover reaches a satisfactory density, this is intensified by the fact that the burned forest extends on rather steep terrain. Also, for the above reasons, flood risk in the lowland residential areas and agricultural fields is also high. For soil erosion and flood risk reduction, small works were constructed in sensitive areas (**Figure 36**), by using the logs of the deadened trees by the fire. The use of logs for protection works makes their construction easy and cheap. Moreover, it offers a temporary occupation to the local forest workers (loggers, resin collectors) who are unemployed since most of the related forest jobs have been lost due to the loss of the forest. The unemployment of forest workers as well as the reduction of tourism activity, due to the aesthetic degradation of the landscape, caused a major downturn of the whole local economy.

Due to the extent of the burned area and the impact on the local economy, additional projects are planned by the Greek state to help local communities recover. Plans that are already applied are related to support tourist activity by providing special allowances for beneficiaries of social tourism specifically for the region of northern Evia. Also, it has been proposed the planting of beekeeping plants, to aid local beekeeping activity.

The logging of burned trees should be reconsidered since up to now most of them remain in place. The wood of the dead trees can be used in various ways and the logging works would offer jobs to forest workers. Moreover, soon, dead trunks will be a hotbed for the excessive growth of fungi and insects that will threaten the existence of the newly growing forest through natural regeneration. Also, the dead trees that will fall to the ground in the future will be an important source of fuel for a new possible fire and at the same time will put obstacles to the access into the forest by foresters or firefighters. The consideration that logging will harm regeneration does not apply in practice given that in Greek natural forests, the regeneration is done by gradual selective thinning and there has been no problem with the success of regeneration. Delaying trunk collection exacerbates the above-mentioned problems and will become more detrimental to regeneration in case of future cutting, as young plants grow, and their stem lose flexibility.

(a)

(b)

Figure 35. Natural regeneration in the burned area (a) pine and (b) broadleaves sprouting leaves (photos of April 2023).

(a)

(b)

Figure 36. Works made of logs for soil erosion (a) and flood risk (b) reduction.

Main interventions for the prevention of severe fires and increase of forest resilience

The strategy to enhance forest resilience to wildfires is based on the following actions:

- Encouragement, through forest management, of broadleaved trees that are more resilient to fire than conifers where it is possible. The plan is to create forest zones made of broadleaved species along the rivers and torrents that could be used as shaded firebreaks in cases of fire since the broadleaved species have a higher resistance to fire.
- Encouragement through forest management of the development of mixed stands of conifers and broadleaved species that could reduce extreme fire characteristics and thus easy fire extinguishing.
- Creation of areas of fuel discontinuity through forest management both horizontally and vertically. This involves the opening and maintenance of fuel breaks to facilitate access for firefighting forces. Exploitation of agricultural cultivations and rangelands as well as roads for preplanned firefighting zones would help greatly the fire suppression efforts.
- Pruning of dead tree branches of the lower part of the tree stem, through forest management and complementary by the aid of beneficiaries of services provided by the forest, such as resin collectors, beekeepers, and shepherds will reduce the probability of transformation of a surface fire to a crown fire.
- The increase of free-ranging livestock grazing that already was applied in the past in the pilot area forests, after the forest recovery will keep in control understory biomass (fuel load). This contributes to regulating shrub biomass and exerts forest thinning influence and cutting of dead tree branches.
- Regular management of combustible biomass where possible, involving the utilization of dead trees and branches to produce useful biomass through mechanized methods.

Forest monitoring in the pilot area should become more intensive in the future through ground missions of multi-purposes nature e.g., forest management supervision, protection from illegal interventions, as well as by exploiting technological ground means (cameras in the visible and infrared-thermal spectrum), and aerial means such as drones and satellites.

The recovery of human activity in the nearby unburned forest such as logging, resin tapping, beekeeping, and ecotourism is important. Because all the forest workers have an interest in keeping the forest healthy and so guard it. In general, in the pilot area, since all the residential areas are near or surrounded by the forest, fire events quickly get noticed and referred to competent authorities by the citizens. The use of volunteers and technological means could greatly improve the early noticing of fire-starting events in remote areas or during the night.

4.2.1.4 Cova Da Beira – Portugal

4.2.1.4.1 Location/ Administrative

The pilot site is in Cova da Beira (study area) in Portugal, in a farm called Quinta da França. Quinta da França occupies a total area of 500 ha, where it holds a significant landscape diversity, partly driven by the presence of two water courses, the Zezêre River, and the Caria stream, and by the agriculture areas and for the 200 ha of autochthonous Pyrenean oak forest (**Figure 37**).

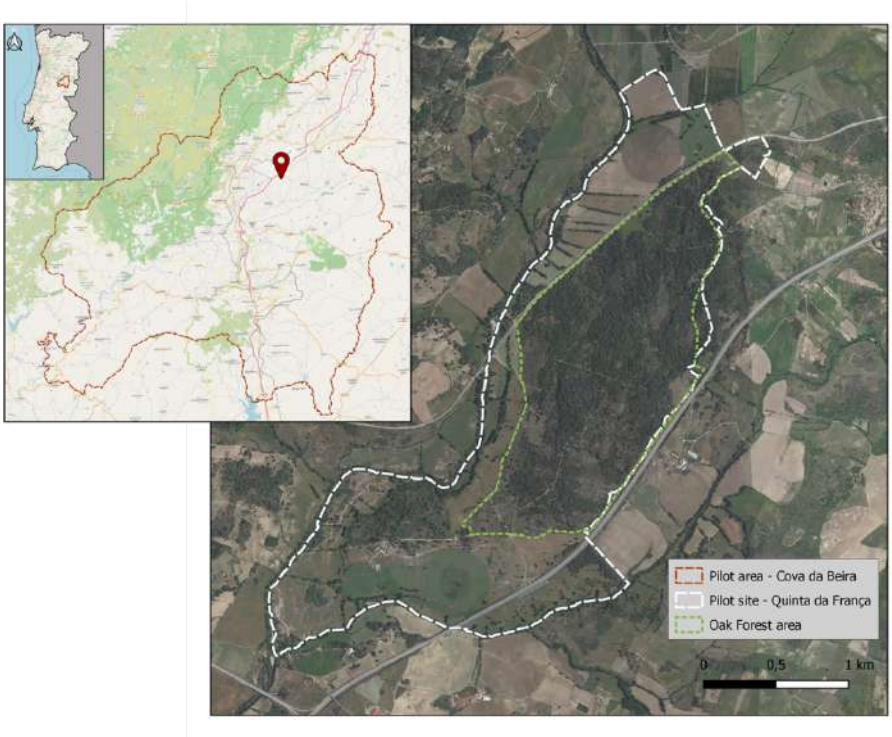

Figure 37. Cova da Beira (pilot area) region and location of the pilot site (Quinta da França).

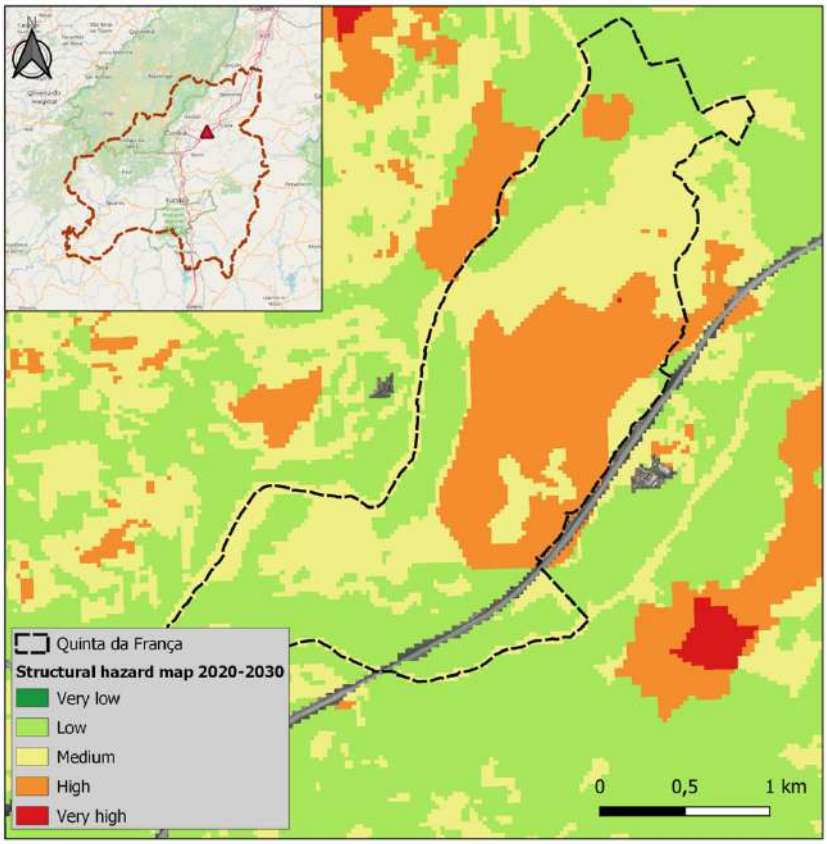

Figure 38. ICNF Structural hazard map to 2020-2030. Source: ICNF.

The 2020 structural hazard map from ICNF (Institute for Nature Conservation and Forests) identifies the oak forest area of Quinta da França as having a "medium to high risk" (**Figure 38**).

4.2.1.4.2 History of Fire

The recent history of fires at Quinta da França is mostly associated to the cessation of agricultural land use of the marginal land, in the areas of steeper slopes and poorer soils (i.e., the landscape unit where most oak forest is located). Until the mid-20th century, this area was used for grazing in natural pastures and for rye production, as these uses were abandoned, the natural processes of secondary succession started, giving place to the unmanaged regeneration of vegetation. Species with higher regeneration potential, in particular broom shrubs (*Cytisus* sp.), blackberry (*Rubus* sp.) and the oak (*Quercus pyrenaica*), expanded their cover contributing to increase the amount of flammable biomass and, therefore, increasing fire hazard. In the case of oak seedlings and sprouts (from vegetative regeneration) the early stages of natural regeneration are particularly susceptible to fire, due to the high density of stems and vertical biomass continuity in some areas.

The recent history of fires comprises two large and severe fires in 1984 (**Figure 39**) and in 1995 (**Figure 40**), which affected most of the 200-ha oak forest patch. After that, forest management actions have been implemented (as described in the next section) to reduce the amount of flammable biomass and create both horizontal breaks (clearings, corridors) and vertical breaks (removal/control of vegetation in the understory). There have been other fires in recent years, notably in 2007, which were controlled affecting much smaller areas and having less severe effects.

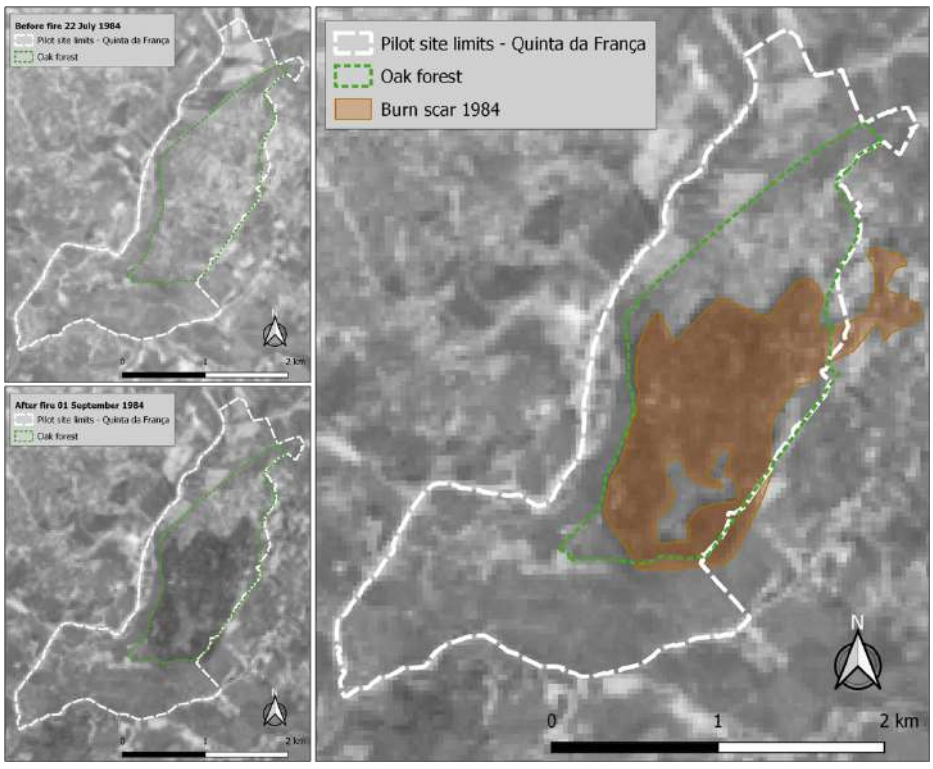

Figure 39. Pilot site before the fire in August 1984 (upper left); Pilot site after the fire in September 1984 (lower left); Delimitation of the burn scar in the oak forest (right). Source: Terraprima and ICNF.

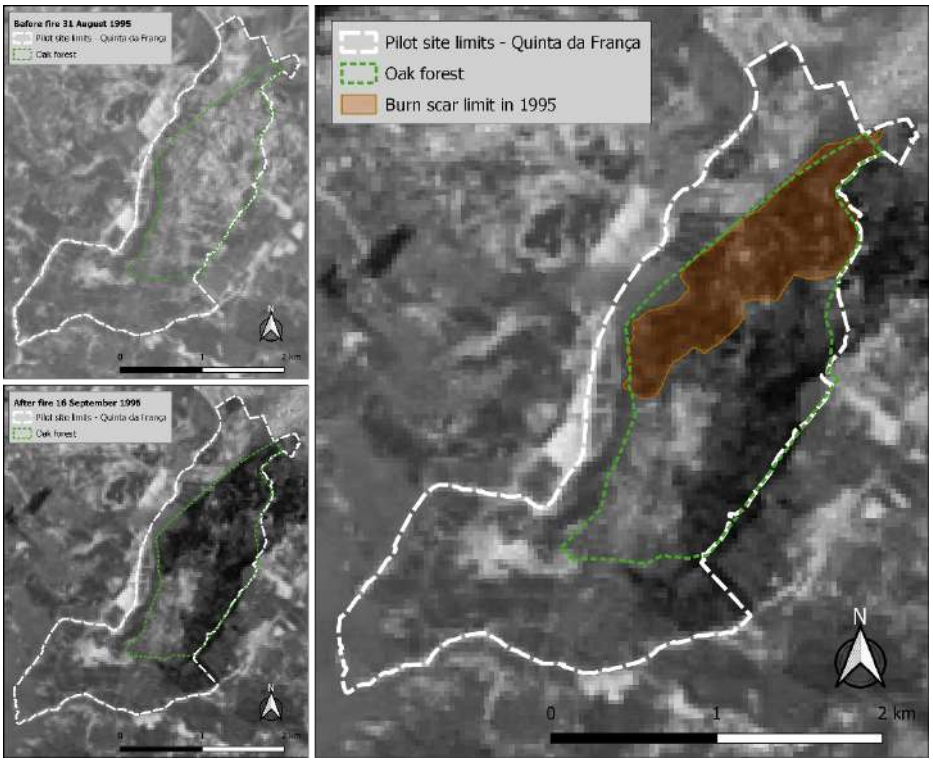

Figure 40. Pilot site before the fire in August 1995 (upper left); Pilot site after the fire in September 1995 (lower left); Delimitation of the burn scar in the oak forest (right). Source: Terraprima and ISA (SCAPEFIRE Project).

4.2.1.4.3 Forest management, prevention, and restoration activities/programmes/strategies

Brief characterization of the post-fire forest environment

The large wildfires in 1984 and 1995 impacted most of the oak forest pilot site. Since then, this area has been undergoing natural (assisted) regeneration, being managed for conservation purposes and for fire prevention. Presently, the area is characterized by a fine-grained mosaic of vegetation cover types, encompassing trees, shrubs, and herbaceous cover, and rock outcrops. These cover types occur intermixed, including areas of sparse tree-covered shrubland, areas of dense canopy with multi-layered understory, and small clearings with natural pastures and scattered trees, including some large mature individuals.

The tree layer has a diverse age structure, with some mature individuals, many young trees and saplings and frequent presence of seedlings. While the overall forest community is still in an early maturity stage, the stand includes areas with closed canopy and relatively tall trees that survived the fire or regenerated vegetatively after it.

The shrub layer is dominated by brooms (*Cytisus sp.).* These leguminous shrubs are characteristic of the sub-serial (regenerating) stages of the deciduous forests of *Q. pyrenaica* in Portugal. Being especially found in areas affected by fire or in abandoned agricultural land. This type of shrub communities tends to be species-poor, flammable and with low conservation value. The herbaceous layer is generally divers, but its richness depends on the composition of the upper layers, being poorer in areas dominated by brooms.

In general, although the biodiversity conservation value is still limited due to the early stage of maturity post-fire, the potential is high, justified by the diversity of species already present and the expected development of the oak forest stand.

Terraprima – responsible for forest management - joined and certified the management of its forest area at Quinta da França through the FSC certification system (Forest Stewardship Council,[2]) in 2008, as a way to demonstrate to third parties its commitment to the principles of sustainability applied to sustainable forest management.

Concurrently, carbon sequestration and storage have been leveraged as significant contributors to forest income, driven by the commercialization of ecosystem services. In 2006, Terraprima entered into an agreement with EDP to receive compensation for carbon storage activities spanning from 2006 to 2012(Terraprima, 2023). Subsequently, the rising popularity of the carbon voluntary market facilitated the maintenance of the certification for carbon storage covering the period from 2013 to 2021.

Main management goals and intervention plan

The management of the oak forest site aims not only at biodiversity conservation but also at the growth and production of deciduous trees, especially *Quercus pyrenaica*, with forestry and energy (biomass) value. Given the recent history of oak forest (natural regeneration occurring in patches, after wildfires), the coverage of the area by Pyrenean oaks is not uniform. There are patches of varying sizes and ages, interspersed with open areas (agricultural lands, pastures, or rock outcrops) or covered with shrubs (primarily brooms). Some of these initially tree-sparse zones have been afforested with pioneer species with high productive potential, such as *Pinus* and *Cupressus*.

From a forestry perspective, the general aims are as follows:

- To establish a resilient system able to cope with market fluctuations, climatic variability, and natural risks;
- To enhance and harmonize the following ecosystem services, seeking compensation for all of them: forest production (both for fuel and high-quality timber) and the associated carbon sequestration, forage production, soil protection, water cycle regulation, biodiversity, recreation (including hunting activities);
- To maximize synergies between forest production and agricultural production, such as introducing livestock grazing in the forest site.

The management plan for the oak forest site foresees the following interventions:

- Enhancing tree density in areas with sparse tree cover through the management of natural regeneration (where applicable) or by planting new species, including coniferous and broadleaf trees, to restore tree coverage and enhance tree diversity;
- Conducting periodic shrub control, primarily targeting dominant pyrophytic species, to mitigate the risk of severe wildfires and facilitate the establishment of diverse herbaceous communities;
- Implementing forest thinning and removal of lower branches to regulate stem density and ladder fuels and establish optimal conditions for the gradual growth of large oak trees over the long term;
- Eliminating trees exhibiting signs of disease or deformities to safeguard forest health and encourage the growth of a stand comprising trees with economic value, in line with a sustainable wood production model;
- Selecting specific trees to preserve, protect, and nurture over the long term with the goal of fostering their complete growth and maturation.

[2] http://info.fsc.org/

- ***Main post-fire interventions for rehabilitation and restoration***
- The existing forest, when Terraprima began managing Quinta da França, was characterized by the presence of a developed riparian gallery and a collection of forested areas in various stages of development. The large forest oak forest site (ca. 200ha) was characterized by the presence of patches of Pyrenean oak and tall brooms with varying degrees of Pyrenean oak regeneration, bearing clear signs of recurrent forest fires, the last significant one occurring in 1995. Following that fire, most of the affected trees were cut.
- The first substantial forest intervention took place at Quinta da França between 2003-2004 in a project co-financed under the AGRO Forest Development Plan. This project involved shrub clearing, fostering the natural regeneration of *Quercus pyrenaica*, correction of stand density and thinning of the more mature oak forest patches, and planting of new trees and species, including *Pinus pinaster* (maritime pine), *Cupressus lusitanica* (cedar of Buçaco), *Prunus avium* (wild cherry), *Tilia spp*. (lime), and *Betula spp*. (birch) in forest clearings. However, the hydrological drought that extended from 2003 to 2005 adversely affected the deciduous plantations, with most of the maritime pine and cedar of Buçaco stands surviving, albeit with some losses. In 2007, new maritime pine plantations were carried out, under a project co-financed by the RURIS Program, covering an area of approximately 33 hectares.
- Complementary to the above actions, the control of shrub encroachment was at the core of forest rehabilitation actions. Mechanized shrub removal took place in 2003 in most of the area, and in 2008 in selected areas. In April 2023, mechanical shrub control was carried out within the oak forest, in areas with higher biomass volume, and along the forest existing paths. Fire breaks paths were maintained clean and new ones were opened with a grader. Furthermore, forest thinning is done regularly in different forest areas considering the age and density of tree stems.
- The use of grazing as a restoration tool was initiated in 2018, with the introduction of free-ranging cattle in a forest section of about 100 ha (contiguous to pastures that are also used by the animals). The main management goal is to maintain both horizontal discontinuities (such as natural pasture areas) and vertical discontinuities (control of ladder fuels) within the understory due to vegetation consumption, trampling, and thinning of lower tree branches. Moreover, the animals also contribute for seed dispersal and to control small patches of invasive trees.
- Another important aspect of the forest rehabilitation and restoration is the monitoring and control of invasive species. In 2003, an intervention was carried out to eliminate the presence of acacias (*Acacia* sp.), which did not achieve the intended success. More recently, cutting followed by consumption of the new shoots by cows was experimented in one of the plots invaded by the species, which had a considerable positive effect on its control. In general, the total area occupied by acacias has remained stable, due to control measures in some areas and expansion into new areas.

Main interventions for prevention of severe fires and forest resilience

The strategy to enhance forest resilience to wildfires is based on four main types of actions:

- Creation of areas of fuel discontinuity both horizontally and vertically. This involves the opening and maintenance of fire breaks to facilitate access and firefighting efforts, the creation or maintenance of natural pastures in forest clearings, and the integration of rock outcrops into the network of discontinuity areas. Additionally, the introduction of free-ranging livestock grazing has been adopted (since 2018) as a means of sustaining both horizontal discontinuities (such as natural pasture areas) and vertical discontinuities (control of ladder fuels) within the understory. This

contributes to regulating shrub biomass and exerts a thinning influence by removing lower tree branches.

- Regular management of combustible biomass, involving mechanized shrub removal and the control of invasive species. Moreover, this objective is also pursued through the integration of livestock grazing within the forest site. However, due to the animals' free-ranging grazing pattern and the moderate stocking density, there is a requirement to supplement this approach with mechanized methods.
- Fire protection is further bolstered by the presence of several permanent ponds located within the agricultural fields (and some temporary and smaller ones within the oak forest), which also serve pastoral purposes. Various hydrant points from the Cova da Beira Irrigation System also contribute to fire protection. The existing forest pond does not retain water throughout the year, making it of limited interest for fire protection purposes.
- In the oak forest area, as part of forest fire prevention efforts, cleaning operations were also carried out along the forest road network, following the decree-law nº124/2006, which establishes the national Forest Fire Defense System. The Portuguese roads authority and the railway company also conducted cleaning operations along the road and railway lines that pass through or are adjacent to Quinta da França.

Forest monitoring

The implementation of the forest management intervention is supported by regular forest monitoring. In particular, the first forest inventory was conducted in 2007, with subsequent repetitions in 2011, 2013, and 2021. Additionally, as part of the commitments undertaken within the framework of sustainable forest management certification, the monitoring of pests and diseases has been conducted annually, with records available for reference. The presence of invasive species is also assessed annually, including an evaluation of their expansion status.

It should also be noted that the monitoring of conservation areas has been carried out over recent years, both due to the legal requirements of the Forest Management Plan (Canaveira et al., 2016) and the involvement of Quinta da França in scientific projects addressing forest conservation and sustainability through grazing. The monitoring purpose is to assess whether these areas and their identified conservation values are being maintained, improved, or degraded. Through monitoring, it is determined if the established management is effective, and if not, it identifies necessary changes.

At Quinta da França, four attributes are monitored, using both field data and aerial photography.

- Extent – this attribute includes the extent and, when applicable, the spatial distribution of relevant habitats. Regarding the oak forest site, it aims to evaluate the maintenance of the area covered and the evolution to more mature successional stages.
- Structure – It includes the balance between the tree layer and the shrub layer; the presence of long-lived trees and of forest clearings (natural pastures and rock outcrops); and the presence of dead trees.
- Composition (trees, shrubs, and herbaceous layers) - This attribute assesses the composition of the tree, shrub, and herbaceous layers, as well as any changes that occur. The favourable classification will be applied in the absence of non-indigenous species and the absence of any signs of accelerated loss (>10% over a five-year period) of species in the tree and shrub layers.

Potential for natural regeneration - of indicator tree and shrub species, specifically: Pyrenean oak, maritime pine, alder, ash, and willow.

4.2.1.5 Podpolanie – Slovakia

4.2.1.5.1 Location/ Administrative

The pilot location is in the Podpolanie micro-region, in the central part of Slovakia (**Figure 41**) – region Banska Bystrica, district Detva.

Figure 41. Location of the Slovak Pilot

The pilot area is agricultural – forest land, with forests in the northern part and agricultural land in the southern part (**Figure 42** and **Figure 43**).

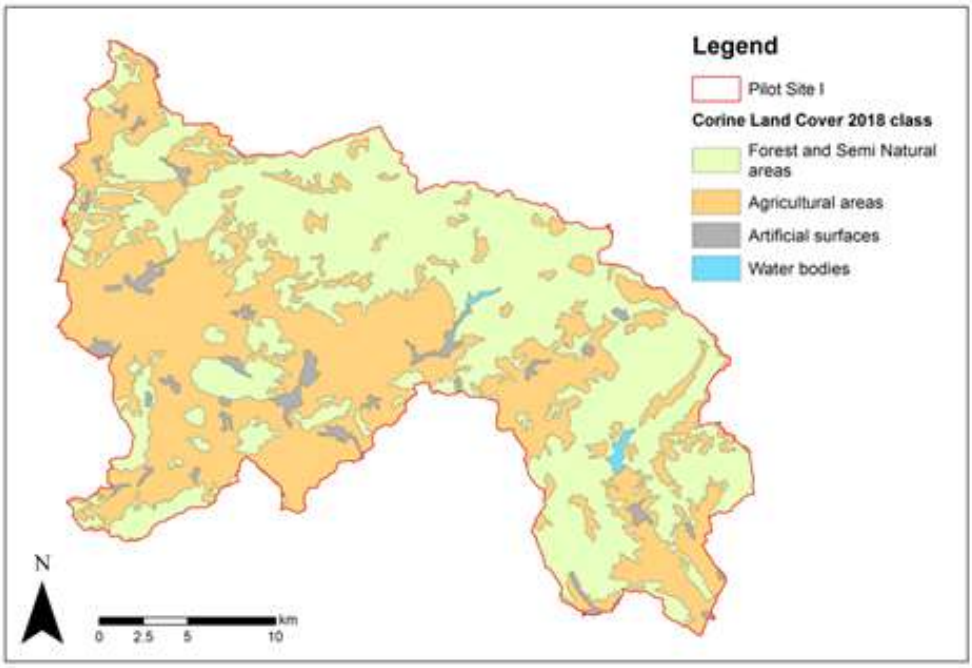

Figure 42. **Land use types in the Podpolanie micro-region**

Figure 43. Landscape of the Podpolanie micro-region

The northern part of the pilot site (almost forest) is under nature protection, particularly because it belongs to Protected Landscape Area Poľana - the Poľana Biosphere Reserve. Protected Landscape Area (PLA) Poľana was launched in 1981 for the protection of inanimate nature, plant, and animal communities, as well as a special landscape character, and declared on the territory of 20,360.48 ha. Of these, there are 3,001.41 ha of agricultural land, and 17,102.36 ha of forest land, 102.50 ha of water areas, 48.62 ha of urban areas and 105.60 ha of other areas. Agricultural land, such as mountain meadows and pastures, is either mowed or grazed by cattle and sheep. Re-cultivation in the recent past, to some degree, has changed the original floristic composition of the grasslands. Despite this, enough natural plant and animal communities is still present.

The forests existing in the pilot site area are managed and administered by the Forests of the Slovak Republic, S.E., specifically the Forest's branch plant Kriváň. The forest management plans are elaborated after the negotiation with the Biospheric Reserve Polana representatives as well as representatives of forest private owners' association.

4.2.1.5.2 History of Fires

In general, the wildfires in the Podpolanie micro-region are mostly caused by human activities. Most often, it is a deliberate human activity associated with the burning of agricultural and grassland areas close to the forest. This activity is typical throughout the territory, particularly in the spring and autumn seasons. It is most pronounced in the period of the survey of meadows and pastures in the territory of the Slovak Republic, which is carried out by the Ministry of Agriculture of the Slovak Republic and whose outputs are used for redistribution of subsidies for the haying of meadows and pastures to their owners or users. This is carried out at 10-yearly intervals. The last survey was carried out in 2022. The fire statistics for 2022 confirmed this fact. In this year also, the most extensive wildfire occurred in the locality of Tisovnik (**Figure 44 and Figure 45**).

Figure 44. **Wild fire consequences – transition from grassland fire to forest fire – Tisovník 2023**

Figure 45. Location of wildfire site in Tisovnik (March 2023)

The wildfire history in the region shows that the highest number of fires occurred in 2011 (89 wildfires), 2012 (160 wildfires), 2017 (83 wildfires) and 2022 (80 wildfires even in March). In 2023 the extremely hot year was not extreme in terms of wildfires occurrence in the region. The most common reason for wildfire initiation is negligence,or carelessness of adults, in particular the burning of grass and dry vegetation (e.g. in 2012 there were 160 wildfires, 153 wildfires due to negligence, 132 wildfires due to grass burning; or in 2017, 83 wildfires, 73 wildfires due to negligence, 51 wildfires due to grass burning).

4.2.1.5.3 Forest management, prevention, and restoration activities/programmes/strategies

Forest management in Slovakia is executed according to the Act on Forests, whose aim is to preserve, improve, and protect forests as a component of the environment and natural wealth of the country for the fulfilment of their irreplaceable functions; to ensure differentiated, professional, and sustainable forest management; to reconcile the interests of society and forest owners; and to create economic conditions for sustainable forest management. Since 2022, when forest management in the national parks and protected areas in Slovakia was transferred from the hands of foresters to the State Nature Conservancy organization, increased attention is being paid to nature conservation in this area over traditional forest management.

In terms of the Act on Forests, as well as the executive legislation arising from it, it is required to reforest the deforested forest areas (also affected by wildfire) within 2 years at the latest. So, any deforested area in Slovakia must be reforested in this interval. There are no special requirements related to forest restoration after the fire from the fire protection legislation or practice. Fire prevention is not a criterium for selection of restoration program.

There are no special requirements related to forest restoration after the fire in the fire protection legislation or practice. Fire prevention is not a criterion for selecting a restoration program. When a period with a high degree of fire danger is declared, everyone is obliged to comply with the principles of fire safety. It is forbidden to smoke, throw burning or smouldering objects, or use open flames on forest land and in its protective zone. Owners, administrators, or managers of forest land in connection with forest fire protection are obliged to ensure patrolling activities in forests and their protective zones, to place the necessary number of fire-fighting tools in a designated place, and to maintain existing passageways, bridleways, and water sources in a condition that allows for the smooth arrival of firefighting units and their use for effective intervention. Forest owners must also take special measures for areas affected by the disaster disturbance, to ensure the prompt removal of timber and other combustible waste, the creation of firebreaks to prevent the spread of fire, and the priority provision of forest roads and highways for fire-fighting equipment. Working machinery, such as forest wheel tractors, harvesters, and other vehicles used in the processing of timber and logging residues, must be equipped with fire extinguishers and effective spark arresters.

4.2.2 Non-European Pilot - Sebangau National Park – Borneo, Indonesia

4.2.2.1 Location/Administrative

Sebangau's forest and peatland were officially designated as a national park via Minister of Forestry Decree No. 423/Menhut/II/2004 on October 19, 2004, encompassing a total area of 568,700 hectares. Sebangau National Park is located across three districts/municipalities in Central Kalimantan Province (see **Figure 46**), with Katingan accounting for 52 percent, Pulang Pisau for 38 percent, and Palangkaraya City for 10 percent of its territorial extent.

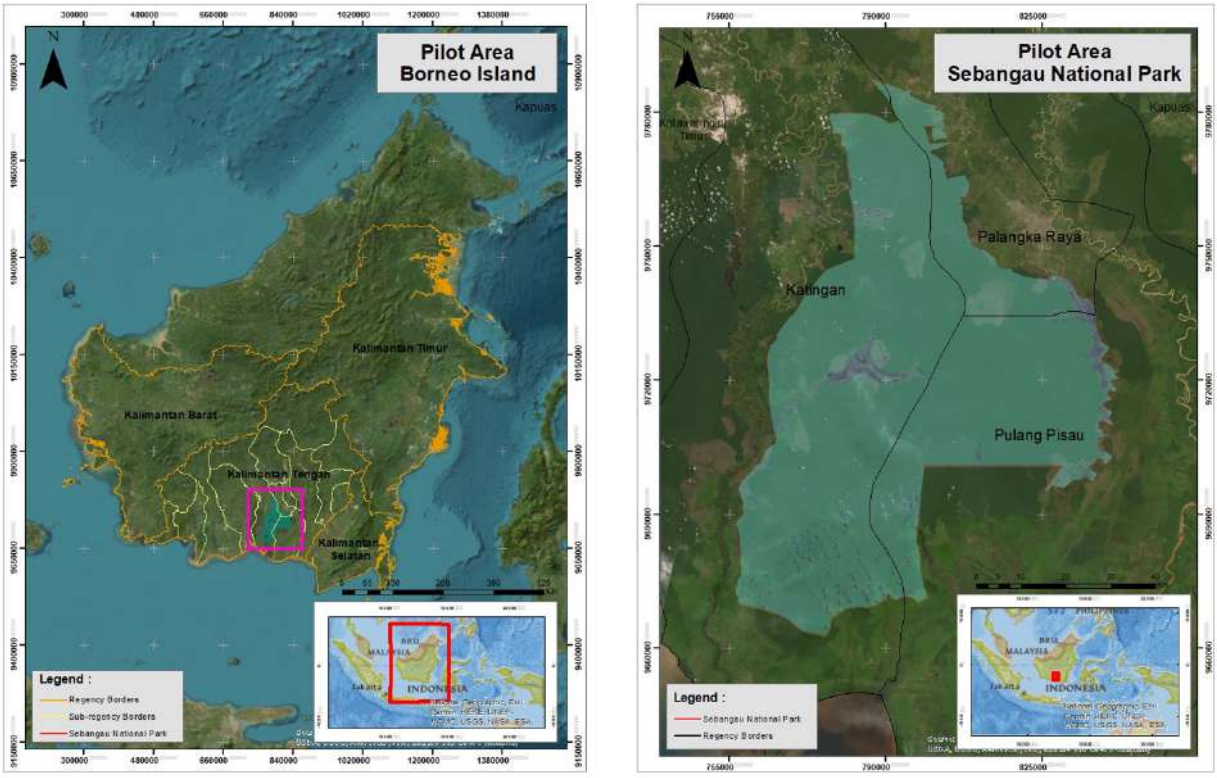

a. b.

Figure 46. a) Sebangau National Park Location in Borneo Island; b) Sebangau National Park Administrative

4.2.2.2 History of Fire

Sebangau National Park deals with the problem of forest fires mostly during the dry season. There are 54,236.87 ha of fires from 2011 to 2020 (Sebangau National Park). From 2011 to 2020, there are three years with the largest effect on the burned area, namely: 2014 (4,364.24 ha), 2015 being the largest one (47,264.54 ha), and 2019 (1,902 ha).

4.2.2.3 Forest management, prevention, and restoration activities/programmes/strategies

Rehabilitation management in Sebangau National Park consist of 4 programs, which are planting program, natural regeneration, canal blocking, and well construction. All programs have been (developed?) considering the characteristic of Sebangau National Park which is peat swamp forest.

Planting

The first programme is vegetation planting in the burnt area. During 2008-2017, an area of 10,944 hectare was successfully recovered. Systematic process conducted to provide suitable growing habitats for plants concerning ecological, physical, management, and social factors. The standard operational program followed to make sure that the program implemented effectively, efficiently, and no further environmental change is expected.

The rehabilitation process of planting activities in Sebangau National Park includes various activities with the following stages:

1. Socialization (pre, monitoring, and evaluation).
2. Survey of planting sites.
3. Preparation of technical plans.
4. Survey of seed abundance (natural extraction).
5. Training in nurseries and planting.

6. Procurement seeds.
7. Procurement of stakes.
8. Planting.
9. Procurement and installation of boreholes.
10. Monitoring and evaluation.
11. Maintenance.

The following information explain the detail process of rehabilitation classified in several stages.

a) Preparation
    1. Coordination with related institutions.
    2. Prepare plant design documents for planting locations block or area.
    3. Prepare implementing organizations such as implementing leaders or supervisors and labour.
    4. Develop a timetable for activities and a rational division of labour.
    5. Prepare areas for conflict and prevent conflicts between residents and workers by socializing.
    6. Preparing materials and equipment.
    7. Re-measurement of location boundaries and erection of plot boundary stakes.
b) Create land preparation work units.
    1. The land unit work unit consists of at least five people.
    2. The head of the work team oversees determining the location of the plant path and concurrently as an activity recorder.
    3. Two team members in charge of making and opening trails.
    4. Two team members manage of making stakes and installing markers in planting holes along the path.
c) Preparation of work equipment
    1. Preparation of land work map in 1:10,000 scale.
    2. Preparation of work equipment, including machetes/machetes, hoes, sign boards and other logistics equipment.
d) Planning
    1. Determine the location of blocks and work plots.
    2. Make a detailed work map of land preparation.
    3. Planning the workforce and budget required.
    4. Make a schedule for the implementation of land preparation work.
e) Implementation
    1. Look for markings for planting paths that will be made.
    2. Make a stub of a clean/plant path 1 meter wide.
    3. At each end of the path are marked with wooden stakes with a minimum diameter of 2 cm with a height minimum 130 cm.
    4. Determine the location of 40,000 holes or 800 holes/ha.
    5. Mark the planting hole with a stake.
f) Recording and reporting
    1. Name of block location and work tile.
    2. Number of planting paths in intensive cultivation - Planned type and number of plants in each plot.
    3. Number of working days that have been used, work performance, and quality profession.
    4. The register book is filled out every day of the activity.
    5. Records of monitoring and evaluation of work by the person in charge of the work unit land preparation.
    6. Activity reports and land preparation work maps must provide relevant information complete.
    7. In monitoring and evaluating activities, a plot is declared complete land preparation.

Planting process is quite challenging due to the characteristic of the peat swamp forest. When the water level is high, plant transport is easy to proceed (using bot) but the planting process is difficult. On the opposite if the water level is low, plant transport is hard since they must walk a far distance inside the forest to reach the allocated area.

The requirement of rehabilitation process is the bureau must make sure that the burned area was 3-5 years since the disaster. By doing so, the soil will be ready to support the growing plant.

Natural Regeneration

Tumbang Nusa is one of the areas left for natural regeneration after fire in 2015. The current condition shows acceptable result of the tree regeneration. Although there is no individual growth yet, but 6000 saplings per hectare and 33,000 seedlings grows exclusively from the two pioneer species of *C. rotundatus* and *Cratoxylon arborescens*.

Post fire 1997, the recovery land demonstrated a spectacular recovery from fires that happened 23 years ago based on the vegetation density at the tree, pole, sapling, and seedling stages. It shows 775 individuals per hectare at the tree and pole stages, 7600 individuals per hectare at the sapling stage, and 106,000 seedling stages of natural regeneration rates. The vegetation species consist of 17 species: *S. belangeran, C. rotundatus, Eugenia sp., C. arborescens, Tetrameristra glabra, S.platycados, Dactylocladus stenostachys, Myristica sp., Knema sp., Campnosperma sp., Dryobalanops sp., Luthocarpus spicatus, Artocarpus sp., Calophyllum sp.*, and two unidentified species with the local name of *pentik and kopi-kopi*.

In another area of Sebangau National Park which was affected by fire in 1988, there grows 675 trees, 4,400 tree at sapling stage, 313,000 tree for seedling stage. The area consists of 16 species, which are *Vatica resak, Litsea elliptica, Ganua motleyana, Knema mandarahan, Cratoxylon arborescens, Dyospiros areolata, Mezzetia parviflora, Xylopia sp., Tetramerista glabra, Terminalia catappa, Litsea firma, Calophyllum sp., Campnosperma sp., Eugenia sp., Shorea leprosula*.

Overall, the natural regeneration process needs 22 to 23 years of recovery since the last fire to reform various vegetation in the area. If there is no recurrent fire, natural regeneration process resulted a good vegetation structure and composition which is like undisturbed sites.

Canal Blocking

The degradation of Sebangau National Park occurs because of canal construction and forest fire. There are 465 canals achieving a total length of 919,213 kilometres built by the companies and the society. Water loss and drought causes peat areas to be more prone to fire. To prevent this, canal blocking is used as a rewetting method to support the natural condition of the forest. The water is blocked to remain in the peat swamp area for as long as possible to maintain the hydrological balance, preventing the drought. The results are achieved by the stabilization of peat swamp water table and peat's increasing level of wetness and humidity.

Sebangau National Park started the canal blocking program in 2006. Spending a lot of fundings, resources, and time, a total of 1,831 canal blocking units were successfully built by 2020.

The following information explain the detail process of canal bocking classified in 3 main stages.

a) Pre-construction
    1. Initial socialization of peat rewetting program as process chain of consent on an initial basis without any coercion.
    2. Field survey.
    3. Determination of the number of canals blocking and selection of block/block design along with its technical specifications.
    4. Consent on an initial basis without any coercion

5. Analysis of the need for human resources and canal blocking materials.
6. Determination of canal blocking time and material mobilization time.
7. Estimating the cost of insulation.
8. The process of forming a group to carry out the construction.
9. Cooperation agreements with construction implementing groups.
10. Technical training.
11. Procurement and mobilization of materials, equipment, and labour.

b) Construction
1. Determination of the location and number of blocks/blocks to be built.
2. Measuring the location of the block/block.
3. Construction of bulkhead structures.
4. Installation of waterproof coatings (tarpaulins, geotextiles, etc.).
5. Entry and stockpiling of infill soil.
6. Installation of the overflow cover (spillway).
7. Tidying job.

c) Post-construction
1. Checking, monitoring, and evaluating the canal blocks that have been built.
2. Demobilization of labour and equipment.
3. Installation of water level monitoring instruments (if needed).
4. Block/bulk/dam maintenance work.

Well Construction

Continuing the above-mentioned problems, restoring the water table of the forest is essential in preventing fire. Well construction function as rewetting tools for dried peatland and for restoring the water surface. It consists of a series of tools in the form of pipes or serial connections PVC pipe installed into peat soil drain or discharge water sources located underground in the aquifer layer of the peat.

Initially, 112 drilling well were built in Sebangau National Park. To improve peat swamp forest as well as fire protection, the Peat Restoration Bureau supported the building of 625 drilling wells in Sebangau National Park. Each well has a 300-meter radius of coverage around it. Communities worked together to construct drilling wells, resulting in the construction of 737 drilling wells in this area.

The aim of constructing a well is to address the issue of surface water supplies becoming scarce during dry season. The peat groundwater level naturally decreases considerably in these circumstances. Natural surface water sources in canals, creeks, rivers, and lakes are quite far-reaching and may experience dryness. Drilled wells are used in peat rehabilitation programme as a water source to moisten the peat, which prevents it from drying out and to reduce its fire proneness during dry season. It can also be utilised as a source of water for quick fire suppression, in case of fire.

The following information explain the detail process of well construction classified in 3 main stages.

a) Pre-construction
1. Initial socialization of peat rewetting program as FPIC process chain.
2. Field survey, for determining the location of wells and the number of simple bore wells as well as selecting a simple borehole design along with its technical specifications.
3. Formation of drill well construction groups and teams.
4. Cooperation agreement.
5. Technical training.
6. Procurement and mobilization of materials, equipment, and labour.

b) Construction
1. Determination of the point and cleaning of the location plan for the placement of the borehole.
2. Preparation of borehole tools and materials.
3. Preparation of borehole injection water pool.
4. Drilling process.

5. Installation of well pipes.
6. Trial of the use of installed bore wells.
7. Foundation casting, marking installation, and taking coordinates.

c) Post-construction
1. Demobilization of tools and labor.
2. Monitoring and evaluation.
3. Drilling well maintenance work.

Based on 2017 BRG Contingency Plan, well construction successfully affected 456,018 hectares of the Sebangau National Park.

4.3 Ecological Resilience Models

Forests worldwide display diverse characteristics, encompassing variations in forest type, environmental conditions, and forest management practices. These distinct attributes give rise to varied responses when disturbances occur, directly influencing forest resilience. Forest resilience refers to the capacity of a forest ecosystem to withstand and recover from disturbances while maintaining its essential functions, structures, identity, and feedback (Triviño et al., 2023). It encompasses the ability of a forest to adapt and adjust to changing external drivers and internal processes, as well as the potential for transformation into new development trajectories (Folke et al., 2010). Forest resilience, shaped by the ecological memory of past ecosystem stability, primarily manifests through species adaptation (Johnstone et al., 2016). Alterations in environmental conditions or shifts in disturbance patterns naturally modify the resilience of forests (Trumbore et al., 2015). Human interventions within forest ecosystems influence both positive and negative impacts on forest resilience, particularly in the context of forest disturbance. Rehabilitation programs and human interventions can be varied in different countries.

Deliverable D6.1 has explained forest characteristics and forest resilience samples in each pilot area. Based on these data, it can be analyzed regarding the relationship between forest characteristics, rehabilitation programs, and forest resilience. In this report, forest type was classified using the FAO global ecological zone map (FAO & UNEP, 2020)(**Figure 47**). The classification of ecoregion and bioregions was based on (Dinerstein et al., 2017) which mapped them at[3] (**Figure 48)**. Fire regimes were categorized using a global fire regime map (Lavorel et al., 2007) (**Figure 49)**. Soil type classification was based on World Soil Information Services (WoSIS) which can be accessed on [4] (Batjes et al., 2020) (**Figure 50**). The climate type was based on Köppen–Geiger climate classification (**Figure 51**). Information on fire events includes the time the forest fire occurred, the value of the fire weather index, and the time range of observations. Forest resilience is described into three parameters, namely magnitude, malleability, and elasticity. The rehabilitation program is a type of program implemented after the fire incident.

[3] https://ecoregions.appspot.com/
[4] https://soilgrids.org/

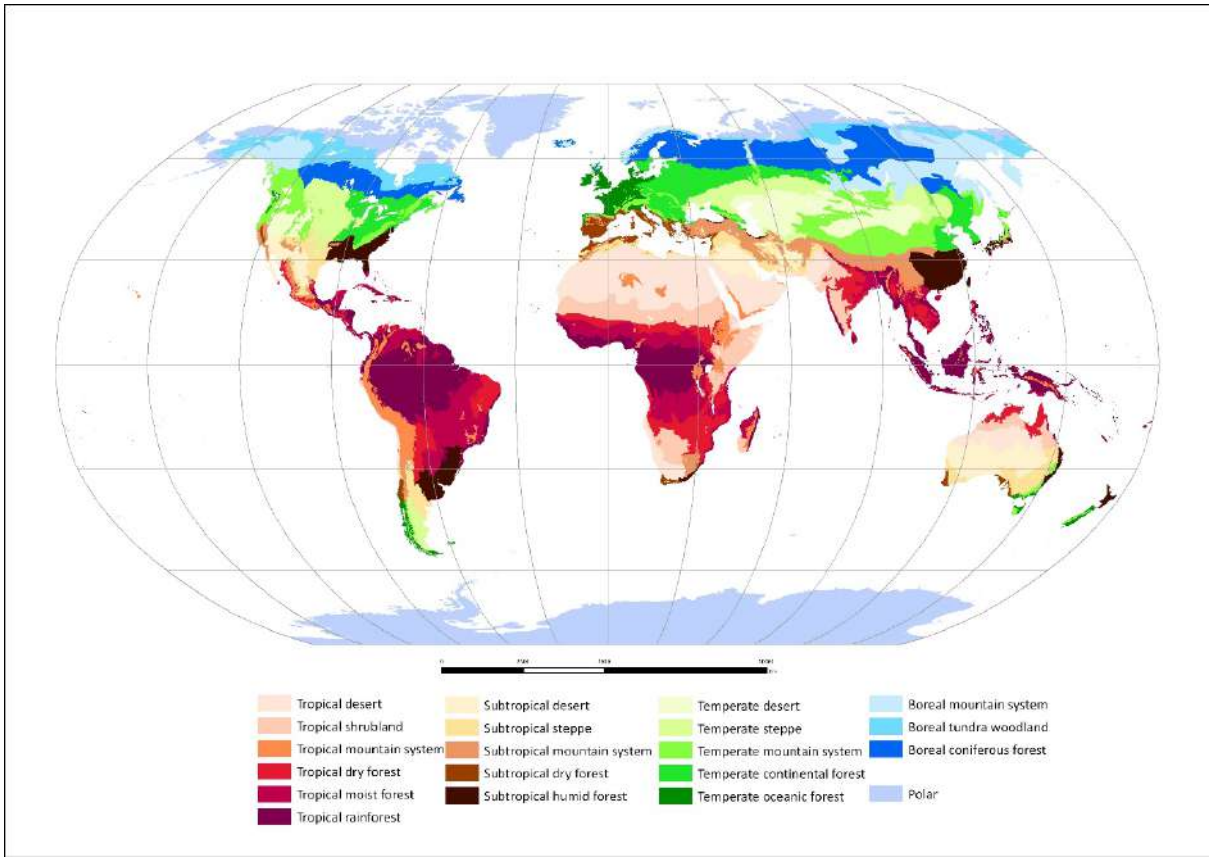

Figure 47. FAO global ecological map

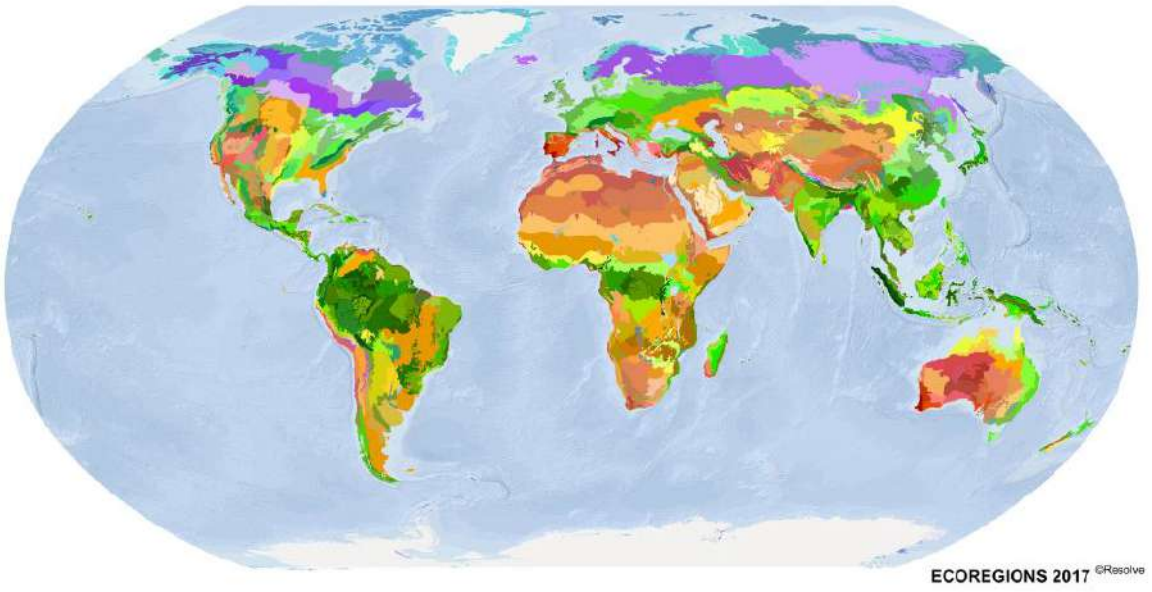

Figure 48. Global ecoregions map[5]

[5] https://ecoregions.appspot.com/

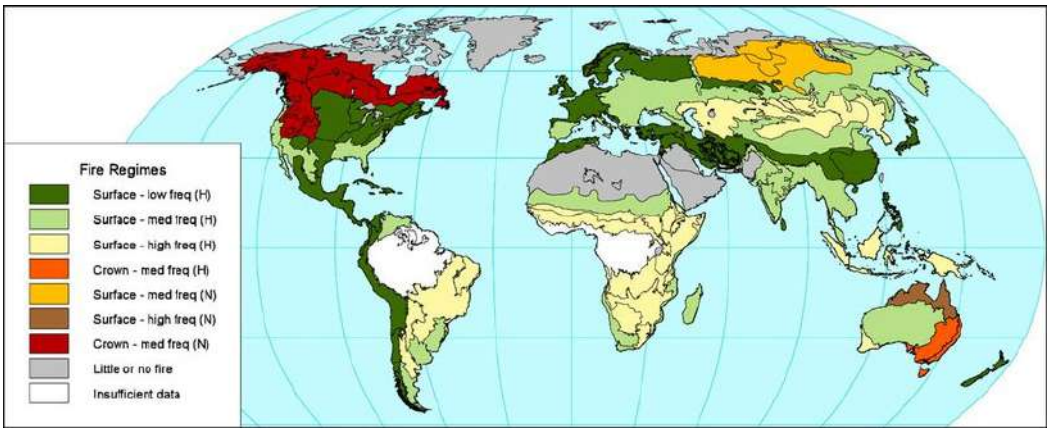

Figure 49. FAO global fire regimes map

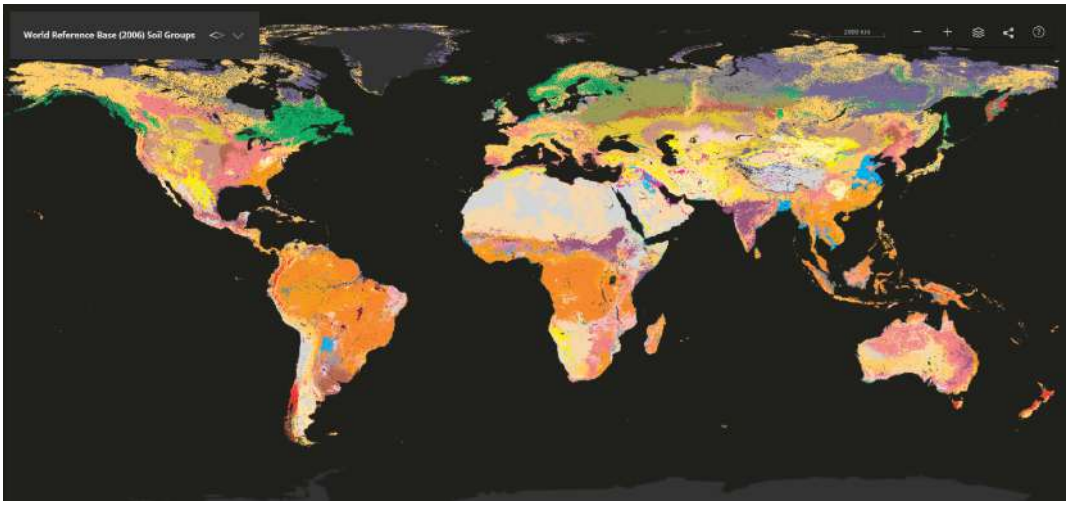

Figure 50. Global soil map from World Soil Information Services (WoSIS)

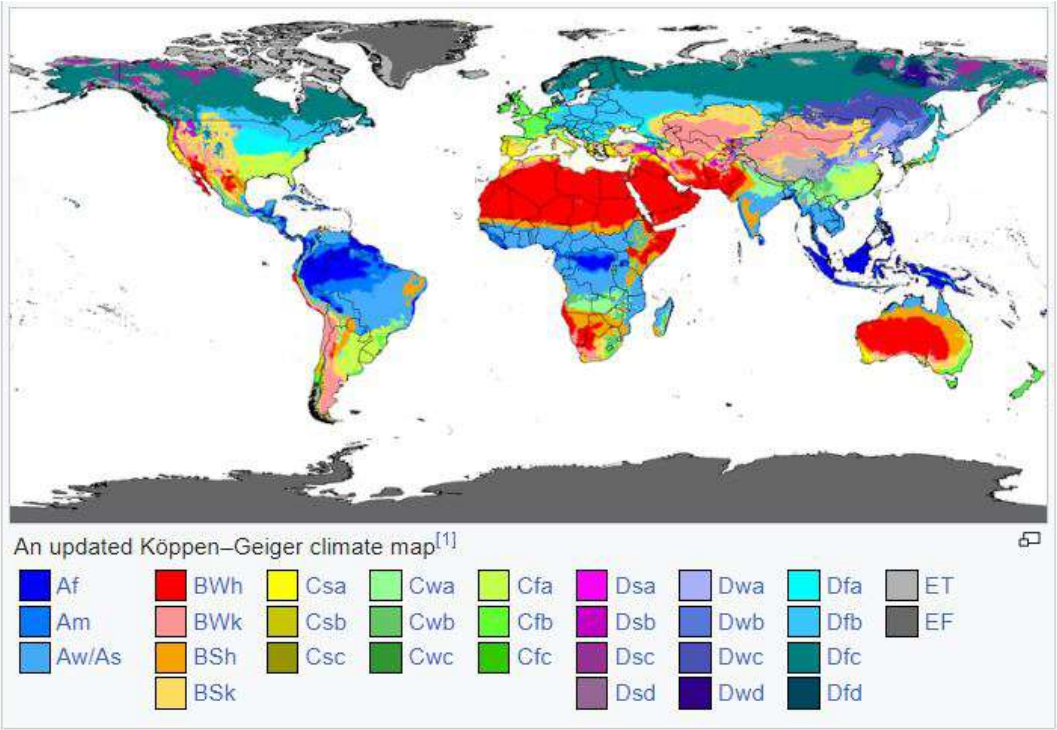

Figure 51. Koppen-Geiger climate classification

In a general overview, the pilot project is categorized into three forest types: subtropical dry forest, temperate continental forest, and tropical rainforest. Subtropical dry forests are represented by: Cova de Beira (Portugal), Gargano (Italy), Tepilora (Italy), and Sterea Ellada (Greece). The temperate continental forest is depicted by Podpol'anie in Slovakia. The tropical rainforest is represented by the Sebangau National Forest in Indonesia. Each forest type has a different response to disturbance (Forzieri et al., 2022).

4.3.1 Subtropical dry forest

The first forest type is subtropical dry forests, specifically classified as part of the Mediterranean Mixed Forest group. This classification encompasses several areas, including Cova de Beira, Gargano, Sterea Ellada, and Tepilora. These forests are in regions with a Mediterranean climate, characterized by dry summers. Mediterranean regions experience a seasonal climate with mild winters that promote the accumulation of fuel and hot, dry summers, that contribute to frequent wildfires ((Fernández-García et al., 2021). Consequently, wildfires have played a vital role in shaping ecological processes within Mediterranean forest ecosystems for countless millennia (Moreira et al., 2020). One key characteristic of Mediterranean forests is the presence of Mediterranean gorse shrublands, which have been described as a fire-prone community (De Luis et al., 2004). General information regarding forest characteristics, fire events, forest resilience, and forest rehabilitation programs at each pilot location. Information on forest characteristics includes forest types, ecoregions, bioregions, fire regimes, and soil types was described in **Table 16.**

Table 16. Forest resilience in subtropical dry forest type

Pilot	Forest type	Bioregions	Ecoregions	Climate type	Fire regime	Fire weather index	Soil type	Fire Events	Time Span	Magnitude	Malleability	Elasticity	Program
Cova de Beira - Quinta da França	Mediterranean forests, woodlands, and scrub	Balearic Sea & West Mediterranean Mixed Forests	Southwest Iberian Mediterranean Sclerophyllous and Mixed Forests, and Northwest Iberian Montane Forests	Hot-summer Mediterranean climate	Surface - medium frequency	30.43	Cambisols; Leptosols and Colluvic regosols	September 2017	2017 - 2019	0.2	0.35	0.0052	
								August 1984	1984-1985	0.17	0.176	0.014	Natural regeneration, planting specific native tree, including periodic shrub control, forest thinning and removal, eliminating diseased tree
								August 1995	1995-1996	0.13	0.53	0.028	Natural regeneration, planting specific native tree, including periodic shrub control, forest thinning and removal, eliminating diseased tree

Pilot	Forest type	Bioregions	Ecoregions	Climate type	Fire regime	Fire weather index	Soil type	Fire Events	Time Span	Magnitude	Malleability	Elasticity	Program
Gargano	Subtropical dryforest	Adriatic Sea & Central Mediterranean Mixed Forests	Italian Sclerophyllous and Semi-Deciduous Forests	Hot-summer Mediterranean climate	Surface - medium frequency	5.61	Cambisols	March 2019	2019 (1 year)	0.05	0.2	0.0075	Natural regeneration, planting, dead tree removal
Sterea Ellada	Subtropical dryforest	Aegean Sea & East Mediterranean Mixed Forests	Eastern Mediterranean Conifer-Broadleaf Forests	Hot-summer Mediterranean climate	Surface - medium frequency	38.7	Luvisols	August 2021	2021 - 2023	0.21	0.33	0.0073	Natural regeneration (preferable), planting,
Tepilora	Subtropical dryforest	Adriatic Sea & Central Mediterranean Mixed Forests	Tyrrhenian-Adriatic Sclerophyllous and Mixed Forests	Hot-summer Mediterranean climate	Surface - medium frequency	17.27	Luvisols	July 2017	2017 - 2018	0.14	0.214	0.0089	
Tepilora (Montiferru)								August 2021	2021-2022	0.2	0.05	0.012	Natural regeneration, planting, cutting, and clearing dead tree, felling, and trimming plant

In terms of fire occurrence, Mediterranean forests typically experience surface fires with a mid-frequency (Mouchet et al., 2017). These forests predominantly feature luvisols and cambisols as their soil types. The Mediterranean region ranks among the world's most fire-prone areas, experiencing a high frequency of fires during the summer season (Fernandes, 2013). The combination of high temperatures, low humidity levels, and dry vegetation significantly increases the risk of fire ignition and spread.

4.3.1.1 Cova de Beira

Cova de Beira is situated in the Balearic Sea & West Mediterranean Mixed Forests bioregion, specifically classified within the Southwest Iberian Mediterranean Sclerophyllous and Mixed Forests ecoregion. Cova de Beira is categorized as the Mediterranean forest region, which is naturally prone to wildfires. In this report, there are three cases of fires in Cova de Beira, which are in 1984, 1995 and 2017 (**Figure 52**, **Figure 53**, and **Figure 54**). Among these occurrences, the wildfire in 2017 was the most extensive in terms of its impact. However, when we compare the fires from 1984 and 1995 to those in 2017, the latter had a lower degree of elasticity. It means that the forest experienced a faster recovery phase during the fires in 1984 and 1995. In 2017 the forest experienced a longer recovery.

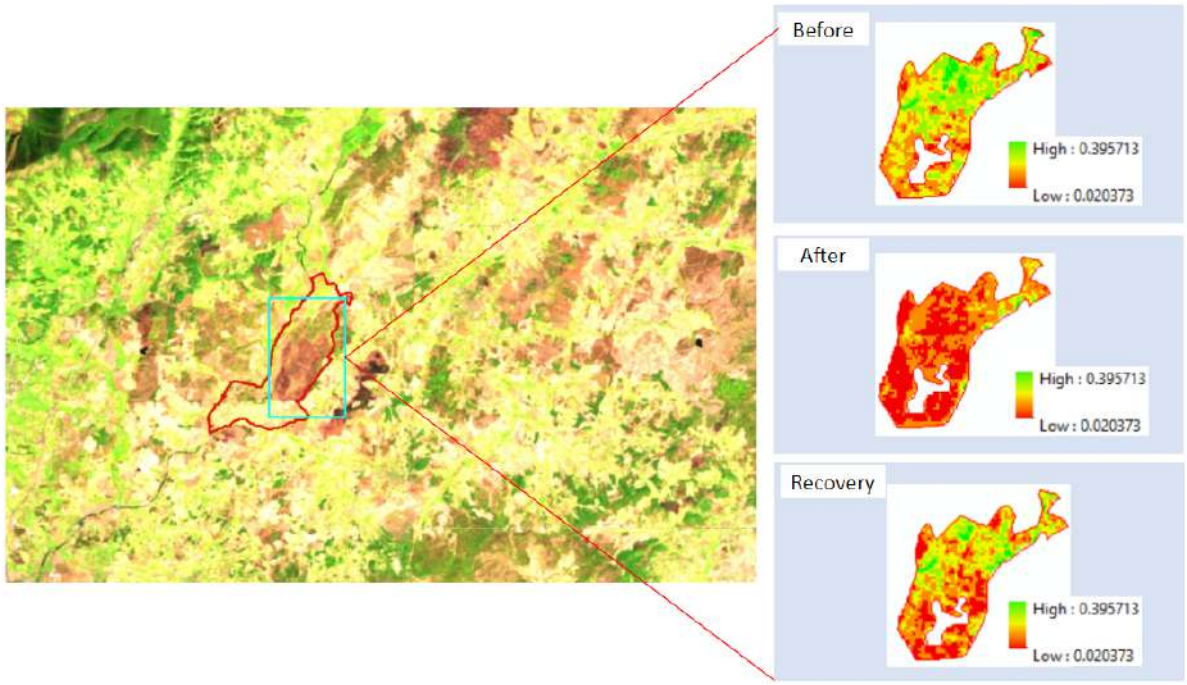

Figure 52. NDVI value of Quinta da França (Cova de Beira) before the fire, after the fire and recovery phase in August 1984 fire event

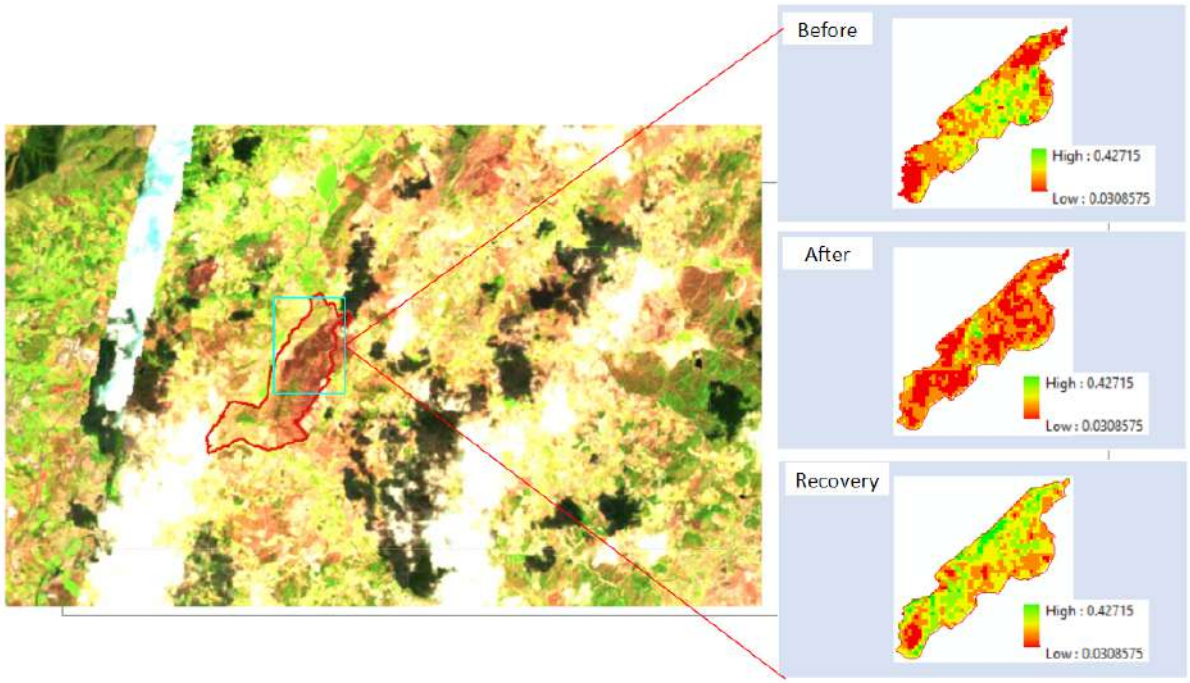

Figure 53. NDVI value of Quinta da França (Cova de Beira) before the fire, after the fire and recovery phase in August 1995 fire event

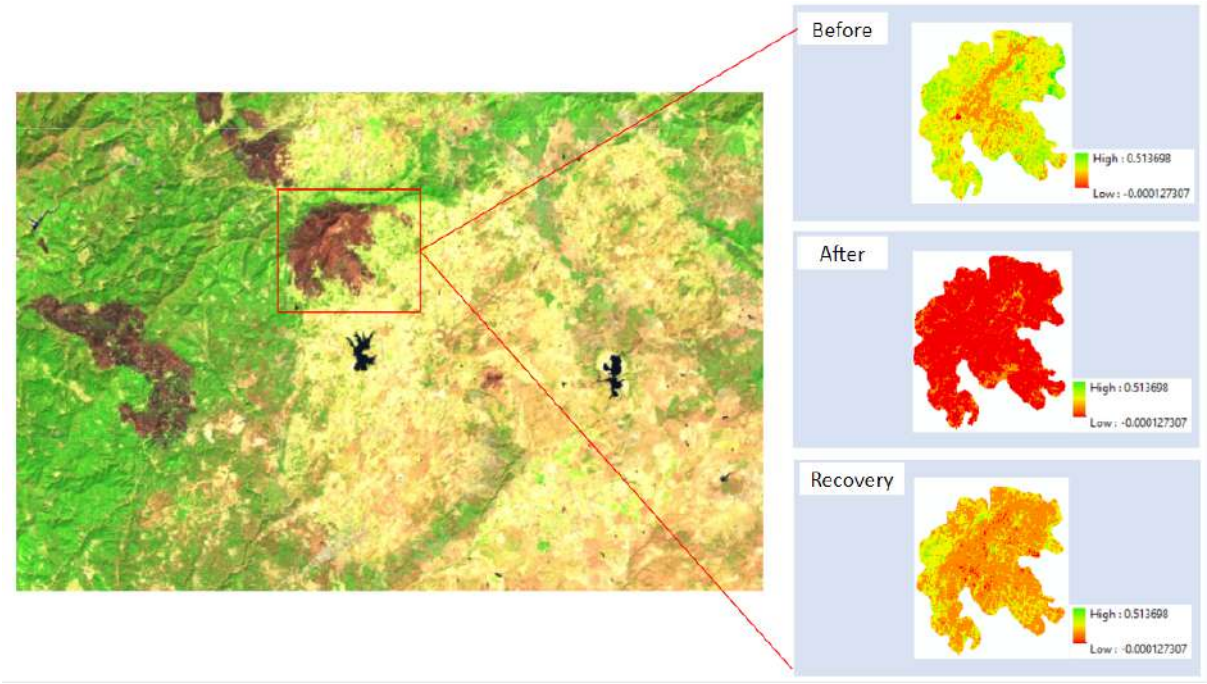

Figure 54. NDVI value of Cova de Beira before the fire, after the fire and recovery phase in August 2017 fire event

The fires in 1984 and 1995 had different locations but were still included in the Quinta de Franca area. The magnitude of the fire in 1984 was higher than in 1995 (**Figure 55**). In the 1995 fire incident, the recovery process occurred more quickly so that the elasticity value was higher. Quinta de Franca only took 7 months for the recovery process. This recovery speed is an indicator of forest resilience.

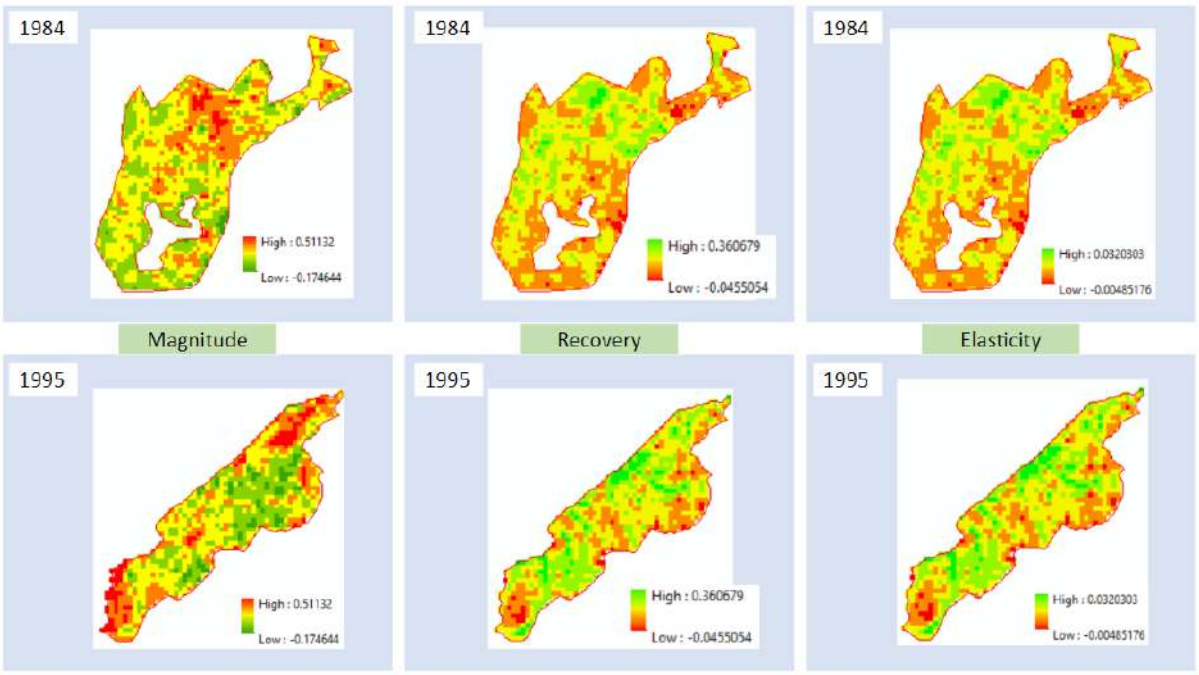

Figure 55. Magnitude, recovery and elasticity of Quinta de Franca, Cova de Beira in 1984 and 1995

The speed at which the recovery process is progressing is a cause for concern in the context of the rehabilitation program undertaken by Quinta de Franca. Several rehabilitation programs carried out by Quinta de Franca include natural regeneration, planting specific native trees, including periodic shrub control, forest thinning and removal, and eliminating diseased trees. This rehabilitation program focuses more on reducing flammable materials and natural regeneration.

4.3.1.2 Sterea Ellada

Sterea Ellada is positioned in the Aegean Sea & East Mediterranean Mixed Forests bioregion, including the Eastern Mediterranean Conifer-Broadleaf Forests ecoregion. The pilot area for Greece is the island of Evia, and more specifically its northern part of the island. In **Figure 56** the conditions before, during and after the fire are clearly visible. The highest fire severity occurred in Sterea Ellada (North Evia) with a magnitude value of 0.21. This fire occurred in August 2021 when the Fire Weather Index (FWI) registered a value of 38.7, indicating an extremely high fire danger level (**Figure 57**). This suggests a clear connection between this fire incident and adverse weather conditions. This event was the mega fire event in North Evia that burned more than 500,000 hectares.

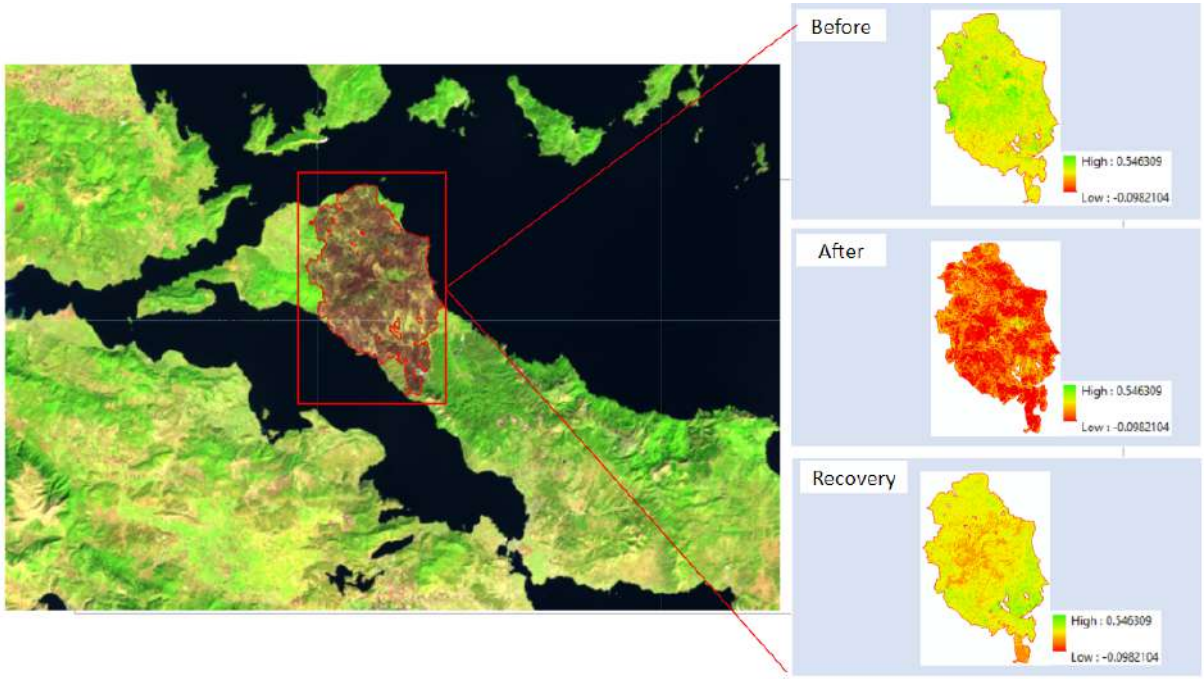

Figure 56. NDVI value of North Evia before the fire, after the fire and recovery phase in August 2021 fire event

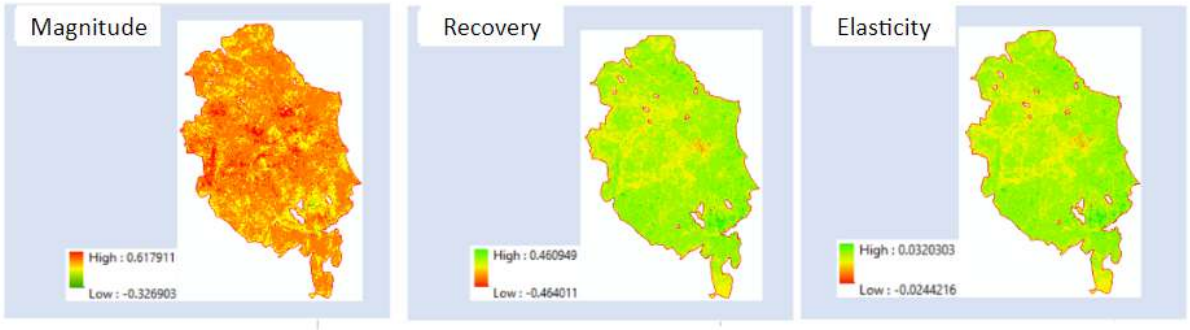

Figure 57. Magnitude, recovery, and elasticity of North Evia in 2021 fire event

North Evia suffered a severe fire with a magnitude value of 0.21. With this damage North Evia took 19 months to recover. The most severe fires occurred in the central spread and the western side of the pilot area, where recovery rates tended to be lower and elasticity lower.

The recovery initiative employed in North Evia primarily involves natural regeneration and the removal of burnt trees. This strategy hinges on the inherent ability and resilience of local vegetation to naturally rejuvenate. The plant species that participated in this recovery process encompassed pine trees and various shrubs. Furthermore, in regions exhibiting high soil moisture levels, such as the riverbeds and banks, where deciduous tree varieties were dominant, these trees managed to withstand the fire and showed signs of leaf regrowth. The capacity of these indigenous deciduous trees to mitigate the fire's impact and their resilience in the face of such challenges positions them as promising natural candidates for enhancing future forest resilience. The North Evia pilot site experienced a relatively fast recovery process compared to other locations.

4.3.1.3 Tepilora

Tepilora belongs to the Tyrrhenian-Adriatic Sclerophyllous and mixed forests. A major fire event occurred in 2021 in the Montiferru area. In this report, the Montiferru fire area is used for program analysis and resilience. In **Figure 58** the conditions before, during and after the fire are clearly visible. Based on the observation, the Montiferru area has a fire magnitude or severity value of 0.2 which indicates the average change in NDVI from before and after the fire.

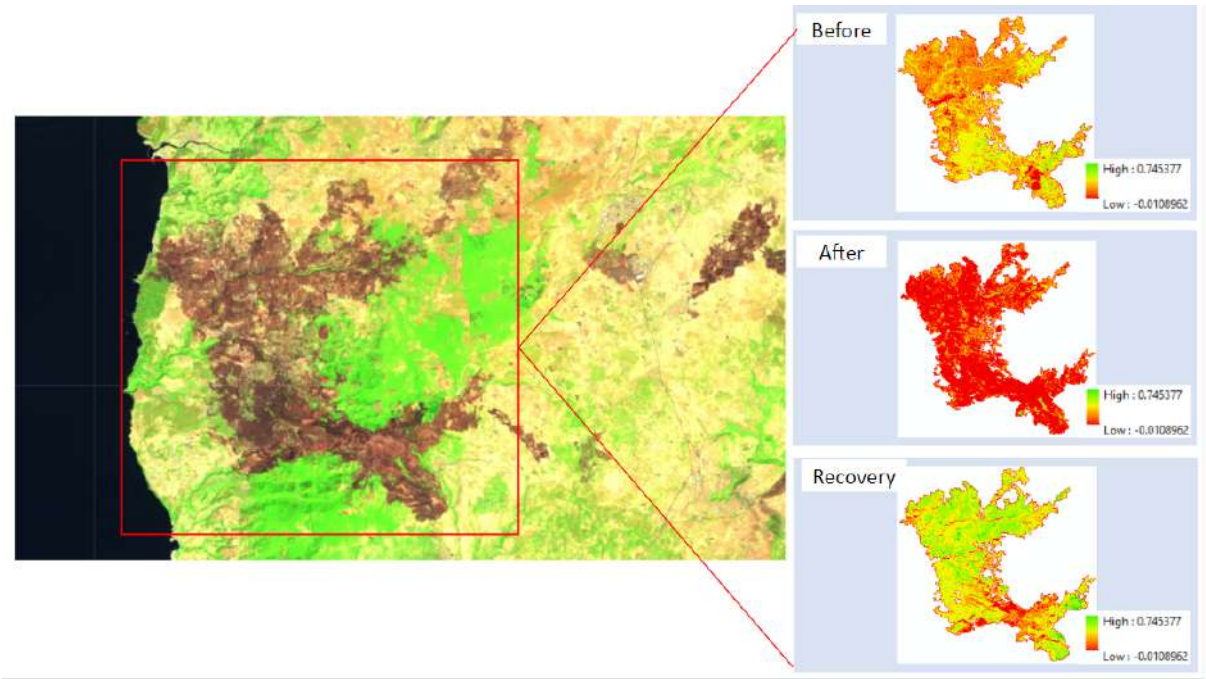

Figure 58. NDVI value Tepilora (Montiferru) before the fire, after the fire and recovery phase in August 2021 fire event

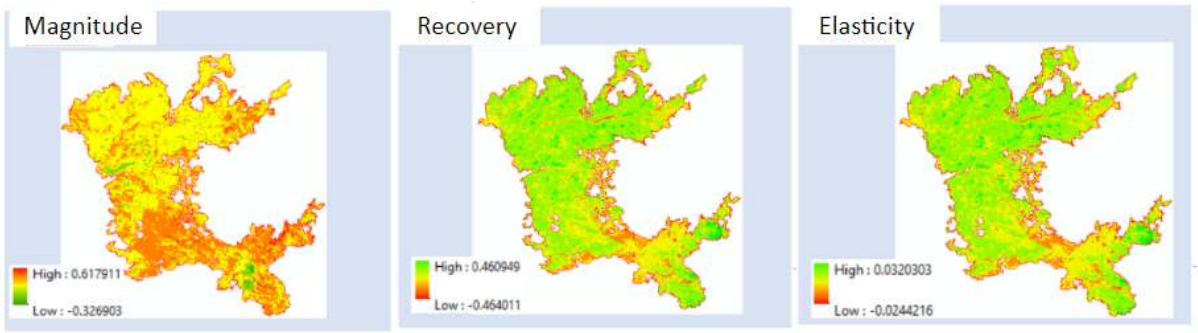

Figure 59. Magnitude, recovery, and elasticity in Montiferru

The distribution of magnitude, recovery and elasticity values is shown in **Figure 59**. The highest fire severity is in the southern part of the fire area. However, in the process of recovery, this section also experienced a rapid recovery process as indicated by the relatively high elasticity values.

The rehabilitation program implemented for this area was mainly natural regeneration, forest construction and replanting. Forest reconstruction was carried out in the early aftermath of the fire. This activity serves to clean up the remnants of the fire. Natural regeneration is aimed at areas that have been affected but where there are still remnants of viable vegetation. While replanting is carried out for affected areas where there is absolutely no vegetation left.

4.3.1.4 Gargano

Gargano includes within the Italian Sclerophyllous and semi-deciduous forests ecoregion. The location of the park on the Mediterranean Sea lends to a climate of high temperatures and moist conditions with precipitation during every season. A relatively significant fire event occurred in March 2019, which is illustrated in **Figure 60** through images captured before the fire, immediately after the fire, and during the recovery phase. Particularly, Gargano experienced the lowest value of magnitude among all locations within the pilot area, signifying the lowest fire intensity (**Figure 61)** Impressively, Gargano National Park took recovery within just 8 months. The highest elasticity values were identified in the north-western portion of the fire-affected area, while the fire's central zone displayed even higher elasticity values, indicating a faster pace of recovery.

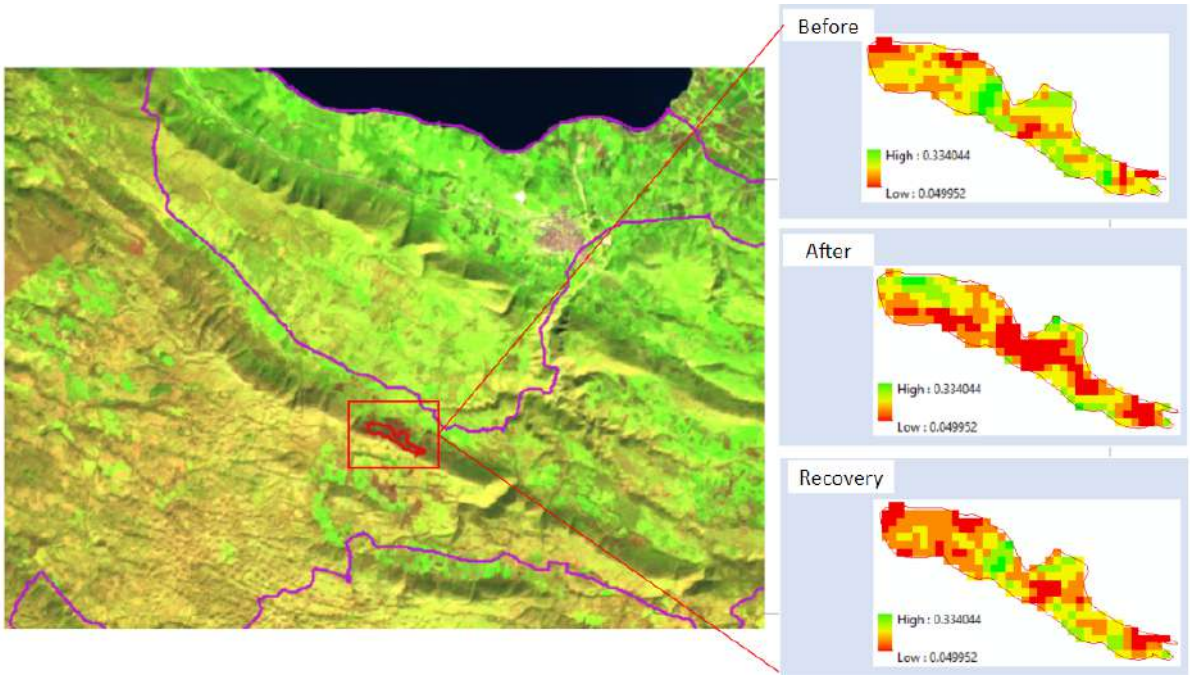

Figure 60. NDVI in Gargano Park before the fire, after the fire and recovery phase in August 2021 fire event

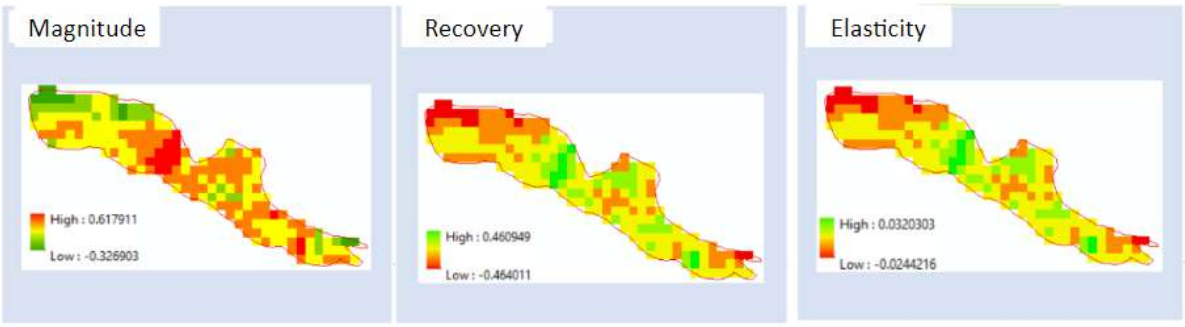

Figure 61. Magnitude, recovery, and elasticity in Gargano Park

The rehabilitation program carried out by Gargano includes natural regeneration, dead tree removal and replanting. The program is carried out in accordance with the characteristics of wildfire and the characteristics of the species. For low intensity fires, no intervention is carried out, only natural regeneration. The speed of forest recovery after a fire depends on the condition of the vegetation.

Based on the results of resilience analysis in the subtropical dry forest, we can conclude that subtropical dry forest in the Mediterranean basin tend to have higher resilience among other pilots. The Mediterranean Forest ecosystem exhibits a high level of resilience to forest fires due to several factors. One key factor is the ability of plant species to recover from fire through resprouting and germination of fire-protected seeds (Rodrigo et al., 2004). This ability allows the vegetation to regenerate quickly after a fire event. Additionally, the presence of fire-resistant structures in plants contributes to their resilience. Fuel characteristics also play a role in the resilience of Mediterranean forests to fire. The fuel characteristics, such as the type and amount of vegetation, can influence fire behaviour and severity (De Luis et al., 2004). However, in general, the Mediterranean ecosystem has adapted to fire and many plant communities, such as shrublands and oak forests, are highly resilient to fire (Pausas et al., 2008). The frequency and intensity of wildfires in the Mediterranean basin can impact the resilience of ecosystems. An increase in fire frequency and intensity can modify the landscape and vegetation structure, altering ecosystem functioning (Buscardo et al., 2010). The higher frequency and intensity of fires expected in the future due to climate change and land use change may pose a greater threat to forest resilience (Hartung et al., 2021). In terms of post-fire recovery, active restoration techniques, such as planting tree saplings, may have implications for the resilience of Mediterranean pine forests. Research suggests that active restoration may decrease the resilience of the plant community and alter the species composition of these forests (Ürker et al., 2018). Therefore, the choice of restoration techniques should be carefully considered to ensure the long-term resilience of the forest ecosystem.

4.3.2 Temperate continental forest

The next forest type is temperate continental forest with a pilot project location in Podpol'anie. This forest is situated within the Carpathian Mountain and Plains mixed forest bioregion and the Carpathian montane forest ecoregion. General information regarding forest characteristics, fire events, forest resilience, and forest rehabilitation programs at each pilot location. Information on forest characteristics includes forest types, ecoregions, bioregions, fire regimes, and soil types was described in **Table 17**. In this region, FWI is classified as surface fire with low frequency. A forest fire event occurred in April 2019, resulting in a fire magnitude of 0.19. This magnitude, when compared to other forested areas, is relatively high. During this fire event, the Fire Weather Index measured at 8.03, indicating a moderate level of fire danger. Podpol'anie shows the highest malleability value among the various forested regions. This suggests that the ecosystem in Podpol'anie tends to be less stable in comparison to other areas.

Table 17. Forest resilience in temperate continental forest type

Pilot	Forest type	Bioregions	Ecoregions	Climate type	Fire regime	Fire weather index	Soil type	Fire Events	Time Span	Magnitude	Malleability	Elasticity	Program
Popdol'anie	Temperate continental forest	Carpathian Mountain & Plains Mixed Forests	Carpathian Montane Forests	Warm-summer humid continental climate	Surface low frequency	8.03	Cambisols	Apr 2019	2019 - 2022	0.19	0.473	0.0068	

Figure 62 described NDVI changes before the fire, after the fire and recovery phase. The fire's intensity is represented by a magnitude value, specifically at 0.19 (as depicted in **Figure 63**). When compared to other forested regions, this magnitude value is relatively high, indicating a more severe level of fire. A higher magnitude value corresponds to greater fire severity. The fires that occurred in Podpol'anie were primarily

concentrated in the northern area, with the magnitude value gradually diminishing in the central part of the fire-affected area.

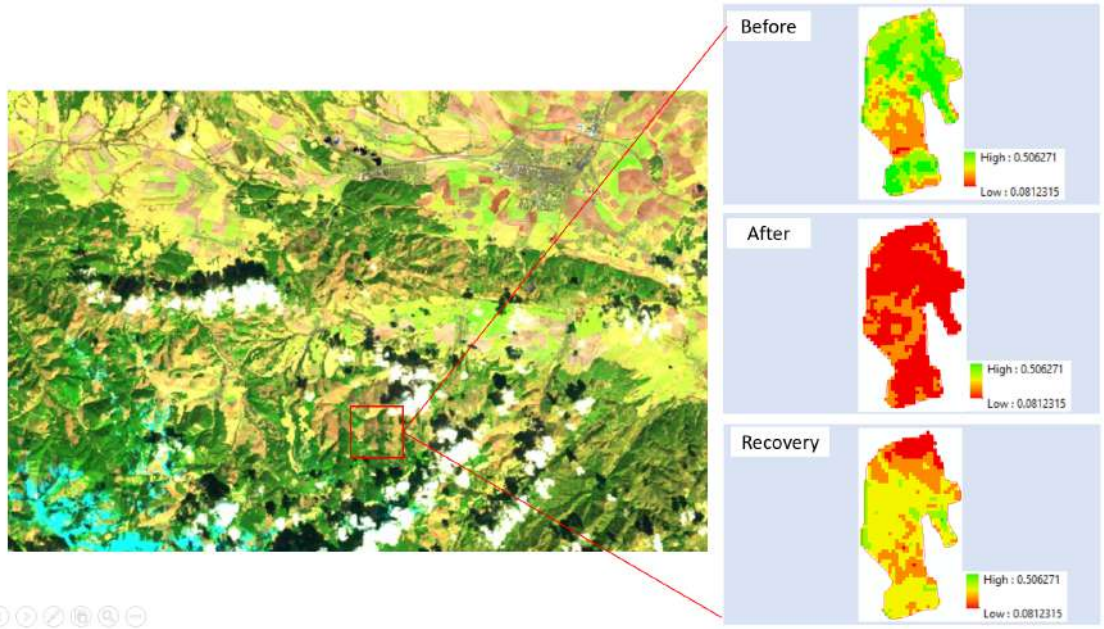

Figure 62. NDVI value Podpolanie before the fire, after the fire and recovery phase in August 2021 fire event

It has been determined that Podpol'anie exhibits a malleability value of 0.19, which suggests a relatively stable ecosystem in this region. When estimating the time required for the forests to return to their stable state, we utilized the elasticity indicator (**Figure 63**). Notably, Podpol'anie underwent a recovery process lasting 41 months. The lowest elasticity values were observed in the northern direction, located in the outermost region affected by the fire. This implies that this area necessitates a longer recovery period. In contrast, areas characterized by moderate to high elasticity values are situated in the southern part of the affected area.

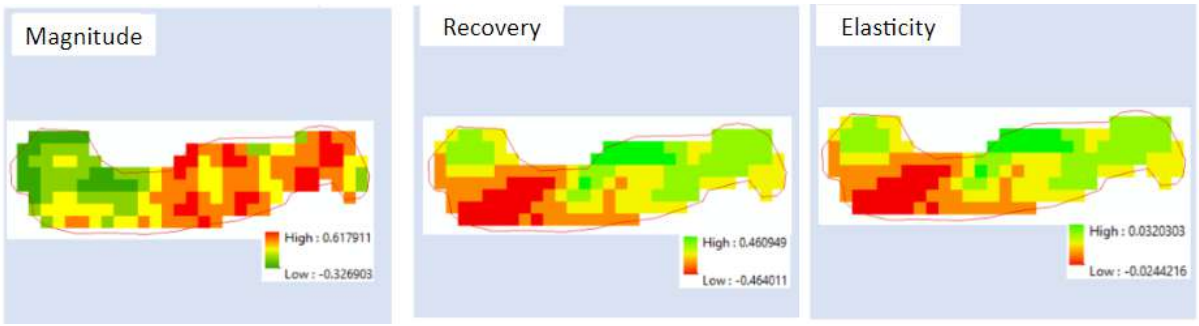

Figure 63. Magnitude, recovery, and elasticity in Podpol'anie

Vegetation composition and land use practices also influence the resilience of temperate forests to fires. Studies have found that the expansion of broad-leaved deciduous forests can lead to fire suppression due to lower flammability, higher forest density, and moister microclimates. This indicates that these types of forests may have higher resilience to fires compared to other forest types (Schwörer et al., 2022). Climate change is also a factor that affects the resilience of temperate continental forests to fires. With the predicted increase in average temperatures and decrease in rainfall, particularly in the southern regions of Europe, there is an increased risk of forest fires. These changing climate conditions can create longer periods of drought in the summer, which increases the likelihood of fires (Milanović et al., 2021)

Forest restoration practices should focus on more than just tree planting. Leach (2006) (Leach, 2006) emphasizes the need to consider the broader landscape context in forest restoration efforts. This may involve restoring natural disturbance regimes, promoting natural regeneration, and enhancing connectivity between forest patches. Furthermore, the program should address the threat of megafires to old-forest species. Jones et al. (2016) (Jones et al., 2016)emphasize the need to reduce the frequency of large, high-severity fires to protect the biodiversity of temperate continental forests.

4.3.3 Tropical rainforest

Sebangau National Park as non-EU partners, situated within the Borneo tropical forest and Sundaland heath forest bioregion, can be further classified into two ecoregions: the Southwest Borneo freshwater swamp forest and the Sundaland heath forest. These areas, characterized by flat, low-lying alluvial floodplains, are subject to periodic flooding, rendering them waterlogged for part of the year. In contrast to neighbouring peat forests, the freshwater swamp forests do not accumulate substantial biomass due to regular flushing and lower acidity (Santika et al., 2023).

Away from the riverbanks, the park falls within the Sundaland heath forest ecoregion, which generally possesses lower nutrient levels compared to freshwater swamp forests. Nevertheless, the soil type in this region typically comprises organic soil or histosols. Concerning fire regimes, this area is categorized as experiencing surface fires with high frequency. The predominant fire type is surface fires, characterized by flames on the ground surface. This relates to the natural flammability of peat soil, making fires in such environments challenging to extinguish as the source of the fire lies beneath the surface. General information regarding forest characteristics, fire events, forest resilience, and forest rehabilitation programs at each pilot location. Information on forest characteristics includes forest types, ecoregions, bioregions, fire regimes, and soil types was described in **Table 18.**

Table 18. Forest resilience in tropical rainforest type

Pilot	Forest type	Bioregion	Ecoregions	Climate type	Fire regime	Fire weather index	Soil type	Fire Events	Time Span	Magnitude	Malleability	Elasticity	Program
Sebangau	Tropical rainforest	Borneo Tropical Forests & Sundaland Heath Forests	Southwest Borneo Freshwater Swamp Forests and Sundaland Heath Forest	Tropical rainforest	Surface high frequency	-5.91	Histosols	October 2015	2015 - 2019	0.19	0.421	0.00524	Natural regeneration, planting, canal blocking, well construction

Sebangau National Park encounters a high frequency of fires, particularly during the dry season, as represented by the 2015 forest fires, which were exacerbated by prolonged drought linked to the El Niño phenomenon. The prolonged dry conditions associated with El Niño created favourable conditions for the ignition and spread of fires (Field et al., 2016) The Indonesian fire environment showed a nonlinear sensitivity to dry conditions during prolonged periods with less than 4 mm/day of precipitation, and this sensitivity appeared to have increased over Kalimantan (Field et al., 2016) These fires were widespread across Southeast Kalimantan, including the Sebangau National Park area. However, the Fire Weather Index

in this region remained relatively low, at 5.91, suggesting that weather factors were not the primary cause of the fires.

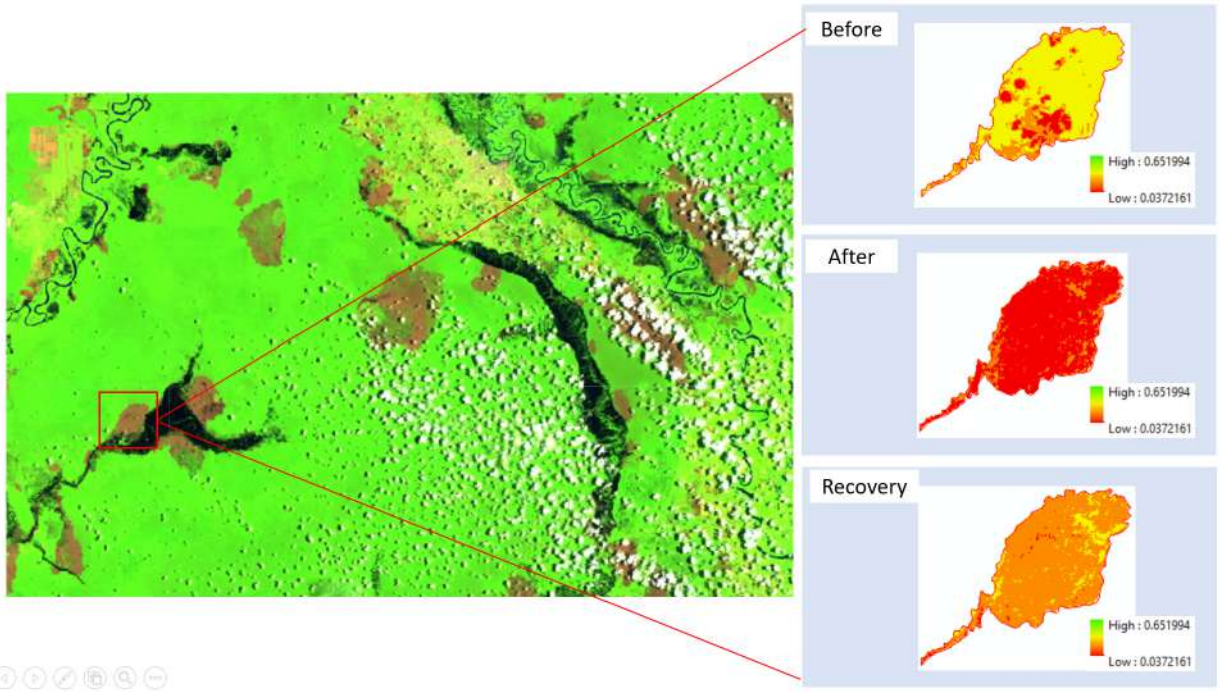

Figure 64. NDVI value of Sebangau before the fire, after the fire and recovery phase in 2015 fire event

The fire incident resulted in a damage magnitude of 0.19, determined by the difference in NDVI (Normalized Difference Vegetation Index) before and after the fire, as shown in the image (**Figure 64 and Figure 65**). Compared to other pilot areas, Sebangau National Park displayed a relatively high damage magnitude, indicating the severity of the fire. The malleability value was also relatively high, signifying a low degree of adaptability, which reflects changes in ecosystem conditions post-fire. The elasticity value was the lowest among the pilots, indicating that the forest took 21 months to recover to its original state, suggesting lower resilience.

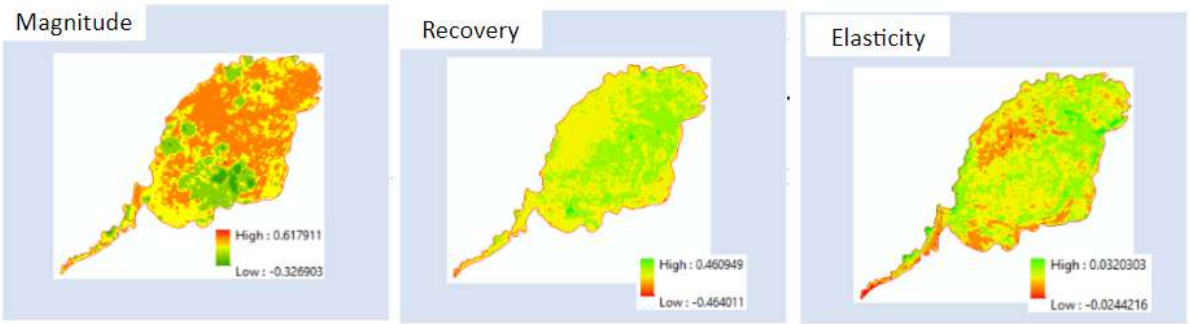

Figure 65. Magnitude, recovery, and elasticity in Sebangau

The recovery program employed within Sebangau National Park encompasses natural regeneration, reforestation, canal blockage, and well construction. Overall, Sebangau National Park exhibits the lowest elasticity due to its location on flammable and challenging-to-extinguish peatland. Moreover, when peatland is exposed to fires, it typically experiences longer period to recover.

Tropical peatland rainforests are unique ecosystems that are highly susceptible to forest fires. Understanding the characteristics of forest fire resilience in these ecosystems is crucial for effective management and conservation efforts. One important characteristic of forest fire resilience in tropical peatland rainforests is the water table level. Peatlands have high water content, which acts as a natural fire barrier. Studies have shown that lower water tables in peatlands, caused by reduced rainfall and increased seasonality, can lead to enhanced peat decomposition and an increased likelihood of fire (Page et al., 2011) These hydrological shifts, combined with human disturbance and increased access, can create fire tipping points where dry weather, fuel availability, and ignition sources converge (Page & Hooijer, 2016). Therefore, maintaining a high-water table is essential for fire resilience in tropical peatland rainforests.

The ability of peat to recover after a fire is another important characteristic of forest fire resilience. Peatlands are particularly vulnerable to smouldering fires that spread vertically underneath the peat, as they limit the peat's ability to fully recover (Widyastuti et al., 2021). Managing fire ignition and spreading is crucial for maintaining the resilience of tropical peatland rainforests.

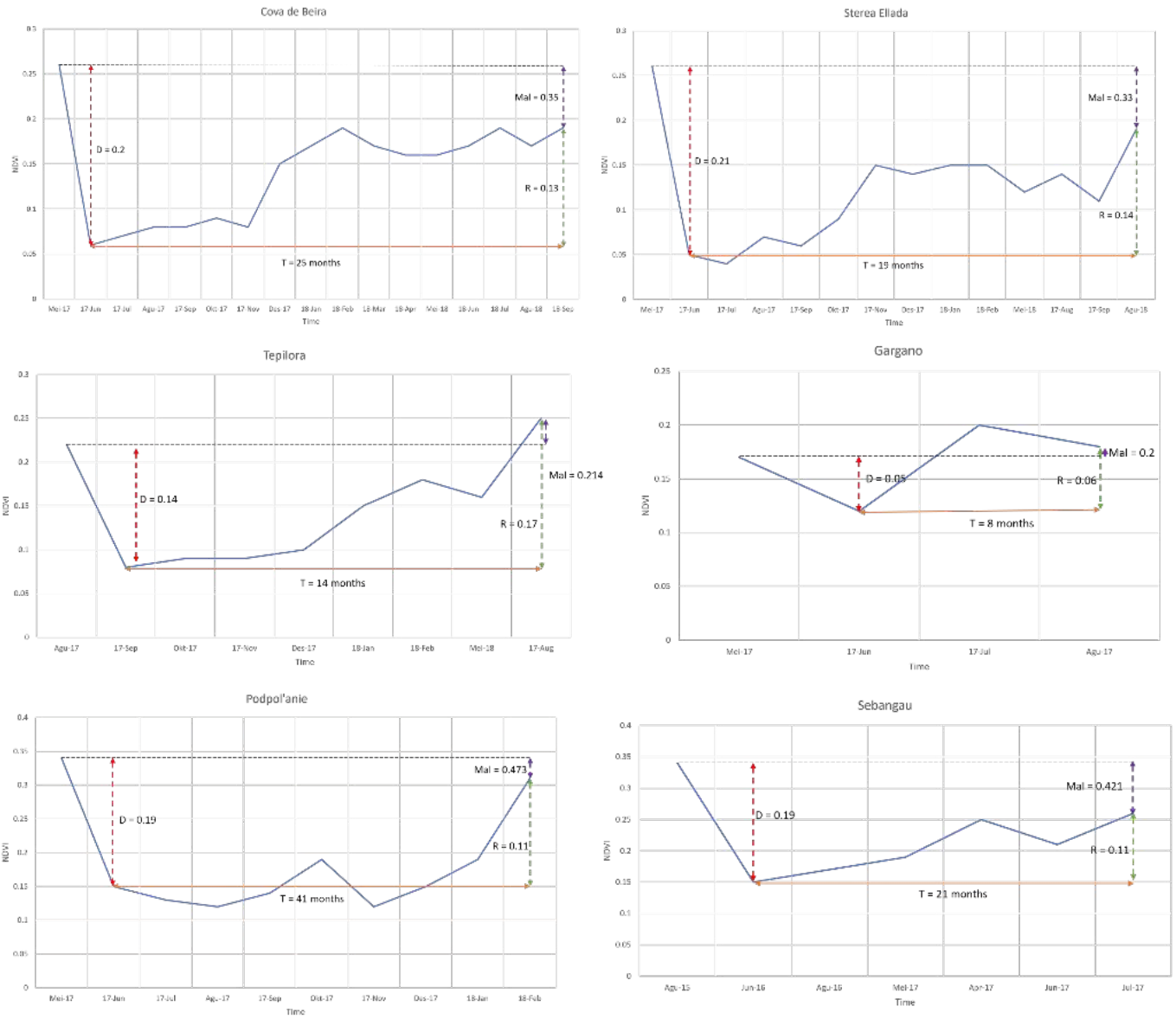

Figure 66. Forest resilience graphics

Based on these findings, it is evident that the Sebangau forest represents a tropical rainforest characterized by a relatively high malleability value and the lowest elasticity value when compared to other forest types **Figure 66**. These results imply that tropical rainforests exhibit lower ecosystem stability and require more time to recover following a fire incident. In contrast, Mediterranean forests demonstrate greater ecosystem stability in the face of fire disturbances and exhibit a faster recovery rate after such events. This is reflected in their low malleability values and high elasticity. On the other hand, temperate continental forests tend to have less stable ecosystems, although it shows a relatively faster recovery compared to tropical rainforests.

Based on the rehabilitation program that has been implemented by each pilot project, natural regeneration is a program implemented by all pilots. Natural regeneration allows for the establishment of diverse plant communities, improves soil quality, and enhances the resilience of forests to future disturbances. The rehabilitation program implemented by each pilot project adapts to the characteristics of the wildfire and the characteristics of the vegetation found in the forest. Rehabilitation programs can help accelerate recovery in forests after fires.

It's important to note that these results should not be generalized to all forest types worldwide due to the limited sample from the pilot area. To gain a comprehensive understanding of forest resilience across various forest types, representative data samples from a wider range of regions are essential. Therefore, the Open Forest Map application addresses this need by providing data that encompasses forest monitoring parameters, facilitating global and accessible forest resilience monitoring.

5 Open Forest Map Tool

This chapter presents the design of open forest maps as a tool aimed to provide long-term monitoring of ecologically resilient processes, focusing mainly on forest ecosystems. This application utilizes historical earth monitoring images, recorded historical climate related data, population, and gross national product. Those variables are provided in spatiotemporal terms with varied resolution. This service also collects wildfire incidents and restoration and rehabilitation programs that have been carried out in the past. In case the wildfire incidents were unavailable, an analysis of the earth monitoring images is carried out to predict the incidents in both size and severity.

Open Forest Map enable big data analysis for all possible related aspects of ecological resilience, such as climate changes, wildfire disturbance, and societal-related aspects. The services allow the expert user to access the data in multiple chart format and make further analysis. The relationship between programs carried out in the past toward the betterment of the forest quality is indicated by the greenness of the forest landscape also shown in the final chart to provide big data based evident of the progress of maintaining the forest in its historical condition.

The limitation of the service for historical conditions is that it cannot take a snapshot of biodiversity in the past. The resolution of the earth monitoring image is unable to reveal what the tree species are and count the quantity of them. This limitation is going to be alleviated by other work packages, such as mobile-based biodiversity monitoring, that allow future digital footprints of biodiversity to be recorded. Therefore, open forest map would be an integrated part of the SILVANUS project.

5.1 Data Acquisition and Pre-Processing

In this tool, three groups of variables are defined. The first group variable is related to forest conditions and is derived from earth monitoring multispectral images. Secondly, a group of variables is related to climates such as temperature, precipitation, and wind. The third is society related data such as population density and gross domestic product. Those variables are collected from available open data providers such as Copernicus, USGS, world population, and the World Bank.

The rest of the historical information is also required, such as the forest fire events in the past, forest rehabilitation programs, and forest management policies. This data is expected to be fulfilled by the pilot owner. In the future, when this prototype has been evaluated, the data sources can be expanded for the public with moderation to ensure data validity.

This application prototype cover analysis for the pilot area under the SILVANUS project for 10 years from 2010 to 2020 subject to data availability.

5.1.1 Data Source

Earth monitoring images come from third-party datasets from USGS and Copernicus that are publicly available. Copernicus is also providing climate-related data overtime in the ERA5 Re-analysis. Societal related data provided by World pop for spatiotemporal population and gross national product world bank. Societal-related data is commonly available at a more granular resolution in national statistical office; therefore, the application also allows national sources for certain data to provide more precise analysis in national level if the data is available. **Table 19** provides the data source for the services, parameters, and time span of this service.

The challenge of processing the streaming data from different sources is the variation in data availability. Earth monitoring images from non-geostationary satellites such as Sentinel and Landsat are available in regular basis with 16-days delays. With this limitation, this service cannot provide an exact date when the wildfire was ignited. Since the service does not aim for real-time monitoring, the delay is still acceptable. The other challenge is the image noise due to the cloud cover. Some images are covered more than 20% by clouds, which leads to low quality analysis. To ensure the quality of analysis, we filtered out the data with more than 20% cloud cover.

5.1.2 Data Acquisition

The OpenForest Map contains diverse data, encompassing three main categories of variables: physical, climate, and socioeconomic (**Table 19**). Among the physical variables are vegetation and land cover, derived from satellite imagery. Typically, the analysis utilizes satellites imagery with multispectral bands like the Landsat and Sentinel satellites. Landsat imagery is widely utilized in forest fire management for various purposes. One of the key applications is estimating forest conditions and fire severity. Landsat imagery, particularly the multi-spectral imagery from the Landsat family of sensors, is used to derive prefire biomass and stand age, which are important factors in assessing fire severity (Zald & Dunn, 2018). Furthermore, Landsat imagery is utilized in mapping tree canopy cover and aboveground biomass (Karlson et al., 2015). In post-fire operations, Landsat imagery is used to analyse fire impacts and develop vegetation recovery plans. Satellite-based maps, including those derived from Landsat data, are used to assess fire damage, and monitor vegetation recovery after a fire event (Quintano et al., 2018; Fernández-Manso et al., 2016). This study utilizes Landsat images to assess historical forest conditions using various calculations, including NDVI, FCD, and NBR. NDVI value serves as a powerful indicator of vegetation health and density, providing insights into the overall condition of forests and their potential vulnerability to environmental changes or human impacts.

Table 19. Data Acquisition the OpenForest Map

Variables	Data Sources	File Format
Physical variables		
FCD (Forest Canopy Density)	Landsat satellite images (https://earthexplorer.usgs.gov/) Sentinel images (https://scihub.copernicus.eu/)	GeoTIFF
NDVI (Normalized Different Vegetation Index)		
NBR (Normalized Burned Ratio)		
Climate variables		
Temperature	ECMWF Reanalysis v5 (ERA5)	netCDF
Precipitation		
Wind speed		
Socioeconomic variables		
Population density	WorlPop database (https://hub.worldpop.org/)	GeoTIFF
GDP	World Bank data (https://data.worldbank.org/)	csv, xml (convertible to shp or GeoJSON)
Data of forest rehabilitation program	Local government	Text (convertible to shp or GeoJSON)

The study utilizes three climate variables, including temperature, precipitation, and wind speed, which are directly linked to forest fire incidents. The study obtained these climate data variables from ERA5 reanalysis data, freely available through the Copernicus Climate Data Store. ERA5 reanalysis data offers comprehensive global climate information with excellent spatial and temporal resolution.

The socio-economic variables in this study consist of population density, GDP (gross domestic product), and forest rehabilitation program data. Population density data was acquired from the World Population Database with a resolution of 1 km x 1 km. It is used to investigate the correlation between the spatial distribution of population density and the occurrence of forest fires. The GDP data represents economic factors relevant to the inhabitants of the forest fire-prone region. This data was obtained from the World Bank database, but the resolution is at the country level. For more detailed economic data, additional information from local government sources can be incorporated. Additionally, the study requires rehabilitation program data from the pilot area to assess the measures taken to mitigate forest fires and aid in their recovery. This data was obtained from the local government organization in each pilot project.

5.1.3 Data Pre-Processing

Earth monitoring images can be directly meaningful for the analysis. There are several preliminary tasks that need to be executed, such as atmospheric correction. This subsection provides some theoretical basis and formulas applied to the implementation of an open forest map.

Radiometric correction

Prior to processing Landsat data, it is necessary to perform radiometric correction to convert the Digital Number values to Top of Atmosphere reflectance (TOA reflectance). According to the Landsat Data User Handbook, the radiometric correction process involves several sequential steps, outlined as follows:

- DN to ToA reflectance

$$\rho\lambda' = M\rho * Qcal + A\rho \quad \textbf{[60]}$$

where:
ρλ' = TOA Planetary Spectral Reflectance, without correction for solar angle. (Unitless)
Mρ = Reflectance multiplicative scaling factor for the band (REFLECTANCEW_MULT_BAND_n from the metadata).
Aρ = Reflectance additive scaling factor for the band (REFLECTANCE_ADD_BAND_N from the metadata).
Qcal = Level 1 pixel value in DN

- Correction for the solar elevation angle

$$\rho\lambda = \frac{\rho\lambda'}{\cos(\theta_{SZ})} = \frac{\rho\lambda'}{\sin(\theta_{SZ})} \quad \textbf{[61]}$$

where:
ρλ = TOA planetary reflectance
θSE = Local sun elevation angle; the scene center sun elevation angle in degrees is provided in the metadata
θSZ = Local solar zenith angle; θSZ = 90° - θSE

- **TOA Reflectance**

$$TOARef = (M\rho * Qcal + A\rho) / Sin (\theta SE) \quad [62]$$

where:
TOARef = TOA reflectance
Mρ = Reflectance multiplicative scaling factor for the band (REFLECTANCEW_MULT_BAND_n from the metadata)
Qcal = Level 1 pixel value in DN
Aρ = Reflectance additive scaling factor for the band (REFLECTANCE_ADD_BAND_N from the metadata)
θSE = Local sun elevation angle; the scene center sun elevation angle in degrees is provided in the metadata

ERA-5 Reanalysis

The fifth generation of the ECMWF's reanalysis of the previous eight decades' worth of global climate and weather is known as ERA5. Data is accessible starting in 1940. For a vast range of atmospheric, oceanic, and land-surface parameters, ERA5 gives hourly estimates. ERA5 provides hourly data, which requires additional processing to be presented on the OpenForest Map. The data displayed in the OpenForest Map, however, is monthly data derived from the original hourly data. The temperature variable utilized is 2m temperature, while the precipitation variable is represented by total precipitation. For wind speed, the 10m u-component and 10m v-component data are used in this study.

5.1.4 Data Processing

5.1.4.1 Multispectral Band for Sentinel

Sentinel-2 is a wide-swath, high-resolution, multi-spectral imaging mission that supports Copernicus Land Monitoring investigations, which include the observation of interior waterways and coastal areas as well as the monitoring of vegetation, soil, and water cover. 13 spectral bands are sampled by the SENTINEL-2 Multispectral Instrument (MSI), including four bands at a spatial resolution of 10 meters, six bands at 20 meters, and three bands at a resolution of 60 meters (**Table 20**).

Table 20. Multispectral Band for Sentinel

Band	Resolution	Central Wavelength	Description
B1	60 m	443 nm	Ultra-Blue (Coastal and Aerosol)
B2	10 m	490 nm	Blue
B3	10 m	560 nm	Green
B4	10 m	665 nm	Red
B5	20 m	705 nm	Visible and Near Infrared (VNIR)
B6	20 m	740 nm	Visible and Near Infrared (VNIR)
B7	20 m	783 nm	Visible and Near Infrared (VNIR)
B8	10 m	842 nm	Visible and Near Infrared (VNIR)
B8a	20 m	865 nm	Visible and Near Infrared (VNIR)
B9	20 m	940 nm	Short Wave Infrared (SWIR)
B10	60 m	1375 nm	Short Wave Infrared (SWIR)
B11	20 m	1610 nm	Short Wave Infrared (SWIR)
B12	20 m	2190 nm	Short Wave Infrared (SWIR)

5.1.4.2 Multispectral Band for Landsat

Landsat 8 was launched on February 11, 2013, and equipped with two sensors: the Operational Land Imager (OLI) and the Thermal Infrared Sensor (TIRS). These sensors offer a spatial resolution of 30 meters for visible, near-infrared (NIR), and shortwave infrared (SWIR) bands, 100 meters for thermal bands, and 15 meters for the panchromatic band **(Table 21**). Landsat 8 has a Sun-Synchronous orbit at an altitude of 705 km, and it captures imagery at a temporal resolution of 16 days.

Table 21. Multispectral Band for Landsat

Band	Resolution	Central Wavelength	Description
B1	30 m	0.43 - 0.45 µm	Coastal Aerosol
B2	30 m	0.450 - 0.51 µm	Blue
B3	30 m	0.53 - 0.59 µm	Green
B4	30 m	0.64 - 0.67 µm	Red
B5	30 m	0.85 - 0.88 µm	Near-Infrared
B6	30 m	1.57 - 1.65 µm	Shortwave Infrared 1
B7	30 m	2.11 - 2.29 µm	Shortwave Infrared 2
B8	15 m	0.50 - 0.68 µm	Panchromatic
B9	30 m	1.36 - 1.38 µm	Cirrus
B10	100 m	10.6 - 11.19 µm	Thermal Infrared Sensor 1
B11	100 m	11.5 - 12.51 µm	Thermal Infrared Sensor 2

5.1.4.3 NDVI calculation

NDVI has been widely used as an indicator of several factors, such as canopy density, biomass, plant health, and vegetation productivity (Rezaei & Ghaffarian, 2021). Furthermore, NDVI is also effective to assess vegetation damage, stress, recovery (Rezaei & Ghaffarian, 2021). NDVI time series monitoring using remote sensing images can be used to determine vegetation growth and recovery regarding ecological resilience program. NDVI is the ratio of the difference between the near-infrared band (NIR) and the red band (R) and the sum of these two bands (Rouse et al., 1974; Yengoh et al., 2015). Where NIR stands for Near-Infrared Light and RED stands for Visible Red Light. The NDVI formula is in the following equation.

$$NDVI = \frac{NIR - R}{NIR + R} \quad \textbf{[63]}$$

5.1.4.4 FCD calculation

Numerous factors have been measured in the evaluation of forest ecosystem condition. Forest canopy density is one of the indicators to monitor forest condition. Forest canopy density indicates percentage of vegetation cover (Rikimaru et al., 2002). Four indexes related to vegetation indices was used to determine forest canopy density. Calculation of forest canopy density was described using the following formula:

Advanced Vegetation Index (AVI)

The AVI formula is in the following:

$$AVI = \sqrt[3]{NIR(1 - RED)(NIR - RED)} \quad \textbf{[64]}$$

This formula is applied to the specific spectral band include red, near infrared, shortwave infrared, blue, green, and thermal band. Bands and wavelengths depend on the specific type of satellite images.

Bare Soil Index (BI)

The BI formula is in the following:

$$BI = \frac{(SWIR + RED) - (NIR + BLUE)}{(SWIR + RED) + (NIR + BLUE)} X\ 100 + 100 \quad \textbf{[65]}$$

Shadow Index (SI)

The SI formula is in the following:

$$SI = \sqrt[3]{(256 - BLUE)(256 - GREEN)(256 - RED)} \quad \textbf{[66]}$$

Thermal Index (TI)

The TI formula is in the following:

$$TI = \frac{K2}{\ln(\frac{K1}{L\lambda})} \quad \textbf{[67]}$$

Vegetation Density (VD)

The VD formula is in the following:

$$VD = \frac{(PCA1 - min)(max' - \min')}{(max - \min)} \quad \textbf{[68]}$$

Scaled Shadow Index (SSI)

The SSI formula is in the following:

$$SSI = \frac{(PCA2 - min)(max' - \min')}{(max - \min)} \quad \textbf{[69]}$$

Forest Canopy Density (FCD)

The FCD formula is in the following:

$$FCD = \sqrt[3]{SSI\ X\ VD + 1} + 1 \quad \textbf{[70]}$$

Where:

NIR is near infrared band; RED is red band; BLUE is blue band; GREEN is green band, SWIR is shortwave infrared band; PCA1 is digital value of principal component analysis between AVI and BI; PCA2 is digital value of principal component analysis between SI and TI; min is minimum value, and max is maximum value, max is maximum value; K1 is constant for thermal conversion band from metadata

(K2_CONSTANT_BAND_x); K2 is constant for thermal conversion band from metadata (K2_CONSTANT_BAND_x); and Lλ is top of atmosphere spectral radiance.

5.1.4.5 NBR calculation

The Normalized Burn Ratio (NBR) is an index specifically designed to emphasize burnt areas in extensive fire zones. It shares a resemblance to NDVI (Normalized Difference Vegetation Index) but distinguishes itself by incorporating both near-infrared (NIR) and shortwave infrared (SWIR) wavelengths in its formula.

$$NBR = \frac{NIR - SWIR}{NIR + SWIR} \quad \textbf{[71]}$$

Where NIR stands for Near-Infrared Light and SWIR stands for Shortwave Infrared Light.

5.2 Application Design

5.2.1 Use Case Diagram

This application receives data stream from the earth observation dataset. We divide the user into end user and authorized user. The use diagram in **Figure 67** shows user interaction between user and application as well as the application with external agent. The task for each user is defined in **Table 22.**

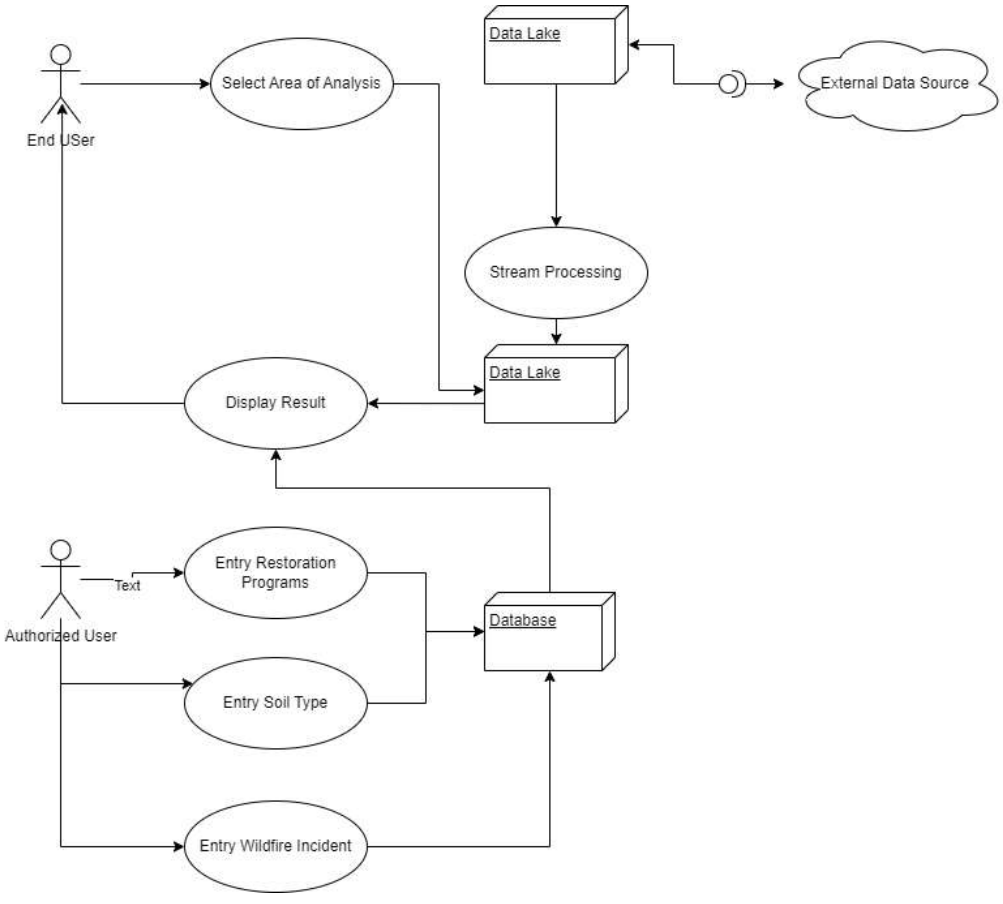

Figure 67. Use Case Diagram

Table 22. Actor and Their Task

Actor	Task
Authorized user	Entry necessary data such as program, geographical location, policy, and soil data Trigger data stream
End User	Identify the location for analysis. Display the result

5.2.2 Database Design

Open Forest Map service needs storage to record the analysis results, and some entities related to the wildfire incident, restoration, and rehabilitation programs. The earth monitoring image and its spatial processing derivations, such as NDVI, FCD and NBR collected as files in big data storage. There is an option to keep all the archives under this application or temporarily save them while processing. The database design is presented in **Figure 68**.

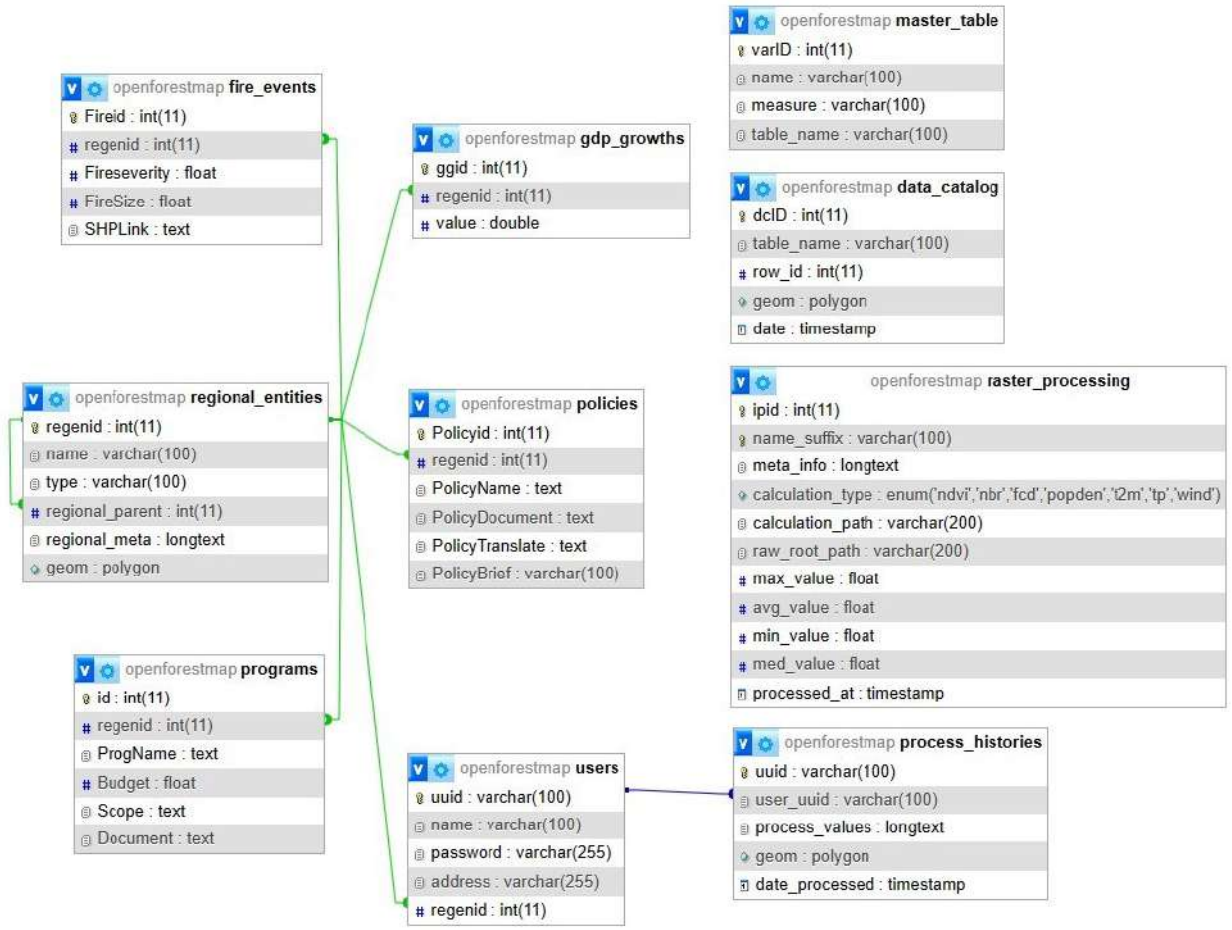

Figure 68. Open Forest Database Design

The database implements polymorphism concepts to enable better communication with the front end. The database is also implementing geometry data types to allow spatial data storage. The polymorphism table implemented in the data catalogue table allows flexibility for future development without interfering with the current services. This is an anticipation if we consider additional variables for further analysis.

The storage is designed to host intermediate processing results from earth monitoring images into NDVI, FCD and NBR while the raster processing output is archived as raster documents. The spatial and temporal data of gross domestic product (GDP) and population density are also stored in the database. Some stakeholders' intervention, such as policies and programs, are carried out in certain spatial space stored in policy and program table. Climate related data such as precipitation and temperature are also considered as the interacting variables towards the ecological resilience stored in climate tables. Soil data are managed in the soil table. Those recorded variables have different units and data ranges. To normalize the data and present it in a single analysis all numerical value will be normalized into standardized range between -1 to 1, and the normalized value is recorded in normalized columns in each table.

5.2.3 Features

This tool aims to record the time series data related to ecological resilience. The data are spatio-temporal covers pilot area, and the functionality is scalable to wider area depend on the data entered to the system. **Table 23** documents the basic functionality of Open Forest Map.

Table 23. The Basic Functionality of Open Forest Map.

No	Functionality	Input/Data Source	Output	User
1	Normal Difference Vegetation Index (NDVI) Calculation	Multispectral Image from Landsat or Sentinel	NDVI MAP	Automatic
2	Forest Canopy Density (FCD) calculation	Multispectral Image from Landsat or Sentinel	FCD MAP	Automatic
3	Temperature data Input	Copernicus ERA5	Temperature Map	Automatic
4	Precipitation data input	Copernicus ERA5	Precipitation Map	Automatic
5	Wind Speen data input	Copernicus ERA5	WindSpeed Map	Automatic
6	Population density	WorldPop	Population Density Map	Automatic
7	Gross National Product Mapping	World Bank	GNP Map	Automatic
8	CORINE landcover data input	Copernicus	Landcover map	Automatic
9	Landscape biodiversity index calculation	Landcover map	Biodiversity Index	User
10	Ecological Resilience Calculation	Time Series NDVI MAP	Elasticity, maleability, Magnitude and trends Ecological Resilience Graph	User
11	Resoration Policy input	User	Policy Map	User

No	Functionality	Input/Data Source	Output	User
12	Restoration Programs Input	User	Restoration Program Map	User
13	Soil Property Input	User	Soil Property Map	User
14	Fire Event Input	User	Fire Event Map	User
15	Graphical Analysis output	User Input Location/Fire Event Map NDVI Map FCD Map Temperature Map Precipitation MAP GNP Map Population Density Map Programs Map	Chart	User

5.2.4 Architectures

The architecture of the system is part of the SILVANUS' project platform. The architecture is divided into three main parts which are the ingestion and data input, data analysis, and data visualization. Data ingestion part would be integrated into the data ingestion platform in the SILVANUS project where all data from third party sources, such as earth observation data from Copernicus and USGS would be stored and managed.

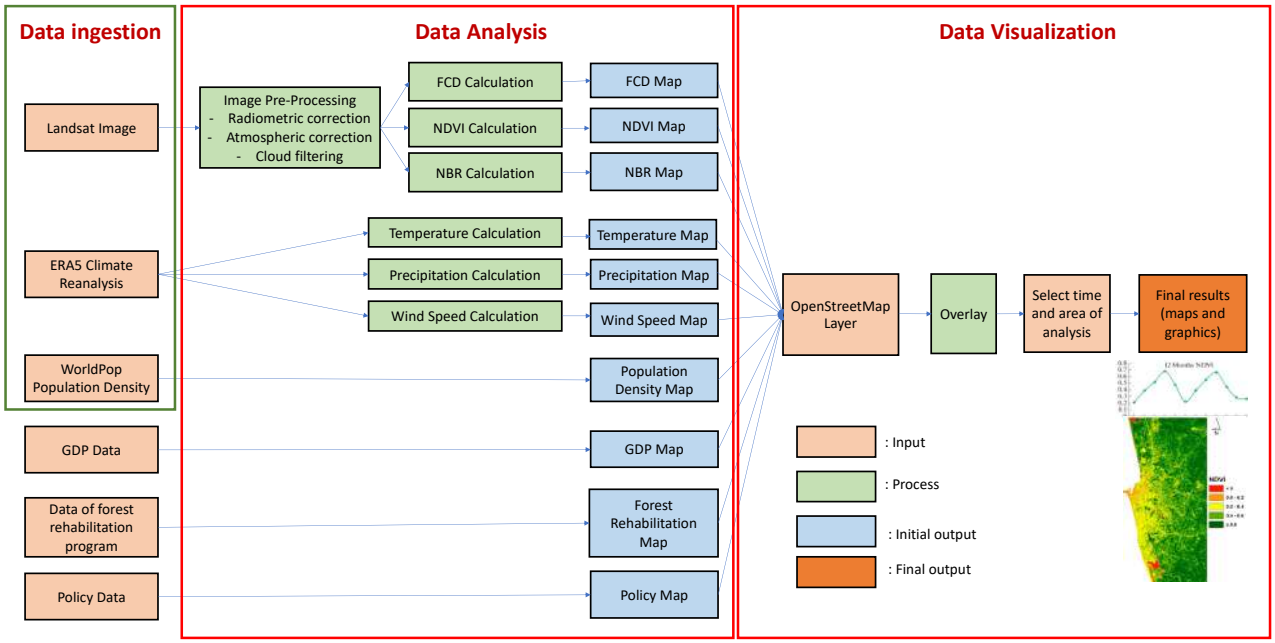

Figure 69. The Application Flow of The System is Part of Silvanus Project Platform

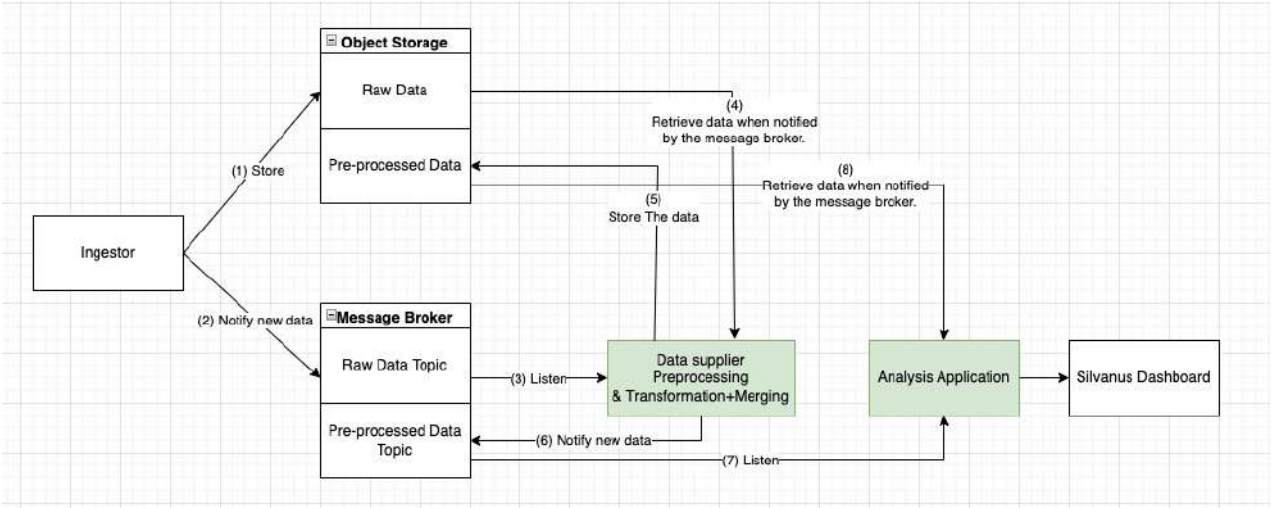

Figure 70. The Architecture of The System is Part of Silvanus Project Platform

The second part is the data analysis where the system provides data transformation and calculation. Data visualization is also integrated with the SILVANUS dashboard, where the results of the analysis are displayed to support the decision-maker in monitoring and make further analysis of forest restoration progress. **Figure 69** and **Figure 70** shows the application flow and the conceptual architecture of the open forest map.

5.2.5 User Interface and output design

Before embarking on the development of the Open Forest Map, it's vital to ensure that the user interface aligns with the needs of our stakeholders. As mentioned earlier, we've categorized stakeholders into two primary groups: the Authorized User and the End User. The Authorized User has the capability to store and upload pertinent documents, thereby ensuring that End Users have access to essential information about the forest. The detail of the Authorized User is integrated to the Silvanus User Management. Authorized user can access the interface provided in **Figure 71, Figure 72,** and **Figure 73** below.

After successfully logging into the system, the Authorized User can input information by selecting the 'Input Variable' button located at the bottom right of the screen. The system will display a right panel containing the information that can be entered by the Authorized User, as illustrated in **Figure 71**.

Subsequently, the Authorized User can select their preferred variable and then fill in the detailed information for it. Within the geometry section, there are three methods to determine the location: drawing manually in a box or free shape, importing from a file, or selecting an administrative location. Adjacent to this, in the 'Variable Data' section, the requirements differ based on the information associated with each variable, as illustrated in **Figure 73**.

Figure 71. Right Panel to Input Information

Figure 72. Spatial selection input for spatio temporal analysis

Figure 73. Geometry Coordinate Options

For the End User, the interface is relatively simple and straight forward to improve the user experience. We divide the information accessibility into two categories: forest features and event-corelated features. To access the information about forest features, the End User can select freely in the map interface, either selecting the map in a square, free form or point. To visualize other forest feature, end user can click the layer icon. Additionally, to access the event correlated feature, the user can select either program, policies, or fire events. The user can access the detail of features both of forest and event-correlated by clicking the geometry area (outlined area). Special only for forest features, user can analyse the correlation of features by clicking the Analyse Area button above. The End User interface is illustrated in **Figure 74, Figure 75,** and **Figure 76.**

For End Users, we've designed the interface to be intuitive and user-friendly to enhance their experience. The accessible information is divided into two main categories: forest features and event-correlated features. To explore the forest features, users have the flexibility to select areas on the map interface, whether through a square, freeform, or point selection. Subsequently, the map will show the visualization of forest features and a timeseries slider for those features. Additionally, to switch the visualization of forest features, users can click on the (layer icon) as illustrated in **Figure 74.**

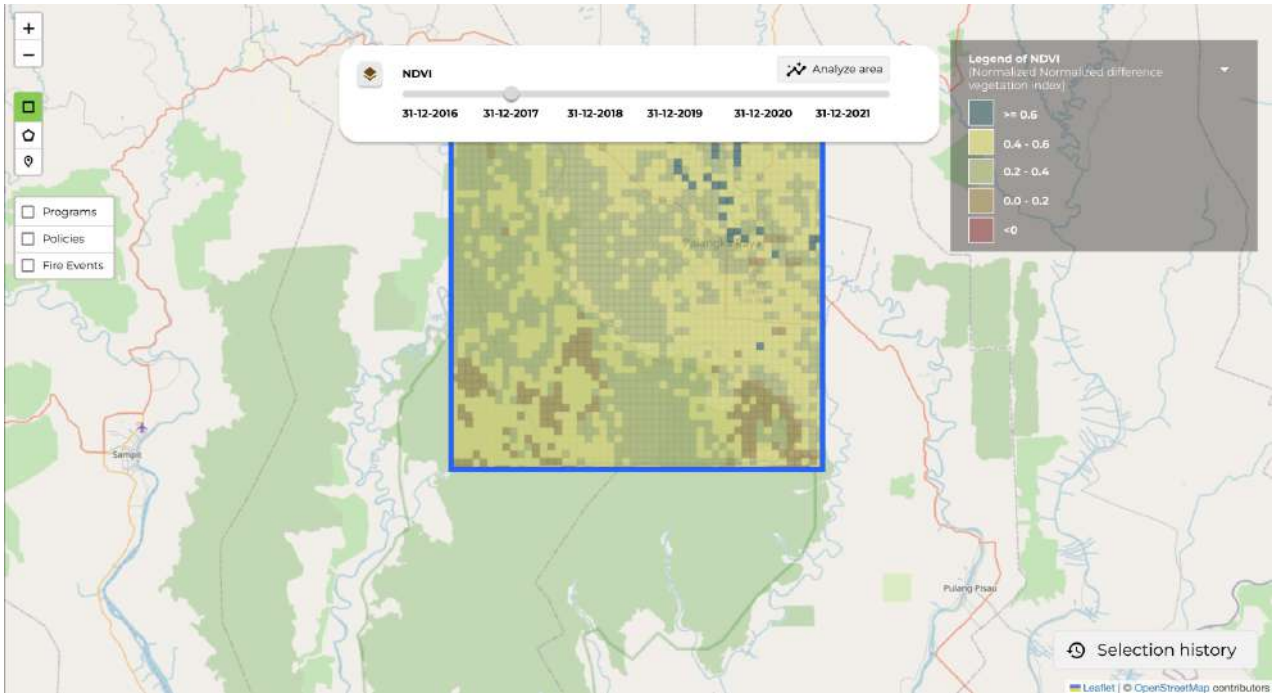

Figure 74. Area Selection to Visualize the Forest Feature

Exclusively for forest features, users have the capability to analyse feature correlations by selecting the 'Analyse Area' button as shown in **Figure 75.**

Figure 75. The Analysis of Forest Feature

On the other hand, event-correlated features can be accessed by selecting from programs, policies, or fire events. Detailed information for both forest and event-correlated features can be viewed by clicking on the designated geometry area (outlined area) as illustrated in **Figure 76**.

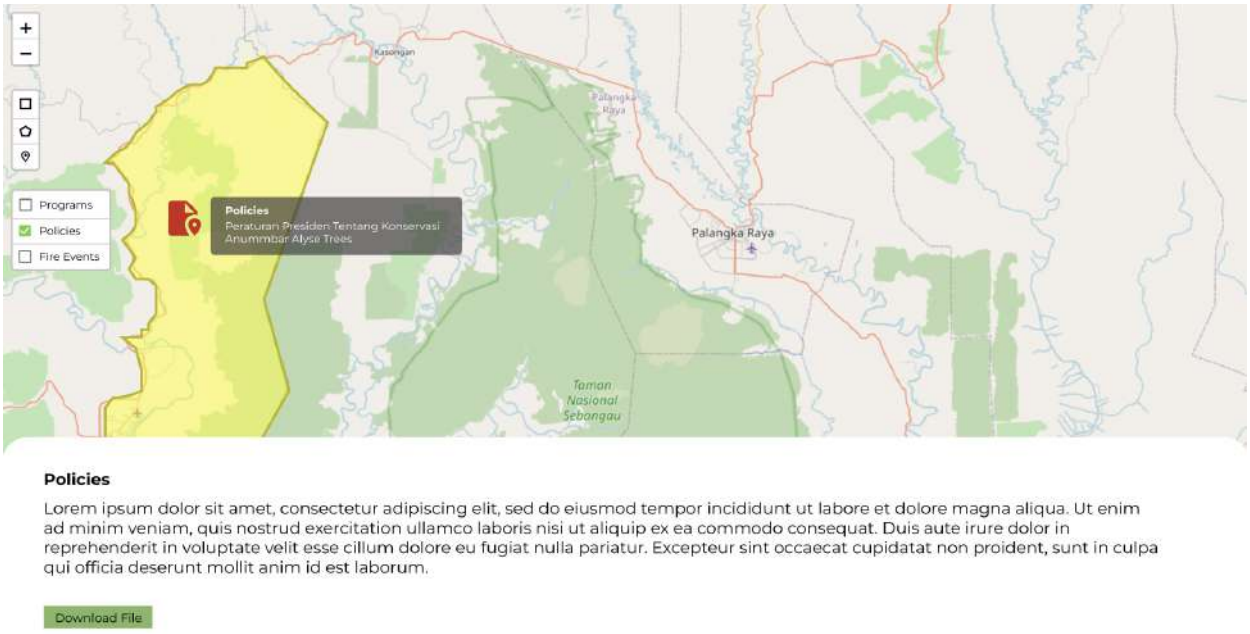

Figure 76. The Detailed Information of Event-Correlated Feature

5.2.5.1 Automatics data stream interface

The open forest map relies on streaming data sources such as Copernicus and USGS services. The open forest map in this stage collects data for a block of multispectral images over the pilot site. All the images are stored in a data lake, and the metadata is collected in the database. As aforementioned above, image

quality is different due to cloud cover problem. To relieve this problem, low-quality images are filtered out and omitted from the subsequent processes. The communication through this service and the data source are handled by the ingestion services of the Silvanus Platform.

5.2.5.2 User data Input

The open forest map needs user data input from authorities in each area. Their inputs comprehend wildfire incident related data, restoration, and rehabilitation program as well as policy. User interface is provided to allow those activities. The user interface for each input activity is shown in figures below (**Figure 77 and Figure 78**).

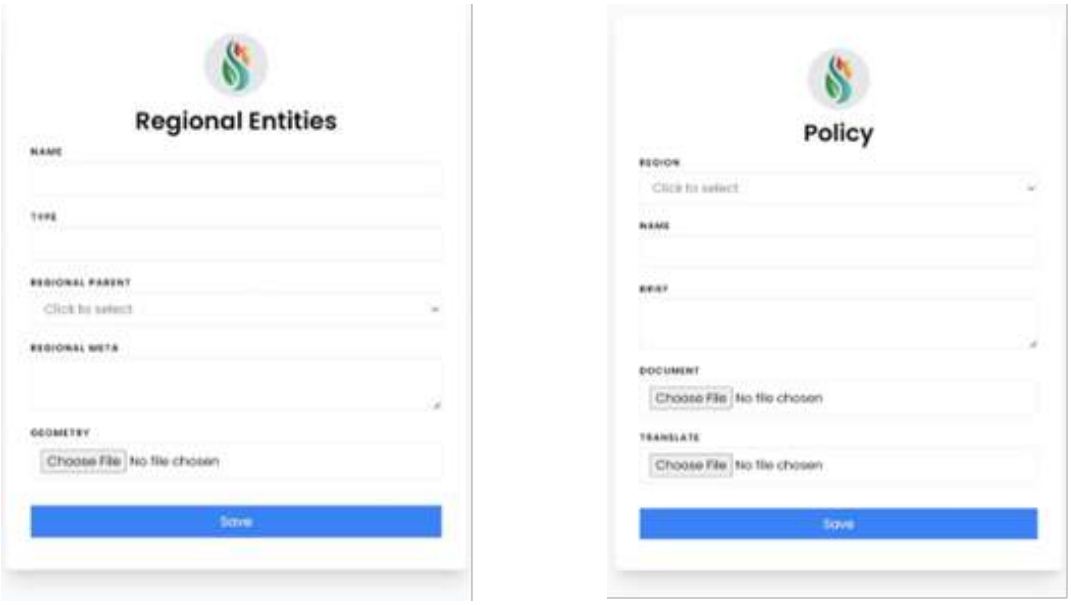

a **b**

Figure 77. a) Regional Entity Input; b) Policy Input in Open Forest Map

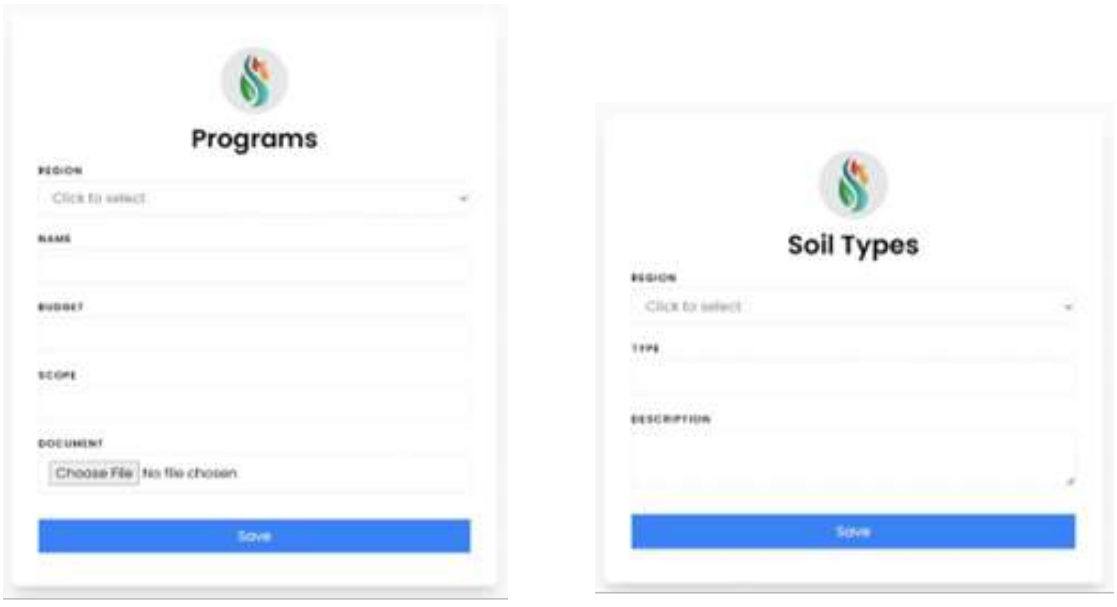

a **b**

Figure 78. a) Program Input; b) Soil data Input

5.2.5.3 Output Analysis Design

The output of the application is provided in two modes: first, the spatial overlay of the analysis result on the map. The spatial output is depicted in **Figure 79, Figure 80,** and **Figure 81**. The spatial output enables the user to interactively select the area of analysis over the provided maps. Secondly, the chart provided allows us to explore the interaction between variables visually. The challenge of data stream analysis is the period variation. Temperature, for example, streams every day, while population density is only available once a year. The rate at which value changes is also different; for example, if temperature is a volatile and can change in an hour, GDP on the other side, need a year to get new value. The differences are natural and therefore to provide meaningful analysis some data needs transformation. For example, the precipitation is summed out during a month, and it will relate to wet and dry month. Another challenge is the data availability, some data are available periodically, such as temperature, precipitation. Some other variables such as NDVI is not always available in periodical basis due to the image quality. To simplify the data presentation, we take da data in monthly basis. **Figure 79** shows the chart of interactions between variables.

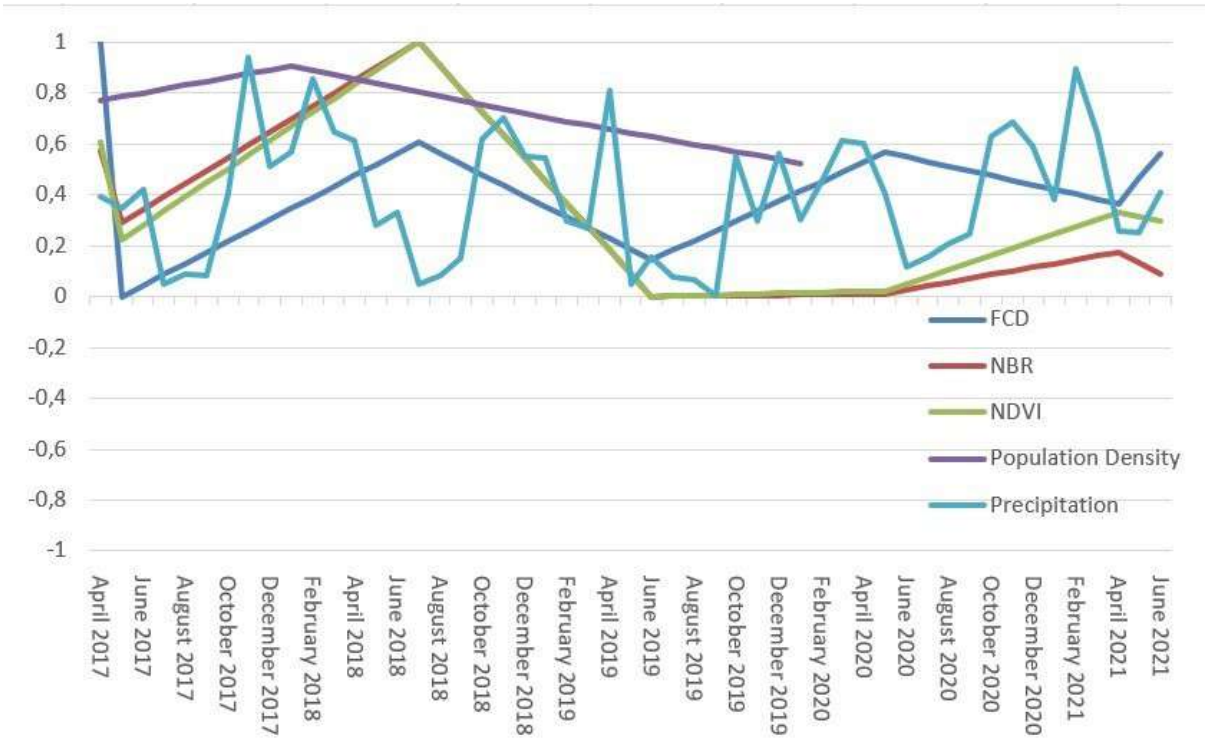

Figure 79. Output design for Time series Data plot

Landscape biodiversity Index is calculated through the Shanoon diversity index from CORINE landscape dataset **Figure 80** shows the landcover map and the calculation of Shannon index's diversity on one of European pilot is equal to 2.24.

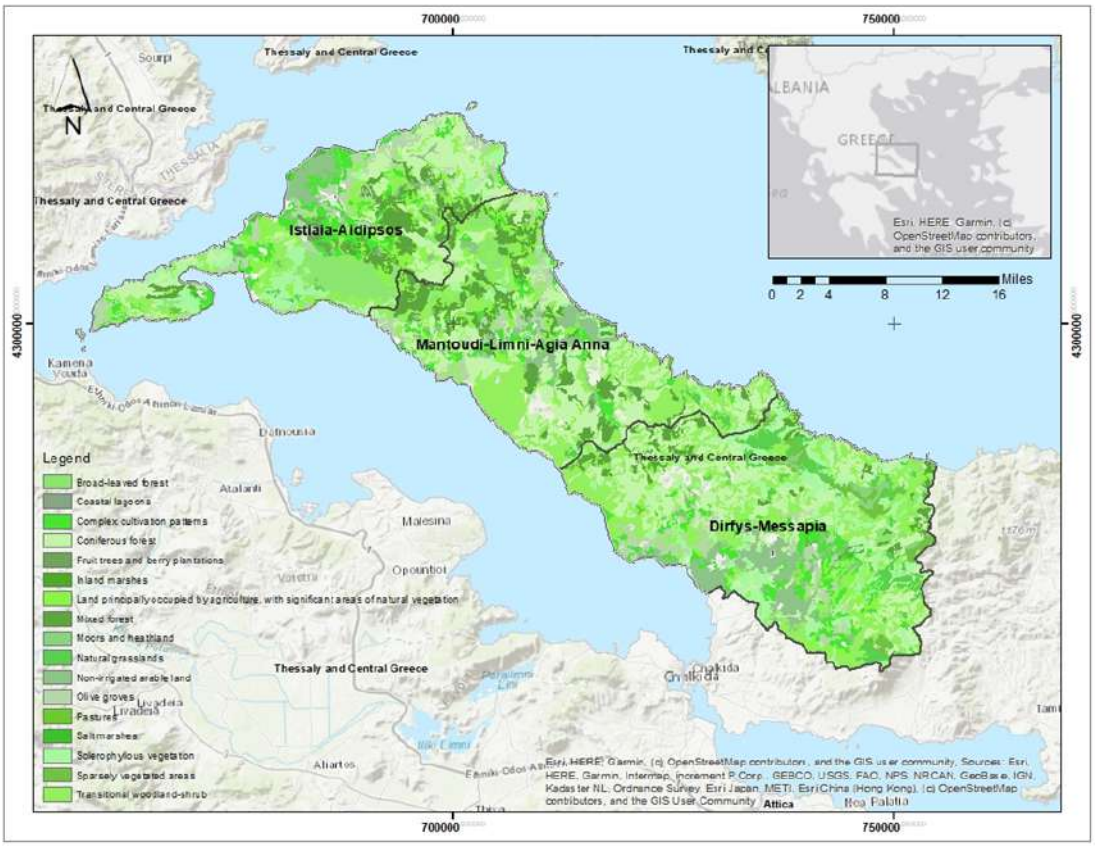

Figure 80. Land Cover Map and Biodiversity Calculation of Sterea Ellada

5.2.5.3.1 Ecological Resilience

Net burn ratio (NBR) a Normalized Difference Vegetation Index (NDVI) over time can indicate the fire severity and recovery speed of the forest. This service gives more attention to historical fires and the differences between NBR to understand the severity of wildfires in the past in a particular location. The service aims to classify the event into a fire severity class over time. **Figure 81** shows the fire severity analysis over time based on a multispectral earth observation image.

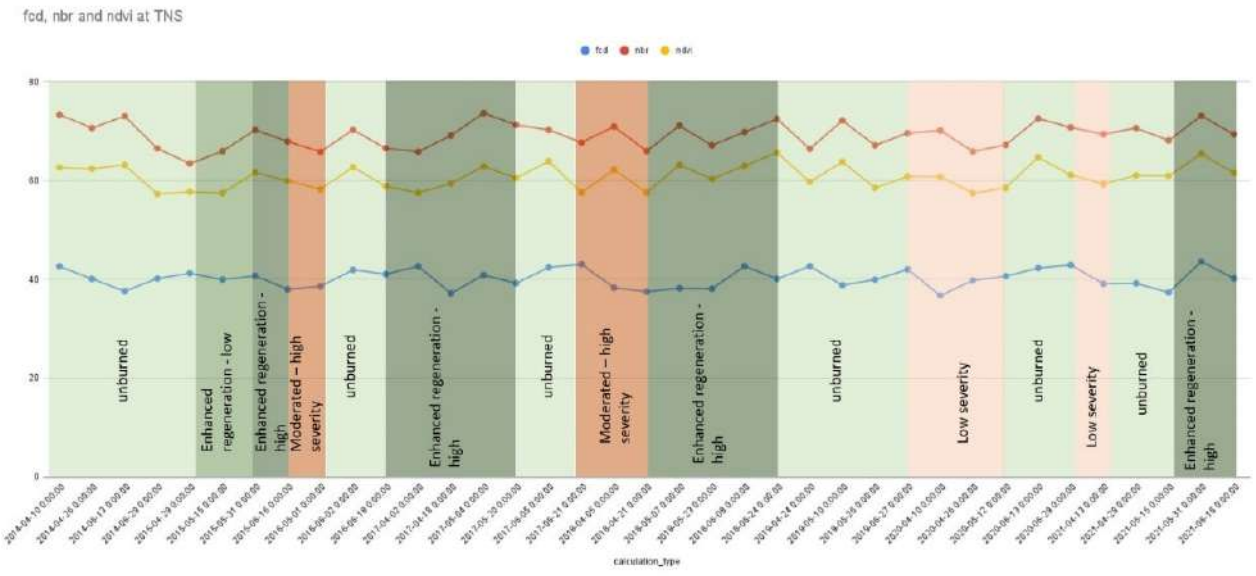

Figure 81. Fire Severity Chart

5.2.5.3.2 Ecological Resilient analysis

Based on the formula that we reported in the deliverable D6.1, ecological resilient is calculated based on amplitude, malleability, and elasticity. This model is implemented in the services, and we can design the output of those calculation throughout all European and non-European pilot in **Figure 82.**

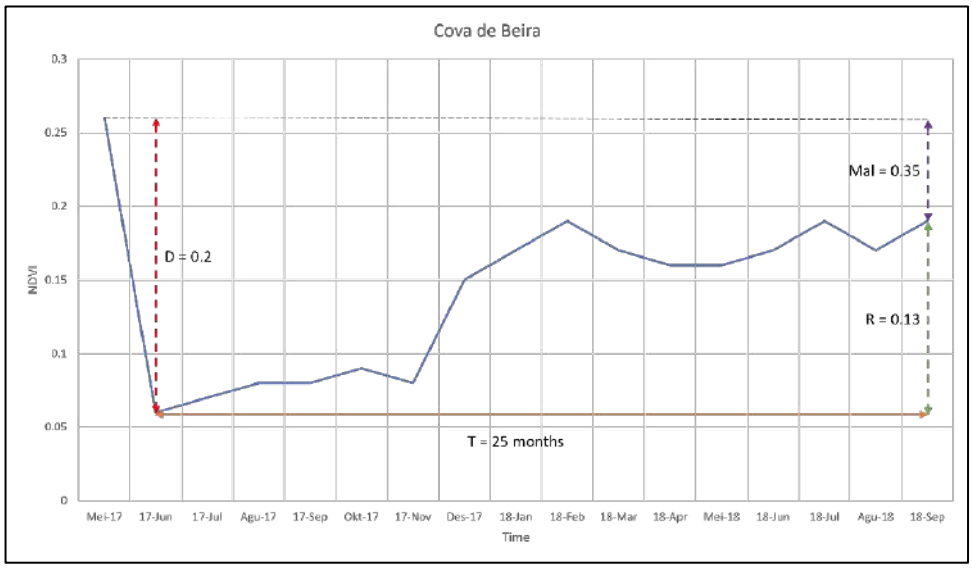

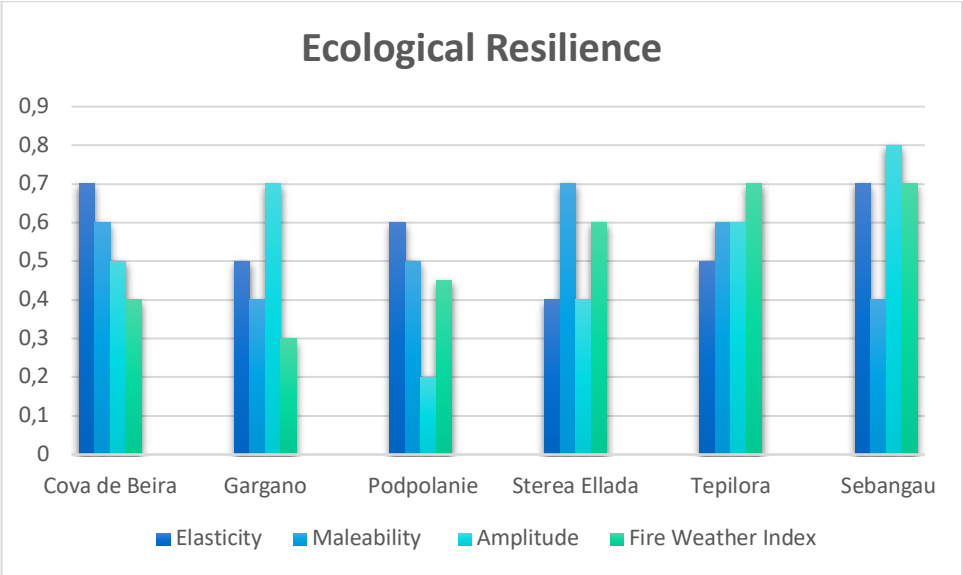

Figure 82. Output Design for Forest Adaptability Parameters versus Disturbance

This service basically can be used in other area of analysis inside or outside the pilot area. The analysis can be done by identifying the data sources needed for the calculation.

5.3 Data Analysis

The calculation results of the 6 available variables are in different scales and units. NDVI, FCD and NBR are in the range of 0 to 1. Temperature, on the other hand, ranging from 0 to 100 degrees Celsius. Precipitation range between 0 to 1 and the population density can achieve 1000 to 30 000 people per km squares. Those

variables need to be normalized into comparable range to properly analyzed. The second challenges are the temporal frequency, those data come in a different period of time; for example, earth monitoring images are available every 16 days. The temperatures, precipitation from ERA-5 reanalysis comes in higher frequency. While the population density is recorded once a year only and it is slow changing value. This condition needs to be tackled by interpolation of the data when it is unavailable.

5.3.1 Time Series Data Plotting

Below, an example of plotting individual variables in two pilot areas is represented. The selected location in the pilot area for analysis has selected by the indication that the area was suffering from wildfire incidents.

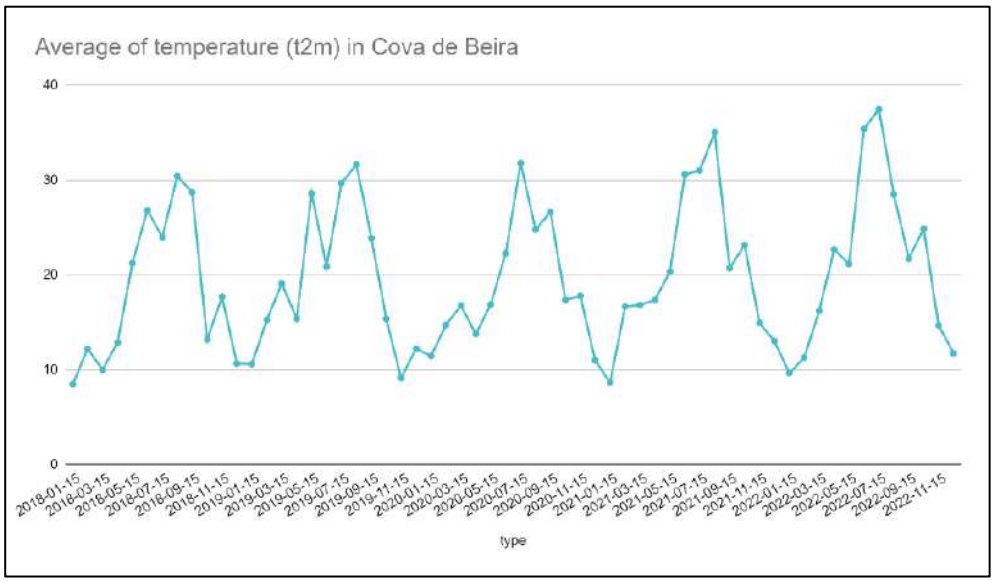

a)

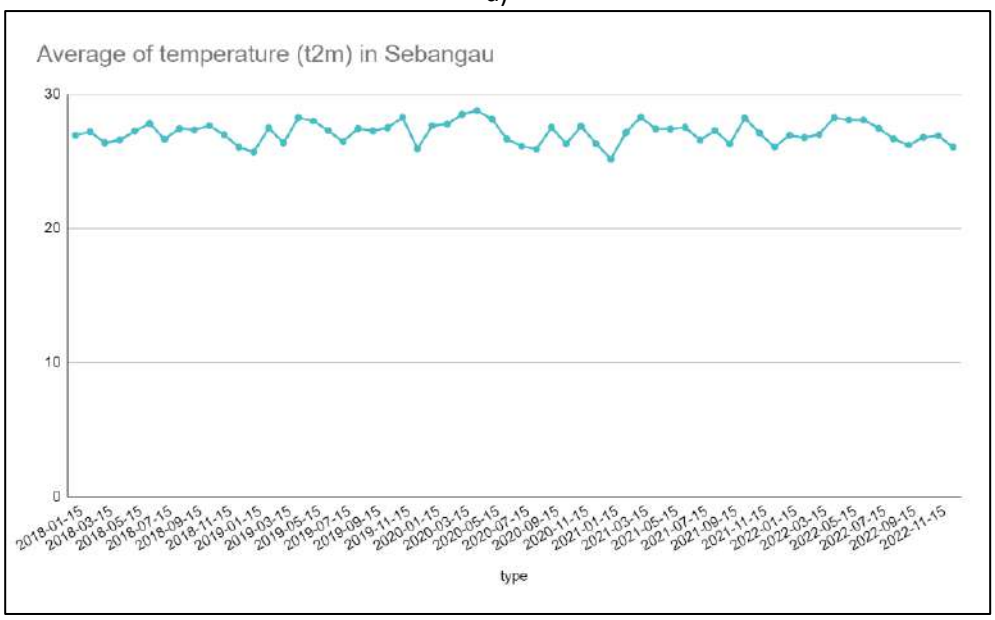

b)

Figure 83. Average of Temperature (t2m) in a) Cova de Beira; b) Sebangau National Park

Figure 83 shows the dynamic changes of the temperature in Cova de Beira pilot and Sebangau National Park. As can be seen, Sebangau National Park is in Indonesia, a tropical country; therefore, the variation is quite low, while on the left, recorded from a European pilot, where the variation between spring, summer, autumn, and winter is quite high. The peak of the temperature is also increasing, and it shows the impact of climate change.

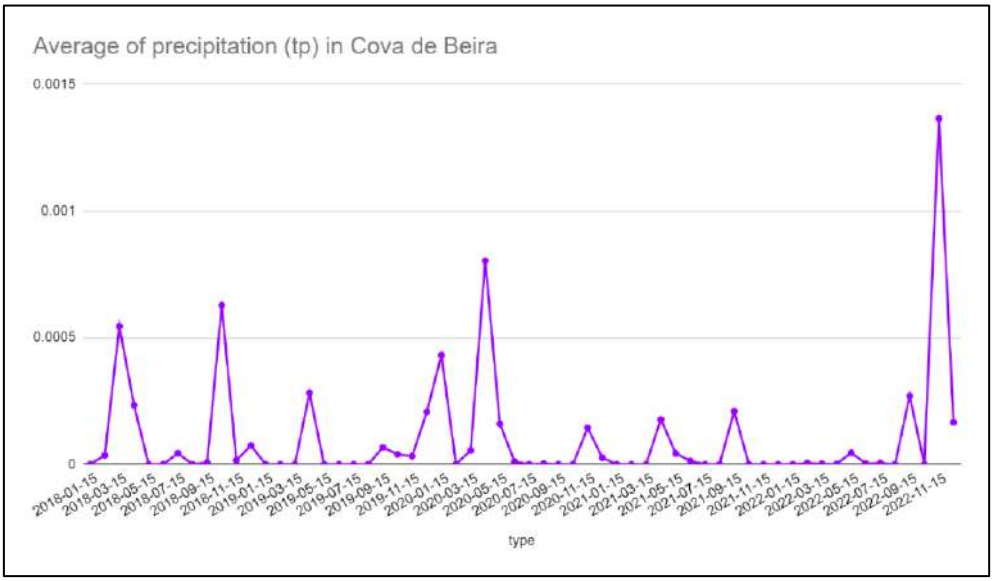

a)

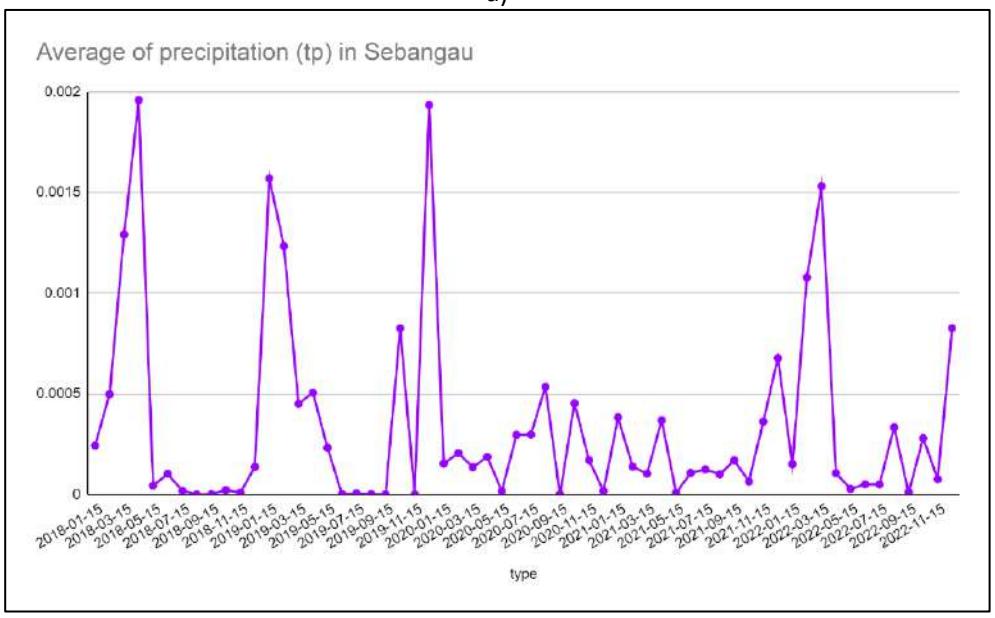

b)

Figure 84. Average of Precipitation (tp) in a) Cova de Beira; b) Sebangau National Park

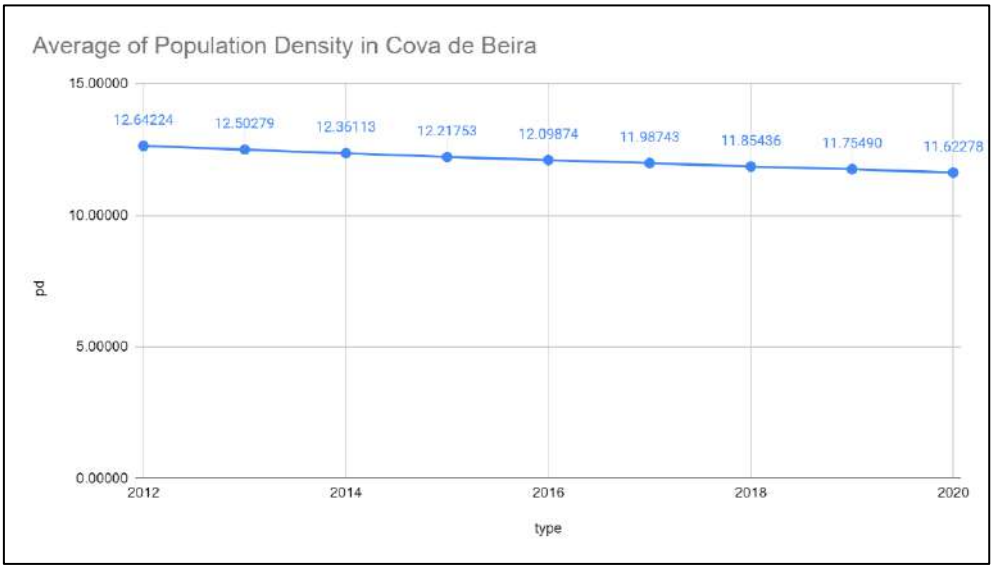

a)

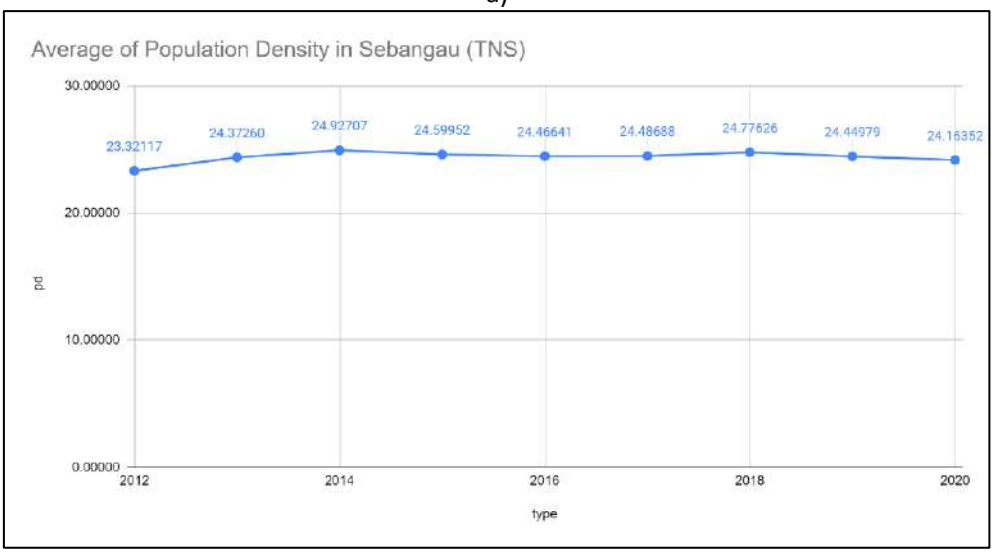

b)

Figure 85. Average of Population Density in a) Cova de Beira; b) Sebangau National Park

As we can see the figures above (**Figure 84, and Figure 85**) have different scales and different temporal scales. To put all the variables in one analysis pipeline, we need to perform data normalization, temporal resampling, and data interpolation whenever needed.

5.3.2 Data Normalization and temporal adjustments

As we can see in the two pilot areas where it was experienced wildfire, the fluctuation of the NDVI, FCD, temperature, and precipitation are shown in **Figure 81, Figure 82, Figure 83, Figure 84, and Figure 85.** Those charts show the different interval values and units of variables. Those data also come with different temporal resolution. To overcome those differences normalization must be carried out to limit all variables to a similar normalized value. Regarding to the temporal resolution, some less frequent data need to be interpolated to fill in the unavailable value at a certain time. **Figure 79** shows the normalized scale and interpolated data throughout the temporal axis. Those time series individual variable plot on its original scale and normalized scale serves further analysis of forest resilience processes.

6 Conclusion

Forest rehabilitation and restoration is an essential process for returning biodiversity and ecosystem that were previously affected by a disturbance. The main drivers of forest change are affected by these factors including temperature, precipitation, fire, drought, windstorm, insect outbreak, pathogens. The degradation of forest condition influences the quality and quantity of abiotic and biotic component in the forest. In general, to interevent in degraded ecosystem, it is crucial to focus on ecological resilience. This involves either restoring the ecosystem to a state equivalent to its native condition or transforming it into a new state (e.g., incorporating adaptive measure like the inclusion of plant species that are better adapted to the level of degradation or anticipated climate changes) that aligns with the management goals for the area and ensures the ecosystem's ability to withstand disturbances.

The concept of ecological resilience used in this project, taken from Holling et al. (1995), Levin and Simon. (2023), is the capacity of forest ecosystems to absorb the disturbance and maintain its normal patterns after being subjected to damage caused by an ecological disturbance. The state of ecological resilience measured in elasticity, malleability, and trend.

One of the impacts of fire events is changing soil conditions change due to extreme heat. Fire releases heat that kills soil microorganism and affects chemical properties in the soil. Those changes lead to soil devaluation into some extend and cause forest production to decline. Fire occurrence influence soil physical properties such as, colour, texture, bulk density, and water repellence. Another property of soil that is affected is its chemical components, such as soil reaction (pH), total organic carbon, soil organic matter and nutrient dynamics. Because of that, soil plays an important role in maintaining forest conditions before and after fire events.

The six pilot project sites encompass forests with distinct characteristics, broadly falling into the categories of subtropical dry forests, temperate continental forests, and tropical rainforests. The analysis of ecological resilience outcomes reveals that these three forest types exhibit varying ecological resilience characteristics, primarily shaped by factors such as climate, soil and rock properties, and vegetation structure. Consequently, a specific rehabilitation program is essential following a wildfire event to ensure the long-term sustainability of each forest type. To enhance forest condition after fire, ecological resilience programs were applied in each of the pilot area considering each intervention of the pilot owner. There are several rehabilitation and restoration conducted in Gargano, Tepilora, Cova da Beira, Podpolanie, Sterea Ellada, and Sebangau National Park.

- In Gargano, natural regeneration take place as the main restoration method. Although in some cases, dead tree removal and reforestation is also conducted depending on the fire intensity.
- In Tepilora, forest reconstitution consists of mechanical, cutting and clearing of dead and compromised individuals, manual forestry reconstitution, felling and trimming plants, and a mixed approach. In post fire program, replanting process is also conducted, if needed.
- In Sterea Ellada, artificial planting is applied as one of the restoration processes. However, natural regeneration is preferrable due to the usual successful recovery of native tree species.
- In Cova da Beira, natural regeneration and planning specific tree species is applied, including periodic shrub control, forest thinning and removal, eliminating diseased tree.
- Last, in Sebangau National Park, both natural regeneration and replanting were conducted. In addition, because of the peat swamp forest condition, canal blocking and well construction enforced to restore soil water table.

In this context, limitation of forest monitoring before and after fire is quite challenging among forest owners. The availability of historical data is mostly unrecorded. Therefore, a platform called **Open Forest Map** to facilitate forest management was generated. Open Forest Map aims to provide a long-term monitoring of the ecological resilient process mainly on forest ecosystems. This application generally uses

historical earth monitoring images, recorded historical climate related data, and other variables such as wildfire incidents, restoration and rehabilitation programs that have been carried out in the past. Open forest maps enable big data analysis for all possible related aspects of ecological resilience such as climate changes, wildfire disturbance as well as community related aspects. The services allow the expert user to access the data in chart format and to make further analysis.

7 REFERENCES

Abatzoglou, J. T., & Williams, A. P. (2016). Impact of anthropogenic climate change on wildfire across western US forests. *Proceedings of the National Academy of Sciences of the United States of America*, *113*(42), 11770–11775. https://doi.org/10.1073/pnas.1607171113

Abraham, J., & Dowling, K. (2017). The Unquantified Risk of Post-Fire Metal Concentration in Soil: a Review. *Water Air Soil Pollution* , *228*(5), 175.

Abrahim, G. M. S., & Parker, R. J. (2008). Assessment of heavy metal enrichment factors and the degree of contamination in marine sediments from Tamaki Estuary, Auckland, New Zealand. *Environmental Monitoring and Assessment*, *136*, 227–238.

Adamu, C. L., & Nganje, T. N. (2010). Heavy metal contamination of surface soil in relationship to land use patterns: A case study of Benue State, Nigeria. *Materials Sciences and Applications*, *1*, 127–134.

Adebayo, O. (2019). Loss of biodiversity:The burgeoning threat to human health. . *Annals of Ibadan Postgraduate Medicine*, *17*(1), 1–3.

Agbeshie, A. A., Abugre, S., Atta-Darkwa, T., & Awuah, R. (2022). A review of the effects of forest fire on soil properties. In *Journal of Forestry Research* (Vol. 33, Issue 5, pp. 1419–1441). Northeast Forestry University. https://doi.org/10.1007/s11676-022-01475-4

Agbeshie, A. A., Logah, V., Opoku, A., Tufour, H. O., Abubakari, A., & Quansah, C. (2020). Mineral nitrogen dynamics in compacted soil under organic amendment. *Scientific African* , *9*, e00488.

Al-Anbari, R., Abdul Hameed, M. J., Obaidy, A. l., & Fatima, H. A. A. (2015). Pollution loads and ecological risk assessment of heavy metals in the urban soil affected by various anthropogenic activities. *International Journal of Advanced Research*, *2*, 104–110.

Allen, C. D., Macalady, A. K., Chenchouni, H., Bachelet, D., McDowell, N., Vennetier, M., Kitzberger, T., Rigling, A., Breshears, D. D., Hogg, E. H. (Ted), Gonzalez, P., Fensham, R., Zhang, Z., Castro, J., Demidova, N., Lim, J. H., Allard, G., Running, S. W., Semerci, A., & Cobb, N. (2010). A global overview of drought and heat-induced tree mortality reveals emerging climate change risks for forests. *Forest Ecology and Management*, *259*(4), 660–684. https://doi.org/10.1016/j.foreco.2009.09.001

Amacher, M. C., O'neill, K. P., & Perry, C. H. (2007). *United States Department of Agriculture Soil Vital Signs: A New Soil Quality Index (SQI) for Assessing Forest Soil Health*. http://www.fs.fed.us/rmrs/

Apostolidis, E., Pagkas, N., Sfouggaris, A., Trigkas, P., Perleros, V., Chavakis, E., Pothos, G., & Adrakta, C. (2022). *Master Plan for the New Forest. Evia after. Program for the reconstruction of North Evia.*

Araya, S. N., Meding, M., & Berhe, A. A. (2016). Thermal alteration of soil physico-chemical properties: a systematic study to infer response of Sierra Nevada climosequence soils to forest fires. *SOIL*, *2*, 351–366.

Arnold, J. G., Srinivasan, R., Muttiah, R. S., & Williams, J. R. (1998). LARGE AREA HYDROLOGIC MODELING AND ASSESSMENT PART I: MODEL DEVELOPMENT. *Journal of the American Water Resources Association*, *34*(1), 73–89. https://doi.org/10.1111/j.1752-1688.1998.tb05961.x

Arocena, J. M. , & Opio, C. (2003). Prescribed fire-induced changes in properties of sub-boreal forest soils. *Geoderma*, *113*(1–2), 1–16.

Arora, V. K., & Melton, J. R. (2018). Reduction in global area burned and wildfire emissions since 1930s enhances carbon uptake by land. *Nature Communications*, *9*(1). https://doi.org/10.1038/s41467-018-03838-0

Aubry-Kientz, M., Dutrieux, R., Ferraz, A., Saatchi, S., Hamraz, H., Williams, J., Coomes, D., Piboule, A., & Vincent, G. (2019). A comparative assessment of the performance of individual tree crowns delineation algorithms from ALS data in tropical forests. *Remote Sensing*, *11*(9), 1–21. https://doi.org/10.3390/rs11091086

Avendaño Salas, C., Sanz Montero, M. E., Cobo Rayán, R., & Gómez Montaña, J. L. (1997). Sediment yield at Spanish reservoirs and its relationship with the drainage area. *19th Symposium of Large Dams*, 863–874.

Bal-Price, A. K., Hogberg, H. T., Buzanska, L., Lenas, P., van Vliet, E., & Hartung, T. (2010). In vitro developmental neurotoxicity (DNT) testing: Relevant models and endpoints. *NeuroToxicology*, *31*(5), 545–554. https://doi.org/10.1016/j.neuro.2009.11.006

Banasik, K., & Walling, D. E. (1996). Predicting Sedimentgraphs for a Small Agricultural Catchment. *Hydrology Research*, *27*(4), 275–294. https://doi.org/10.2166/nh.1996.0010

Bathurst, J. C., Iroumé, A., Cisneros, F., Fallas, J., Iturraspe, R., Novillo, M. G., Urciuolo, A., Bièvre, B. de, Borges, V. G., Coello, C., Cisneros, P., Gayoso, J., Miranda, M., & Ramírez, M. (2011). Forest impact on floods due to extreme rainfall and snowmelt in four Latin American environments 1: Field data analysis. *Journal of Hydrology*, *400*(3–4), 281–291. https://doi.org/10.1016/j.jhydrol.2010.11.044

Batjes, N. H., Ribeiro, E., & van Oostrum, A. (2020). Standardised soil profile data to support global mapping and modelling (WoSIS snapshot 2019). *Earth System Science Data*, *12*(1), 299–320. https://doi.org/10.5194/essd-12-299-2020

Bemporad, G. A., Alterach, J., Amighetti, F. F., Peviani, M., & Saccardo, I. (1997). A distributed approach for sediment yield evaluation in Alpine regions. *Journal of Hydrology*, *197*(1–4), 370–392. https://doi.org/10.1016/0022-1694(95)02978-8

Blake, G., & Hartge, K. (1986). Bulk Density. In G. , Campbell, R. , Jackson, M. , Mortland, D. , Nielsen, & A. Klute (Eds.), *Methods of Soil Analysis, Part I. Physical and Mineralogical Methods: Vol. SSSA Book Series: 5* (Second Edition, pp. 1–1188).

Boerner, R. E. C. , Hart, S. , & Huang J. (2009). Impacts of Fire and Fire Surrogate treatments. *Ecological Applications*, *19*(2), 338–358.

Bonan, G. B. (2008). Forests and climate change: Forcings, feedbacks, and the climate benefits of forests. *Science*, *320*(5882), 1444–1449. https://doi.org/10.1126/science.1155121

Breure, A. M. (2004). Soil biodiversity: measurements, indicators, threats and soil functions. . *SOIL AND COMPOST ECO-BIOLOGY* .

Brown, J. H., Gillooly, J. F., Allen, A. P., Savage, V. M., & West, G. B. (2004). TOWARD A METABOLIC THEORY OF ECOLOGY. *Ecology*, *85*(7), 1771–1789. https://doi.org/10.1890/03-9000

Brown, R. T., Agee, J. K., & Franklin, J. F. (2004). Forest Restoration and Fire: Principles in the Context of Place. *Conservation Biology*, *18*(4), 903–912. https://doi.org/10.1111/j.1523-1739.2004.521_1.x

Bryson, L. K. (2015). *An erosion and sediment delivery model for semi-arid catchments.* Rhodes University.

Bünemann, E. K., Bongiorno, G., Bai, Z., Creamer, R. E., De Deyn, G., de Goede, R., Fleskens, L., Geissen, V., Kuyper, T. W., Mäder, P., Pulleman, M., Sukkel, W., van Groenigen, J. W., & Brussaard, L. (2018). Soil quality – A critical review. *Soil Biology and Biochemistry*, *120*, 105–125. https://doi.org/10.1016/j.soilbio.2018.01.030

Buscardo, E., Rodríguez-Echeverría, S., Martín, M. P., De Angelis, P., Pereira, J. S., & Freitas, H. (2010). Impact of wildfire return interval on the ectomycorrhizal resistant propagules communities of a

Mediterranean open forest. *Fungal Biology*, *114*(8), 628–636. https://doi.org/10.1016/J.FUNBIO.2010.05.004

Caeiro, S., Costa, M. H., Ramos, T. B., Fernandes, F., Silveira, N., & Coimbra, A. (2005). Assessing heavy metal contamination in Sado Estuary sediment: An index analysis approach. . *Ecological Indicators*, *5*, 151–169.

Campos, I., & Abrantes, N. (2021). Forest fires as drivers of contamination of polycyclic aromatic hydrocarbons to the terrestrial and aquatic ecosystems. In *Current Opinion in Environmental Science and Health* (Vol. 24). Elsevier B.V. https://doi.org/10.1016/j.coesh.2021.100293

Canaveira, P., Martins, H., & Alves, M. (2016). *Plano de Gestão Florestal da Quinda da França 2012 – 2026*.

Cañizares, J. C., Copeland, S. M., & Doorn, N. (2021). Making sense of resilience. *Sustainability (Switzerland)*, *13*(15). https://doi.org/10.3390/su13158538

Carrington, M. E. (2010). Effects of Soil Temperature during Fire on Seed Survival in Florida Sand Pine Scrub. . *International Journal of Forestry Research*, 1–10.

Certini, G. (2005). Effect of fire on properties of soil. A review. *Oecologia*, *143*, 1–10.

Chazdon, R. L. (2008). Beyond Deforestation: Restoring Forests and Ecosystem Services on Degraded Lands. *Science*, *320*(5882), 1458–1460. https://doi.org/10.1126/SCIENCE.1155365

Chokkalingam, U., Sabogal, C., Almeida, E., Carandang, A. P., Gumartini, T., De Jong, W., Brienza, S., Lopez, A. M., Murniati, Nawir, A. A., Wibowo, L. R., Toma, T., Wollenberg, E., & Zaizhi, Z. (2005). Local participation, livelihood needs, and institutional arrangements: Three keys to sustainable rehabilitation of degraded tropical forest lands. *Forest Restoration in Landscapes: Beyond Planting Trees*, 405–414. https://doi.org/10.1007/0-387-29112-1_58/COVER

Choromanska, U., & DeLuca, T. M. (2002). Microbial activity and nitrogen mineralization in forest mineral soils following heating: Evaluation of post-fire effects. . *Soil Biology and Biochemistry*, *34*, 263–271.

Coakley, S. M., Scherm, H., & Chakraborty, S. (1999). Climate change and plant disease management. *Annual Review of Phytopathology*, *37*(February 1999), 399–426. https://doi.org/10.1146/annurev.phyto.37.1.399

Collins, K. M., Price, O. F., Penman, T. D., Collins, K. M., Price, O. F., & Penman, T. D. (2015). Spatial patterns of wildfire ignitions in south-eastern Australia. *International Journal of Wildland Fire*, *24*(8), 1098–1108. https://doi.org/10.1071/WF15054

Cook, B. I., Smerdon, J. E., Seager, R., & Coats, S. (2014). Global warming and 21st century drying. *Climate Dynamics*, *43*(9–10), 2607–2627. https://doi.org/10.1007/s00382-014-2075-y

Cui, X., Gibbes, C., Southworth, J., & Waylen, P. (2013). Using remote sensing to quantify vegetation change and ecological resilience in a semi-arid system. *Land*, *2*(2), 108–130. https://doi.org/10.3390/land2020108

Da Silva, R. M., Santos, C. A. G., & Silva, A. M. (2014). PREDICTING SOIL EROSION AND SEDIMENT YIELD IN THE TAPACURÁ CATCHMENT, BRAZIL. *Journal of Urban and Environmental Engineering*, 75–82. https://doi.org/10.4090/juee.2014.v8n1.075082

Dakos, V., & Kéfi, S. (2022). Ecological resilience: what to measure and how. *Environmental Research Letters*, *17*(4), 043003. https://doi.org/10.1088/1748-9326/ac5767

De Luis, M., Baeza, M. J., Raventós, J., & González-Hidalgo, J. C. (2004). Fuel characteristics and fire behaviour in mature Mediterranean gorse shrublands. *International Journal of Wildland Fire*, *13*(1), 79–87. https://doi.org/10.1071/WF03005

de Vente, J., & Poesen, J. (2005). Predicting soil erosion and sediment yield at the basin scale: Scale issues and semi-quantitative models. *Earth-Science Reviews*, *71*(1–2), 95–125. https://doi.org/10.1016/j.earscirev.2005.02.002

Dekker, L. W., & Ritsema, C. J. (1994). How water moves in a water repellent sandy soil: 1. Potential and actual water repellency. . *Water Resour. Res.*, *30*, 2507–2517.

Dendy, F. E., & Bolton, G. C. (1976). Sediment yield-runoff drainage area relationships in the United States. *Journal of Soil and Water Conservation*, *31*, 264–266.

Desmet, P., & Govers, G. (1996). A GIS procedure for automatically calculating the USLE LS factor on topographically complex landscape units. . *Journal of Soil and Water Conservation*, *51*(5), 427–433.

Diaz-Delgado, R., Lloret, F., Pons, X., & Terradas, J. (2002). Satellite Evidence of Decreasing Resilience in Mediterranean Plant Communities after Recurrent Wildfires. *Ecology*, *83*(8), 2293. https://doi.org/10.2307/3072060

Dinerstein, E., Olson, D., Joshi, A., Vynne, C., Burgess, N. D., Wikramanayake, E., Hahn, N., Palminteri, S., Hedao, P., Noss, R., Hansen, M., Locke, H., Ellis, E. C., Jones, B., Barber, C. V., Hayes, R., Kormos, C., Martin, V., Crist, E., … Saleem, M. (2017). An Ecoregion-Based Approach to Protecting Half the Terrestrial Realm. *BioScience*, *67*(6), 534–545. https://doi.org/10.1093/BIOSCI/BIX014

Doran, J. W. (2002). Soil health and global sustainability: translating science into practice. *Agriculture, Ecosystems & Environment*, *88*(2), 119–127. https://doi.org/10.1016/S0167-8809(01)00246-8

Doran, J. W., & Parkin, T. B. (1994). Defining and assessing soil quality. In J.W. Doran, D.C. Coleman, D.F. Bezdicek, & B.A. Stewart (Eds.), *Defining soil quality for a sustainable environment* (Vol. 35, pp. 1–21). SSSA Special Publication, Soil Science Society of America and American Society of Agronomy.

Dudley, N., Schlaepfer, R., Jeanrenaud, J.-P., Jackson, W., & StoltonJill, S. (2006). *Forest Quality: Assessing Forests at a Landscape Scale (Earthscan Forestry Library)*. Earthscan.

Enríquez-de-Salamanca, Á. (2022). Effects of Climate Change on Forest Regeneration in Central Spain. *Atmosphere*, *13*(1143), 1–11.

Erawaty Silalahi, E. T. M., Anita, S., & Teruna, H. Y. (2021). Comparison of Extraction Techniques for the Determination of Polycyclic Aromatic Hydrocarbons (PAHs) in Soil. *Journal of Physics: Conference Series*, *1819*(1). https://doi.org/10.1088/1742-6596/1819/1/012061

Escudey, M., Arancibia-Miranda, N., Pizarro, C., & Antilén, M. (2015). Effect of ash from forest fires on leaching in volcanic soils. *Catena*, *135*, 383–392. https://doi.org/10.1016/j.catena.2014.08.006

Espelta, J. M., Retana, J., & Habrouk, A. (2003). Resprouting patterns after fire and response to stool cleaning of two coexisting Mediterranean oaks with contrasting leaf habits on two different sites. *Forest Ecology and Management*, *179*(1–3), 401–414. https://doi.org/10.1016/S0378-1127(02)00541-8

FAO, & UNEP. (2020). The State of the World's Forests 2020. *The State of the World's Forests 2020*. https://doi.org/10.4060/CA8642EN

Ferguson, R. I. (1986). River Loads Underestimated by Rating Curves. *Water Resources Research*, *22*(1), 74–76. https://doi.org/10.1029/WR022i001p00074

Fernandes, P. M. (2009). Combining forest structure data and fuel modelling to classify fire hazard in Portugal. *Annals of Forest Science*, *66*(4), 415–415. https://doi.org/10.1051/forest/2009013

Fernandes, P. M. (2013). Fire-smart management of forest landscapes in the Mediterranean basin under global change. *Landscape and Urban Planning*, *110*(1), 175–182. https://doi.org/10.1016/j.landurbplan.2012.10.014

Fernández-García, V., Marcos, E., Huerta, S., & Calvo, L. (2021). Soil-vegetation relationships in Mediterranean forests after fire. *Forest Ecosystems*, *8*(1). https://doi.org/10.1186/s40663-021-00295-y

Ferro, V., & Porto, P. (2000). Sediment Delivery Distributed (SEDD) Model. *Journal of Hydrologic Engineering*, *5*(4), 411–422. https://doi.org/10.1061/(ASCE)1084-0699(2000)5:4(411)

Field, R. D., van der Werf, G. R., Fanin, T., Fetzer, E. J., Fuller, R., Jethva, H., Levy, R., Livesey, N. J., Luo, M., Torres, O., & Worden, H. M. (2016). Indonesian fire activity and smoke pollution in 2015 show persistent nonlinear sensitivity to El Niño-induced drought. *Proceedings of the National Academy of Sciences*, *113*(33), 9204–9209. https://doi.org/10.1073/pnas.1524888113

Folke, C., Carpenter, S. R., Walker, B., Scheffer, M., Chapin, T., & Rockström, J. (2010). Resilience thinking: Integrating resilience, adaptability and transformability. *Ecology and Society*, *15*(4). https://doi.org/10.5751/ES-03610-150420

Forzieri, G., Dakos, V., McDowell, N. G., Ramdane, A., & Cescatti, A. (2022). Emerging signals of declining forest resilience under climate change. *Nature*, *608*(7923), 534–539. https://doi.org/10.1038/s41586-022-04959-9

Foster, I., Harrison, S., & Clark, D. (1997). Soil Erosion in the West Midlands: An Act of God or Agricultural Mismanagement? *Geography*, *82*, 231–239.

Gardner, W. (1986). Water Content. In Arnold Klute (Ed.), *Methods of Soil Analysis, Part I. Physical and Mineralogical Methods* (pp. 1–1188). American Society of Agronomy, Inc. Soil Science Society of America.

Gavrilovic, S. (1970). Modern ways of calculating the torrential sediment and erosion mapping. In *Yugoslav Committee for International Hydrological decade* (Vol. 1, pp. 85–100).

Gee, G., & Bauder, J. (1986). Particle-size Analysis. In Arnold Klute (Ed.), *Methods of Soil Analysis, Part I. Physical and Mineralogical Methods* (pp. 1–1188). American Society of Agronomy, Inc. Soil Science Society of America.

Gu, Y. G., Gao, Y. P., & Lin, Q. (2016). Contamination, bioaccessibility and human health risk of heavy metals in exposed-lawn soils from 28 urban parks in southern China's largest city, Guangzhou. *Applied Geochemistry*, *67*, 52–58. https://doi.org/10.1016/J.APGEOCHEM.2016.02.004

Guo, K. ;, Wang, B. ;, Niu, X. A., Guo, K., Wang, B., & Niu, X. (2023). A Review of Research on Forest Ecosystem Quality Assessment and Prediction Methods. *Forests 2023, Vol. 14, Page 317*, *14*(2), 317. https://doi.org/10.3390/F14020317

Gyssels, G., Poesen, J., Bochet, E., & Li, Y. (2005). Impact of plant roots on the resistance of soils to erosion by water: a review. *Progress in Physical Geography: Earth and Environment*, *29*(2), 189–217. https://doi.org/10.1191/0309133305pp443ra

Hartung, M., Carreño-Rocabado, G., Peña-Claros, M., & van der Sande, M. T. (2021). Tropical Dry Forest Resilience to Fire Depends on Fire Frequency and Climate. *Frontiers in Forests and Global Change*, *4*, 755104. https://doi.org/10.3389/FFGC.2021.755104/BIBTEX

Hobbs, R. J., & Harris, J. A. (2001). Restoration Ecology: Repairing the Earth's Ecosystems in the New Millennium. *Restoration Ecology*, *9*(2), 239–246. https://doi.org/10.1046/J.1526-100X.2001.009002239.X

Holling, C. S. (1973). *Resilience and Stability of Ecological Systems on JSTOR*. https://www.jstor.org/stable/2096802

Hosseini, M., Nunes, J. P., Pelayo, O. G., Keizer, J. J., Ritsema, C., & Geissen, V. (2018). Developing generalized parameters for post-fire erosion risk assessment using the revised Morgan-Morgan-Finney model: A test for north-central Portuguese pine stands. *CATENA*, *165*, 358–368. https://doi.org/10.1016/J.CATENA.2018.02.019

Hossner, L. R. (1996). Dissolution of Total Elemental Analysis. In D. L. ; P. A. L. ; H. P. A. ; L. R. H. ; S. P. N. ; T. M. A. ; J. C. T. ; S. M. E. Sparks (Ed.), *Methods of soil analysis. Part 3 - chemical methods.* (Vol. 5, pp. 49–64). Soil Science Society of America Inc.

Hubbell, S. P. (2005). Neutral theory in community ecology and the hypothesis of functional equivalence. *Functional Ecology*, *19*(1), 166–172. https://doi.org/10.1111/j.0269-8463.2005.00965.x

Hughes, D. A., & Slaughter, A. (2015). Daily disaggregation of simulated monthly flows using different rainfall datasets in southern Africa. *Journal of Hydrology: Regional Studies*, *4*(PB), 153–171. https://doi.org/10.1016/J.EJRH.2015.05.011

Ibáñez, I., Acharya, K., Juno, E., Karounos, C., Lee, B. R., McCollum, C., Schaffer-Morrison, S., & Tourville, J. (2019). Forest resilience under global environmental change: Do we have the information we need? A systematic review. *PLoS ONE*, *14*(9). https://doi.org/10.1371/journal.pone.0222207

Iglesias, T., Cala, V., & Gonzalez, J. (1997). Mineralogical and chemical modifications in soils affected by a forest fire in the Mediterranean area. *Science of The Total Environment*, *204*(1), 89–96. https://doi.org/10.1016/S0048-9697(97)00173-3

Inbar, A., Lado, M., Sternberg, M., Tenau, H., & Ben-Hur, M. (2014). Forest fire effects on soil chemical and physicochemical properties, infiltration, runoff, and erosion in a semiarid Mediterranean region. *Geoderma*, *221–222*, 131–138. https://doi.org/10.1016/J.GEODERMA.2014.01.015

Inengite, A., Abasi, C., & Walter, C. (2015). Application of Pollution Indices for the Assessment of Heavy Metal Pollution in Flood Impacted Soil. *International Research Journal of Pure and Applied Chemistry*, *8*(3), 175–189. https://doi.org/10.9734/IRJPAC/2015/17859

Jha, M., Gassman, P. W., Secchi, S., Gu, R., & Arnold, J. (2004). EFFECT OF WATERSHED SUBDIVISION ON SWAT FLOW, SEDIMENT, AND NUTRIENT PREDICTIONS. *Journal of the American Water Resources Association*, *40*(3), 811–825. https://doi.org/10.1111/j.1752-1688.2004.tb04460.x

Jolly, W. M., Cochrane, M. A., Freeborn, P. H., Holden, Z. A., Brown, T. J., Williamson, G. J., & Bowman, D. M. J. S. (2015). Climate-induced variations in global wildfire danger from 1979 to 2013. *Nature Communications*, *6*. https://doi.org/10.1038/ncomms8537

Jones, G. M., Gutierrez, J. R., Tempel, D. J., Whitmore, SA., Berigan, W. J., & Peery, M. Z. (2016). Megafires an emerging threat to old-forest species. *Front Ecol Environ*, *14*(6), 300–306.

Julien, P. Y., & Simons, D. B. (1985). Sediment Transport Capacity of Overland Flow. *Transactions of the ASAE*, *28*(3), 755–762. https://doi.org/10.13031/2013.32333

Kainyande, A., Auch, E., & Okoni-Williams, A. (2023). Local perceptions of the socio-demographic changes triggered by large-scale plantation forests: Evidence from rural communities in Northern Province of Sierra Leone. *Environmental Challenges*, *11*, 100694. https://doi.org/10.1016/J.ENVC.2023.100694

Kalra, Y. P., & Maynard, D. G. (1991). Methods manual for forest soil and plant analysis. *Forestry Canada, Northwest Region, Northern Forestry Centre Edmonton, Alberta*, 116.

Karydas, C. G., & Panagos, P. (2018). The G2 erosion model: An algorithm for month-time step assessments. *Environmental Research*, *161*, 256–267. https://doi.org/10.1016/j.envres.2017.11.010

Keesstra, S., Wittenberg, L., Maroulis, J., Sambalino, F., Malkinson, D., Cerdà, A., & Pereira, P. (2017). The influence of fire history, plant species and post-fire management on soil water repellency in a Mediterranean catchment: The Mount Carmel range, Israel. *CATENA*, *149*, 857–866. https://doi.org/10.1016/J.CATENA.2016.04.006

Keizer, J. J., Silva, F. C., Vieira, D. C. S., González-Pelayo, O., Campos, I., Vieira, A. M. D., Valente, S., & Prats, S. A. (2018). The effectiveness of two contrasting mulch application rates to reduce post-fire erosion in a Portuguese eucalypt plantation. *CATENA*, *169*, 21–30. https://doi.org/10.1016/j.catena.2018.05.029

Ketterings, Q. M., Bigham, J. M., & Laperche, V. (2000). Changes in Soil Mineralogy and Texture Caused by Slash-and-Burn Fires in Sumatra, Indonesia. *Soil Science Society of America Journal*, *64*(3), 1108–1117. https://doi.org/10.2136/sssaj2000.6431108x

Kinnell, P. I. A. (2005). Raindrop-impact-induced erosion processes and prediction: a review. *Hydrological Processes*, *19*(14), 2815–2844. https://doi.org/10.1002/hyp.5788

Kinnell, P. I. A., & Risse, L. M. (1998). USLE-M: Empirical Modeling Rainfall Erosion through Runoff and Sediment Concentration. *Soil Science Society of America Journal*, *62*(6), 1667–1672. https://doi.org/10.2136/sssaj1998.03615995006200060026x

Kirkby, M. J. (1976). Tests of the random network model, and its applications to basin hydrology. . *Earth Surf. Processes*, *1*, 197–212.

Kloster, S., Mahowald, N. M., Randerson, J. T., & Lawrence, P. J. (2012). The impacts of climate, land use, and demography on fires during the 21st century simulated by CLM-CN. *Biogeosciences*, *9*(1), 509–525. https://doi.org/10.5194/BG-9-509-2012

Koutsoyiannis, D., & Tarla, K. (1987). Sediment yield estimations in Greece. . *Technika Chronika*, *A7*(3), 127–154.

Kowalska, J. B., Mazurek, R., Gąsiorek, M., & Zaleski, T. (2018). Pollution indices as useful tools for the comprehensive evaluation of the degree of soil contamination–A review. *Environmental Geochemistry and Health*, *40*(6), 2395–2420. https://doi.org/10.1007/s10653-018-0106-z

Krcho, J. (1992). Georelief and its cartographic modelling by complex digital model (CDM) from geographical information systém (GIS) point of view. . In *Acta Facultatis Rerum Naturalium Universitatis Comenianae* (Vol. 33, pp. 3–132).

Lamb, D., & Gilmour, D. (2003). *Rehabilitation and Restoration of Degraded Forests*. IUCN, Gland, Switzerland and Cambridge, UK and WWF, Gland, Switzerland. http://www.iucn.org

Landsberg, J. J., & Waring, R. H. (1997). A generalised model of forest productivity using simplified concepts of radiation-use efficiency, carbon balance and partitioning. *Forest Ecology and Management*, *95*(3), 209–228. https://doi.org/10.1016/S0378-1127(97)00026-1

Larsen, J. B., Angelstam, P., Bauhus, J., Carvalho, J. F., Diaci, J., Dobrowolska, D., Gazda, A., Gustafsson, L., Krumm, F., Knoke, T., Konczal, A., Kuuluvainen, T., Mason, B., Motta, R., Pötzelsberger, E., Rigling, A., & Schuck, A. (2022). *Closer-to-Nature Forest Management From Science to Policy 12 2 From Science to Policy 12*. https://doi.org/10.36333/fs12

Lavorel, S., Flannigan, M. D., Lambin, E. F., & Scholes, M. C. (2007). *Vulnerability of land systems to fire : Interactions among humans , climate , the atmosphere , and ecosystems Vulnerability of land systems to fire : Interactions among humans , climate , the atmosphere , and ecosystems*. *June 2014*. https://doi.org/10.1007/s11027-006-9046-5

Leach, M. K. (2006). Forest Restoration in Landscapes: Beyond Planting Trees. *Restoration Ecology*, *14*(2), 322–323. https://doi.org/10.1111/J.1526-100X.2006.00138.X

Li, Q., Ahn, S., Kim, T., & Im, S. (2021). Post-Fire Impacts of Vegetation Burning on Soil Properties and Water Repellency in a Pine Forest, South Korea. *Forests*, *12*(6), 708. https://doi.org/10.3390/f12060708

Linden, P. Van Der. (2015). Climate Change 2007 : Impacts , Adaptation and Vulnerability INTERGOVERNMENTAL PANEL ON CLIMATE CHANGE Climate Change 2007 : Impacts , Adaptation and Vulnerability Working Group II Contribution to the Intergovernmental Panel on Climate Change Summary for. *Environmental Research Letters*, *March*.

Liu, M., Liu, X., Wu, L., Tang, Y., Li, Y., Zhang, Y., Ye, L., & Zhang, B. (2021). Establishing forest resilience indicators in the hilly red soil region of southern China from vegetation greenness and landscape metrics using dense Landsat time series. *Ecological Indicators*, *121*, 106985. https://doi.org/10.1016/J.ECOLIND.2020.106985

Long, E. R., Macdonald, D. D., Smith, S. L., & Calder, F. D. (1995). Incidence of adverse biological effects within ranges of chemical concentrations in marine and estuarine sediments. *Environmental Management*, *19*(1), 81–97. https://doi.org/10.1007/BF02472006

Lopes, A. R., Prats, S. A., Silva, F. C., & Keizer, J. J. (2020). Effects of ploughing and mulching on soil and organic matter losses after a wildfire in Central Portugal. *Cuadernos de Investigación Geográfica*, *46*(1), 303–318. https://doi.org/10.18172/cig.3768

Lucas-Borja, M. E., Plaza-Álvarez, P. A., Gonzalez-Romero, J., Sagra, J., Alfaro-Sánchez, R., Zema, D. A., Moya, D., & de las Heras, J. (2019). Short-term effects of prescribed burning in Mediterranean pine plantations on surface runoff, soil erosion and water quality of runoff. *Science of The Total Environment*, *674*, 615–622. https://doi.org/10.1016/J.SCITOTENV.2019.04.114

Lykoudi, E., & Zarris, D. (2004). The influence of drainage network formation and characteristics over a catchment's sediment yield. . *2nd International Conference on Fluvial Hydraulics*, 793–800.

Mann, M. E., Rahmstorf, S., Kornhuber, K., Steinman, B. A., Miller, S. K., & Coumou, D. (2017). Influence of Anthropogenic Climate Change on Planetary Wave Resonance and Extreme Weather Events. *Scientific Reports*, *7*(January). https://doi.org/10.1038/srep45242

Martínez, J., Vega-Garcia, C., & Chuvieco, E. (2009). Human-caused wildfire risk rating for prevention planning in Spain. *Journal of Environmental Management*, *90*(2), 1241–1252. https://doi.org/10.1016/J.JENVMAN.2008.07.005

Mataix-Solera, J., Cerdà, A., Arcenegui, V., Jordán, A., & Zavala, L. M. (2011). Fire effects on soil aggregation: A review. *Earth-Science Reviews*, *109*(1–2), 44–60. https://doi.org/10.1016/j.earscirev.2011.08.002

Mather, A. S. (2007). Recent Asian forest transitions in relation to foresttransition theory. *International Forestry Review*, *9*(1), 491–502. https://doi.org/10.1505/ifor.9.1.491

Mazurek, R., Kowalska, J., Gąsiorek, M., Zadrożny, P., Józefowska, A., Zaleski, T., Kępka, W., Tymczuk, M., & Orłowska, K. (2017). Assessment of heavy metals contamination in surface layers of Roztocze National Park forest soils (SE Poland) by indices of pollution. *Chemosphere*, *168*, 839–850. https://doi.org/10.1016/j.chemosphere.2016.10.126

McCann Kevin Shear. (2000). The diversity–stability debate. *Nature*, *405*(6783), 228–233. https://doi.org/10.1038/35012234

McWethy, D. B., Pauchard, A., García, R. A., Holz, A., González, M. E., Veblen, T. T., Stahl, J., & Currey, B. (2018). Landscape drivers of recent fire activity (2001-2017) in south-central Chile. *PLOS ONE*, *13*(8), e0201195. https://doi.org/10.1371/JOURNAL.PONE.0201195

Milanović, S., Milanović, S. D., Marković, N., Pamučar, D., Gigović, L., & Kostić, P. (2021). Forest fire probability mapping in eastern serbia: Logistic regression versus random forest method. *Forests*, *12*(1), 1–17. https://doi.org/10.3390/f12010005

Miranda, B. R., Sturtevant, B. R., Stewart, S. I., Hammer, R. B., Miranda, B. R., Sturtevant, B. R., Stewart, S. I., & Hammer, R. B. (2011). Spatial and temporal drivers of wildfire occurrence in the context of rural development in northern Wisconsin, USA. *International Journal of Wildland Fire*, *21*(2), 141–154. https://doi.org/10.1071/WF10133

Mitas, L., & Mitasova, H. (1998). Distributed soil erosion simulation for effective erosion prevention. *Water Resources Research*, *34*(3), 505–516. https://doi.org/10.1029/97WR03347

Mitášová, H., & Hofierka, J. (1993). Interpolation by Regularized Spline with Tension: II. Application to Terrain Modeling and Surface Geometry Analysis. *Mathematical Geology*, *25*, 657–669.

Mitášová, H., & Mitas, L. (1993). Interpolation by regularized spline with tension : I. Theory and implementation. *Mathematical Geology* , *25*, 641–655.

Moore, I. D., & Burch, G. J. (1986). Modelling Erosion and Deposition: Topographic Effects. *Transactions of the ASAE*, *29*(6), 1624–1630. https://doi.org/10.13031/2013.30363

Moreira, F., Ascoli, D., Safford, H., Adams, M. A., Moreno, J. M., Pereira, J. M. C., Catry, F. X., Armesto, J., Bond, W., González, M. E., Curt, T., Koutsias, N., McCaw, L., Price, O., Pausas, J. G., Rigolot, E., Stephens, S., Tavsanoglu, C., Vallejo, V. R., … Fernandes, P. M. (2020). Wildfire management in Mediterranean-type regions: paradigm change needed. *Environmental Research Letters*, *15*(1), 011001. https://doi.org/10.1088/1748-9326/ab541e

Moreira, F., & Vallejo, R. (2009). Living with wildfires : what science can tell us : a contribution to the Science-Policy dialogue. In *In Birot (2009) Living with wildfires : what science can tell us* (pp. 53–58). European Forest Institute.

Morgan, R. P. C. (1995). *Soil erosion and conservation* (Davidson D.A., Ed.; 2nd ed.). Longman, J. Wiley, Prentice Hall PTR.

Morgan, R. P. C. (2001). A simple approach to soil loss prediction: a revised Morgan–Morgan–Finney model. *CATENA*, *44*(4), 305–322. https://doi.org/10.1016/S0341-8162(00)00171-5

Morgan, R. P. C. (2005). *Soil erosion and conservation* (3rd ed.). Blackwell.

Morgan, R. P. C., Morgan, D. D. V., & Finney, H. J. (1984). A predictive model for the assessment of soil erosion risk. *Journal of Agricultural Engineering Research*, *30*, 245–253. https://doi.org/10.1016/S0021-8634(84)80025-6

Mouchet, M. A., Paracchini, M. L., Schulp, C. J. E., Stürck, J., Verkerk, P. J., Verburg, P. H., & Lavorel, S. (2017). Bundles of ecosystem (dis)services and multifunctionality across European landscapes. *Ecological Indicators*, *73*, 23–28. https://doi.org/10.1016/j.ecolind.2016.09.026

Mulder, T., & Syvitski, J. P. M. (1996). Climatic and Morphologic Relationships of Rivers: Implications of Sea-Level Fluctuations on River Loads. *The Journal of Geology*, *104*(5), 509–523. https://doi.org/10.1086/629849

Müller, G. (1969). Index of geoaccumulation in sediments of the Rhine River. . *GeoJournal*, *2*(3), 108–118.

Muñoz-Rojas, M. (2018). Soil quality indicators: critical tools in ecosystem restoration. *Current Opinion in Environmental Science & Health*, *5*, 47–52. https://doi.org/10.1016/J.COESH.2018.04.007

Neary, D. G., Klopatek, C. C., DeBano, L. F., & Ffolliott, P. F. (1999). Fire effects on belowground sustainability: a review and synthesis. *Forest Ecology and Management*, *122*(1–2), 51–71. https://doi.org/10.1016/S0378-1127(99)00032-8

Neary, D. G., Ryan, K. C., & DeBano, L. F. (2005). *Wildland fire in ecosystems: effects of fire on soils and water*. https://doi.org/10.2737/RMRS-GTR-42-V4

Nelson, D., & Sommers, L. (1996). Total Carbon, Organic Carbon, and Organic Matter. . In D. L. Sparks, A. L. Page, P. A. Helmke, R. H. Loeppert, P. N. Soltanpour, M. A. Tabatabai, C. T. Johnston, & M. E. Sumner (Eds.), *Methods of Soil Analysis* (pp. 961–1010). Soil Science Society of America, American Society of Agronomy. https://doi.org/10.2136/sssabookser5.3

Nørnberg, P., Vendelboe, A. L., Gunnlaugsson, H. P., Merrison, J. P., Finster, K., & Jensen, S. K. (2009). Comparison of the mineralogical effects of an experimental forest fire on a goethite/ferrihydrite soil with a topsoil that contains hematite, maghemite and goethite. *Clay Minerals*, *44*(2), 239–247. https://doi.org/10.1180/claymin.2009.044.2.239

Oliver, T. H., Heard, M. S., Isaac, N. J. B., Roy, D. B., Procter, D., Eigenbrod, F., Freckleton, R., Hector, A., Orme, C. D. L., Petchey, O. L., Proença, V., Raffaelli, D., Suttle, K. B., Mace, G. M., Martín-López, B., Woodcock, B. A., & Bullock, J. M. (2015). Biodiversity and Resilience of Ecosystem Functions. *Trends in Ecology & Evolution*, *30*(11), 673–684. https://doi.org/10.1016/J.TREE.2015.08.009

Padilla, F. M., Mommer, L., de Caluwe, H., Smit-Tiekstra, A. E., Visser, E. J. W., & de Kroon, H. (2019). Effects of extreme rainfall events are independent of plant species richness in an experimental grassland community. *Oecologia*, *191*(1), 177–190. https://doi.org/10.1007/s00442-019-04476-z

Page, S. E., & Hooijer, A. (2016). In the line of fire: The peatlands of Southeast Asia. *Philosophical Transactions of the Royal Society B: Biological Sciences*, *371*(1696). https://doi.org/10.1098/rstb.2015.0176

Page, S. E., Rieley, J. O., & Banks, C. J. (2011). Global and regional importance of the tropical peatland carbon pool. *Global Change Biology*, *17*(2), 798–818. https://doi.org/10.1111/j.1365-2486.2010.02279.x

Panagos, P., Karydas, C. G., Gitas, I. Z., & Montanarella, L. (2012). Monthly soil erosion monitoring based on remotely sensed biophysical parameters: a case study in Strymonas river basin towards a functional pan-European service. *International Journal of Digital Earth*, *5*(6), 461–487. https://doi.org/10.1080/17538947.2011.587897

Parlak, M. (2011). Effect of heating on some physical, chemical and mineralogical aspects of forest soil. *Bartın Orman Fakültesi Dergisi* , *13*, 143–152.

Pastor, J., & Post, W. M. (1986). Influence of climate, soil moisture, and succession on forest carbon and nitrogen cycles. *Biogeochemistry*, *2*(1), 3–27. https://doi.org/10.1007/BF02186962

Pausas, J. G., Bladé, C., Valdecantos, A., Seva, J. P., Fuentes, D., Alloza, J. A., Vilagrosa, A., Bautista, S., Cortina, J., & Vallejo, R. (2004). Pines and oaks in the restoration of Mediterranean landscapes of Spain: New perspectives for an old practice — a review. *Plant Ecology 2004 171:1*, *171*(1), 209–220. https://doi.org/10.1023/B:VEGE.0000029381.63336.20

Pausas, J. G., Llovet, J., Rodrigo, A., Vallejo, R., Pausas, J. G., Llovet, J., Rodrigo, A., & Vallejo, R. (2008). Are wildfires a disaster in the Mediterranean basin? – A review. *International Journal of Wildland Fire*, *17*(6), 713–723. https://doi.org/10.1071/WF07151

Pausas, J. G., & Vallejo, V. R. (1999). The role of fire in European Mediterranean ecosystems. In *Remote Sensing of Large Wildfires* (pp. 3–16). Springer Berlin Heidelberg. https://doi.org/10.1007/978-3-642-60164-4_2

Pejman, A., Nabi Bidhendi, G., Ardestani, M., Saeedi, M., & Baghvand, A. (2015). A new index for assessing heavy metals contamination in sediments: A case study. *Ecological Indicators*, *58*, 365–373. https://doi.org/10.1016/J.ECOLIND.2015.06.012

Pereira, P., Francos, M., Brevik, E. C., Ubeda, X., & Bogunovic, I. (2018). Post-fire soil management. *Current Opinion in Environmental Science & Health*, *5*, 26–32. https://doi.org/10.1016/J.COESH.2018.04.002

Petersen, R., & Calvin, l. (1996). Sampling. In D. L. Sparks, A. L. Page, P. A. Helmke, R. H. Loeppert, P. N. Soltanpour, M. A. Tabatabai, C. T. Johnston, & M. E. Sumner (Eds.), *Methods of Soil Analysis* (pp. 1–17). Soil Science Society of America, American Society of Agronomy. https://doi.org/10.2136/sssabookser5.3

Plaza-Álvarez, P. A., Lucas-Borja, M. E., Sagra, J., Zema, D. A., González-Romero, J., Moya, D., & De las Heras, J. (2019). Changes in soil hydraulic conductivity after prescribed fires in Mediterranean pine forests. *Journal of Environmental Management*, *232*, 1021–1027. https://doi.org/10.1016/j.jenvman.2018.12.012

Pozo, R. A., Galleguillos, M., González, M. E., Vásquez, F., & Arriagada, R. (2022). Assessing the socio-economic and land-cover drivers of wildfire activity and its spatiotemporal distribution in south-central Chile. *Science of The Total Environment*, *810*, 152002. https://doi.org/10.1016/J.SCITOTENV.2021.152002

Qingjie, G., Deng, J., Yunchuan, X., Qingfei, W., & Liqiang, Y. (2008). Calculating Pollution Indices by Heavy Metals in Ecological Geochemistry Assessment and a Case Study in Parks of Beijing. *Journal of China University of Geosciences*, *19*(3), 230–241.

Quansah, C. (1982). *Laboratory experimentation for the statistical derivation of equations for soil erosion modelling and soil conservation design*. Cranfield Institute of Technology.

Rawat, D., Khanduri, V. P., Sati, S. P., Ahmad, T., Riyal, M., & Mishra, P. (2020). Impact of forest fire on soil quality and resilience potential: A review. *Adrri Journal of Agriculture and Food Sciences*, *4*(6), 2023–5204.

Redda+. (2022). *What is Forest Restoration?* https://redda.com.br/en/what-is-forest-restoration/

Renard, K. G. , Foster, G. R. , Yoder, D. C. , & McCool, D. K. (1994). RUSLE revisited: Status, questions, answers, and the future. *Journal of Soil Snd Water Conservation*, *49*(3), 213–220.

Renard, K. G., Foster, G. R., Weesies, G. A., McCool, D. K., & Yoder, D. C. (1997). *Predicting soil erosion by water : a guide to conservation planning with the Revised Universal Soil Loss Equation (RUSLE)* (Vol. 703).

Renard, K. G., Foster, G. R., Weesies, G. A., & Porter, J. P. (1991). RUSLE: Revised Universal Soil Loss Equation. . *Journal of Soil and Water Conservation*, *46*(1), 30–33.

Reyer, C. P. O., Rammig, A., Brouwers, N., & Langerwisch, F. (2015). Forest resilience, tipping points and global change processes. *Journal of Ecology*, *103*(1), 1–4. https://doi.org/10.1111/1365-2745.12342

Reyes, O., García-Duro, J., & Salgado, J. (2015). Fire affects soil organic matter and the emergence of Pinus radiata seedlings. *Annals of Forest Science*, *72*(2), 267–275. https://doi.org/10.1007/s13595-014-0427-8

Rezaei, R., & Ghaffarian, S. (2021). Monitoring forest resilience dynamics from very high-resolution satellite images in case of multi-hazard disaster. *Remote Sensing*, *13*(20). https://doi.org/10.3390/rs13204176

Rikimaru, A., Roy, P. S., & Miyatake, S. (2002). Tropical forest cover density mapping. *Tropical Ecology*, *43*(1), 39–47.

Robichaud, P. R., Lewis, S. A., Brown, R. E., Bone, E. D., & Brooks, E. S. (2020). Evaluating post-wildfire logging-slash cover treatment to reduce hillslope erosion after salvage logging using ground measurements and remote sensing. *Hydrological Processes*, *34*(23), 4431–4445. https://doi.org/10.1002/hyp.13882

Rodrigo, A., Retana, J., & Picó, F. X. (2004). DIRECT REGENERATION IS NOT THE ONLY RESPONSE OF MEDITERRANEAN FORESTS TO LARGE FIRES. *Ecology*, *85*(3), 716–729. https://doi.org/https://doi.org/10.1890/02-0492

Rodrigues, M., Jiménez-Ruano, A., Peña-Angulo, D., & de la Riva, J. (2018). A comprehensive spatial-temporal analysis of driving factors of human-caused wildfires in Spain using Geographically Weighted Logistic Regression. *Journal of Environmental Management*, *225*, 177–192. https://doi.org/10.1016/J.JENVMAN.2018.07.098

Romagnoli, F., Cadei, A., Costa, M., Marangon, D., Pellegrini, G., Nardi, D., Masiero, M., Secco, L., Grigolato, S., Lingua, E., Picco, L., Pirotti, F., Battisti, A., Locatelli, T., Blennow, K., Gardiner, B., & Cavalli, R. (2023). Windstorm impacts on European forest-related systems: An interdisciplinary perspective. *Forest Ecology and Management*, *541*, 121048. https://doi.org/10.1016/J.FORECO.2023.121048

Rouse, J. W. , Jr., Haas, R. H., Schell, J. A., Deering, D. W., Haas, R. H., Schell, J. A., & Deering, D. W. (1974). monitoring vegetation systems in the great plains with erts. *NASA. Goddard Space Flight Center 3d ERTS-1 Symp., Vol. 1, Sect. A*.

Ruiz-Pérez, G., & Vico, G. (2020). Effects of Temperature and Water Availability on Northern European Boreal Forests. *Frontiers in Forests and Global Change*, *3*(April), 1–18. https://doi.org/10.3389/ffgc.2020.00034

Sadeghi, M., Petrosino, P., Ladenberge, A., Albanese, S., Andersso, n M., Morris, G., Lima, A., & De Vivo, B. (2013). Ce, La and Y concentrations in agricultural and grazing-land soils of Europe. *Journal of Geochemical Exploration*, *133*, 202–213. https://doi.org/10.1016/j.gexplo.2012.12.007

Sadeghi, S. H. R., Gholami, L., Khaledi, D. A., & Saeidi, P. (2014). A review of the application of the MUSLE model worldwide. *Hydrological Sciences Journal*, *59*(2), 365–375. https://doi.org/10.1080/02626667.2013.866239

Sadeghi, S. H. R., Mizuyama, T., Miyata, S., Gom, i T., Kosugi, K., Mizugak, S., & Onda, Y. (2007). Is MUSLE apt to small steeply reforested watershed? *Journal of Forest Research*, *12*(4), 270–277. https://doi.org/10.1007/s10310-007-0017-9

Salis, M., Del Giudice, L., Robichaud, P. R., Ager, A. A., Canu, A., Duce, P., Pellizzaro, G., Ventura, A., Alcasena-Urdiroz, F., Spano, D., & Arca, B. (2019). Coupling wildfire spread and erosion models to quantify post-fire erosion before and after fuel treatments. *International Journal of Wildland Fire*, *28*(9), 687–703. https://doi.org/10.1071/WF19034

San-Miguel-Ayanz, J., Moreno, J. M., & Camia, A. (2013). Analysis of large fires in European Mediterranean landscapes: Lessons learned and perspectives. *Forest Ecology and Management*, *294*, 11–22. https://doi.org/10.1016/J.FORECO.2012.10.050

Santika, T., Muhidin, S., Budiharta, S., Haryanto, B., Agus, F., Wilson, K. A., Struebig, M. J., & Po, J. Y. T. (2023). Deterioration of respiratory health following changes to land cover and climate in Indonesia. *One Earth*, *6*(3), 290–302. https://doi.org/10.1016/j.oneear.2023.02.012

Satheeshkumar, S., Venkateswaran, S., & Kannan, R. (2017). Rainfall–runoff estimation using SCS–CN and GIS approach in the Pappiredipatti watershed of the Vaniyar sub basin, South India. *Modeling Earth Systems and Environment*, *3*(1), 24. https://doi.org/10.1007/s40808-017-0301-4

Schmeer, S. R., Kampf, S. K., MacDonald, L. H., Hewitt, J., & Wilson, C. (2018). Empirical models of annual post-fire erosion on mulched and unmulched hillslopes. *CATENA*, *163*, 276–287. https://doi.org/10.1016/j.catena.2017.12.029

Schultz, C. A., Mattor, K. M., & Moseley, C. (2016). Aligning policies to support forest restoration and promote organizational change. *Forest Policy and Economics*, *73*, 195–203. https://doi.org/10.1016/J.FORPOL.2016.09.015

Schwörer, C., Gobet, E., van Leeuwen, J. F. N., Bögli, S., Imboden, R., van der Knaap, W. O., Kotova, N., Makhortykh, S., & Tinner, W. (2022). Holocene vegetation, fire and land use dynamics at Lake Svityaz, an agriculturally marginal site in northwestern Ukraine. *Vegetation History and Archaeobotany*, *31*(2), 155–170. https://doi.org/10.1007/s00334-021-00844-z

Seidl, R., Thom, D., Kautz, M., Martin-Benito, D., Peltoniemi, M., Vacchiano, G., Wild, J., Ascoli, D., Petr, M., Honkaniemi, J., Lexer, M. J., Trotsiuk, V., Mairota, P., Svoboda, M., Fabrika, M., Nagel, T. A., & O Reyer, C. P. (2017). *Forest disturbances under climate change*. https://doi.org/10.1038/NCLIMATE3303

Seidl, R., Thom, D., Kautz, M., Martin-Benito, D., Peltoniemi, M., Vacchiano, G., Wild, J., Ascoli, D., Petr, M., Honkaniemi, J., Lexer, M. J., Trotsiuk, V., Mairota, P., Svoboda, M., Fabrika, M., Nagel, T. A., & Reyer, C. P. O. (2017). Forest disturbances under climate change. *Nature Climate Change 2017 7:6*, *7*(6), 395–402. https://doi.org/10.1038/nclimate3303

SER. (2004). *Restoration Resource Center What is Ecological Restoration?* Society for Ecological Restoration International Science & Policy Working Group . https://www.ser-rrc.org/what-is-ecological-restoration/

Shakesby, R. A. (2011). Post-wildfire soil erosion in the Mediterranean: Review and future research directions. *Earth-Science Reviews*, *105*(3–4), 71–100. https://doi.org/10.1016/J.EARSCIREV.2011.01.001

Shakesby, R. A., & Doerr, S. H. (2006). Wildfire as a hydrological and geomorphological agent. *Earth-Science Reviews*, *74*(3–4), 269–307. https://doi.org/10.1016/J.EARSCIREV.2005.10.006

Shtober-Zisu, N., & Wittenberg, L. (2021). Wildfires as a Weathering Agent of Carbonate Rocks. *Minerals*, *11*(10), 1091. https://doi.org/10.3390/min11101091

Sjöström, J., & Granström, A. (2023). Human activity and demographics drive the fire regime in a highly developed European boreal region. *Fire Safety Journal*, *136*, 103743. https://doi.org/10.1016/J.FIRESAF.2023.103743

Slaughter, A. R., Hughes, D. A., Retief, D. C. H., & Mantel, S. K. (2017). A management-oriented water quality model for data scarce catchments. *Environmental Modelling & Software*, *97*, 93–111. https://doi.org/10.1016/j.envsoft.2017.07.015

Soti, P. G., Purcell, M., & Jayachandran, K. (2020). Soil biotic and abiotic conditions negate invasive species performance in native habitat. *Ecological Processes*, *9*(1), 18. https://doi.org/10.1186/s13717-020-00220-1

Suding, K. (2011). Toward an Era of Restoration in Ecology: Successes, Failures, and Opportunities Ahead. *Https://Doi.Org/10.1146/Annurev-Ecolsys-102710-145115*, *42*. https://doi.org/10.1146/ANNUREV-ECOLSYS-102710-145115

Suding, K., Higgs, E., Palmer, M., Callicott, J. B., Anderson, C. B., Baker, M., Gutrich, J. J., Hondula, K. L., LaFevor, M. C., Larson, B. M. H., Randall, A., Ruhl, J. B., & Schwartz, K. Z. S. (2015). Committing to ecological restoration: Efforts around the globe need legal and policy clarification. *Science*, *348*(6235), 638–640. https://doi.org/10.1126/science.aaa4216

Syvitski, J. P. M., Peckham, S. D., Hilberman, R., & Mulder, T. (2003). Predicting the terrestrial flux of sediment to the global ocean: a planetary perspective. *Sedimentary Geology*, *162*(1–2), 5–24. https://doi.org/10.1016/S0037-0738(03)00232-X

Syvitski, J. P., & Morehead, M. D. (1999). Estimating river-sediment discharge to the ocean: application to the Eel margin, northern California. *Marine Geology*, *154*(1–4), 13–28. https://doi.org/10.1016/S0025-3227(98)00100-5

Tadesse, K. A. (2016). A Review on Effects of Fire and Traditional Practices of Soil. Burning on Soil Physico-Chemical Properties. *Journal of Biology*, *6*(1).

Terraprima. (2023). *Carbon sequestration contract with EDP*. Https://Www.Terraprima.Pt/En/Projecto/13.

Thomas, G. W. (1996). Soil pH and Soil Acidity. In D. L. Sparks, A. L. Page, P. A. Helmke, R. H. Loeppert, P. N. Soltanpour, M. A. Tabatabai, C. T. Johnston, & M. E. Sumner (Eds.), *Methods of Soil Analysis. Part 3. Chemical Methods* (pp. 475–490). Soil Science Society of America, American Society of Agronomy. https://doi.org/10.2136/sssabookser5.3

Thomaz, E. L. (2018). Ash Physical Characteristics Affects Differently Soil Hydrology and Erosion Subprocesses. *Land Degradation & Development*, *29*(3), 690–700. https://doi.org/10.1002/ldr.2715

Thompson, I., Mackey, B., McNulty, S., & Mosseler, A. (2009). *Forest Resilience, Biodiversity, and Climate Change*.

Triviño, M., Potterf, M., Tijerín, J., Ruiz-Benito, P., Burgas, D., Eyvindson, K., Blattert, C., Mönkkönen, M., & Duflot, R. (2023). Enhancing Resilience of Boreal Forests Through Management Under Global Change: a Review. *Current Landscape Ecology Reports 2023 8:3*, *8*(3), 103–118. https://doi.org/10.1007/S40823-023-00088-9

Trumbore, S., Brando, P., & Hartmann, H. (2015). Forest health and global change. *Science (New York, N.Y.)*, *349*(6250), 814–818. https://doi.org/10.1126/SCIENCE.AAC6759

Tuomisto, H., Poulsen, A. D., Ruokolainen, K., Moran, R. C., Quintana, C., Celi, J., & Cañas, G. (2003). Linking floristic patterns with soil heterogeneity and satellite imagery in Ecuadorian Amazonia. *Ecological Applications*, *13*(2), 352–371. https://doi.org/10.1890/1051-0761(2003)013[0352:LFPWSH]2.0.CO;2

Ulery, A. L., & Graham, R. C. (1993). Forest Fire Effects on Soil Color and Texture. *Soil Science Society of America Journal*, *57*(1), 135–140. https://doi.org/10.2136/sssaj1993.03615995005700010026x

Ulery, A. L., Graham, R. C., & Bowen, L. H. (1996). Forest Fire Effects on Soil Phyllosilicates in California. *Soil Science Society of America Journal*, *60*(1), 309–315. https://doi.org/10.2136/sssaj1996.03615995006000010047x

Ulery, A. L., Graham, R. C., Goforth, B. R., & Hubbert, K. R. (2017). Fire effects on cation exchange capacity of California forest and woodland soils. *Geoderma*, *286*, 125–130. https://doi.org/10.1016/j.geoderma.2016.10.028

Ürker, O., Tavşanoğlu, Ç., & Gürkan, B. (2018). Post-fire recovery of the plant community in Pinus brutia forests: active vs. indirect restoration techniques after salvage logging. *IForest - Biogeosciences and Forestry*, *11*(5), 635. https://doi.org/10.3832/IFOR2645-011

Vallejo, V. R., Arianoutsou, M., & Moreira, F. (2012). *Fire Ecology and Post-Fire Restoration Approaches in Southern European Forest Types*. 93–119. https://doi.org/10.1007/978-94-007-2208-8_5

Van Oost, K., Govers, G., & Desmet, P. (2000). Evaluating the effects of changes in landscape structure on soil erosion by water and tillage. *Landscape Ecology*, *15*(6), 577–589. https://doi.org/10.1023/A:1008198215674

Van Rompaey, A. J. J., Verstraeten, G., Van Oost, K., Govers, G., & Poesen, J. (2001). Modelling mean annual sediment yield using a distributed approach. *Earth Surface Processes and Landforms*, *26*(11), 1221–1236. https://doi.org/10.1002/esp.275

Varela, M. E., Benito, E., & Keizer, J. J. (2010). Effects of wildfire and laboratory heating on soil aggregate stability of pine forests in Galicia: The role of lithology, soil organic matter content and water repellency. *CATENA*, *83*(2–3), 127–134. https://doi.org/10.1016/J.CATENA.2010.08.001

Varol, M. (2011). Assessment of heavy metal contamination in sediments of the Tigris River (Turkey) using pollution indices and multivariate statistical techniques. *Journal of Hazardous Materials*, *195*, 355–364. https://doi.org/10.1016/J.JHAZMAT.2011.08.051

Verma, S., & Jayakumar, S. (2012). Impact of forest fire on physical, chemical and biological properties of soil: A review. *Proceedings of the International Academy of Ecology and Environmental Sciences*, 168–176.

Vieira, D. C. S., Malvar, M. C., Martins, M. A. S., Serpa, D., & Keizer, J. J. (2018). Key factors controlling the post-fire hydrological and erosive response at micro-plot scale in a recently burned Mediterranean forest. *Geomorphology*, *319*, 161–173. https://doi.org/10.1016/J.GEOMORPH.2018.07.014

Vieira, D. C. S., Serpa, D., Nunes, J. P. C., Prats, S. A., Neves, R., & Keizer, J. J. (2018). Predicting the effectiveness of different mulching techniques in reducing post-fire runoff and erosion at plot scale with the RUSLE, MMF and PESERA models. *Environmental Research*, *165*, 365–378. https://doi.org/10.1016/J.ENVRES.2018.04.029

Walkley, A., & Black, I. A. (1934). An examination of the Degtjareff method for determining soil organic matter, and a proposed modification of the chromic acid titration method. *Soil Science*, *37*(1), 29–38. https://doi.org/10.1097/00010694-193401000-00003

Walling, D. E. (1983). The sediment delivery problem. *Journal of Hydrology*, *65*(1–3), 209–237. https://doi.org/10.1016/0022-1694(83)90217-2

Wang, N., & Bao, Y. (2011). Modeling forest quality at stand level: A case study of loess plateau in China. *Forest Policy and Economics*, *13*(6), 488–495. https://doi.org/10.1016/J.FORPOL.2011.05.012

Wattez, J., & Courty, M. A. (1987). Morphology of ash of some plant materials. Soil micromorphology. *Proceedings of the Seventh International Working Meeting on Soil Micromorphology*, 677–683.

Webb, R. H., & Griffiths, P. G. (2001). *Sediment Delivery by Ungaged Tributaries of the Colorado River in Grand Canyon*.

Widyastuti, K., Imron, M. A., Pradopo, S. T., Suryatmojo, H., Sopha, B. M., Spessa, A., & Berger, U. (2021). PeatFire: An agent-based model to simulate fire ignition and spreading in a tropical peatland ecosystem. *International Journal of Wildland Fire*, *30*(2), 71–89. https://doi.org/10.1071/WF19213

Williams, J. R. (1975). Sediment-Yield Prediction with Universal Equation Using Runoff Energy Factor. . *Proceedings of the Sediment Yield Workshop: "Present and Prospective Technology for Predicting Sediment Yield and Sources"*, 244–252.

Williams, J. R., & Berndt, H. D. (1977). Sediment Yield Prediction Based on Watershed Hydrology. *Transactions of the ASAE*, *20*(6), 1100–1104. https://doi.org/10.13031/2013.35710

Wischmeier, W., & Smith, D. (1978). *Predicting rainfall erosion losses: A guide to conservation planning* (Vol. 537). U.S. Department of Agriculture .

Wittenberg, L., van der Wal, H., Keesstra, S., & Tessler, N. (2020). Post-fire management treatment effects on soil properties and burned area restoration in a wildland-urban interface, Haifa Fire case study. *Science of The Total Environment*, *716*, 135190. https://doi.org/10.1016/J.SCITOTENV.2019.135190

Yengoh, G. T., Dent, D., Olsson, L., Tengberg Compton, A. E., & Iii, J. T. (2015). *Use of the Normalized Diff erence Vegetation Index (NDVI) to Assess Land Degradation at Multiple Scales Current Status, Future Trends, and Practical Considerations*. Springer International Publishing. http://www.springer.com/series/8868

Yusiharni, E., & Gilkes, R. J. (2012). Changes in the mineralogy and chemistry of a lateritic soil due to a bushfire at Wundowie, Darling Range, Western Australia. *Geoderma*, *191*, 140–150. https://doi.org/10.1016/j.geoderma.2012.01.030

Zanchi, C., & Torri, D. (1980). Evaluation of rainfall energy in central Italy. In M. de Boodt & D. Gabriels (Eds.), *Assessment of Erosion* (pp. 133–142). John Wiley and Sons Ltd.

Zavala, L. M., De Celis, R., & Jordán, A. (2014). How wildfires affect soil properties. A brief review. *Cuadernos de Investigación Geográfica*, *40*(2), 311–332. https://doi.org/10.18172/cig.2522

Zema, D. A. (2021). Postfire management impacts on soil hydrology. In *Current Opinion in Environmental Science and Health* (Vol. 21). Elsevier B.V. https://doi.org/10.1016/j.coesh.2021.100252

Zema, D. A., Lucas-Borja, M. E., Fotia, L., Rosaci, D., Sarnè, G. M. L., & Zimbone, S. M. (2020). Predicting the hydrological response of a forest after wildfire and soil treatments using an Artificial Neural Network. *Computers and Electronics in Agriculture*, *170*, 105280. https://doi.org/10.1016/J.COMPAG.2020.105280

Zhai, T., Wang, J., Jin, Z., Qi, Y., Fang, Y., & Liu, J. (2020). Did improvements of ecosystem services supply-demand imbalance change environmental spatial injustices? *Ecological Indicators*, *111*(July 2018). https://doi.org/10.1016/j.ecolind.2020.106068

Zhao, Q., Yu, S., Zhao, F., Tian, L., & Zhao, Z. (2019). Comparison of machine learning algorithms for forest parameter estimations and application for forest quality assessments. *Forest Ecology and Management*, *434*, 224–234. https://doi.org/10.1016/J.FORECO.2018.12.019

Zituni, R., Wittenberg, L., & Malkinson, D. (2019). The effects of post-fire forest management on soil erosion rates 3 and 4 years after a wildfire, demonstrated on the 2010 Mount Carmel fire. *International Journal of Wildland Fire*, *28*(5), 377–385. https://doi.org/10.1071/WF18116